Model hibridnog električnog vozila u frekvencijskoj domeni za predviđanje potrošnje i emisija

Kozina, Ante

Doctoral thesis / Disertacija

2024

Degree Grantor / Ustanova koja je dodijelila akademski / stručni stupanj: **University of Split, Faculty of Electrical Engineering, Mechanical Engineering and Naval Architecture / Sveučilište u Splitu, Fakultet elektrotehnike, strojarstva i brodogradnje**

Permanent link / Trajna poveznica: https://urn.nsk.hr/urn:nbn:hr:179:657972

Rights / Prava: In copyright/Zaštićeno autorskim pravom.

Download date / Datum preuzimanja: **2025-01-13**

Repository / Repozitorij:

Repository of the Faculty of Electrical Engineering, Mechanical Engineering and Naval Architecture - University of Split

SVEUČILIŠTE U SPLITU
FAKULTET ELEKTROTEHNIKE, STROJARSTVA I BRODOGRADNJE

Ante Kozina

MODEL HIBRIDNOG ELEKTRIČNOG VOZILA U FREKVENCIJSKOJ DOMENI ZA PREDVIĐANJE POTROŠNJE I EMISIJA

DOKTORSKI RAD

Split, 2024.

SVEUČILIŠTE U SPLITU
FAKULTET ELEKTROTEHNIKE, STROJARSTVA I BRODOGRADNJE

Ante Kozina

Model hibridnog električnog vozila u frekvencijskoj domeni za predviđanje potrošnje i emisija

DOKTORSKI RAD

Split, 2024.

Doktorski rad je izrađen na Katedri za toplinske strojeve, Zavoda za strojarstvo i brodogradnju, Fakulteta elektrotehnike, strojarstva i brodogradnje, Sveučilišta u Splitu

Mentor: prof. dr. sc. Gojmir Radica

Rad br. 207

Povjerenstvo za ocjenu disertacije:

1. prof. dr. sc. Branko Klarin, Sveučilište u Splitu, FESB, Split

2. prof. dr. sc. Zoran Lulić, Sveučilište u Zagrebu, FSB, Zagreb

3. prof. dr. sc. Tomislav Mrakovčić, Sveučilište u Rijeci, TF, Rijeka

4. prof. dr. sc. Sandro Nižetić, Sveučilište u Splitu, FESB, Split

5. doc. dr. sc. Željko Penga, Sveučilište u Splitu, FESB, Split

Povjerenstvo za obranu disertacije:

1. prof. dr. sc. Branko Klarin, Sveučilište u Splitu, FESB, Split

2. prof. dr. sc. Zoran Lulić, Sveučilište u Zagrebu, FSB, Zagreb

3. prof. dr. sc. Tomislav Mrakovčić, Sveučilište u Rijeci, TF, Rijeka

4. prof. dr. sc. Sandro Nižetić, Sveučilište u Splitu, FESB, Split

5. doc. dr. sc. Željko Penga, Sveučilište u Splitu, FESB, Split

Disertacija obranjena dana: 13. prosinca 2024.

Model hibridnog električnog vozila u frekvencijskoj domeni za predviđanje potrošnje i emisija

Sažetak:

Doktorski rad predstavlja objedinjeno istraživanje koje čine četiri objavljena rada u uglednim znanstvenim časopisima prema skandinavskom modelu. Područje znanstvenog istraživanja usmjereno je na procjene emisija i potrošnje goriva u stvarnim uvjetima upotrebe vozila primarno pokretanih motorima s unutarnjim izgaranjem. U svrhu kvalitetnijeg predviđanja emisija, potrošnje goriva i potrošnje energije razvijen je model hibridnog električnog vozila na temelju modalne analize uz primjenu odgovarajućeg dijagrama toka energije definiranog prema funkcionalnoj podjeli. Razvijeni model povezuje pojedinačne emisije i potrošnju energije s uzdužnom dinamikom vozila. Provedenim istraživanjem utvrđeno je kako je na razvijeni model moguće uspješno primijeniti globalnu strategiju upravljanja, temeljenu na pravilima, u više različitih standardnih ciklusa vožnje i u stvarnim uvjetima upotrebe. Predloženi model validiran je u odnosu na kontrolni model prema Novom europskom ciklusu ispitivanja, Globalno usklađenom ispitnom ciklusa te u okolnostima koje repliciraju stvarne uvjete upotrebe. Rezultati provedene usporedbe pokazuju točnije predviđanje emisija i potrošnje goriva sa značajno manjom relativnom pogreškom na razini ciklusa u odnosu na rezultate postojećih modalnih modela. U radu je provedeno i eksperimentalno istraživanje u cilju utvrđivanja količina emisija ispušnih plinova u stvarnim uvjetima upotrebe ispravnih vozila, kao i u slučaju vozila s kvarom na sustavima kontrole emisija. Zaključci istraživanja pridonijeli su razumijevanju utjecaja stvarnih uvjeta upotrebe kao i dugotrajne eksploatacije na emisije te sustave njihove kontrole.

Ključne riječi:

hibridna električna vozila, emisijski modeli, modalni modeli, kontrola emisija, strategije upravljanja

Model of hybrid electric vehicle in the frequency domain for consumption and emission prediction

Abstract:

This doctoral thesis presents a comprehensive study comprising four published papers in reputable scientific journals, adhering to the Scandinavian model. The research primarily focuses on assessing emissions and fuel consumption under real-world conditions for vehicles primarily powered by internal combustion engines. To improve the accuracy of emission and consumption predictions, an innovative hybrid electric vehicle model was developed based on modal emissions analysis. This model incorporates energy flow diagrams that are based on their purpose. The developed model integrates the longitudinal dynamics of the vehicle and energy flows with fuel consumption and individual emissions. The research demonstrates the successful application of a global rule-based energy management strategy to the developed model across various standard driving cycles and under real-world conditions as defined by Real Driving Emissions (RDE) regulations. The model was validated against control models using the New European Driving Cycle (NEDC), Worldwide Harmonized Light Vehicles Test Cycle (WLTC), and real-world driving conditions. Comparative results show that the proposed model provides more accurate predictions of emissions and consumption, with significantly lower relative error in tested driving cycles compared to existing modal models based on Vehicle Specific Power (VSP) analysis. Additionally, the thesis includes experimental research on exhaust gas emissions from vehicles under real driving conditions. This research was conducted on both fully operational vehicles and those with malfunctioning emission control systems. The findings contribute to a deeper understanding of the impact of real-world driving conditions and long-term vehicle operation on emissions and the performance of emission control systems.

Keywords:

hybrid electric vehicles, emission models, modal models, emission control, energy management strategies.

Zahvala

Prije svega posebnu zahvalnost izražavam prof. dr. sc. Gojmiru Radici, najprije kao čovjeku, a onda i kao mentoru na vođenju, dugogodišnjem strpljenju i savjetima tijekom cijelog studija. Zahvaljujem se kolegama s katedre za toplinske strojeve i termodinamiku na pomoći i savjetima, posebno kolegi Tinu Vidoviću na aktivnom sudjelovanju u istraživanju i objavama znanstvenih radova. Također se zahvaljujem kolegama s katedre za motore i vozila zagrebačkog FSB-a na ustupanju opreme, prostora i vlastitog vremena koje je bilo daleko iznad mojih očekivanja. Hrvatska zaklada za znanost poduprla je ovaj rad u sklopu projekta IP-2020-02-6249. Prijateljima i rodbini koji su svoje slobodno vrijeme uložili u ovaj rad, onima koji su me potakli na odluku o studiju i onima koji su mi ustupili svoja vozila i opremu upućujem jedno veliko hvala. S toplinom u srcu zahvaljujem svojim roditeljima Veselki i Stanku koji su uz nesebičnu ljubav i strpljivost pomogli da izrastem u osobu kakva sam danas. Hvala na potpori mojim najboljim prijateljima još od djetinjstva, sestri Ivanki i bratu Marku koji su uvijek bili u blizini. Na kraju najvažniju zahvalnost izražavam svojoj supruzi Anđeli, sinovima Luki i Marku te kćeri Ivani na pruženoj ljubavi, potpori i strpljenju koje su imali za mene jer su možda na najteži način iskusili teret mog profesionalnog razvoja.

Nakon svakog životnog uspjeha ne zaboravimo da:

„*Čovjekova vrijednost sastoji se u onome što on jest, a ne u tome što radi ili posjeduje*".

Sv. Ivan Pavao II

Sadržaj

Popis slika

Popis kratica

AFR	Omjer zraka i goriva (*engl. Air to Fuel Ratio*)
BMEP	Srednji efektivni tlak (*engl. Brake Mean Effective Pressure*)
CD	Pražnjenje baterije (*engl. Charge Depleting*)
CFD	Računalna dinamika fluida (*engl. Computational Fluid Dynamics*)
CS	Održavanje konstantne razine napunjenosti (*engl. Charge Sustain*)
DOC	Dizelski oksidacijski katalizator (*engl. Diesel Oxidation Catalyst*)
DPF	Filter dizelskih čestica (*engl. Diesel Particulate Filter*)
DVA	Dvostruko aktiviranje ventila (*engl. Double Valve Actuation*)
EGR	Recirkulacija ispušnih plinova (*engl. Exhaust Gas Recirculation*)
EMS	Strategije upravljanja energijom (*engl. Energy Management Strategy*)
EV	Električno vozilo (*engl. Electric Vehicle*)
FHEV	Potpuno hibridno električno vozilo (*engl. Full Hybrid Electric Vehicle*)
GPF	Filter benzinskih čestica (*engl. Gasoline Particulate Filter*)
HEV	Hibridno električno vozilo (*engl. Hybrid Electric Vehicle*)
HP-EGR	Visokotlačna recirkulacija ispušnih plinova (*engl. High Pressure Exhaust Gas Recirculation*)
IMEP	Indicirani srednji efektivni tlak (*engl. Indicated Mean Effective Pressure*)
ISFC	Indicirana specifična potrošnja goriva (*engl. Indicated Specific Fuel Consumption*)
^{0}KV	Kut koljenastog vratila
LNT	Katalizator NOx-a u uvjetima siromašne smjese (*engl. Lean NOx Trap*)
LP-EGR	Niskotlačna recirkulacija ispušnih plinova (*engl. Low Pressure Exhaust Gas*
MSUI	Motor s unutarnjim izgaranjem
NEDC	Novi europski ispitni ciklus (*engl. New European Driving Cycle*)
OBD	Dijagnostika na vozilu (*engl. On Board Diagnostic*)
PEMS	Prijenosni sustav za mjerenje emisija (*engl. Portable Emissions Measurement System*)

PHEV	Hibridno električno vozilo s mogućnosti napajanja iz električne mreže (*engl. Plug-in Hybrid Electric Vehicle*)
PMEP	Srednji efektivni tlak izmjene radne tvari (*engl. Pumping Mean Effective Pressure*)
PM	Masa čestica (*engl. Particulate Matter*)
PMS	Strategija upravljanja snagom (*engl. Power Management Strategy*)
PN	Broj čestica (*engl. Particulate Number*)
RDE	Emisije u stvarnim uvjetima upotrebe (*engl. Real Driving Emissions*)
SCR	Selektivna katalitička redukcija (*engl. Selective Catalytic Reduction*)
SoC	Stanje napunjenosti baterije (*engl. State of Charge*)
STP	Stanica za tehnički pregled
VCS	Pomak zatvaranja ventila (*engl. Valve Closing Shift*)
VOS	Pomak otvaranja ventila (*engl. Valve Opening Shift*)
VSP	Specifična snaga vozila (*engl. Vehicle Specific Power*)
WLTC	Globalno usklađeni ispitni ciklus za laka vozila (*engl. Worldwide Harmonized Light Vehicles Test Cycle*)

1. UVOD

Doktorski rad izrađen je na temelju skupa od četiri objavljena znanstvena rada [1-4] po skandinavskom modelu. Objavljeni radovi čine zaokruženu znanstveno-istraživačku cjelinu i daju novi znanstveni doprinos u području tehničkih znanosti. U uvodnom dijelu predstavljena je motivacija i hipoteza znanstvenog istraživanja, zatim je opisan postupak istraživanja koji je korišten u potvrdi hipoteze uz elaborirane temeljne znanstvene doprinose rada.

1.1. Motivacija i hipoteza

Stalno povećanje transportnih potreba i težnja čovječanstva za samoodrživosti usmjerava proizvođače vozila prema tehnologijama koje doprinose smanjenju štetnih emisija, posebice ugljikovog dioksida. Pojedine zemlje poput EU-a i nekih dijelova SAD-a najavljuju zabranu prodaje osobnih automobila pogonjenih fosilnim gorivima [5], dok je ova zabrana teško primjenjiva na manje razvijene dijelove svijeta s lošijom infrastrukturom [6]. Dugoročni je cilj EU-a značajno smanjenje emisija stakleničkih plinova u transportu [7], planirano je od 2025. godine smanjiti emisije CO_2 za dodatnih 15 % u odnosu na 2021. za nova putnička vozila i laka komercijalna vozila. Prema [8], na svim razinama hibridizacije udio novoregistriranih HEV-a, ovisno o nivou ambicioznosti redukcije CO_2, trebao bi biti između 29 % i 56 % do 2030. Posljednjih 15 godina brzohodni motori s unutarnjim izgaranjem postigli su vrlo visoku učinkovitost, dizelski postižu vršnu učinkovitost i veću od 40 % [9], ali teško da mogu ispuniti zahtjeve sljedećeg Euro 7 emisijskog propisa [10, 11] kao samostalni pogonski sklop [12]. Osnovni je razlog tome sporo postizanje radne temperature motora i sustava za kontrolu emisija, neučinkovito raspolaganje mehaničkom energijom i veliki pad učinkovitosti kod niskih opterećenja. Pad učinkovitosti povezan je s izostankom rekuperacije mehaničke energije kočenja i radom motora u radnoj točki koja je ograničena trenutnim zahtjevom korisnika. Zbog loše definicije starijih emisijskih propisa proizvođači su trebali osigurati poštivanje graničnih vrijednosti samo u uskom području radnih parametara vozila koja uključuje ispitni ciklus. Posljednjih desetak godina ostvaren je napredak u pogledu stvarnog poštivanja zakonskih graničnih vrijednosti emisija u značajno većem dijelu uvjeta vožnje uvođenjem RDE ispitivanja (*engl. Real Driving Emissions*) kao sastavnog dijela procesa tipskog odobrenja. Daljnji napredak očekuje se u osiguravanju poštivanja graničnih vrijednosti svih emisija u cijelom eksploatacijskom periodu vozila. Pokazalo se da s porastom složenosti pogonskih sustava, osobito sustava kontrole emisija, raste i utjecaj kvarova na povećanje količine emisija. Područje emisija vozila u dugotrajnoj eksploataciji i osobito u slučajevima kvarova sustava njihove kontrole nije dovoljno istraženo. Hibridna električna vozila (HEV) koja kombiniraju prednosti

potpuno električnih vozila (EV) i klasičnih vozila, imaju visok stupanj fleksibilnosti kao i mogućnost ispunjavanja šireg spektra zahtjeva u vožnji, ali isto tako i veću osjetljivost na ranije spomenute kvarove. Neophodni sustavi za regulaciju emisija, koje zahtijevaju najnoviji emisijski propisi, zahtijevaju brzo dostizanje radne temperature kao i periodične regeneracije. Za postizanje navedenih uvjeta ključan je veći broj stupnjeva slobode upravljanja energijom koji omogućuju HEV. Najznačajnija prednost u odnosu na klasična vozila pogonjena samo motorom s unutarnjim izgaranjem (MSUI) je daleko učinkovitije raspolaganje mehaničkom energijom kroz mogućnost uštede energije regenerativnim kočenjem ili spremanjem viška energije kod pomaka radnog područja prema onom s najvišom učinkovitosti MSUI-ja. Prednost je i u korištenju manjih, lakših i jednostavnijih jednorežimskih motora s unutarnjim izgaranjem. Najznačajnija prednost HEV vozila u odnosu na potpuno električna vozila je superioran doseg s jednim punjenjem i brzina dopunjavanja koja se postiže upotrebom kemijske energije goriva umjesto električne [13]. Zbog navedenog, hibridna električna vozila su svakako jedno od ključnih rješenja za povećanje učinkovitosti i smanjenje emisija osobito uz primjenu ekološki prihvatljivih, sintetičkih, CO_2 neutralnih goriva prihvatljive cijene [14] ili alternativnih goriva poput ukapljenog plina sa značajno manjim emisijama i CO_2 otiskom [15] u zemljama u razvoju. Takvi pogonski sustavi svakako će naći svoju primjenu u teškim kamionima za velike udaljenosti, u civilnim vozilima posebnih primjena, terenskim vozilima i vozilima za vojne svrhe [16] u sljedećim razdobljima bez obzira na stupanj elektrifikacije cestovnog prometa. Predviđanje udjela HEV-a u budućnosti je vrlo teško predvidjeti zbog prilično ambicioznih i promjenjivih planova reduciranja CO_2 emisija. Za stvaranje kvalitetnog upravljanja hibridnih vozila, uzimanjem u obzir specifičnosti načina rada motora s unutarnjim izgaranjem, potrebno je dobro poznavanje svih njegovih sustava, a osobito onih koji direktno utječu na emisije ispušnih plinova. Mogućnost izbora različitih radnih parametara motora s unutarnjim izgaranjem u svakom trenutku omogućava kvalitetniji pristup upravljanja sustavima za kontrolu ispušnih emisija i potpuno rješavanje njihovih najvećih problema u eksploataciji [2]. Naznačene su prednosti omogućene zbog visoke složenosti HEV sustava, a koja je i ujedno najveći nedostatak u smislu brojnosti sklopova i pronalaska optimalnog načina upravljanja koji predstavlja jedan od najvećih izazova. Više razine hibridizacije, odnosno potpuna hibridna električna vozila FHEV i hibridna vozila s mogućnosti napajanja iz električne mreže PHEV su još složenije jer dopuštaju veći broj stupnjeva slobode. Osnovne strategije upravljanja energijom su strategije povezane s upravljanjem u stvarnom vremenu, kao i globalna optimizacija koju je teško implementirati u stvarnom vremenu, ali je korisna u procjeni potrošnje goriva i emisija tijekom jednog ciklusa [17]. Unatoč tome što su razvijeni različiti

pristupi modeliranja klasičnih i hibridnih cestovnih vozila, čiji je detaljan pregled dan u drugom poglavlju ovog rada, pronalazak optimalnog rješenja složenih modela i dalje predstavlja veliki problem. Upotreba više izvora energije i visoka kompleksnost sustava pogona HEV zahtijeva složeniji sustav upravljanja na visokoj razini za što su potrebni složeni modeli u korisničkom i računalnom smislu. Modeliranje MSUI-ja u užem smislu kao i modeliranje sustava za kontrolu emisija, njihova nelinearnost, složeni međusobni utjecaji i ovisnost o velikom broju parametara, koji su detaljno elaborirani u objavljenom preglednom znanstvenom radu [2], čine fizikalne i analitičke modele presloženima. Zbog prethodno navedenog vrlo je teško implementirati pojedinačne modele svih komponenti MSUI-ja i svih sustava kontrole emisija kod modeliranja kompletnih hibridnih vozila pri čemu se javlja potreba za alternativnim modelima iz koje proizlaze ciljevi i hipoteza ovog doktorskog rada.

Glavni je cilj doktorskog rada predložiti novi model hibridnog vozila temeljen na modalnoj analizi energije, emisija i potrošnje goriva. Modalni pristup modeliranju podrazumijeva generiranje matrice ili mape koja povezuje izlazne vrijednosti modela, kao što su emisije, potrošnje goriva i potrošnje energije, s rasponima ulaznih varijabli koje opisuju ponašanje vozila. Na taj način se izlazne varijable modela raščlanjuju prema rasponima ili modovima ulaznih varijabli. Ukupne emisije vozila se dobivaju iz produkta određenog obrasca ponašanja i udjela provedenog unutar određenog svakog raspona. Ta bi metoda trebala omogućiti brži i lakši dolazak do unaprijed postavljenog cilja optimizacije HEV-a, ili se može koristiti kao smjernica koja klasični fizikalni model vodi do optimalnog rješenja izbjegavajući lokalne minimume. Također, predloženi model bi trebao zadržati prednosti modalnih emisijskih modela u smislu što manjeg broja unutarnjih varijabli, što mu osigurava upotrebu u grupnim procjenama emisija. Model se temelji na stvarnim emisijama vozila, potrošnji goriva i energije koji su mjereni u stvarnim uvjetima vožnje prema RDE pravilima koja su danas obvezni segment procesa tipskog odobrenja svakog vozila.

Hipoteza znanstvenog istraživanja u doktorskom radu je sljedeća:

- Na temelju modalne analize te definiranog toka energije prema funkciji moguće je formirati inovativni model hibridnog električnog vozila u frekvencijskoj domeni koji povezuje uzdužnu dinamiku vozila i energetske tokove s potrošnjom goriva, učinkovitošću i pojedinačnim emisijama vozila.

1.2. Znanstvene metode i znanstveni doprinos

Cjelokupno znanstveno istraživanje obuhvaćeno doktorskim radom, prikazano Tablicom 1, usmjereno je rješavanju problema zadovoljavanja strogih emisijskih propisa i CO_2 emisija u stvarnim uvjetima upotrebe i u cjeloživotnoj eksploataciji. Istraživanje je rezultiralo objavom šest radova na međunarodnim znanstvenim konferencijama te četiri znanstvena rada u A kategoriji. Radovi [3] i [4] su potvrdili hipotezu, dok su radovi [1] i [2] kao i radovi na međunarodnim znanstvenim konferencijama te kvalifikacijski ispit, pridonijeli razumijevanju i usmjeravanju k potvrdi hipoteze rada. U Tablici 1 podebljanim su tekstom naglašeni zaključci i problemi koji su usmjeravali daljnje istraživanje, a plavom su bojom naglašeni objavljeni rezultati u časopisima A kategorije.

Tablica 1. Prikaz znanstvenog istraživanja.

AKTIVNOST	REZULTATI I ZAKLJUČCI ISTRAŽIVANJA
Pregledom literature utvrđeni su najveći izazovi vozila pokretani motorima s unutarnjim izgaranjem u cestovnom prometu	• **Stroge emisijski propisi i ograničenja CO_2 emisija u stvarnim uvjetima upotrebe i u eksploataciji do kraja radnog vijeka**
	• **Povećanje učinkovitosti ključnih komponenti vozila pojedinačno** • **Razumijevanje rada sustava za kontrolu emisija i detekcija najvećih izazova** • **Analiza ponašanja sustava kontrole emisija u stvarnim uvjetima eksploatacije** • **Povećanje učinkovitosti raspolaganja energijom kompletnog vozila – HEV, veliki problem predstavljaju složeni načini predviđanja emisija**
Povećanje učinkovitosti ključnih komponenti vozila pojedinačno	• Najveći potencijal je utjecaj na učinkovitost motora s unutarnjim izgaranjem • Primjena CFD 1D/QD modela u testiranju koncepta smanjenja gubitaka izmjene radne tvari benzinskog atmosferskog motora s direktnim ubrizgavanjem goriva u cilindar • **Rezultati pokazuju porast učinkovitosti kod niskih opterećenja na razini Atkinson i Miller ciklusa koji su već u širokoj upotrebi;** mogućnost ispitivanja na prednabijanim motorima; **CFD modeli nisu prikladni kao komponente modela kompletnog vozila**
Razumijevanje rada sustava za kontrolu emisija, njihovo poboljšanje i utjecajni parametri	• Istraživanje utjecajnih čimbenika na emisije i na učinkovitost sustava za njihovu kontrolu • Izrada preglednog rada o svim komercijalno dostupnim sustavima za kontrolu emisija • Nužnost sustavnog pristupa koji razmatra zajednički učinak svih podsustava vozila. Dane su smjernice dostizanja emisijskih propisa i konceptualna usporedba mogućih kombinacija različitih sustava s aspekta kontrole emisija, potrošnje goriva, održavanja, veličine i cijene izvedbe • **Potreba za istraživanjem utjecaja kvara pojedinih sustava na količine emisija u stvarnim uvjetima upotrebe.**

	• **Teško ostvarivi ciljevi sljedećih propisa bez upotrebe hibridnih pogonskih sustava** • **Vrlo složeni fizikalno-empirijski modeli sustava kontrole emisija**
Analiza ponašanja sustava kontrole emisija u stvarnim uvjetima eksploatacije Predstavljanje modalnog modela HEV-a na osnovi modalnih emisija.	• Istraživanje utjecaja zakazivanja komponenti za kontrolu emisija na njihovu količinu • Eksperimentalno istraživanje količine emisija u stvarnim uvjetima upotrebe na vozilima s ispravnim i neispravnim sustavima za kontrolu emisija • Količine NO_X emisija iznad važećeg praga kod novijih vozila, višestruko povećanje svih emisija osim CO_2 u slučajevima kvarova komponenti. CO emisije kod dizelskih vozila ispod zakonskog praga i u slučaju kvara oksidacijskog katalizatora. • Prijedlog načina kontrole uređaja za kontrolu emisija u sklopu redovnih TP bez investicija u novu opremu. • Na osnovi izmjerenih podataka predstavljen modalni model klasičnog i HEV te predstavljen maksimalni potencijal učinaka hibridizacije ispitivanog vozila
Validacija novog modela HEV-a	• Određivanje performansi i upotrebljivosti novog modalnog modela • Izrada novog modela klasičnog i HEV na osnovi eksperimentalnih podataka te izrada kontrolnog fizikalnog modela klasičnog i HEV te njihova usporedba • Novi model HEV pokazuje znatno bolje rezultate u usporedbi s modalnim modelima HEV obrađenih u literaturi
Procjena emisija HEV-a pomoću kontinuirane raspodjele vjerojatnosti	• Analitička formulacija primjene kontinuirane raspodjele vjerojatnosti u izradi modalnih emisijskih modela • Primjena modela na općeniti model HEV-a

Metode i tijek istraživanja po fazama prikazani su na slici 1. Pregledom literature utvrđeno je da su dugoročni planovi smanjenja emisija CO_2 i nadolazećih emisijskih propisa najveći izazov opstanka MSUI-ja u cestovnim vozilima. U prvom koraku istraživanja primijenjen je numerički model motora sa svrhom ispitivanju koncepta povećanja ukupne učinkovitosti benzinskog MSUI-ja kroz povećanje učinkovitosti izmjene radne tvari. Potvrđena je hipoteza o značajnom povećanju učinkovitosti primjenom novog koncepta, ali bez značajnih prednosti u odnosu na metode koje su već u komercijalnoj upotrebi. Istraživanje je pokazalo da je visoka razina složenosti CFD modele MSUI-ja čini neprikladnima u modeliranju vozila, čime je istraživanje usmjereno prema jednostavnijim emisijskim modelima vozila. Druga faza istraživanja je inicirana problemima količina emisija i potrošnje goriva u stvarnim uvjetima upotrebe, odnosno problemima u eksploataciji i problemima njihova predviđanja. Napravljen je pregled literature iz područja formiranja emisija i sustava kontrole emisija s naglaskom na sustave najproblematičnijih emisija dizelskih vozila u svrhu razumijevanja njihova ponašanja kod izrade modela i u eksploataciji. Istraživanje upućuje na vrlo složena ponašanja sustava kontrole emisija u uvjetima stvarne eksploatacije i gotovo nemoguće zadovoljavanje graničnih

vrijednosti sljedećih emisijskih propisa bez upotrebe hibridnih pogonskih sustava. Treća faza istraživanja uključuje eksperimentalna mjerenja emisija i ključnih parametara vozila te njihovu obradu. Osnovna je svrha analiza problema emisija u trajnoj eksploataciji i prijedlog izrade modalnih emisijskih modela klasičnih i hibridnih vozila. Četvrta faza istraživanja se isključivo odnosi na validaciju predloženih modela i načine njihova daljnjeg poboljšanja što je ključni dio hipoteze ovog rada. Ovaj dio istraživanja je detaljnije objašnjen u daljnjem izlaganju.
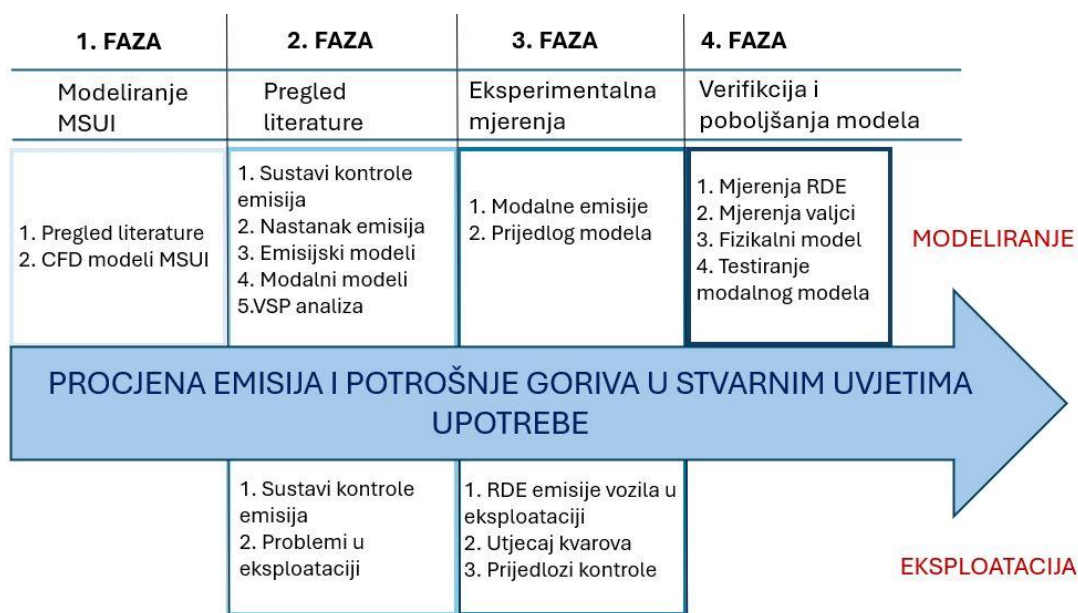
Slika 1. Metode i faze istraživanja.

U svrhu potvrđivanja postavljene hipoteze izrađen je novi model vozila temeljen na modalnoj analizi, izvršeno je vrednovanje modela određivanjem odstupanja od stvarnih vrijednosti u različitim ciklusima vožnje. Najrelevantniji postupak bila bi usporedba rezultata s rezultatima mjerenja stvarnog hibridnog električnog vozila u različitim ciklusima vožnje. Osnovni je nedostatak ovakvog postupka visoka cijena opreme i same provedbe mjerenja. Zbog navedenog je primijenjen alternativni i znatno složeniji postupak koji je shematski prikazan na slici 2., prema kojem je provedena usporedba s klasičnim modelom hibridnog električnog vozila razvijenom u AVL-ovom programskom paketu CruiseM. S obzirom na tok energije i informacija, CruiseM model je formiran kao unapredni (*engl. Forward*) kvazistatički model. Pojedini sklopovi opisani su karakterističnim fizikalnim veličinama dok se procjena emisija i potrošnje goriva zasniva na pripadajućim mapama. Mape potrošnje goriva i emisija definirane su u ovisnosti o statičkim radnim točkama motora s unutarnjim izgaranjem i dobivene su mjerenjem na mjernim valjcima u laboratorijskim uvjetima.

Modalni model je formiran kao unatražni (*engl. Backward*) kinematički model prema analizi rezultata mjerenja potrošnje goriva, emisija i trenutne snage u stvarnim uvjetima vožnje u skladu s RDE procedurom. U istim uvjetima verificiran je i klasičan CruiseM model. Model je formiran diskretnom analizom učestalosti izmjerenih emisija i potrošnje goriva unutar određenih raspona pogonske snage. Polazna je pretpostavka da su odnosi količina pojedinačnih emisija prema jediničnoj pogonskoj energiji približno jednaki unutar promatranog raspona snage, bez obzira na vozni ciklus. To znači da su vrijednosti pojedinačnih specifičnih emisija ili potrošnje goriva po jedinici mehaničke energije j-tog razreda jednake omjeru ukupne količine emisija ili potrošnje goriva razreda i njegove ukupne energije. Razred snage podrazumijeva promatrano područje raspona snage između njene, unaprijed definirane, minimalne i maksimalne vrijednosti. Za svaki ispitni ciklus vožnje moguće je odrediti učestalost pojave svakog razreda snage i njegovu potrebnu pogonsku energiju, a time i količinu emisija i potrošnju goriva.
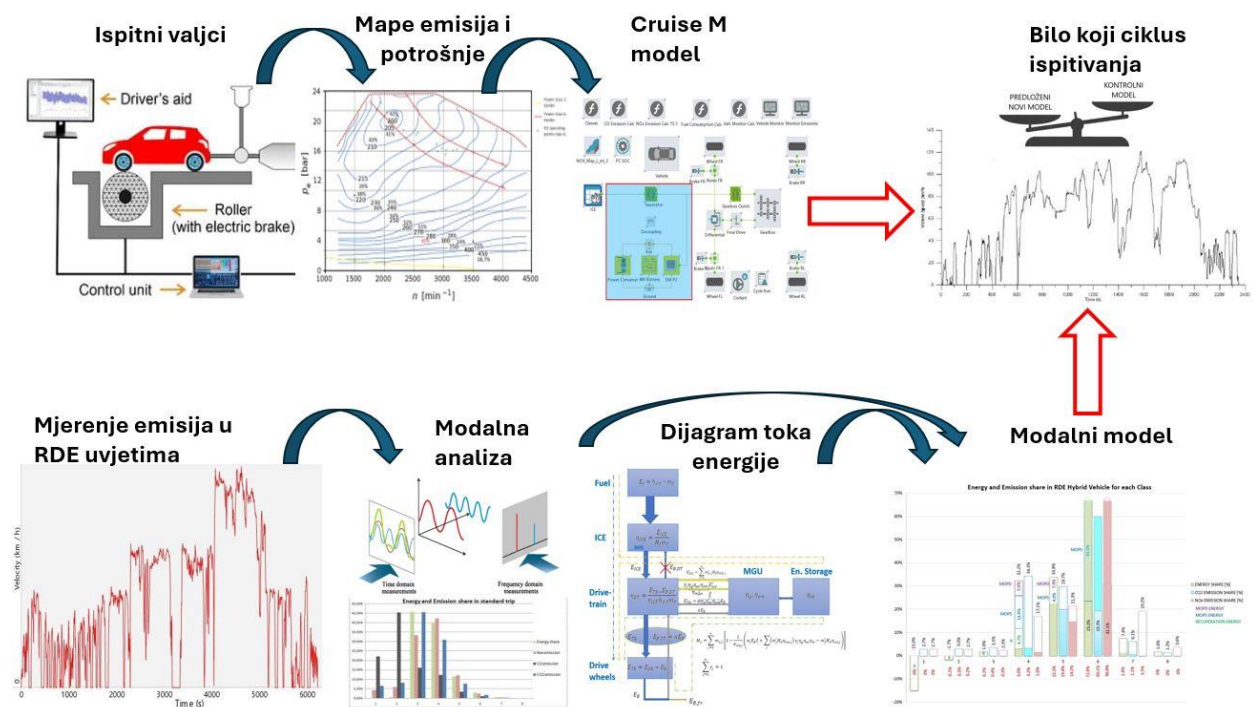
Slika 2. Proces izrade i vrednovanja modela.

Oba su modela, pod istim uvjetima s istim komponentama hibridizirana u paralelno hibridno električno vozilo, složeni CruiseM fizikalni kontrolni model i novi modalni model. Budući da klasična, nehibridna, vozila imaju samo jedan stupanj slobode, relativno je jednostavno model primijeniti na pojedini ciklus, dok je za hibridna vozila potrebno definirati strategiju upravljanja

na najvišoj razini. Zbog jednostavnosti implementacije i kasnije usporedbe rezultata odabrana je strategija upravljanja energijom temeljena na pravilima jer se kao takva može upotrijebiti na oba modela. Budući da je CruiseM model daleko složeniji po broju varijabli i parametara, primijenjena strategija upravljanja prilagođena je njegovim postavkama dok novorazvijeni modalni model oponaša tu strategiju. Na kraju su uspoređeni dobiveni rezultati oba modela, novorazvijeni VSP (*engl. Vehicle Specific Power*) modalni model s CruiseM modelom na klasičnom i hibridnom vozilu u realnim uvjetima upotrebe RDE te u NEDC i WLTC ciklusima.

Izvorni znanstveni doprinosi ovog doktorskog rada su sljedeći:

- Razvoj i vrednovanje novog modela klasičnog i hibridnog električnog vozila temeljenog na modalnim emisijama koji obuhvaća procjenu potrošnje goriva, emisija, potrebne snage pogonskih komponenti i potrebne energije.

- Procjena emisija i potrošnje goriva vozila primjenom globalne strategije upravljanja energijom temeljene na pravilima na predloženom modelu hibridnog električnog vozila u različitim ciklusima vožnje.

- Procjena utjecaja stvarnih uvjeta upotrebe i trajne eksploatacije vozila na emisije i ponašanje sustava kontrole emisija.

1.3. Objavljeni radovi na kojima se temelji doprinos

Doktorski rad predstavlja osnovu i pregled četiri objavljena znanstvena rada na kojima se temelji doprinos zajedno sa zaključcima koji iz njih proizlaze. Objavljeni znanstveni radovi na kojima se temelji doprinos disertacije su sljedeći:

[1] A. Kozina, G. Radica, S. Nižetić, "Increasing engine efficiency at part load with the exhaust valve control: A simplified modelling approach", *International journal of exergy, 26 (2018), 1/2; 131-152 doi:10.1504/IJEX.2018.092510*

[2] A. Kozina, G. Radica, S. Nižetić, "Analysis of methods towards reduction of harmful pollutants from Diesel engines ", *Journal of cleaner production, 262 (2020), 1-20 doi: 10.1016/j.jclepro.2020.121105*

[3] A. Kozina, G. Radica, S. Nižetić, "Emission analysis of Diesel Vehicles in circumstances of emission regulation system failure: A case study", *Journal of energy resources technology, 144 (2021), 8; 082307, 13 doi:10.1115/1.4053070*

[4] A. Kozina, T. Vidović, G. Radica, A. Vučetić, "A New Vehicle-Specific Power Model for the Estimation of Hybrid Vehicle Emissions", *Energies 2023, 16, 8094.* *https://doi.org/10.3390/en16248094*

1.4.   Pregled organizacije disertacije

Motivacija i hipoteze istraživanja predstavljeni su u uvodnom dijelu doktorskog rada. Predstavljene su metode istraživanja i izvorni znanstveni doprinosi, dok je na kraju uvodnog poglavlja dan popis objavljenih znanstvenih radova na kojima se temelji doprinos disertacije. Drugo poglavlje obuhvaća pregled postojećeg eksperimentalnog i analitičkog istraživanja iz područja sustava kontrole emisija, modeliranja emisija, modeliranja klasičnih i hibridnih vozila, upotrebe modalne analize u emisijskim modelima klasičnih i hibridnih vozila i dijagrame toka energije. Objavljeni pregledni rad na kojem se temelji dio ukupnog doprinosa također je dio poglavlja u kojima su analizirana dosadašnja istraživanja. Poglavlje završava zaključkom kako je nedovoljno istraženo područje emisija i emisijskih modela klasičnih i hibridnih vozila, s obzirom na postojeće znanstvene spoznaje. U trećem poglavlju dan je detaljan osvrt na eksperimentalna istraživanja doktoranda. U četvrtom poglavlju dan je pregled objavljenih radova na kojima se temelji doprinos s istaknutim pojedinačnim doprinosima, kao i s doprinosima doktoranda na svakom od radova. Peto poglavlje daje zaključke doktorskog rada te smjerove budućih istraživanja. Priložena je korištena literatura u istraživanju i na kraju su priloženi znanstveni radovi na kojima se temelji doprinos disertacije.

2. PREGLED DOSADAŠNJIH ISTRAŽIVANJA IZ PODRUČJA RADA

Modeliranje cjelokupnog vozila zahtjevan je proces kojim se obuhvaća široko područje istraživanja s nekoliko ključnih elemenata. Najsloženiji dio modela vozila je model motora s unutarnjim izgaranjem u širem smislu kao i njegovi emisijski modeli. Emisijski modeli i modeli potrošnje goriva vozila uvjetovani su složenim predviđanjem s jedne strane i ograničenim brojem varijabli koja im ograničava širinu upotrebe s druge strane. Zbog izrazite prednosti u vidu količine varijabli i jednostavnosti primjene, modalni emisijski modeli vozila vrlo se često koriste u pojedinačnim i grupnim procjenama emisija i potrošnje goriva vozila. Najveći je nedostatak ove grupe modela ograničena točnost, osobito kod novijih generacija pogonskih sustava koji uključuju sustave kontrole emisija osjetljive na dinamiku vožnje i hibridne pogonske sustave s visokim razinama hibridizacije. Kod hibridnih vozila zbog specifičnosti rada motora s unutarnjim izgaranjem i pogonskih elemenata sekundarnog izvora energije formiranje modela se dodatno komplicira, te uvjetuje uvođenje tokova energije unutar modela. Iz prethodno navedenog pregledno poglavlje, osim šireg područja modeliranja emisija i potrošnje goriva klasičnih i hibridnih vozila, obuhvaća modalne emisije, obuhvaća poglavlje o nastanku emisija i sustavima za njihovu kontrolu te dijagrame toka energije HEV-a.

2.1. Emisije, modeli emisija i sustavi za njihovu regulaciju

Kako bi se ispunili zahtjevi novijih emisijskih propisa i istovremeno povećala učinkovitost motora, motori s unutarnjim izgaranjem postaju sve složeniji sa sve većim brojem upravljačkih sustava i sustava za kontrolu emisija. U preglednom radu [2] analizirane su različite metode i sustavi kontrole emisije motora s unutarnjim izgaranjem, posebice tehnike recirkulacije ispušnih plinova koje reguliraju emisije tijekom njihovog stvaranja, kao i tehnike naknadne obrade ispušnih plinova pomoću različitih vrsta katalitičkih pretvarača i filtriranje čestica. Također se objašnjavaju problemi odstupanja od postojećih emisijskih propisa i načini njihova ispunjavanja. Analizirani su mehanizmi nastanka pojedinih emisija i njihova povezanost s parametrima rada motora. Objašnjeni su problemi koji su se javljali pri korištenju pojedinih metoda za smanjenje emisija u specifičnim radnim uvjetima motora. Istražen je utjecaj sustava

za kontrolu emisija na parametre rada motora, njegovu trajnost kao i na potrošnju goriva odnosno emisija CO_2.

Idealnim izgaranjem 1 kg dizelskog goriva nastaje približno 3,1 kg CO_2 i 1,3 kg vodene pare uz oslobađanje topline. Osim vode i ugljikovog dioksida, tijekom izgaranja goriva u motoru nastaje i oko 1 % štetnih tvari u obliku plinova i sitnih čestica od kojih najznačajniji količinski utjecaj na zdravlje ljudi imaju različiti oksidi dušika, NO_X, sitne čestice, PM, ugljikov monoksid, CO, neizgorjeli ugljikovodici, HC i sumporov dioksid, SO_2. Približne volumne udjele produkata izgaranja prikazuje slika 3.
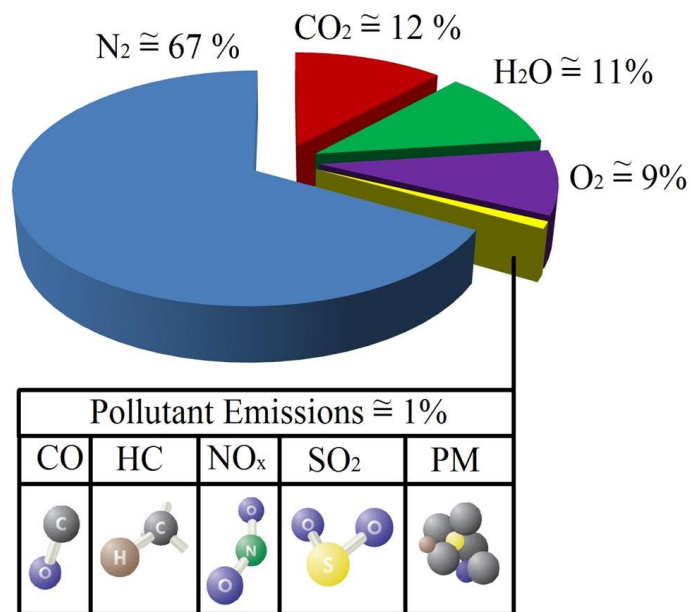
Slika 3. Prosječni sastav ispušnih plinova dizelskog motora [18].

Mehanizam nastajanja **emisija NOx-a** je gotovo isključivo vezan za temperaturu izgaranja, pretičak kisika i vrijeme trajanja visokih temperatura izgaranja (> 1600 °C) [19], čiji su trendovi prikazani dijagramom na slici 4.
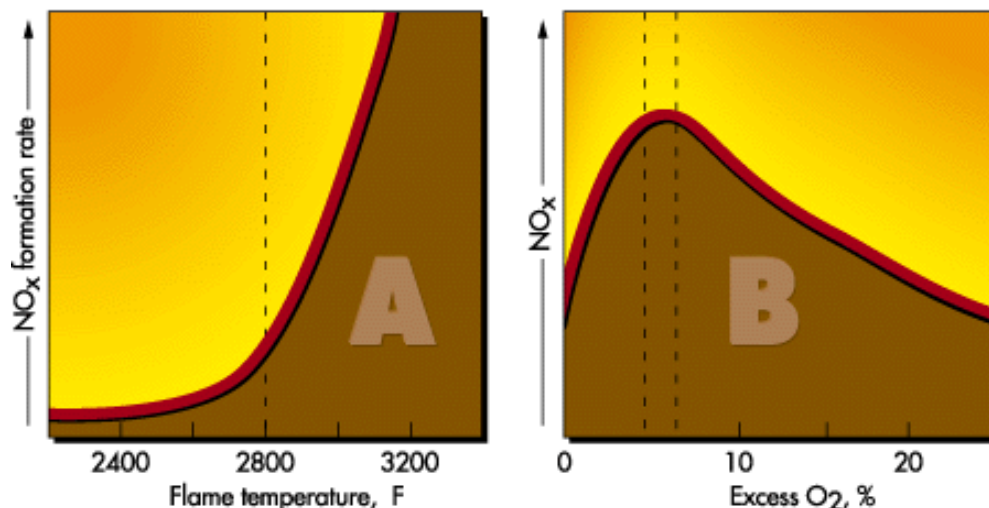
Slika 4. Formiranje NO$_X$ emisija u ovisnosti o temperaturi izgaranja i pretičku kisika [20].

Definirana su četiri mehanizma nastajanja NO$_X$ [21]: „prompt" mehanizam, termalni mehanizam, stvaranje NO$_X$ preko N$_2$O i stvaranje NO$_X$ iz dušika korištenog kao gorivo. U dizelskim motorima stvaranje NO primarno se odvija termalnim mehanizmom na koji se odnosi većina korištenih modela. Čisti empirijski modeli temelje se na korelaciji između operativnih parametara motora kao što su temperatura i tlak u cilindru na emisije NO$_X$-a. Empirijski NO$_X$ modeli valjani su samo za uski raspon operativnih uvjeta i ne mogu predvidjeti vrijednosti izvan kalibracijskog raspona. U analitičkim modelima uzima se u obzir kemijski mehanizam stvaranja NO$_X$-a. Ovi modeli predviđaju NO$_X$ u širem rasponu operativnih uvjeta za različite tipove/konfiguracije motora. Analitički modeli najčešće se koriste u kombinaciji s dvozonskim ili višezonskim modelima izgaranja, pretpostavljajući jednolik tlak u cilindru. Svaka zona tretira se kao jedan termodinamički sustav s određenom temperaturom i sastavom plinova. Koncentracija pojedine komponente izračunava se koristeći detaljan kemijski mehanizam. Ovaj model koristi tzv. prošireni Zeldovichev mehanizam [22] za stvaranje NO koji je dominantan nad ostalim oksidima dušika. Osim empirijskih i analitičkih modela postoje i statistički modeli koji koriste direktno usrednjene podatke mjerene u prometu [23] ili te iste podatke koriste za treniranje različitih neuralnih mreža [24].

Čestice čađe nastaju zbog nepotpunog izgaranja goriva, tako veće emisije čađe upućuju na neadekvatno izgaranje i lošu učinkovitost [25]. Čestice čađe uglavnom su sastavom čisti ugljik, s nekim organskim spojevima adsorbiranim na njihovim površinama, poput aromatskih spojeva i neizgorenih ugljikovodika [26]. Promjer čestica kreće se od 15 do 30 nm pri temperaturi ispuha većoj od 500 °C. Ispod 500 °C ugljikovodici velike molekulske mase se adsorbiraju na česticama, uzrokujući povećanje njihove veličine [27]. Na formiranje čađe utječu tlak,

temperatura i pretičak zraka, u dizelskim motorima se ono događa u temperaturnom rasponu od 1000 do 2800 K i tlakovima od 50 do 100 bar, s dovoljno zraka za cjelovito izgaranje goriva [28]. Formiranje čađe u osnovi je složen proces prijelaza iz plinovite u čvrstu fazu, koji se završava u nekoliko milisekundi. Sastav goriva i nečistoće također utječu na formiranje čađe u motorima s kompresijskim paljenjem. Ako gorivo sadrži značajniju količinu sumpora on povećava masu čestica tako što oksidira u SO_2 koji se apsorbira na susjednim česticama čađe i reagira s ugljikovodicima [29]. Povećanje omjera ugljika prema vodiku u gorivu dovodi do većeg broja čestica čađe, a smanjuje se s porastom udjela kisika u gorivu [30]. Generiranje vrtloga povećava turbulenciju u komori izgaranja i ubrzava brzinu izgaranja što rezultira smanjenjem količine čestica čađe. Ranije ubrizgavanje smanjuje formiranje čađe, dok zakašnjelo povećava [31]. Veće količine čestica nastaju pri nagloj promjeni opterećenja motora, odnosno u dinamičnim uvjetima vožnje. Metoda višestrukog ubrizgavanja učinkovita je u ograničavanju formiranja čađe [32] jer vremenski razmak između dva ubrizgavanja omogućuje ulazak svježeg zraka u mlaz spreja, povećavajući lokalni pretičak zraka.

Hiroyasu je dao jednostavnu formulaciju za izračunavanje brzine formiranja mase čađe koja se dobije razlikom između brzine formiranja i brzine oksidacije čađe tijekom izgaranja [33]. Nagle, Strickland i Constable proširili su Hiroyasuov model tako da su u oksidaciji čađe uzeti u obzir raspored i lokacija ugljikovih atoma na površini čestica čađe. Mjesta su podijeljena na reaktivnija mjesta i manje reaktivna mjesta. Kako temperatura raste, manje reaktivna mjesta prelaze u reaktivnija mjesta; empirijske jednadžbe dane su u [34]. Ovi empirijski modeli ne uzimaju u obzir detaljne informacije o mehanizmu formiranja čađe i neovisni su o vrsti goriva, također fronta predviđena ovim modelom ne slaže se sa strukturom plamena u blizini mlaznice [35]. Stoga, detaljne informacije o formiranju predviđene čađe znaju odstupati od mjerenih rezultata. Navedeni su modeli vrlo popularni u akademskoj zajednici zbog jednostavnosti implementacije u već postojeća programska rješenja.

Emisije ugljikova monoksida iz motora s unutarnjim izgaranjem kontroliraju se prvenstveno omjerom zraka i goriva [36]. Kod bogate smjese koncentracije CO u ispušnim plinovima kontinuirano rastu s opadanjem omjera zraka i goriva, odnosno kako se povećava količina viška goriva. Za smjese siromašne gorivom koncentracije CO u ispušnim plinovima malo variraju i niske su, reda veličine promila molarnog udjela. Budući da benzinski motori često rade blizu stehiometrijskog omjera, pri djelomičnom opterećenju, a ovisno o modelu mogu koristiti bogatu smjesu pri visokim opterećenjima; emisije CO su značajne i potrebno ih je kontrolirati. Također, zbog potrebe za obogaćivanjem smjese kada je motor hladan, emisije

CO tijekom zagrijavanja motora u pravilu su značajno veće nego emisije u potpuno zagrijanom stanju. Tijekom prijelaznih opterećenja motora i tijekom ubrzanja i usporavanja kontrola doziranja goriva ključna je u količini CO emisija. Tako da količina CO emisija tijekom dinamičnih uvjeta vožnje može biti značajno veća nego kod stacionarnog opterećenja. S druge strane, dizelski motori uvijek rade s velikim viškom zraka te posljedično emisije CO iz dizelskih motora su relativno niske. Razine CO opažene u ispušnim plinovima benzinskih motora niže su od maksimalnih vrijednosti izmjerenih unutar komore za izgaranje, ali su značajno više od ravnotežnih vrijednosti. Na temelju toga može se zaključiti da su procesi koji upravljaju razinama CO u ispušnim plinovima kinetički kontrolirani [37]. Modeli predviđanja CO temelje se na analitičkom opisu brzina reakcije CO s hidroksilnim radikalom OH i brzine oksidacije CO s okolnim kisikom. Budući da se najveća koncentracija CO emisija (80-90 %) u odnosu na cijeli ciklus ispušta prilikom hladnog starta, razvijeni su mnogi specijalizirani modeli koji razmatraju emisije upravo u tom području. U [38] predstavljen je detaljan fizikalni model katalizatora koji se sastoji od 13 kemijskih reakcija i 9 reakcija za pohranu kisika. U [39] razmatra se kemijska pretvorba ugljikovog monoksida i neizgorjelih ugljikovodika u procesu oksidacije uz detaljno modeliranje prijenosa topline koji su ključni kod procjene učinkovitosti katalizatora.

U benzinskim motorima **neizgorjeli ugljikovodici, HC** mogu imati različite načine formacija te je stoga vrlo teško pružiti cjelovit opis njihova procesa nastajanja, pogotovo u 1D ili kvazidimenzionalnim uvjetima. Ipak, postoje fenomenološki modeli koji uzimaju u obzir glavne mehanizme nastajanja i predviđaju trendove nastanka ugljikovodika kao funkciju radnih parametara motora. Prema [40] glavni su izvori neizgorjelih ugljikovodika sljedeći:

1. Dio smjese ulazi u mikropraznine unutar cilindra i ne izgara u potpunosti.

2. Pare goriva apsorbiraju se u sloj ulja i talože na stijenkama cilindra tijekom usisa i kompresije. Sljedeća desorpcija događa se kada tlak u cilindru padne tijekom ekspanzije, što onemogućava potpuno izgaranje.

3. U blizini stijenke cilindra plamena se fronta prijevremeno gasi zbog gubitka topline na stijenkama, ostavljajući tanak sloj neizgorene mješavine goriva i zraka.

4. Izravan protok pare goriva u ispušni sustav tijekom preklapanja ventila.

Prva dva mehanizma smatraju se najvažnijima i trebaju biti uzeti u obzir u termodinamičkim modelima. Kako su opisani učinci vezani za samu geometriju komore izgaranja, ne mogu se

fizikalno opisati u kvazidimenzionalnom pristupu, ali se mogu uključiti usvajanjem prilagodljivih poluempirijskih korelacija.

U daljnjem su razmatranju naglašeni samo osnovni principi djelovanja i uži problemi vezani za daljnje istraživanje modeliranja, utjecaja na emisije u različitim uvjetima upotrebe i utjecaja kvara sustava, dok je u preglednom radu [2] obrađeno široko područje regulacije emisija. Generalno sustave kontrole emisija možemo podijeliti na one koji djeluju u mjestu nastanka, kao recirkulacija ispušnih plinova, i one koji djeluju na postojeće emisije, kao što su katalitički pretvarači i filtri čestica.

Recirkulacija ispušnih plinova (*engl. Exhaust Gas Recirculation*, *EGR*) je najčešća tehnologija za smanjenje emisije NO_X u motorima s unutarnjim izgaranjem. Recirkulirani plinovi smanjuju vršne temperature izgaranja unutar komore za izgaranje potrebne za stvaranje NO_X emisija [41]. Niže vršne temperature izgaranja posljedica su usporavanja izgaranja i većeg toplinskog kapaciteta ispušnih plinova u odnosu na svježi zrak koji zamjenjuju. Osim pozitivnog utjecaja na NO_X emisije, EGR negativno utječe i na PM, CO i HC emisije ovisno o udjelu, kako je prikazano na slici 5.
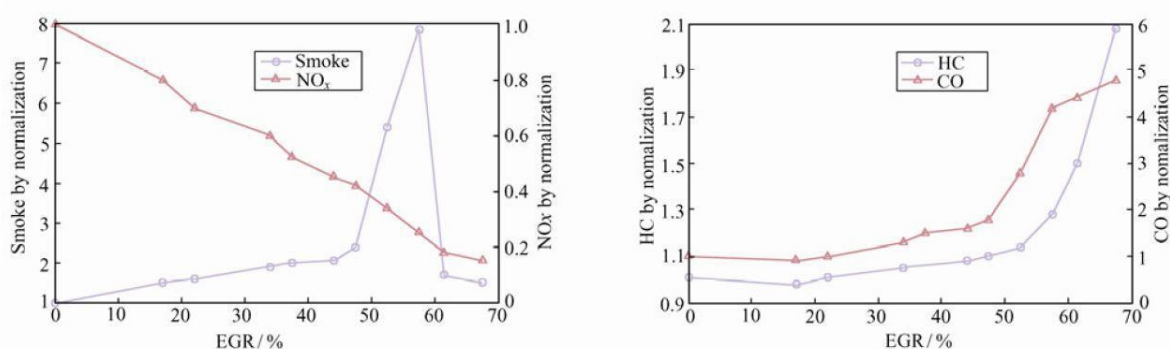
Slika 5. Utjecaj EGR-a na NO_X, PM, HC i CO emisije [42].

EGR tehnologija se osim u svrhu smanjenja NO_X emisija, kod benzinskih motora, koristi za smanjenje gubitaka usisa i smanjenje vjerojatnosti nastanka detonantnog izgaranja. Učinak EGR-a se najčešće izvodi povratom iz ispušnog kolektora kao visokotlačni HP-EGR, povratom plinova nizstrujno od turbopunjača kao niskotlačni LP-EGR ili interno unutar same komore izgaranja prikladnim odabirom preklapanja ventila. Prema [43] porast količine visokotlačnog HP-EGR-a pomiče radnu točku turbopunjača prema nižoj učinkovitosti sa smanjenim protokom zraka uz smanjenje brzine turbopunjača i povećanje vremena odziva na promjenu opterećenja. Utjecaj ovisi o karakteristikama cjelovitog ispitivanog sustava, o tipu recirkulacije i o trenutnoj količini recirkuliranih plinova. U [43] je pokazana ovisnost vremena odziva s 2 bar na 9 bar srednjeg

efektivnog tlaka o količini recirkuliranih plinova koja je povezana s odgovarajućim emisijskim propisom, slika 6.
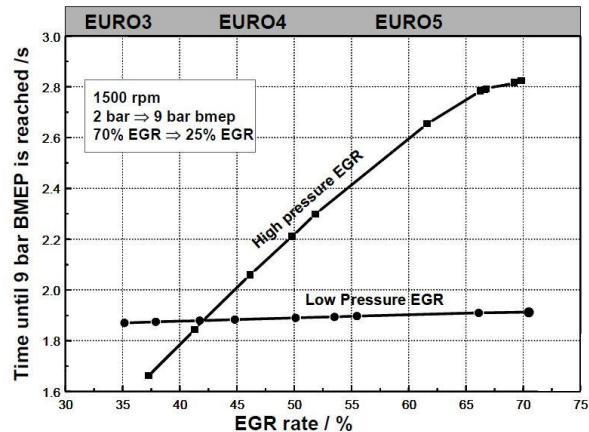
Slika 6. Odziv motora kod različitih euro propisa za HP i LP EGR [43].

Tijekom vremena odziva kao i kod visokih opterećenja EGR se u pravilu potpuno zatvara što uzrokuje značajno povećanje emisija u dinamičkim uvjetima vožnje. Povećanje omjera LP/HP EGR ima pozitivan učinak na vrijeme odziva motora pri niskom i dinamičkom opterećenju [44, 45], što je posebno bitno u cestovnim vozilima. Najveći je nedostatak HP-EGR sustava korištenje nepročišćenih ispušnih plinova zbog čega je većina kvarova uzrokovana taloženjem čađe koja se nakuplja u EGR ventilu, hladnjacima i usisnom kolektoru.

Katalizator trostrukog djelovanja je najčešće korišteni sustav za kontrolu emisija, njegova je najveća prednost što se oksidacija ugljikovog monoksida, oksidacija ugljikovodika i redukcija dušikovog oksida odvijaju istovremeno. Ima visoku učinkovitost u uskom području omjera zrak/gorivo (*engl. Air to Fuel Ratio*, AFR) i pri visokim radnim temperaturama [46]. Utjecaj omjera zraka i goriva na učinkovitost prikazana je dijagramom na slici 7.
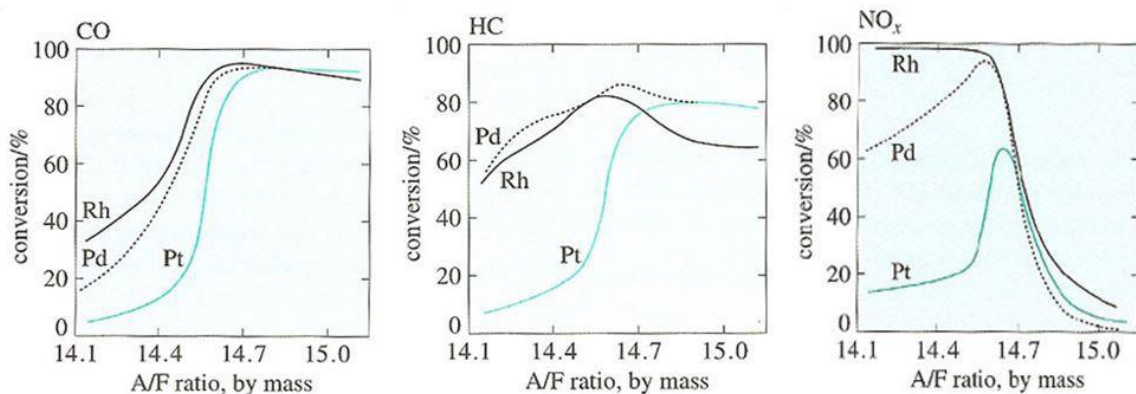
Slika 7. Učinkovitost različitih katalizatora na redukciju CO, HC i NOx u funkciji AFR-a[42].

U području siromašne smjese potpuno izostaje redukcija NO_X-a tako da nisu pogodni za dizelske i benzinske motore sa slojevitim ubrizgavanjem koji u svrhu eliminacije NO_X koriste selektivnu katalitičku redukciju, katalizatore u uvjetima siromašne smjese i njihove kombinacije.

Katalizator dušikovih oksida u uvjetima siromašne smjese (*engl. Lean NO$_X$ Trap, LNT*) sastoji se od oksidacijskog katalizatora, adsorbera za privremeno skladištenje NO_2 u uvjetima siromašne smjese i redukcijskog katalizatora [46]. Jedan od nedostataka je faza regeneracije koja se odvija u obogaćenoj smjesi i koja traje oko 2 do 5 sekundi u intervalima od 1 do 3 minute, što uzrokuje povećanje potrošnje goriva do 10 % [47]. Na učinkovitost pretvorbe utječe vrijeme provedeno u režimu siromašne smjese, vrijeme provedeno u režimu obogaćene smjese i radna temperatura [48]. Na slici 8. prikazan je utjecaj radnih režima i radnih temperatura na učinkovitost komercijalnog LNT katalizatora.
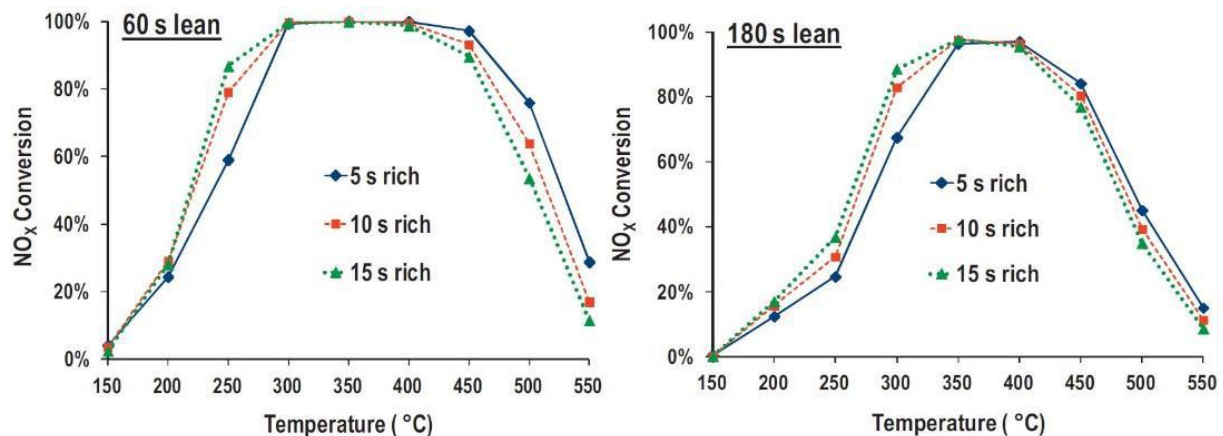
Slika 8. Stupanj učinkovitosti NO$_X$ u LNT za period od 60 s i 180 s [47].

Toplinsko starenje i kontaminacija sumporom dva su glavna čimbenika koji dovode do pada performansi LNT katalizatora. Nakon kontaminacije sumporom potrebno je provesti proces desulfatizacije jedinice za skladištenje NO_X-a. Potpuna desulfatizacija zahtijeva znatno više temperature od normalnih radnih temperatura, iznad 650 °C u bogatoj smjesi, gdje se javlja problem termičkog starenja kojem je ovaj katalizator sklon. Unatoč nedostacima u vidu povećanja potrošnje goriva, osjetljivosti na nečistoće i podložnosti toplinskom starenju, buduća primjena LNT katalizatora zajamčena je nižom cijenom i manjim potrebnim prostorom za smještaj od ostalih sustava za redukciju NO_X-a u siromašnom režimu rada.

Selektivna katalitička redukcija (*engl. Selective Catalytic Reduction, SCR*) kombinira aktivnu kontrolu i katalizator koji reducira NO_X emisije dodavanjem vanjskog redukcijskog reagensa, koji je obično tekućina na bazi uree. Sastoji se od mješavine deionizirane vode i čiste

uree s udjelom od 32,5 % [49]. SCR katalizator postiže stopu pretvorbe NO_X između 80 i 95 % u normalnim uvjetima korištenja [50] i pokazuje visoku stabilnost u dugotrajnom radu [51], zbog čega ova tehnologija postavlja standarde u redukciji emisija NO_X u uvjetima rada motora sa siromašnom smjesom. Glavni su nedostaci SCR tehnologije visoka radna učinkovitost u uskim temperaturnim područjima jer učinkovito rade na temperaturama iznad 190 °C, veliki dodatni prostor koji zauzimaju sve komponente ovog katalizatora i dodatna tekućina koju treba dopunjavati [52]. Dijagram na slici 9. pokazuje vrlo visoku učinkovitost i jaku osjetljivost različitih SCR katalizatora na temperaturu, posebno u području niskih temperatura.
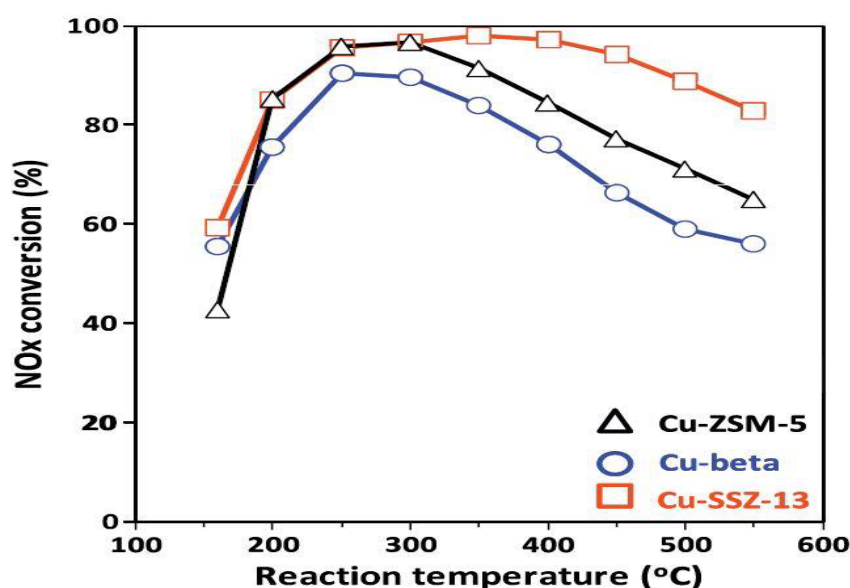
Slika 9. Temperaturna ovisnost redukcije NO_X za različite katalitičke materijale [53].

Jak utjecaj na povećanje učinkovitosti redukcije NO_X-a pri niskim temperaturama SCR katalizatora ima omjer NO_2/NO, slika 10. Pri 200 °C i 10 ppm NH_3, SCR s čistim NO ima učinkovitost od 21 % i s omjerom 1:1, njegova se učinkovitost pretvorbe povećava do 93 % [54]. Uobičajeni ukupni udio NO_2 u dušikovim oksidima dizelskih ispušnih plinova je samo 5 -10 %. Taj se udio povećava korištenjem visokokvalitetnog platinastog oksidacijskog katalizatora koji je postavljen uzstrujno, ali ne rješava u potpunosti problem niskotemperaturne pretvorbe budući da su mu također potrebne povišene temperature za učinkovitu pretvorbu NO u NO_2.
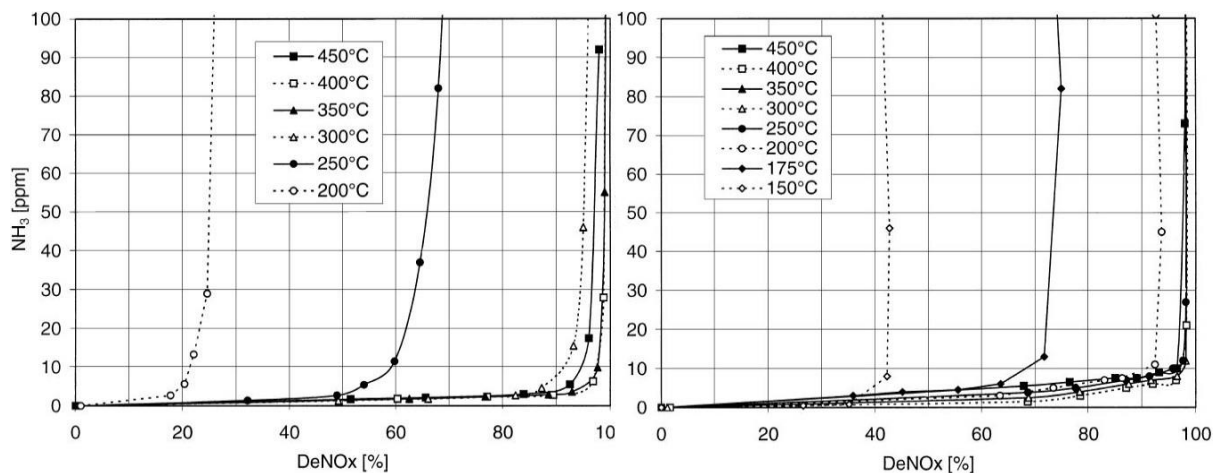
Slika 10. Učinkovitost redukcije NO$_X$: a) s čistim NO i b) s mješavinom NO$_2$/NO 1:1[54].

SCR za redukciju NO$_X$-a koristi amonijak koji se dobiva termolizom 32 % uree u katalizatoru uzlazno od SCR-a, čiji je zadatak i dekompozicija čvrstih produkata zaostalih iz nepotpune termolize za čiji su raspad bez prisutnosti katalizatora potrebne temperature od 600°C. Slika 11. prikazuje učinkovitost razgradnje uree u ovisnosti o temperaturi termolize za različite materijale katalizatora koji također spuštaju temperature dekompozicije krutih produkata između 200 °C i 290 °C [55].
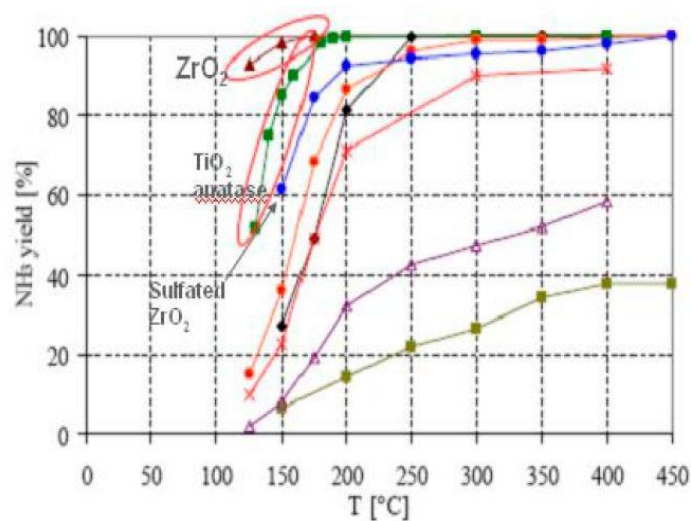
Slika 11. Utjecaj temperature termolize na učinkovitost razgradnje uree [55].

Kombinacija LNT SCR redukcijskih katalizatora NO$_X$-a ostvaruje prednosti u vidu visoke učinkovitosti, kompaktnosti i niže cijene zbog izostanka sustava ubrizgavanja i razgradnje uree jer je izvor amonijaka LNT katalizator u vremenu obogaćene smjese. Ovisnosti o radnim parametrima slične su kao u pojedinačnim sustavima i detaljno su objašnjeni u [2] kao i njihove konfiguracije, učinkovitosti, te problemi eksploatacije.

Filter čestica osnovni je sustav za smanjenje emisije čestica dizelskih motora (*engl. Diesel Particulate Filter, DPF)* ili kod benzinskih motora (*engl. Gasoline Particulate Filter, GPF*). Riječ je o mehaničkom filteru koji zaustavlja čestice iz ispušnih plinova, uključujući čvrsti ugljik (čađu) i fine čestice, dok ostatak ispušnih plinova prolazi kroz filter. Nakon određenog razdoblja korištenja filter je zasićen, stupanj onečišćenja se procjenjuje kao i kod standardnih mehaničkih filtera prema diferencijalnom tlaku između ulaza i izlaza filtera. Prema [56] povećanje protutlaka od 200 mbar dovodi do povećanja specifične potrošnje goriva za približno 2 %. Nakon što je filtar zasićen česticama čađe do unaprijed određene granice, čestice se moraju ukloniti, odnosno regenerirati filter. Osim čestica čađe, filter zadržava i čestice pepela koje se regeneracijom ne mogu ukloniti pa je potreban servis filtera. Kod vozila u cestovnom prometu većinom se koristi kombinacija aktivne i pasivne regeneracije. Pasivna se regeneracije događa na nižim temperaturama, između 200 i 300 °C, reakcijom čestica čađe s NO_2; na ovaj način filter čestica sudjeluje u smanjenju emisija NO_X-a. Kvaliteta pasivne regeneracije, kao i učinkovitost redukcije NO_X-a, ovisi o količini raspoloživog NO_2 na čiju količinu utječe kvaliteta i temperatura uzstrujnog oksidacijskog katalizatora. Prema [57] uz korištenje aditiva za sniživanje temperature pasivne regeneracije kod komercijalnog nekataliziranog DPF-a učinkovitost redukcije NO_2 kretala se oko 44 %. Oksidacija čestica čađe u kisiku je vrlo spora reakcija pa je za aktivnu regeneraciju potrebna znatno viša temperatura od 550 °C do 600 °C, ili oko od 100 °C do 200 °C niže temperature kod korištenja kataliziranih filtera ili ubrizgavanjem katalizatora. Takve se temperature osiguravaju dodatnim izgaranjem goriva u oksidacijskom katalizatoru postavljenom uzstrujno. Posebno su opasne regeneracije kod jako velikih akumulacija čađe, jer pri visokim temperaturama i dovoljno kisika čađa vrlo brzo izgara i može podići temperaturu iznad 900 °C, unatoč aktiviranoj zaštiti od prekomjernih temperatura, što može uzrokovati trajna oštećenja DPF-a. Aktivna regeneracija zbog potrebe dodatnog grijanja utječe na povećanje potrošnje goriva za 2 do 3 %, dok se kod pasivne regeneracije taj utjecaj smanjuje za oko 80 % [58].

Na osnovi spoznaja o svim dostupnim sustavima kontrole emisija vozila, s fokusom na najproblematičnije emisije dizelskih vozila, razvijen je dijagram, prikazan na slici 12., koji jasno prikazuje načine postizanja različitih emisijskih razina. S gledišta najproblematičnijih emisija, linije 1, 2 i 3 predstavljaju tehnologije motora u užem smislu, bez ikakvih sustava za kontrolu emisije. Položaj i oblik linija uvjetovan je stupnjem razvoja motora u užem smislu, koji ovisi o različitim primijenjenim tehnologijama ubrizgavanja, prednabijanja, vrtloženja u komori izgaranja, izmjene radnog medija, omjera kompresije itd. Linija 1 predstavlja motor s

najvišim stupnjem razvoja, dok je položaj točaka P1, P2 i P3 određen trenutnim postavkama motora. Kako ograničenja CO_2 emisija i potrošnje goriva dolaze u prvi plan, polazišna su linija MSUI s najvišim stupnjem razvoja, podešeni prema najnižoj potrošnji goriva bez obzira na pojedine emisije. Korištenje efikasnih sustava kontrole emisija omogućava im zadovoljavanje različitih europskih propisa o graničnim vrijednostima emisija štetnih tvari u svim uvjetima upotrebe.
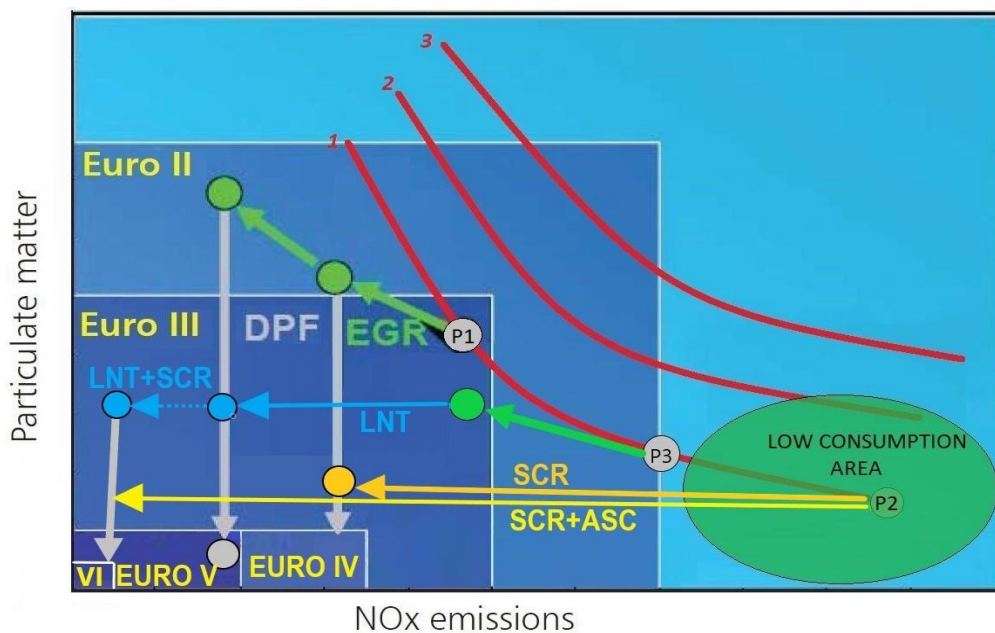
Slika 12. Učinak različitih tehnologija kontrole emisija u cilju dostizanja različitih emisijskih razina [2].

Rad [2] je obuhvatio različite tehnike i sustave čija je osnovna svrha kontrola ili smanjenje emisija štetnih tvari s naglaskom na najproblematičnije NO_X i PM emisije. Obrađeni su gotovo svi poznati učinci utjecajnih parametara na svaki sustav pojedinačno, što je pridonijelo razumijevanju složenih fizikalnih i analitičkih modela ponašanja. Pregledom dosadašnjih istraživanja utvrđeno je iznimno složeno predviđanje svakog pojedinog sustava na pojedine emisije, ali i određeni nedostatak u području istraživanja zajedničkog djelovanja više podsustava koji čine cjelovito rješenje. Prema detaljnoj analizi postojećih tehnologija dane su smjernice s procjenom kvalitete rješenja u vidu usporedba različitih rješenja cjelovitih sustava kontrole emisija s aspekta učinka na najutjecajnije emisije, potrošnju goriva, održavanje, veličinu i cijenu izvedbe na slici 13.

Technical solution	Emissions						Packaging	Maintenance	Costs	Comments
	NOx	PM/PN	CO₂	NH₃	CO	THC				
HP EGR Cooled HP EGR [DOC] [DPF]	BASELINE									Pure NOx reduction potential. Commonly used up to Euro 6b. Failed in RDE.
High EGR combustion HP/LP EGR [DOC] [DPF]	⊕	○	○	○	○	○○ ⊖	⊖	○○ ⊖	⊖	Insufficient NOx reduction potential for future euro norms. Possible HEV application in smaller vehicles.
Lean NOx Trap System HP EGR [DOC] [DPF] [LNT]	⊕⊕	○	⊖	⊖	○	○	⊖⊖	○○ ⊖	⊖⊖	Suitable for smaller vehicles. Sensitive to sulfur content in fuel. NOx reduction potential affects fuel consumption.
SCR System HP EGR [DOC] [DPF] [SCR]	⊕⊕⊕	○	⊕	⊖⊖	○	○	⊖⊖⊖	⊖⊖	⊖⊖⊖	Very robust and large system. Suitable for highly and midium loaded engine in large engine.
Close-coupled SCR/ASC System HP EGR [DOC] [DPF] [SCR] [ASC]	⊕⊕⊕⊕	○	⊕⊕	○	○	○	⊖⊖⊖	⊖⊖	⊖⊖⊖⊖	Very efficient NOx reduction system also suitable for low loaded engine. Able to meet all future standards of harmful emissions, especially in combination with HEV
	⊕ -better than baseline			○ -same as baseline						
	⊖ -worse than baseline			○ -same as baseline, fully satisfied requirements						

Slika 13. Usporedba različitih koncepata sustava kontrole emisija dizelskih vozila [2].

Glavni zaključci koji su odredili smjernice daljnjeg istraživanja su sljedeći:

1. Sustavi kontrole emisija pružaju visoku učinkovitost samo u određenom rasponu djelovanja, koji je kod klasičnih (nehibridnih) pogonskih sustava gotovo u potpunosti određen zahtjevima korisnika.

2. Veliki broj utjecajnih parametara i međusobna ovisnost sustava za kontrolu emisija čini fizikalne i empirijske modele presloženima kod modeliranja kompletnih vozila.

3. Učinkovitost sustava kontrole emisija nije jednoznačno određena trenutnom radnom točkom MSUI-ja, nego jako ovisi o smjeru i brzini dostizanja radne točke i o povijesti događaja koji opisuju tromost sustava.

4. Korištenje učinkovitijih sustava kontrole emisija povećava utjecaj (polu) hladnih startova na ukupne količine emisija.

5. Sustavi kontrole emisija podložni su kvarovima, osobito u uvjetima rada izvan predviđenih okvira, te mogu utjecati na ispravnost ostalih sustava MSUI-ja, dok će neispravnost kompleksnijih sustava imati veće posljedice na porast količine emisija u stvarnim uvjetima upotrebe.

6. Sustavi kontrole mogu se prilagoditi uvjetima koji vladaju prilikom ispitivanja emisija i potrošnje goriva za vrijeme tipskog odobrenja.

2.2. Modeliranje klasičnih i HEV i strategije upravljanja

Zbog velike složenosti različitih sustava pogona HEV obrađeno je široko područje modeliranja svih njegovih sklopova. Zahtjevi pojedinih modela s obzirom na klasifikaciju HEV-a prema arhitekturi obrađeni su u literaturi [59-68] i stupnju hibridizacije [13, 59, 61, 63, 69]. Razvijeni su različiti pristupi modeliranja cestovnih vozila s različitim razinama detaljizacije. Strogu podjelu modela potrošnje goriva i emisijskih modela vozila nije moguće precizno odrediti jer većina rješenja uključuje različite pristupe i načine upotrebe, klasičnih i hibridnih vozila. Načelna podjela emisijskih modela vozila s obzirom na razmjere upotrebe prema [70] prikazana je na slici 14. Također, prikazani su primjeri primjena i ulaznih podataka potrebnih za procjenu emisija komponenti ispušnih plinova vozila.
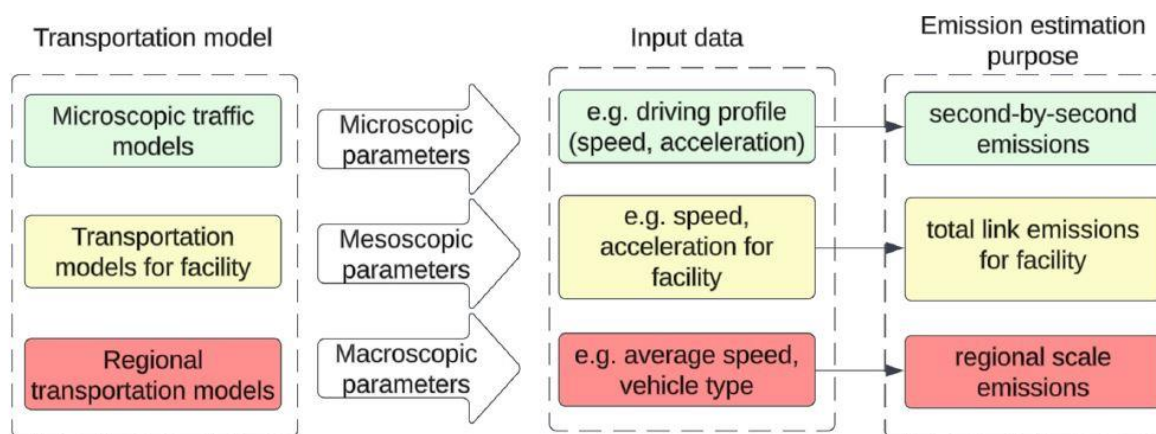
Slika 14. Podjela modela s obzirom na razmjere upotrebe [70].

Mikroskopski modeli emisija i potrošnje goriva uzimaju u obzir svako vozilo pojedinačno [71], obrađuju veliku količinu podataka s rezolucijom oko 1s koji se odnose na mjerenja parametara vozila kao što su ubrzanje i brzina, kao i parametara ceste kao što su nagib terena i koordinate položaja. Mikromodeli mogu se klasificirati prema vrsti ulaznih podataka [70]; na temelju profila trenutne brzine [72] (Enviver Versit, Roundabout EM), na temelju parametara vozila kao što je snaga ili specifična snaga (MOVES, CSIRO, CMEM, VT-CPFM) ili na temelju kombinacija prethodno navedenih metoda.

Makroskopski modeli koriste se za procjenu emisija, potrošnje goriva i utjecaja cestovnog prometa na okoliš. Uglavnom formiraju se kao regresijski modeli koji se temelje na parametru prosječne brzine vožnje na analiziranoj dionici ceste (2.1), gdje je:

$$F = f(v) = a + b\frac{1}{v} + cv + dv^2 \tag{2.1}$$

Područje ovog rada većinom je ograničeno na mikroemisijske modele pojedinačnih vozila koje možemo općenito zapisati kao funkciju koja povezuje količine pojedinih emisija x s ulaznim varijablama (2.2),

$$J_x = f(u) \qquad\qquad (2.2)$$

gdje je *x∈(potrošnje goriva ili el. Energije, emisija CO₂, NOₓ, CO, HC....)*

Jedna od klasifikacija mikromodela, s obzirom na način formiranja emisijskih modela prema [72], prikazana je na slici 15.
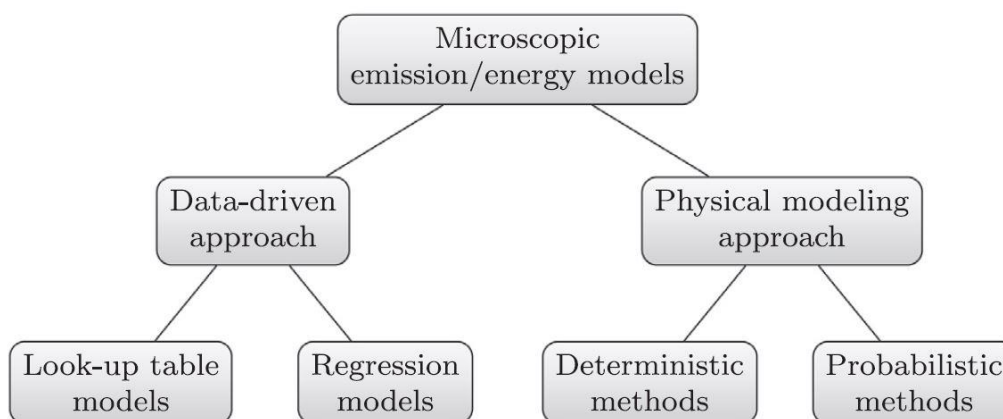
Slika 15. Podjela emisijskih modela i modela potrošnje goriva odnosno energije [72].

Pristup na osnovi mjernih podataka uključuje tablične i regresijske modele. Tablični su modeli zasnovani na emisijskim mapama koje opisuju ponašanje pojedinih emisija i potrošnje goriva u odnosu na promatrane parametre, pri čemu su to najčešće brzina i ubrzanje [73]. Prednost pristupa relativno je jednostavna upotreba zbog ovisnosti o vanjskim varijablama. Osnovni nedostaci vezani su za kreiranje emisijskih mapa na ispitnim stolovima u stacionarnom stanju gdje nisu zastupljeni tranzijentni uvjeti što uzrokuje određene pogreške [74]. Regresijski modeli koriste prikupljene podatke kako bi „obučili" model da što točnije oponaša te podatke. Ulazni su podaci obično brzina, ubrzanje ili potrebna snaga pogona, a izlazni količine pojedinih emisija odnosno potrošnja goriva. Zbog izrazite nelinearne ovisnosti emisija o ulaznim varijablama ovi modeli često se oslanjaju na neuralne mreže za pronalazak najboljeg rješenja, što uz visoku rezoluciju podataka često predstavlja veliko računalno opterećenje. Modeli su kritizirani zbog uobičajenog korištenja ulaznih podataka s dinamometra umjesto stvarnih uvjeta upotrebe jer su takvi modeli davali značajno niže vrijednosti emisija u odnosu na realne emisije [75, 76]. Navedeni modeli također ne sadrže nikakvu fizikalnu interpretaciju pojava koje opisuju. Suprotno pristupu na osnovi mjernih podataka, fizikalni pristup modeliranju podrazumijeva

povezivanje parametara i varijabli modela s fizikalnim značenjem. Prema [71] fizikalni modeli mogu biti deterministički i probabilistički. Deterministički fizikalni modeli podrazumijevaju određivanje funkcije količine emisija i potrošnje goriva u ovisnosti o stvarnim varijablama u određenom trenutku. Probabilistički modeli koriste se kada stvarne vrijednosti ulaznih varijabli nisu dostupne. Na primjeru trenutne brzine kao ulazne varijable, umjesto profila brzine koriste se uprosječene brzine na određenim rutama ili područjima uz dodatak slučajnih poremećaja. Autori u [70] uspoređuju modalni model na osnovi matrice trenutne brzine i ubrzanja s fizikalnim modelom gdje je cjelokupan proces nastanka emisija podijeljen na komponente prema fizikalnim pojavama koje ih uzrokuju. Osnovni nedostaci korištenja matrice trenutna brzina-ubrzanje su sljedeći: zanemarivanje nagiba, oslanjanje na statičke rezultate mjerenja, pogreške zbog uprosječenih vrijednosti protoka emisija unutar istog polja matrice te vrlo ograničen broj podataka unutar određenih polja. Najveći je izazov determinističkog fizikalnog modela prikupljanje i obrada velikog broja varijabli kao i definiranje analitike fizikalnih pojava različitih utjecajnih mehanizama. Autori u [17] bave se modeliranjem i upravljanjem HEV-om te predlažu kombiniranu podjelu postojećih modela HEV-a prema načinu upravljanja i prema dinamici na kinematičke unatražne, kvazistatičke unapredne i dinamičke modele.

Kinematički unatražni (*engl. backward*) pristup, prikazan na slici 16., polazi od krajnjih komponenti pogona, tj. od kotača koji zahtijevaju određeni moment odnosno snagu da bi zadovoljili predodređeni ciklus. Protok informacija ide u smjeru suprotnom od toka energije, tj. od pogonskih kotača prema prijenosu i motoru s unutarnjim izgaranjem, odnosno prema električnom stroju i baterijama. Slabosti ovog pristupa proizlaze iz pretpostavke da se kretanje vozila apsolutno poklapa s unaprijed predloženim ciklusom vožnje i uobičajenog korištenja stacionarnih mapa ili tabela učinkovitosti. Pretpostavka o savršenom poklapanju stvarne brzine s unaprijed određenim obrascem ciklusa je osobito nevjerodostojna kada zahtjevi za ubrzanjem i brzinom premašuju performanse vozila. Ovaj pristup obično se kombinira sa statičkim modelima uz zanemarivanje prijelaznih ponašanja, npr. uzrokovanih promjenom temperature MSUI-ja, tj. ne uzima u obzir hladne startove. Pojednostavljeni model prijelaznih pojava kao niza stacionarnih stanja ograničava njegovu upotrebu na preliminarne procjene potrošnje goriva i emisija [17].
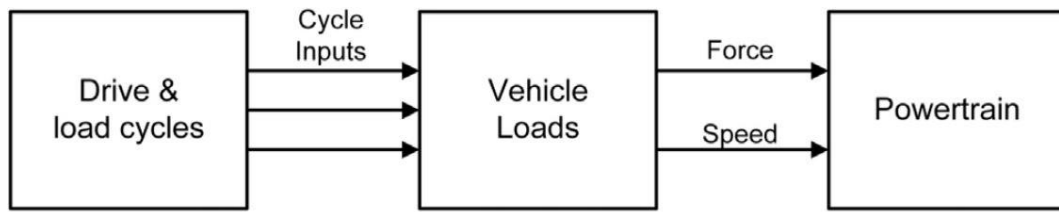
Slika 16. Kinematički unatražni pristup [17].

Kvazistatički unapredni (*engl. forward*) **pristup.** Kvazistatički pristup pretpostavlja da su u određenom kratkom vremenskom intervalu sve ulazne varijable konstantne te polazi od zahtjeva korisnika za promjenom brzine na osnovi želje za poštivanjem unaprijed zadanog obrasca brzine i ide u smjeru toka energije [77]. Prethodno navedeni sustav shematski je prikazan na slici 17. Zahtjev korisnika se preko pedale akceleratora i odgovarajućeg regulatora prenosi na MSUI koji ima svoje karakteristike i brzinu odziva. Moment se prenosi na sustav prijenosa koji ima svoje gubitke i prijenosni omjer i tako sve do kotača koji trebaju ostvariti potreban moment. Kvazistatički unapredni pristup je pogodniji za detaljno modeliranje i dinamička opterećenja jer vodi računa o odzivu i tranzijentima određenih sustava vozila [78]. Prikladnost i točnost ovog pristupa uvelike ovisi o tipu provedene simulacije. Kada je u pitanju procjena potrošnje goriva ili količina NO_X emisija, ovakav pristup daje prihvatljive rezultate, dok kod procjene količine čestica i prijelaznih pojava vezanih za odziv turbopunjača radi veće pogreške i zahtijeva detaljniji simulacijski model motora koji bolje opisuje tranzijentno ponašanje [17]. Unatoč navedenim nedostacima, zbog visoke složenosti modela HEV-a i visoke složenosti modeliranja dinamičkog ponašanja motora s unutarnjim izgaranjem, kvazistatički unapredni modeli često se primjenjuju za modeliranje hibridnih vozila [79, 80].
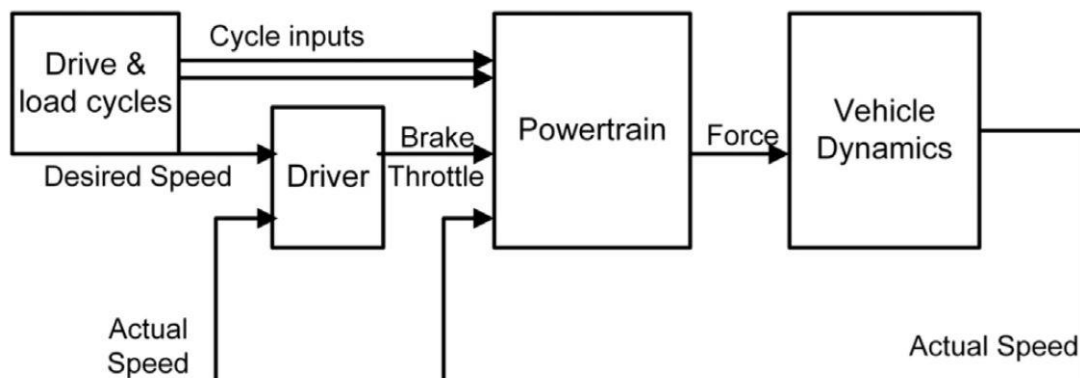
Slika 17. Kvazistatički unapredni model vozila [17].

Dinamički model vozila karakterizira osim opisa prijelaznih pojava uzdužne dinamike vozila i opis prijelaznih pojava motora s unutarnjim izgaranjem koji uključuje i kašnjenje turbopunjača te hladne startove. Sa stajališta upravljanja preferira se tok informacija prema naprijed kao kod unapredng modela [17, 78]. Razlika u potrošnji goriva između stacionarnog stanja i prijelaznih stanja može biti značajna. Prema istraživanjima autora [81-83], potrošnja goriva tijekom prijelaznih stanja je između 6 i 30 % u izrazito dinamičkim uvjetima veća od stacionarne. Metode za predviđanje prijelaznih pojava dijele se na metode koje su temeljene na korekcijama ustaljenog stanja te na metode temeljene na izravnom predviđanju upotrebom dinamičkih varijabli. Autori [81, 82, 84] koriste metode temeljene na korekcijama ustaljenog stanja uz korekcijske faktore masenog protoka zraka, brzine vrtnje motora i temperature. Istraživanja [84] pokazuju da ovakav dinamički model u izrazito promjenjivim uvjetima brzine vrtnje i opterećenja motora smanjuje grešku predviđanja potrošnje goriva s 20 % za statički model na manje od 2 %. Autori u [83] navode kao osnovni nedostatak ovog pristupa složen način mjerenja korekcijskih faktora, osobito masenog protoka što mu ograničava širu primjenu. Autori u [85] koriste model vozila temeljen na izravnom predviđanju upotrebom dinamičkih varijabli i njihovih proteklih vrijednosti u fiksno definiranom periodu. U istom radu kao ulazi modela koriste se lako mjerljivi podaci brzina i ubrzanje. Unatoč dobrim rezultatima u pojedinim aplikacijama nedostatak ovakvog modela je taj što ne uzima u obzir uzdužni nagib ceste odnosno promjenu visine, a što mu ograničava upotrebu na ceste bez velikih visinskih promjena. Kod modeliranja hibridnih vozila ne postoji mogućnost razlikovanja više izvora energije, a što je također bitno ograničenje modela. U radu [83] izrađen je model koji kombinira prednosti prethodno navedenih tranzijentnih modela, koristi metodu korekcije ustaljenog stanja, koja uzima u obzir uzdužni nagib ceste, dok su korekcijski faktori brzina i ubrzanje lako mjerljivi elementi modela. Pogreška modela [32] smanjuje se na polovicu tijekom tranzijentnih opterećenja u odnosu na statički model i 2,7 % do 4,6 % u odnosu na model temeljen na dinamičkim varijablama brzine i ubrzanja razvijen u [72]. Točniji opis ponašanja emisija i potrošnje goriva dobiva se višedimenzionalnim ili detaljnim jednodimenzionalnim numeričkim modelima dinamike fluida, korištenim u [1]. Navedeni modeli omogućavaju da se izrazito dinamični događaji, kao što su nagle promjene momenta i brzine vrtnje, pouzdano simuliraju s velikom točnosti. Veliki je nedostatak ovakvog pristupa dinamičkog modeliranja složenost modela koja zahtijeva velike ljudske i računalne resurse te vrijeme za obradu podataka. Primjena

ovakvog tipa modeliranja najčešće je ograničena na specifična područja istraživanja koja se bave razvojem motora s unutarnjim izgaranjem [1, 86].

Snažan razvoj računala omogućio je razvoj računalnih metoda i napredak u razvoju simulacijskih softvera za različite komponente i topologije vozila. Dio programskih paketa oslanja se na modalnu analizu odnosno na grupiranje podataka prema vanjskim varijablama, kao primjerice snaga na kotačima, brzina i/ili ubrzanje. Primjeri paketa koji koriste modalnu analizu su CMEM (Comprehensive Modal Emission Model) [87], VERSIT i MOVES koji koristi VSP analizu [88]. Drugi je pristup oslanjanje na unutarnje varijable i opis osnovnim fizikalnim veličinama, kao što su sila, moment, brzina, kutna brzina, ubrzanje, kutno ubrzanje, masa i moment inercije, gdje se svaka komponenta prikazuje analitički. Ovakav pristup najjednostavnije je implementirati unutar računalnih simulacija. Virtual Test Bed (VTB), Power electronics simulator (PSIM), Simplorer, i V-ELph su primjeri programskih alata koji se oslanjaju na fizikalne modele [89]. Dio simulacijskih modela hibridnih vozila se za nelinearne komponente koje su neprikladne za matematički opis oslanja na mape i krivulje koje opisuju različite veličine u ovisnosti o jednom ili više parametara [78, 89-93]. Jedan od češće korištenih je ADVISOR [78, 89, 90, 94, 95], koji je razvio Američki nacionalni institut za obnovljive izvore NREL u MATLAB/SMULINK okruženju. Specifičan je po tome što koristi mješoviti unapredni i unatražni pristup, dok su pojedine komponente vozila izrađene kao kvazistatički modeli, što ga ograničava na veće vremenske intervale. Nadalje, oslanja se na unutarnje varijable i eksperimentalne modele u obliku tablica i mapa učinkovitosti [89]. Powertrain System Analysis Toolkit PSAT razvijen je u Matlab / Simulink okruženju i koristi unapredni pristup modeliranju [80] dok Hybrid Powertrain Simulation Program HPSP koristi unatražni pristup [91]. CruiseM je softverski paket s grafičkim sučeljem koji je razvila tvrtka AVL i koji se može konfigurirati da koristi unapredni i unatražni pristup kao i njihove kombinacije ovisno o zahtjevima simulacije [4, 92, 96]. Za dinamičke modele MSUI-ja AVL je razvio poseban programski paket BOOST koji koristi kvazidimenzionalne, odnosno jednodimenzionalne modele za opis procesa unutar cilindra, i opise usisa i ispuha [97], te FIRE koji se oslanja na višedimenzionalne modele računalne dinamike fluida. Odabir pogodnog programskog paketa i metode ovisi o zahtjevima za brzinom i točnosti, koji ovise o izboru modela. Primjerice numerički modeli motora zasnovani na CFD-u daju najbolje rezultate u smislu točnosti i dinamike vremenski i prostorno ovisnih pojava, međutim zbog složenosti modela i vremena trajanja analize navedeni je pristup apsolutno neprihvatljiv kod modeliranja kompletnog pogonskog sklopa ili cijelog vozila.

Kroz kvalifikacijski ispit [98] obrađene su najčešće korištene **strategije upravljanja energijom** HEV-a čiji ishod ovisi o kvaliteti modela na koji su primijenjene. Polazna točka pronalaska optimalnog rješenja je definiranje funkcije cilja koja ovisi o specifičnostima primjene. U najvećem broju slučajeva strategija upravljanja energijom svodi se na kompromis između minimalizacije potrošnje goriva, odnosno emisija ispušnih plinova [63], povećanje trajnosti komponenti poput baterija, ispunjavanje zahtijeva za snagom, osiguravanje voznih karakteristika i komfora [64], slika 18.
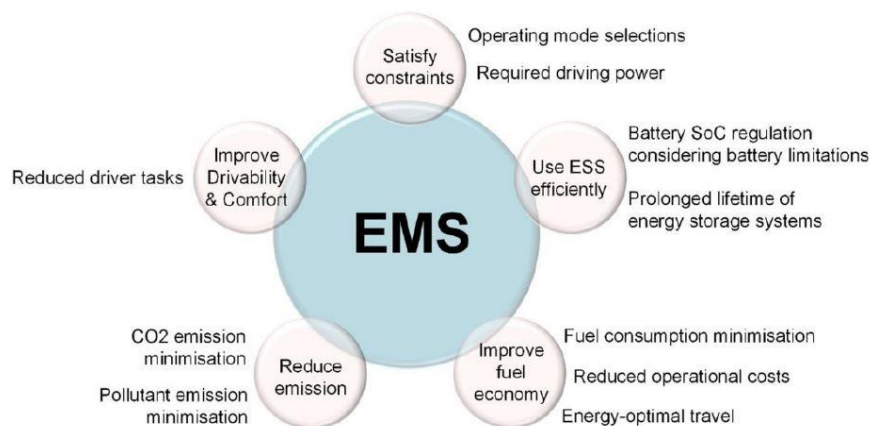
Slika 18. Osnovni zahtjevi EMS HEV-a [99].

Velik broj familija strategija upravljanja energijom EMS (*engl. Energy Management Strategy*), neki autori koriste izraz PMS (*engl. Power Management Strategy*), obrađen je u literaturi i nije jednostavno napraviti jednoznačnu klasifikaciju zbog isprepletanja različitih pristupa unutar jedne fleksibilne strategije. Kao osnovnu podjelu [62, 100] navode offline EMS koje su pogodne za globalnu optimizaciju, a temelje se na unaprijed poznatom ciklusu vožnje i online EMS za određivanje trenutno optimalnog rješenja u realnom vremenu. Autori [63, 99, 101-103] dijele familije EMS-a na one temeljene na pravilima (*engl. Role Based*) unutar kojih se sustav pogona ponaša, i one temeljene na optimizaciji (*engl. Optimization Based*) parametara sa svrhom određivanja najboljeg rješenja, primjer takve klasifikacije je prikazan na slici 19.
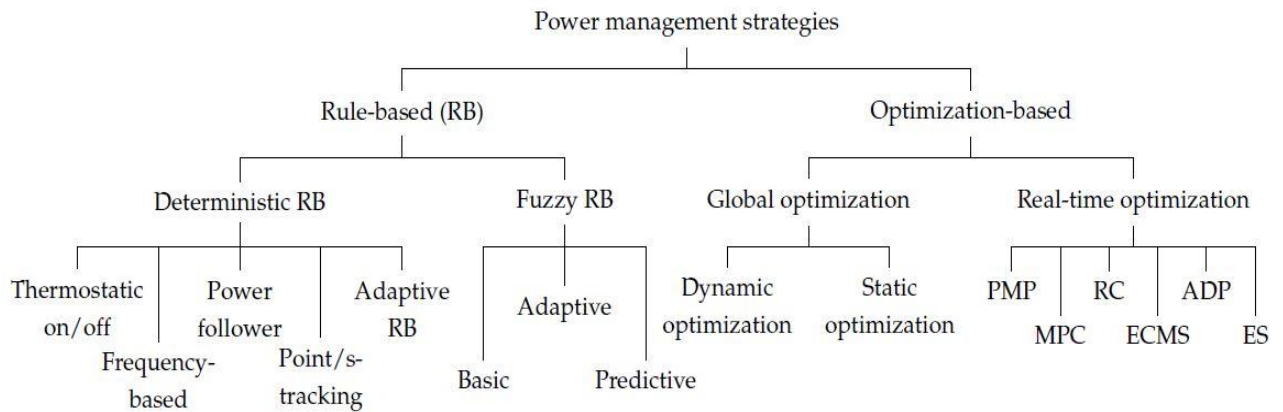
Slika 19. Klasifikacija EMS [103].

Strategije u realnom vremenu ili online strategije primjenjuju trenutna pravila upravljanja energijom temeljena na budućim pretpostavkama kako bi minimizirali ukupnu funkciju troška. Globalne ili offline metode zbog svoje prirode tj. poznavanja ciklusa unaprijed i složenosti nisu primjenjive u realnom vremenu, ali s druge strane predstavljaju referentna rješenja koja se mogu koristiti kao mjerila uspješnosti i dobar alat za analizu te procjenu učinkovitosti online metoda. U pravilu je cilj postići što bolji rezultat sa što manje upotrijebljenih ljudskih i računalnih resursa u što kraćem vremenu. Pregled različitih metoda, s obzirom na računalno opterećenje i optimalnost rješenja, prikazan je na slici 20., gdje se vidi da postizanje boljeg rješenja traži veće računalno opterećenje odnosno vrijeme pronalaska optimalne strategije upravljanja energijom.
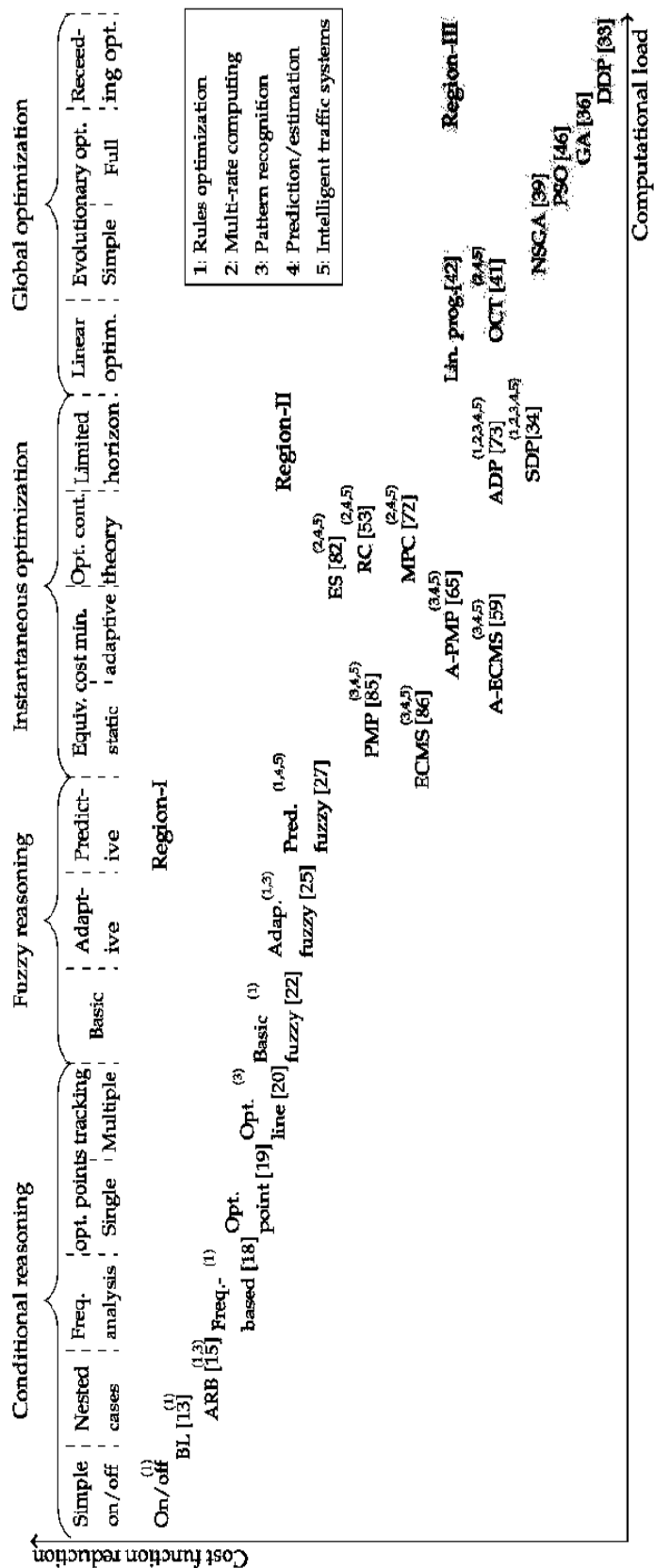
Slika 20. Usporedba različitih strategija upravljanja energijom [103].

2.3. Modalna analiza pomoću specifične snage

Jimenez [104] je prvi predložio metodu koja definira specifične emisije i potrošnju goriva prema parametru specifične snage vozila, tj. analizu prema specifičnoj snazi (*engl. Vehicle Specific Power, VSP*), iako je autor u [105] ranije doveo u vezu emisije i potrošnju goriva s pozitivnom kinetičkom energijom što je na tragu VSP definicije. Specifična snaga vozila definirana je kao trenutna snaga po jedinici mase vozila. Trenutna snaga koju generira motor s unutarnjim izgaranjem troši se na svladavanje aerodinamičkog otpora i otpora kotrljanja te na povećanje kinetičke i potencijalne energije vozila (2.3).

$$VSP = \frac{\frac{d}{dt}(KE + PE) + F_{roll} \cdot v + F_{aero} \cdot v}{m}$$

$$= \frac{\frac{d}{dt}\left(\frac{1}{2}m \cdot (1 + \varepsilon_i) \cdot v^2 + mgh\right) + C_R \cdot mg \cdot v + \frac{1}{2}\rho_a C_D A(v + v_w)^2 \cdot v}{m} \quad (2.3)$$

$$= v \cdot (a \cdot (1 + \varepsilon_i) + g \cdot grade + g \cdot C_R) + \frac{1}{2}\rho_a \frac{C_D A}{m}(v + v_w)^2 \cdot v$$

Koristeći tipične parametre temeljene na prosječnim vrijednostima koeficijenta otpora zraka i koeficijenta otpora kotrljanja za putničko vozilo srednje klase i gustoću zraka pri 20 ⁰C, izraz (2.4) prelazi u [104]:

$$VSP = v \cdot (a \cdot 1.1 + 9{,}81 \cdot grade + 0{,}0135) + \frac{1}{2} \cdot 1{,}207 \cdot 0.0005 \cdot (v + v_w)^2 \cdot v$$

$$= v \cdot (a \cdot 1.1 + 9{,}81 \cdot grade\% + 0{,}0132) + 3.2 \cdot 10^{-4} \cdot (v + v_w)^2 \cdot v \quad (2.4)$$

U VSP analizi uglavnom se koriste rasporedi modalnih razreda s konstantnim rasponima jednake širine. Dio pogreške modalnih emisija čini usrednjavanje unutar razreda jer su iste definirane kao maseni protoci u jedinici vremena koji u energetski zastupljenijim razredima, u pravilu, rastu sa snagom. Osim specifične snage korišteni su drugi parametri kao brzina, ubrzanje i nagib ceste [70, 105, 106], koji su direktno mjerljivi, ali sa slabijom korelacijom prema emisijama i potrošnji goriva. Mnogi modeli koji nisu primarno nastali na VSP analizi koriste VSP parametar zbog jake korelacije VSP-a s emisijama i potrošnjom goriva [107].

Također koriste se u modelima koji zahtijevaju nešto veće točnosti kao usporedbe emisija između različitih goriva, E85 i benzina kod osobnih putničkih vozila [108]. Autori u [109] koriste VSP modele za procjene emisija i potrošnje goriva autobusa pogonjenih gorivnim člancima i dizelskim motorima. Autor u [110] koristi VSP analizu u svrhu poboljšanja predviđanja modalnih modela s parametrom brzine na način da radi procjenu utjecaja promjene opterećenja brojem putnika gradskih autobusa na modalne emisije i potrošnju goriva prema parametru brzine. Osnovni razlog provedene korekcije je neosjetljivost originalnog modela na promjenu opterećenja. Autori u [111] ispituju u realnim uvjetima 10 različitih automobila i dovode u korelaciju potrošnju goriva prema VSP parametru. U istom je utvrđeno kako je za vozila pokretana motorima s elektroničkim ubrizgavanjem korelacija između potrošnje goriva i specifične snage linearna, dok je kod starijih vozila, koja koriste rasplinjače, eksponencijalna funkcija. Odstupanja modela u odnosu na izmjerene podatke samo su kod jednog vozila bila veća od 16 %. Autor u literaturi [83] u razvoju dinamičkog modela potrošnje goriva temeljenog na korekciji ustaljenog stanja koristi VSP parametar u razvoju tranzijentnog modula kao i za filtriranje mjernih podataka u svrhu odbacivanja ekstrema mjernih rezultata svakog raspona koji su u normalnoj raspodjeli izvan 3σ, prema [112]. Unatoč velikom uzorku podataka na osnovi kojih [112] razvija tranzijentni VSP model, kao i korištenju 3σ filtera, ipak uzrokuje veliku relativnu pogrešku procjene veću od 30 %. Razlog visoke pogreške leži u korištenju univerzalnog modela za više vozila, ali i u jednostavnom prikupljanju podataka s OBD modula umjesto instalacije daleko točnijeg PEMS uređaja. Autor u literaturi [113] analizira upravljanje pogonom i energijom na PHEV vozilu, dovodi u korelaciju promjenu stupnja napunjenosti (*engl. State of Charge, SoC*) odnosno snagu baterije s VSP parametrom, posebno za uključen MSUI, a posebno za isključen. VSP analizu koristi za procjenu preostalog SoC-a u CS i CD modu, ne bavi se analizom emisija. Funkcija SoC iz modela vrlo dobro aproksimira izmjerene podatke s koeficijentom R^2 oko 0,99. Autor u literaturi [114] izrađuje VSP model s 14 raspona snage FHEV vozila tako što mjeri emisije i potrošnju goriva pomoću PEMS uređaja, a zatim vrši validaciju modela prema NEDC ciklusu u kojem je vozilo tipski odobreno. Nedostatak oslanjanja na podatke NEDC ciklusa je problem ispitivanja na „Golden Vehicle" vozilu što sigurno utječe na točnost modela. Koristi pojednostavljenu univerzalnu definiciju VSP-a prema [104] što pojednostavljuje model, ali i smanjuje točnost. Odstupanje modela od certificiranih podataka prema NEDC protokolu je u potrošnji goriva -3,2 %, CO emisija +18,1 % i NO_X emisija 26,2 %. Navedeno odstupanje CO_2 emisija nije u skladu s potrošnjom goriva. Najbitniji razlog slabog funkcioniranja klasičnih VSP modela kod hibridnih vozila, za razliku od klasičnih, slaba je korelacija VSP parametra s emisijama i potrošnjom goriva. Razlog je

postojanje dva izvora energije od kojih je samo jedan odgovoran za emisije i potrošnju goriva, dok strategija upravljanja energijom određuje njihove odnose. Samo je nekoliko autora različitim korekcijama pokušalo povezati emisije i potrošnju goriva hibridnih vozila s VSP parametrom. Wang je u [115] detektirao problem korištenja klasične definicije VSP analize kod HEV-a s visokim stupnjem hibridizacije u vidu vrlo slabe korelacije potrošnje goriva, odnosno CO_2 emisija a VSP parametrom vozila. Na osnovi analiziranih podataka uvidio je potrebu uključivanja unutarnjih varijabli unutar VSP modela. U istom radu autor predlaže uvođenje VSP parametra u odnosu na snagu motora, umjesto u odnosu na pogonsku snagu vozila, čime povećava koeficijent korelacije s $R^2=0.11$ na $R^2=0.98$ u uvjetima gradske vožnje, slika 21.
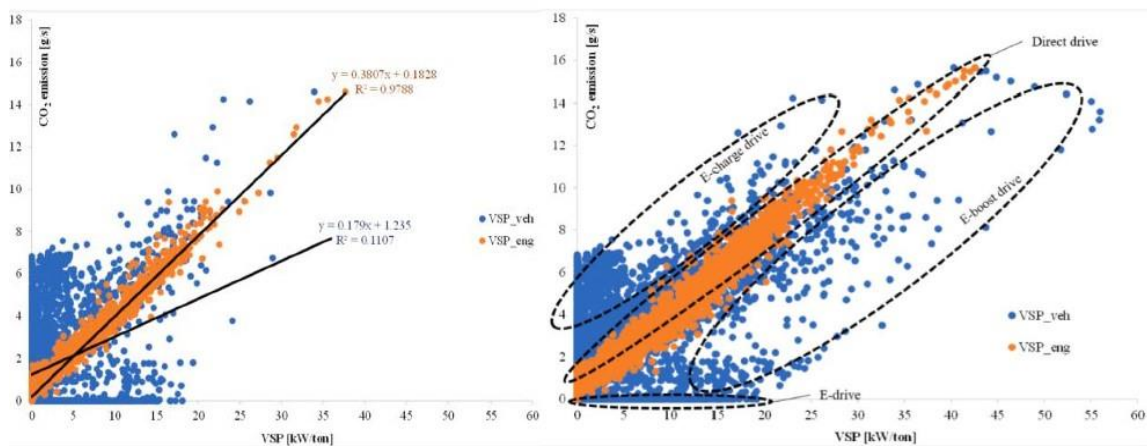
Slika 21. Usporedba korelacije CO_2 emisija s VSP parametrom vozila i VSP parametrom motora [115].

Duarte i ost. u [116] koriste VSP metodu za određivanje korelacije između potrošnje goriva i specifične snage vozila za više kategorija vozila, ukupno 20, pogonjenih dizelskim, benzinskim ili hibridnim pogonom. Specifičnost je pristupa u pronalaženju funkcija modela koje u zavisnosti o VSP parametru najbolje opisuju potrošnju goriva različitih vozila, te naknadna korekcija modela posebno klasičnih, a posebno hibridnih vozila linearnom funkcijom. Cjelokupno područje rada podijeljeno je na tri zasebna dijela koji su opisani konstantom za VSP<-10, kvadratnom aproksimacijom za -10<VSP<10 i linearnom za VSP>10. Dok se klasična vozila ponašaju prilično ujednačeno i zahtijevaju manji upliv linearne korekcije, modeli hibridnih vozila značajno odstupaju ovisno o primijenjenoj konfiguraciji; upliv linearne korekcije je čak suprotan za različita vozila. Razlozi osjetljivosti hibridnih modela na konfiguraciju leže u različitim postavkama strategije upravljanja energijom i različitim primijenjenim tehnologijama MSUI-ja. Iz istog razloga modeli istog proizvođača

pokazuju ista obilježja. Odstupanja potrošnje goriva korigiranih modela HEV-a su između -3,6 % i 6,8 %. Pristup pokazuje da je moguće izraditi upotrebljiv VSP model potrošnje goriva hibridnog vozila koji dobro replicira postojeće stanje upotrebom linearnih korekcijskih faktora bez utjecaja na strategiju upravljanja odnosno na same uzroke odstupanja, zbog čega vozila s drugačijim strategijama zahtijevaju potpuno različite korekcije osnovnog modela. Mera i ost. [117] grade vrlo složen korekcijski VSP model benzinskih hibridnih vozila s motorima s direktnim i indirektnim ubrizgavanjem i dizelskih hibridnih vozila sa samo EGR kontrolom NO_X emisija i kombinacijom EGR-SCR sustava. Odabrana su vozila s različitim tehnologijama motora s unutarnjim izgaranjem zbog izrazito različitih ponašanja ukupnih NO_X emisija [2]. Svaki VSP raspon dijeli se na *m x m* područja opterećenja i brzine vrtnje za koje se definiraju mape pojedinih emisija. Faktor korekcije definiran je kao odnos emisija koje proizlaze iz mapa motora i emisija pripadajućeg VSP raspona. Drugi parametar je τ koji definira najmanji broj podataka u svakoj od jediničnih *m* podjela. Parametri *m* i τ optimiraju se za svaki pojedini model zasebno odnosno prema grupama, posebno za benzinska, posebno za dizelska vozila. U pogledu CO_2 emisija najveći dobitak ovakvog pristupa je vidljiv tamo gdje standardni VSP model generira najveću pogrešku, tj. kod vozila pogonjenog benzinskim motorom s direktnim ubrizgavanjem u gradskim uvjetima vožnje gdje je primjerice greška modela smanjena s 27,9 % na 10,3 %, dok je pogreška tipskog modela 2,1 % veća u odnosu na individualni. Kod NO_X modela svih testiranih vozila ostvareno je povećanje točnosti, ali je pogreška i dalje znatno veća u odnosu na CO_2 emisije i potrošnju goriva. Prednosti su modela značajno povećanje točnosti kod CO_2 emisija osobito gdje standardni VSP generira najveću grešku i relativno malo odstupanje tipskog modela od individualnog. Povećanje točnosti NO_X modela nije toliko značajno, međutim nedostatak je i vrlo složen postupak dobivanja modela višeparametarskom optimizacijom i Paretovom analizom. Zhai i ost. [118] izrađuju model emisija i potrošnje goriva FHEV-a na osnovi modalne VSP analize, uvode osnovnu logiku upravljanja energijom koja uključuje samo vrijeme rada motora s unutarnjim izgaranjem prema kriteriju produkta brzine i ubrzanja. Prednost je ovakvog pristupa mogućnost uvođenja dodatnih parametara nagiba ceste i SoC u logike pokretanja i zaustavljanja motora s unutarnjim izgaranjem, što u radu nije primijenjeno jer je testiranje provedeno isključivo na valjcima, a SoC je zanemaren. Osnovni je nedostatak modela nemogućnost utjecaja na odnose između pojedinih izvora energije za vrijeme rada MSUI-ja. Nadalje, procjena regenerirane energije nije objašnjena u radu zbog čega primjena bilo kakve strategije upravljanja energijom, osim kopiranja postojećeg ponašanja, nije moguća. Jedan od uzroka pojedinačnih odstupanja leži u činjenici da su modalne emisije definirane kao maseni protoci u jedinici vremena čime se u odnosu na definiciju količine

pojedinih emisija po jedinici vučne energije otvara mogućnost dodatne pogreške. Također ovakva definicija modalnih emisija preko uprosječenog protoka dodatno komplicira zapis funkcije cilja kao polazne točke određivanja strategije upravljanja.

2.4. Dijagram toka energije HEV-a

Poznavanje tokova energije i energetska analiza ključni su elementi za razumijevanje dobitaka sustava hibridnog pogona, u smislu povećanja ukupne učinkovitosti i smanjenja emisija ispušnih plinova. Ako promatramo vozilo s konvencionalnim pogonom, motor s unutarnjim izgaranjem pretvara kemijsku energiju goriva u mehaničku energiju. Mehanička energija najvećim se dijelom koristi za pokretanje vozila i manjim dijelom za pogon pomoćnih sustava. Kod hibridnih pogona je situacija bitno drugačija, zahtjev za snagom je zbroj snage koja dolazi iz kemijske energije tj. motora s unutarnjim izgaranjem i snage koja dolazi iz baterije, odnosno snage električnog stroja koja može imati i pozitivan i negativan predznak.

Energetski tokovi u literaturi [119] uglavnom se opisuju kao skup fizikalnih i empirijskih modela pojedinačnih komponenti od kojih se vozilo sastoji. Navedeni koncept koristan je kod klasičnog fizikalnog pristupa modeliranju vozila zbog detaljnog opisa, dok je za modalne modele preopsežan. Detaljan i opširan energetski analitički samostojeći (*engl. stand alone*) koncept razvio je Katrašnik [120] gdje on definira tokove energije za gotovo sve poznate topologije hibridnih pogona; serijsku, paralelnu, serijsko-paralelnu i kompleksnu. Na osnovi dijagrama toka energije izvodi jednadžbe temeljene na energetskoj bilanci, koje daju detaljan opis svih energetskih tokova i gubitaka svih elemenata sustava. Tokovi su energije dvosmjerni s tim da su za svaki element definirani gubici odnosno učinkovitosti za ulaz i izlaz energije prema svakom susjednom elementu, slika 22.
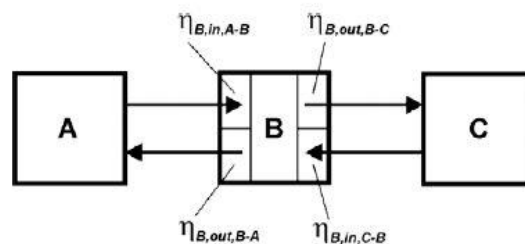
Slika 22. Podjela gubitaka elementa B kod dvosmjernog toka energije [120].

Analiza emisija i potrošnje goriva obično se predviđa za određeni ispitni ciklus vožnje, zbog toga je cjelokupna energija koja prolazi kroz pojedine elemente sustava sumirana vrijednost za cijeli ciklus (2.5).

$$W_{A-B} = \int_0^{t_{tc}} P(t)_{A-B}^* \, dt \tag{2.5}$$

Definirani tokovi energije za oba smjera, smjer A-B je definiran prema (2.6):

$$P(t)_{A-B}^* = \begin{cases} P(t)_{A-B}, & P(t)_{A-B} \geq 0 \\ 0, & P(t)_{A-B} < 0 \end{cases} \tag{2.6}$$

Posebno je definiran tok energije u suprotnom smjeru B-A (2.7):

$$P(t)_{B-A}^* = \begin{cases} -P(t)_{A-B}, & P(t)_{A-B} < 0 \\ 0, & P(t)_{A-B} \geq 0 \end{cases} \tag{2.7}$$

Pretpostavlja se pozitivni tok kad energija ulazi u element, a negativni kad iz njega izlazi, razlika ulaznog i izlaznog toka su gubici elementa W_B (2.8):

$$W_B = \sum_{i=1}^{n_{inflow}} W_{i-B} - \sum_{j=1}^{n_{outflow}} W_{B-j} \tag{2.8}$$

Kad se uvrste faktori gubitaka na ulaznoj i izlaznoj strani elementa, izraz prelazi u (2.9):

$$0 = \sum_{i=1}^{n_{inflow}} \eta_{B,in,i-B} W_{i-B} - \sum_{j=1}^{n_{outflow}} \frac{1}{\eta_{B,out,i-B}} W_{B-j} \tag{2.9}$$

Prednost Katrašnikove definicije toka energije je primjenjivost na sve topologije, stupnjeve hibridizacije i na sve elemente koji se nalaze u sustavu. Osnovni je nedostatak ogroman broj varijabli koji za posljedicu ima visoku složenost modela. Zbog navedenog razvijen je vlastiti dijagram toka energije orijentiran i prema funkciji [121], slika 23. Plava isprekidana linija predstavlja tok energije vozila s klasičnim pogonom, kemijska energija goriva se u MSUI-ju pretvara u mehanički rad s koeficijentom iskorištenja koji jako ovisi o položaju radne točke. Dalje mehanička energija prolazi kroz sustav pogona do pogonskih kotača s gubicima mjenjača i završnog prijenosa. Tok energije regenerativnog kočenja označen je zelenom linijom, energija kočenja se uzima s kotača i pretvara u povoljan oblik za spremanje, te se ponovno vraća istim putem do pogonskih kotača. Gubici energije su definirani na sljedećim elementima: završni prijenos, mjenjač, električni stroj u generatorskom režimu, baterija, električni stroj u motornom režimu, mjenjač i završni prijenos uz koeficijent ograničenja α. Treći tok opisuje spremanje

viška mehaničke energije iz MSUI-ja u spremnik i vraćanje energije na pogonske kotače, isti je označen žutom isprekidanom linijom. Gubici energije su definirani na sljedećim elementima: električni stroj u generatorskom režimu, baterija, električni stroj u motornom režimu, mjenjač i završni prijenos. Ovaj tok energije omogućava pomak radne točke odnosno trenutnog radnog područja MSUI-ja prema energetski ili emisijski povoljnijem radnom području. Navedena definicija toka energije prema funkciji uvelike pojednostavljuje zapis funkcije cilja, a time i definiranje strategije upravljanja uz minimalan broj unutarnjih varijabli.
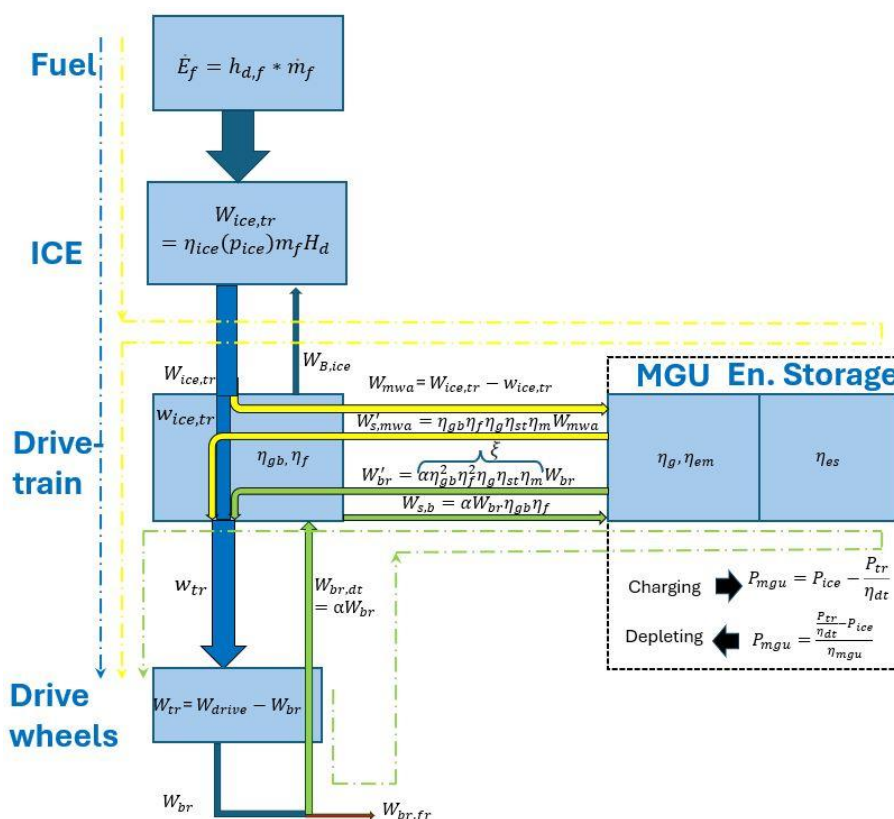
Slika 23. Dijagram toka energije paralelnog HEV-a prema [121].

2.5. Sažetak postojećeg stanja i smjernice daljnjeg istraživanja

Specifičnosti emisijskih modela su posljedica složenih procesa nastajanja emisija unutar komore izgaranja i složenih procesa u sustavima za kontrolu emisija. Njihov opis ovisi o varijablama koji su mjerljive isključivo unutar samog sustava, a na vrlo kompleksan način su povezani s radnim parametrima motora s unutarnjim izgaranjem i što je detaljno obrađeno na

početku ovog poglavlja i kroz pregledni rad [2]. Pregled osnovnih karakteristika različitih emisijskih modela i modela potrošnje goriva prikazan je na slici 24.
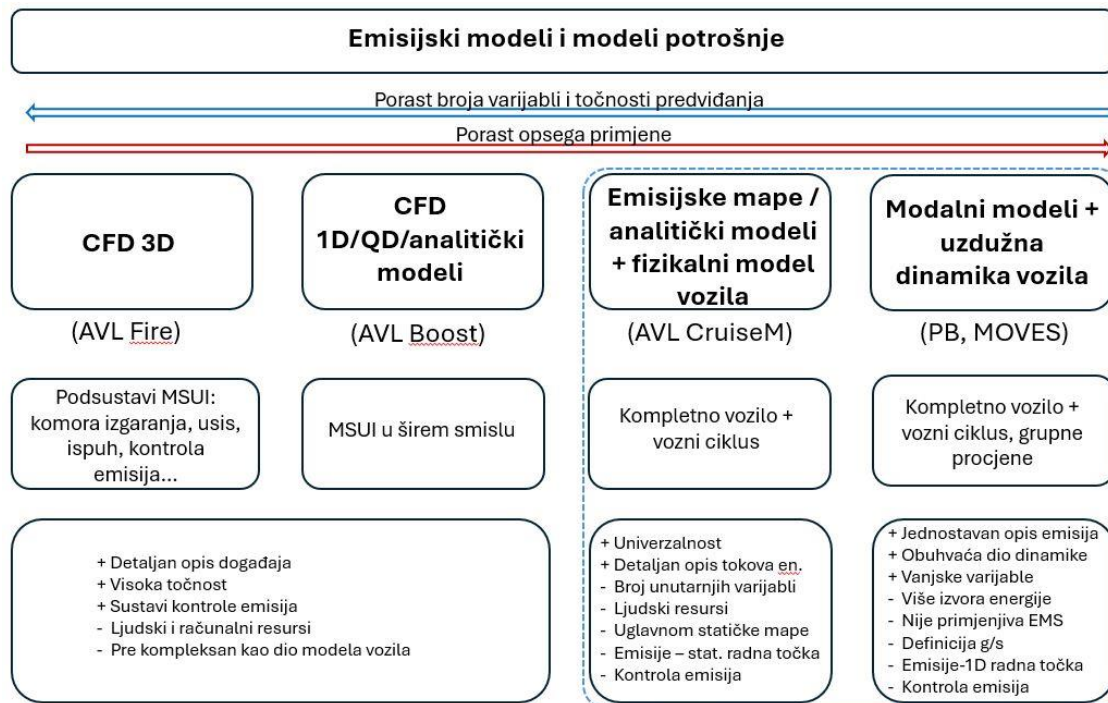
Slika 24. *Pregled različitih emisijskih modela i modela potrošnje goriva.*

Numerički, jedno ili višedimenzionalni emisijski modeli i modeli potrošnje goriva (modeli izgaranja), kao i složeni empirijski modeli koji se oslanjaju na velike brojeve unutarnjih varijabli, koriste se u specifičnim područjima istraživanja kao što je razvoj MSUI-ja, kao primjerice u radu [1], ali nisu prihvatljivi u modeliranjima kompletnih vozila. Kombinacija fizikalnih modela uzdužne dinamike vozila i energetskih tokova pogonskih sustava vozila sa stacionarnim emisijskim mapama, i mapama potrošnje goriva, predstavljaju uobičajen način modeliranja klasičnih i hibridnih vozila. Takvi su modeli nezamjenjivi u području razvoja pojedinačnih sustava zbog fizikalnog opisa svih ključnih komponenti. Osnovni su nedostaci zanemarivanje tranzijentnih utjecaja na količine emisija i potrošnju goriva koje je vrlo teško povezati s vanjskim varijablama kao i za ogroman broj varijabli, osobito kad su u pitanju hibridna vozila. Predviđanje emisija vezano je isključivo za trenutnu radnu točku motora, dok su smjer dostizanja radne točke, kao i povijest događaja, najčešće zanemareni unatoč značajnom utjecaju osobito na sustave za kontrolu emisija [2]. Zbog izrazitih prednosti u vidu ovisnosti većinom o vanjskim lako dostupnim varijablama i značajno jednostavnijem zapisu, modalni

modeli prikladni su u procjenama emisija i potrošnje goriva vozila, osobito u stvarnim uvjetima upotrebe i u grupnim procjenama. Modalni modeli na osnovi pogonske snage ili specifične pogonske snage VSP-a pokazuju značajno bolju korelaciju s parametrima MSUI-ja u odnosu na ostale skupine modalnih modela, a time i s emisijama i potrošnjom goriva samih vozila. Jedan od uzroka pojedinačnih odstupanja leži u činjenici da je klasična VSP definicija modalnih emisija definirana kao maseni protok u jedinici vremena [104]. Na ovaj se način u odnosu na definiciju količine pojedinih emisija po jedinici vučne energije otvara mogućnost dodatne pogreške unutar svakog modalnog razreda, ovisno o njegovoj širini. Primjena modalnih modela na hibridna vozila slabo je zastupljena u literaturi zbog slabije korelacije klasične definicije VSP parametra s emisijama i potrošnjom goriva, iz razloga postojanja dva izvora energije od kojih je samo jedan odgovoran za emisije i potrošnju goriva [115], dok strategija upravljanja energijom regulira njihove odnose. Najčešće se koriste samo djelomični modeli HEV-a temeljeni na VSP analizi za procjenu grupne potrošnje goriva i emisija HEV-a u različitim uvjetima vožnje. Ovi modeli ne primjenjuju tokove energije koji su neophodni u izradi strategije upravljanja i njezinoj optimizaciji, odnosno procjenu maksimalne učinkovitosti hibridizacije. Autori modalnih modela hibridnih vozila obrađenih u literaturi [116-118] uglavnom korigiraju klasični VSP model regresijskim faktorima u svrhu poboljšanja predviđanja emisija i potrošnje goriva, ali bez značajne uzročno-posljedične interpretacije koja bi dovela do zaključaka o uzrocima odstupanja. Unatoč korekcijama, točnosti predviđanja emisija i potrošnje goriva znatno su lošiji u usporedbi s modalnim modelima klasičnih vozila.

S obzirom na postojeće znanstvene spoznaje, prethodno obrađene u ovom poglavlju, može se zaključiti da područje modalnih modela nije dovoljno istraženo i da postoji značajan prostor za poboljšanje u području modeliranja hibridnih vozila. Potrebno je predložiti novi model emisija i potrošnje goriva hibridnog vozila temeljen na potpuno drugačijem pristupu koji će zadržati prednosti sadašnjih modalnih modela u vidu broja varijabli, uz uključivanje specifičnosti i rješavanje nedostataka postojećih modela hibridnih vozila, nedostatka VSP modela i problema tranzijentnog ponašanja. Shematski prikaz nastanka modela prikazan je na slici 25.
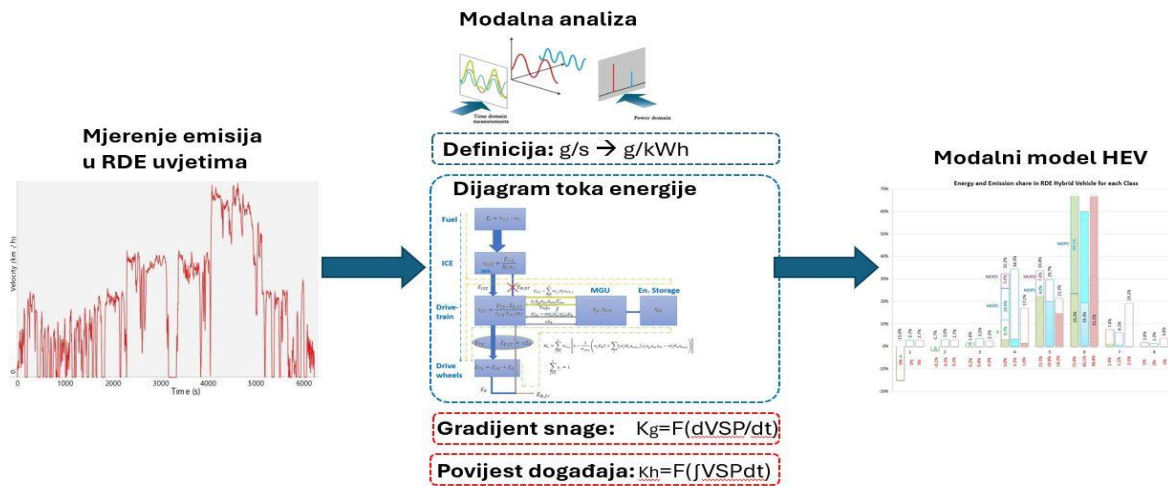
Slika 25. Planirani elementi emisijskog modela HEV-a.

Osnovni preduvjet kvalitetnog predviđanja emisija i potrošnje goriva hibridnog vozila podrazumijeva mogućnost primjene strategija upravljanja energijom na najvišoj razini koje omogućavaju razlikovanje više od jednog izvora energije. Strategija upravljanja definira se u odnosu na tokove energije čije univerzalne definicije, orijentirane prema elementu [120], oslanjaju se na relativno velik broj unutarnjih varijabli koje treba svesti na najmanju moguću mjeru uz zadržavanje točnosti na zadovoljavajućoj razini. To je moguće postići korištenjem predloženog toka energije, hibridnog vozila, orijentiranog prema funkciji [121]. Definicija modalnih emisija po jedinici pogonske energije povećava točnost predviđanja unutar modalnog razreda u odnosu na klasičnu definiciju masenog protoka. Korištenje ulaznih podataka iz stvarnih uvjeta upotrebe umjesto podataka iz stacionarnih uvjeta uključuje dio tranzijentnog ponašanja emisijskog modela. Za kvalitetnije predviđanje emisija kod izraženijih tranzijenata i hladnih startova nije dovoljno definiranje emisija u trenutnoj radnoj točki koja uključuje uprosječenu dinamiku. Naime, potrebno je uključiti utjecaj gradijenta snage kao i povijest događaja koji su većinom povezani sa sustavima kontrole emisija [2].

3. PROVEDENO EKSPERIMENTALNO I NUMERIČKO ISTRAŽIVANJE I RAZVOJ EMISIJSKOG MODELA

3.1. Primjena numeričkog 1D/QD modela motora u ispitivanju koncepta povećanja učinkovitosti izmjene radne tvari kod benzinskog motora pri djelomičnom opterećenju

Pregledom literature, nadolazeći emisijski propisi [10, 122], raskorak u odnosu na emisije u stvarnim uvjetima upotrebe [75, 123, 124] i dugoročni planovi o ograničenjima CO_2 emisija [7] detektirani su kao najveći izazovi, a možda i ključni problemi opstanka vozila pokretanih motorima s unutarnjim izgaranjem. Prijedlozi rješenja dijelom leže u boljim predviđanjima emisija i potrošnje goriva kroz kvalitetnije modele kao i u povećanju učinkovitosti ključnih komponenti pogona. Prvi je korak eksperimentalnog istraživanja primjena numeričkog modela u ispitivanju koncepta povećanja ukupne učinkovitosti benzinskog MSUI-ja kroz povećanje učinkovitosti izmjene radne tvari.

Glavni je cilj rada [1] potvrditi hipotezu da je moguće značajno povećati ukupnu učinkovitost pri niskim opterećenjima kod benzinskog motora s direktnim ubrizgavanjem i fiksnom geometrijom usisa i ispuha dodatnim otvaranjem ispušnog ventila u taktu kompresije.

Zbog prirode rada benzinskog motora s približno stehiometrijskim omjerom zraka i goriva u gotovo cijelom rasponu opterećenja potrebno je vršiti regulaciju količine usisanog radnog medija. Kod klasičnih motora regulacija snage vrši se zaklopkom na usisu odnosno prigušenjem koje uzrokuje značajne gubitke kod izmjene radne tvari, odnosno utječe na ukupnu učinkovitost prema (3.4). Prethodno opisani efekt je osobito izražen kod niskih opterećenja gdje je potreba za prigušenjem veća. Za potrebe ovog istraživanja korišten je AVL-ov programski paket BOOST koji koristi kvazidimenzionalni model (qD) za simuliranje pojava unutar cilindra i jednodimenzionalni model (1D) za simuliranje usisa i ispuha. Kao model izgaranja korištena je Vibeova funkcija i Woschni model prijenosa topline. Shematski prikaz korištenog modela motora prikazan je na slici 26. Odabrani su parametri niskog opterećenja i brzine vrtnje koji približno odgovaraju NEDC ciklusu i to 2000 o/min i srednjeg efektivnog tlaka (*engl. Brake Mean Effective Pressure*) BMEP 2 bar, 3 bar i 4 bar kako za standardni model motora tako i za novi model.
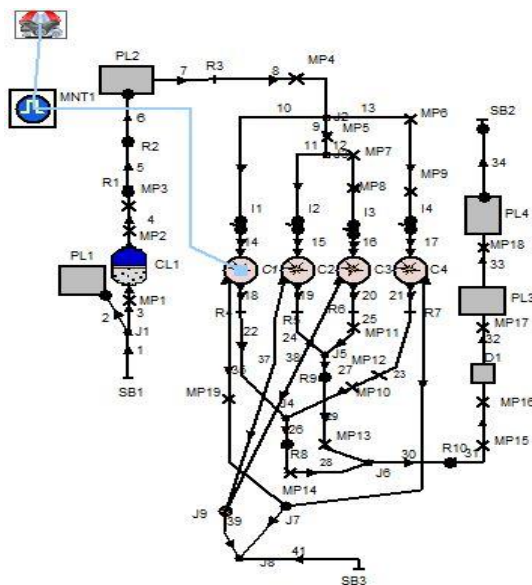
Slika 26. Grafički prikaz testnog modela motora u programskom paketu AVL-Boost.

Ključni promatrani parametri su srednji indicirani efektivni tlak IMEP definiran prema (3.1), IMEP-hp odnosno srednji efektivni tlak u cilindru za vrijeme takta kompresije i ekspanzije te srednji efektivni tlak izmjene radnog medija za vrijeme takta usisa i ispuha PMEP. Omjer ovih dvaju tlakova IMEP-hp/PMEP je mjera za učinkovitost motora, a još se naziva i učinkovitost izmjene radne tvari k_{ex} (3.3). Indicirana učinkovitost motora η_i predstavlja učinkovitost pretvorbe kemijske energije goriva u mehaničku, prije mehaničkih gubitaka trenja (3.2), gdje se uvrštavanjem u (3.3) dobije izraz koji dovodi u vezu učinkovitost izmjene radne tvari s ukupnom indiciranom učinkovitosti (3.4).

$$IMEP = IMEP_{hp} + PMEP \tag{3.1}$$

$$\eta_i = \frac{\int_{CD} p_c dv}{m_f h_d} = \frac{\frac{1}{Vc} Vc \int_{CD} p_c dv}{m_f h_d} = \frac{V_c\, IMEP}{m_f h_d} \tag{3.2}$$

$$k_{ex} = \frac{IMEP_{hp}}{|PMEP|} \tag{3.3}$$

$$\eta_i = \eta_{hp} \left(1 - \frac{1}{k_{ex}} \right)$$
(3.4)

Prikaz gubitaka i učinkovitosti izmjene radne tvari najbolje je vidljiv u p-V dijagramu, dio ispod linije atmosferskog tlaka, točnije tlaka koji vlada u kućištu koljenastog vratila, a koji predstavlja gubitke u radu motora. Omjer površina koje zatvara petlja iznad linije atmosferskog tlaka IMEP-hp i površine koje zatvara petlja ispod te linije PMEP-a, predstavlja učinkovitost izmjene radne tvari. Iz dijagrama na slici 27. vidljiv je značajan pad učinkovitosti izmjene radne tvari kod djelomičnog opterećenja, isti je prikazan crvenom linijom.
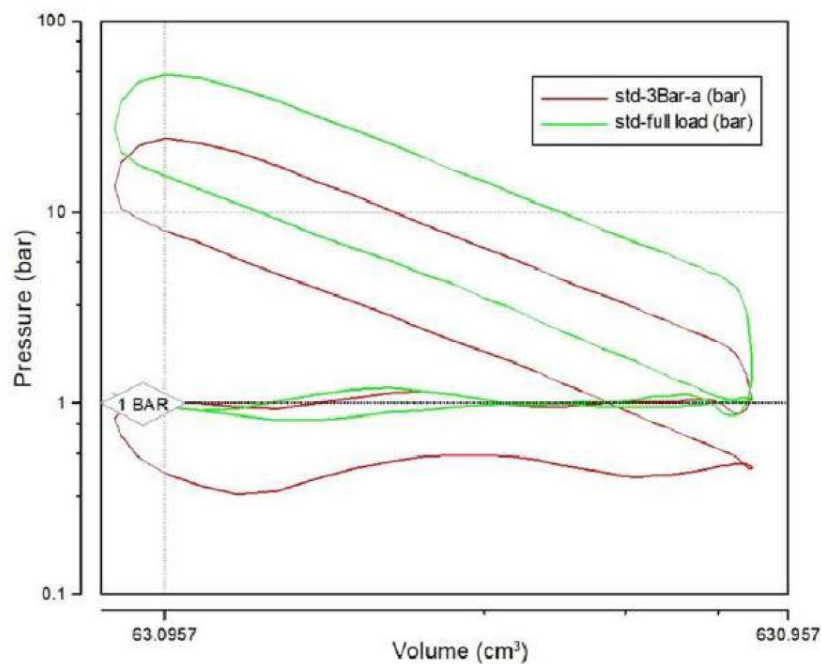
Slika 27. Indikatorski dijagrami testiranog motora [1].

Crvena krivulja na slici 27. prikazuje primjer rezultata indikatorskog dijagrama standardne verzije testiranog proračunskog modela pri 2000 o/min i srednjem efektivnom tlaku 3 bar, dok druga krivulja prikazuje tlak u istom cilindru pri jednakoj brzini vrtnje s potpuno otvorenom zaklopkom na usisu, tj. maksimalnim opterećenjem. Testni model motora raspolaže fiksnom fazom usisnih ventila i s mogućnošću potpune kontrole faze otvaranja i zatvaranja dodatnog ispušnog ventila radi smanjenja gubitaka za vrijeme usisa. Slika 28. prikazuje krivulju podizaja kod testiranja novog pristupa smanjenja gubitaka izmjene radne tvari dodatnim otvaranjem ispušnog ventila. Varijabla VOS pomiče kut otvaranja, a varijabla VCS kut zatvaranja dodatnog ispušnog ventila.
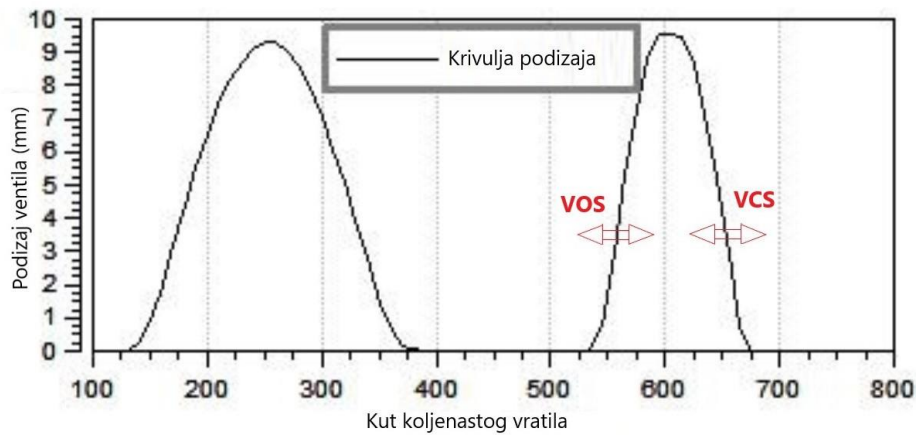
Slika 28. Podizaj ispušnih ventila u odnosu na kut koljenastog vratila.

Primjer rezultata simulacije prikazan je na slici 29. koja prikazuje ovisnost indicirane potrošnje goriva za opterećenje BMEP = 2 bar o pomacima kutova otvaranja i zatvaranja dodatnog ventila u odnosu na početno stanje opisano krivuljom podizaja.
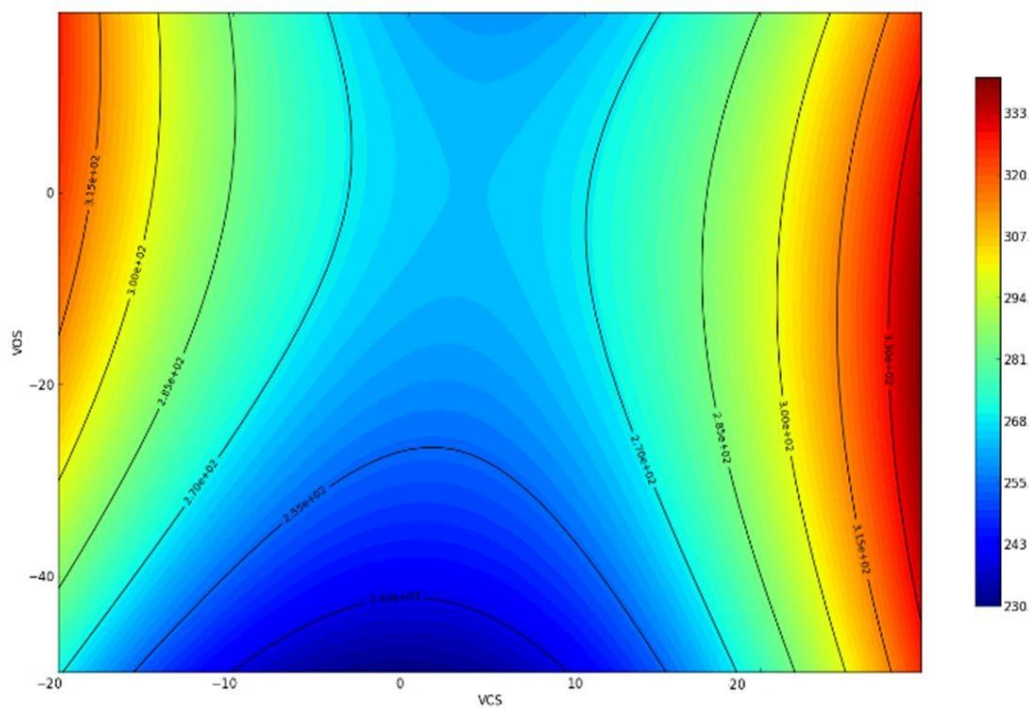
Slika 29. Ovisnost ISFC-ja o pomaku VOS-a i VCS-a (°KV) za 2 bar BMEP-a.
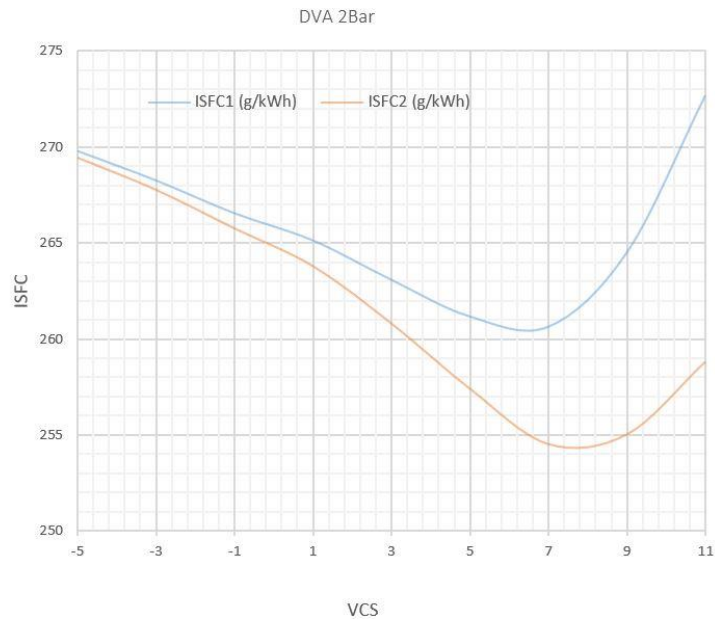
Slika 30. Ovisnost ISFC-ja o pomaku VCS-a (ºKV) za 2 bar BMEP-a.

Tablica 2. Usporedba rezultata ispitivanja

		Standardni motor			DVA 2bar		DVA 3bar		DVA 4bar	
		2 bar	3 bar	4 bar	Rezultat	Promjena	Rezultat	Promjena	Rezultat	Promjena
BMEP	bar	2,00	3,00	4,00	2,00	0,00%	3,00	0,00%	4,00	0,00%
FMEP	bar	0,94	0,94	0,94	0,94	0,00%	0,94	0,00%	0,94	0,00%
IMEP-hp	bar	**3,57**	**4,49**	**5,42**	**3,01**	**-15,69%**	**3,98**	**-11,36%**	**4,98**	**-8,12%**
PMEP	bar	**-0,63**	**-0,55**	**-0,48**	**-0,08**	**-87,30%**	**-0,07**	**-86,91%**	**-0,07**	**-85,21%**
PMEP-i	bar	**0,39**	**0,46**	**0,53**	**0,94**	**139,74%**	**0,94**	**104,35%**	**0,94**	**77,36%**
PMEP-e	bar	-1,01	-1,01	-1,01	-1,02	0,69%	-1,01	0,00%	-1,01	0,00%
IMEP-hp/PMEP		**5,67**	**8,16**	**11,29**	**37,63**	**563,97%**	**55,28**	**577,12%**	**70,14**	**521,17%**
VCS	°CA				7,00		0,00		-7,00	
DVA-VC	°CA				672,00		665,00		658,00	
Efektivni komp. omjer	–	10,5	10,5	10,5	5,21	-50,43%	4,78	-54,52%	4,09	-61,08%
BSFC	g/kWh	397,1	333,1	300,1	382,88	-3,58%	320,21	-3,87%	289,36	-3,58%
ISFC	**g/kWh**	**271,3**	**254,2**	**243,3**	**260,65**	**-3,93%**	**243,44**	**-4,23%**	**233,98**	**-3,83%**
Učinkovitost motora	–	0,208	0,248	0,275	0,216	3,85%	0,258	4,03%	0,286	4,00%
Indicirana Učinkovitost	**–**	**0,305**	**0,326**	**0,339**	**0,325**	**6,56%**	**0,342**	**4,91%**	**0,354**	**4,42%**
Maksimalni tlak u cilindru	bar	19,7	24,2	28,7	16,04	-18,58%	20,25	-16,32%	24,71	-13,90%

Pronalazak optimalnog rješenja je dvodimenzionalni problem u ovisnosti o pomaku zatvaranja i pomaku otvaranja ventila, ali se za svako pojedino opterećenje može svesti na jednodimenzionalni, slika 30., jer se približno optimalni rezultati postižu za minimalne vrijednosti VOS-a, koji je ograničen donjom granicom od 0 stupnjeva, odnosno početkom takta

kompresije. Najmanja opterećenja motora zahtijevaju najdulje kutove otvaranja ventila zbog najvećeg viška radnog medija, s tim da je ograničavajući kut zatvaranja vezan za početak ubrizgavanja goriva u cilindar zbog čega učinkovitost za veće kutove naglo opada. Određeni su optimalni kutovi pomaka otvaranja od 7, 0 i -7 °KV-a za opterećenja 2, 3 i 4 bar BMEP-a te isti jako ovise o geometrijskim karakteristikama motora, s tim da korelacija između duljine otvorenosti i srednjeg efektivnog tlaka ostaje. Detaljni rezultati ispitivanja prikazani tablicom 2. pokazuju značajan napredak u odnosu na standardan motor s fiksnom geometrijom usisa i ispuha [1]. Specifična potrošnja goriva odnosno CO_2 emisije smanjene su između 3,83 % i 4,23 %, ukupni gubici izmjene plinova u cilindrima smanjeni su između 85 % i 87 %, dok je učinkovitost izmjene radne tvari porasla za više od šest puta čime je dokazana hipoteza rada [1]. Dobici smanjenjem gubitaka izmjene radne tvari nešto su manji od očekivanih zbog povećanih gubitaka topline. Zanimljiv je i podatak o maksimalnim tlakovima u cilindru, prvenstveno sa stajališta ekologije i trajnosti motora, koji su niži od 13, 9 % do 18,6 % u odnosu na standardni motor pri jednakim opterećenjima. Najveći dobici ispitivanog pristupa su pri najmanjim opterećenjima i postignuti su minimiziranjem gubitaka izmjene radnog medija za vrijeme usisa, dok pri velikim opterećenjima benefiti ovakvog pristupa nestaju. Isti je motor uz dodatak kontrole usisnih ventila testiran u Atkinsonovu i Millerovu ciklusu koji su danas u serijskoj primjeni. Budući da su ostvareni slični rezultati s komercijalno ispitanim metodama, daljnji razvoj koncepta kod atmosferskih motora nije potreban. Ideja za primjenu ovakvog koncepta proizišla je iz područja prednabijanih motora koje može biti jedan od smjerova daljnjih istraživanja ovdje predloženog pristupa. Kod atmosferskih motora gornja granica tlaka koji vlada u cilindru je približno atmosferski tlak, dok je kod prednabijanih motora to tlak prednabijanja. Samim time imamo na raspolaganju veće područje povećanja učinkovitosti, i ne samo smanjenjem gubitaka tijekom usisa kod niskih opterećenja nego je moguće dobiti pozitivan rad korištenjem energije prednabijanja turbopunjača, bez namjernog narušavanja njegove učinkovitosti, kroz ekspanziju u cilindru tijekom takta usisa. Ako promatramo sa stajališta redukcije gubitaka izmjene radne tvari i toplinskih tokova, primijenjeni model predstavlja optimum između razine složenosti i kvalitete dobivenih podataka. Nedostatak modela u smislu točnosti je nemogućnost procjene utjecaja na promjene u učinkovitosti izgaranja zbog promjena u vrtloženju, za čiju je procjenu nužno korištenje značajno složenijeg trodimenzionalnog CFD modela komore izgaranja. S druge strane, unatoč univerzalnosti i visokoj razini točnosti u pogledu procjene emisija štetnih tvari, upotreba CFD modela je najčešće neprihvatljiva kod modeliranja emisija i modela potrošnje goriva kompletnih vozila, zbog izrazite kompleksnosti i potrebe za velikim ljudskim i računalnim resursima, zbog čega je

upravo fokus istraživanja premješten na proučavanje prihvatljivijih modela opisanih u preglednom poglavlju.

3.2. **Predstavljanje modalnog modela hibridnog električnog vozila i analiza utjecaja kvara sustava za regulaciju emisija na njihov nastanak temeljena na metodi grupiranja snage**

Iz opširnog proučavanja postojeće literature iz područja sustava za kontrolu emisija kroz objavljeni pregledni rad [2] kao i modeliranja MSUI-ja 1D/QD modelom u [1], proizašli su ključni zaključci o daljnjem smjeru istraživanja.

Najveći dio problema emisija cestovnih vozila vezan je za količine emisija štetnih tvari i emisija CO_2 u stvarnim uvjetima upotrebe kao i u trajnoj eksploataciji. Raskorak između emisija štetnih tvari novih vozila u stvarnim uvjetima upotrebe i graničnih vrijednosti odgovarajućih emisijskih propisa dobro je istražen nakon „Dieselgate" afere [75, 125]. Postojeća istraživanja obuhvaćaju uglavnom novija vozila u početku eksploatacijskog perioda [75, 126] jer se relativno skupa istraživanja provode u razvijenim dijelovima svijeta. Količine emisija štetnih tvari neispravnih vozila, vozila u dugotrajnoj eksploataciji i prijedlozi načina rješavanja problema kontrole nisu dovoljno obrađeni u postojećoj literaturi.

Ključni problem sljedećih generacija vozila u cestovnom prometu je zadovoljavanje strogih emisijskih propisa u svim uvjetima upotrebe i ambiciozni planovi smanjenja emisija CO_2, što je nedostižno bez hibridnih pogonskih sustava. Problemi klasičnih vozila koje rješavaju hibridni pogoni vezani su za brzinu zagrijavanja katalitičkih sustava kontrole emisija, utjecaje sustava recirkulacije ispušnih plinova na brzinu odziva kod promjene opterećenja i bolju kontrolu opterećenja kod sustava s periodičnom regeneracijama poput regeneracije filtera čestica ili LNT katalizatora [2]. Kombinacija visoke složenosti sustava za kontrolu emisija i specifičnosti hibridnih pogonskih sustava stvaraju potrebu za kvalitetnijim modelima HEV-a u smislu točnosti predviđanja, dok je primjerice istraživanje [1] pokazalo da visoka razina složenosti CFD modele MSUI-ja čini neprikladnima u modeliranju vozila.

Iz navedene problematike je proizašlo pet hipoteza znanstvenog istraživanja objavljenog u [3]:

1. Količine emisija štetnih tvari vozila u eksploataciji, sa svim ispravnim komponentama za njihovo smanjenje, iznad su zakonom propisanih za vozila tipski odobrena prema NEDC laboratorijskom ciklusu ispitivanja u stvarnim propisanim uvjetima upotrebe.

2. Količine štetnih emisija u stvarnim uvjetima upotrebe vozila s kvarom sustava za kontrolu emisija višestruko premašuju zakonom propisane granice i kod vozila koja normalno prolaze tehničku kontrolu ispravnosti. Navedena su odstupanja izraženija kod vozila koja su tipski odobrena prema strožim emisijskim propisima.

3. Na temelju podataka iz stacionarnog ispitivanja, u sklopu godišnjeg periodičnog pregleda, moguće je utvrditi neispravnost sustava za kontrolu emisija dizelskih vozila bez investiranja u dodatnu opremu stanica za tehnički pregled.

4. Na osnovi modalne analize podataka o pogonskoj snazi, emisijama štetnih tvari i potrošnji goriva, uz primjenu toka energije, moguće je formirati modalne emisijske modele klasičnog i hibridnog vozila.

5. Na predloženi model moguće je primijeniti strategiju upravljanja energijom temeljenu na pravilima te odrediti maksimalne učinke hibridnog pogona u smislu smanjenja emisija štetnih tvari i potrošnje goriva.

Za mjerenje i procjenu emisija odabrana je metoda grupiranja snage [127] koja se temelji na Jimenezovoj VSP analizi [104]. Određivanje količine emisija ovom metodom temelji se na procjeni normizacijom na distribuciju standardne frekvencije snage te podrazumijeva njihovo mjerenje i bilježenje u stvarnim uvjetima vožnje na cesti uz uobičajene uvjete opterećenja i načina vožnje. Ispitivanja svih šest vozila provedena su na istoj ruti prikazanoj na slici 31.
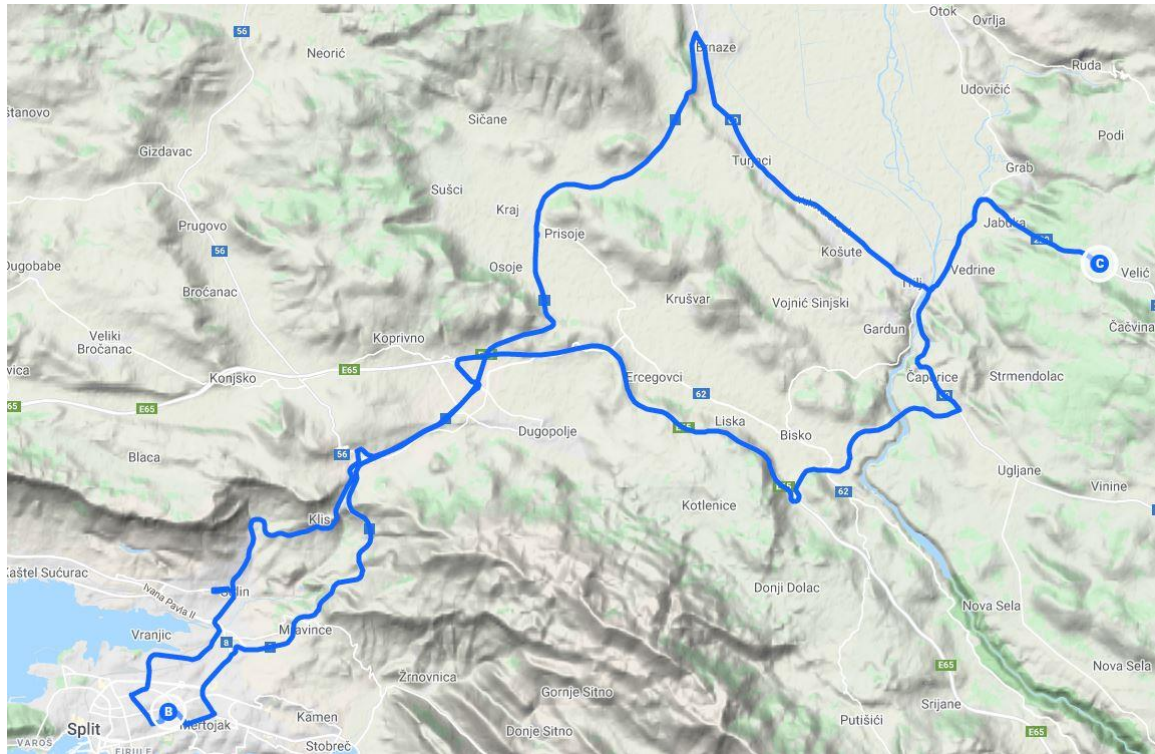
Slika 31. Prikaz testne rute na topografskoj karti.

Za mjerenje sastava ispušnih plinova korišten je analizator ispušnih plinova *MRU Vario Plus Industrial* čiji je princip mjerenja temeljen na elektrokemijskom efektu za mjerenje O_2, NO i NO_2 te metodi nedisperzivne infracrvene spektrometrije za mjerenje CO, CO_2, HC i SO_2. Analizator plinova opremljen je Pittotovom cijevi za mjerenje brzine i sondom Pt100 za mjerenje temperature ispušnih plinova. Za potrebe ovog mjerenja izrađena je posebna mjerna cijev s prilagodljivim priključcima na ispušne cijevi svih ispitivanih vozila te priključcima za analizator i Pittot cijev, slika 32.

Slika 32. Oprema za mjerenje emisija postavljena na vozilo.

Snaga na pogonskim kotačima određena je iz momenta i kutne brzine kotača. Sustav mjerenja momenta na pogonskim kotačima također je izrađen u laboratoriju za toplinske strojeve i prilagođen je svakom vozilu zasebno. Moment je mjeren direktno postavljanjem tenzometarskih traka na pogonsku osovinu jednog kotača. Signal s rotirajuće osovine prikupljen je preko bežičnog programabilnog dvokanalnog predajnika *Sg-Link-OEM-LXRS* tvrtke *Lord Microstrain*, slika 33.
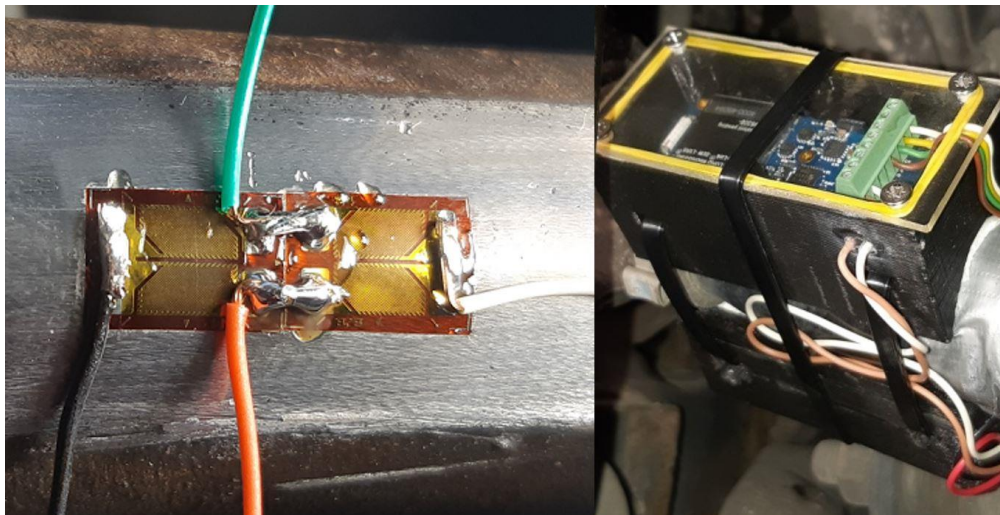
Slika 33. Mjerenje momenta direktno na pogonskoj osovini vozila.

Brzina vozila, nadmorska visina i prijeđeni put mjereni su i uz pomoć komunikacijskog sučelja temeljenog na ELM 327 koji preko OBD-a (*engl. On Board Diagnostic*) komunicira s računalima vozila. Brzina je mjerena preko broja okretaja pogonskih kotača, a korigirana signalom brzine s GPS-a.

3.2.1 Emisije vozila pokretanih dizelskim motorima u stvarnim uvjetima upotrebe i analiza utjecaja kvara sustava za regulaciju emisija na njihov nastanak temeljena na metodi grupiranja snage

Rezultati provedenog istraživanja potvrđuju prvu hipotezu ovog rada, odnosno poznatu problematiku emisija ispušnih plinova u stvarnim uvjetima vožnje ispravnih vozila [125, 128]. Unatoč tome što su u svrhu ispitivanja korištena rabljena vozila s dugim periodom eksploatacije, rezultati mjerenja slični su očekivanim rezultatima za nova vozila. Iz dobivenih podataka vidljivo je da kod vozila sa svim ispravnim komponentama postoje značajna odstupanja između izmjerenih rezultata dobivenih RDE metodom grupiranja snage i graničnih vrijednosti emisija prema kojima je vozilo tipski odobreno. Odstupanje je veće kod novijih vozila, sa strožim emisijskim propisima. Uzrok odstupanja CO_2 emisija, odnosno potrošnje goriva, prikazanog grafikonom na slici 36. je isključivo u korištenju zastarjelog NEDC ciklusa tipskog odobrenja koji loše aproksimira stvarne uvjete upotrebe [75]. Uzrok značajnog odstupanja emisija NO_X-a u odnosu na deklarirane vrijednosti krije se u korištenju visokotlačnog sustava recirkulacije ispušnih plinova koji dobro funkcionira u NEDC uvjetima tipskog odobrenja, dok mu u stvarnim uvjetima upotrebe veća prosječna snaga MSUI-ja uz dinamičniju vožnju značajno reduciraju učinkovitost. Također normalan rad EGR sustava u takvim uvjetima nepovoljno djeluje na trajnost MSUI-ja, potrošnju goriva i PM/PN emisije [43]. CO emisije su znatno ispod propisanih granica zbog prirode rada motora u režimu siromašne smjese, kvalitetnog izgaranja u kombinaciji s visokoučinkovitim oksidacijskim katalizatorima [2].

Drugi dio istraživanja daje uvid u problematiku vozila s neispravnim komponentama za kontrolu emisija koja je slabo zastupljena u literaturi. Kvarovi sustava za kontrolu NO_X emisija, u ovom slučaju većinom EGR, ali i DPF u određenoj mjeri, značajno povećavaju količine dušikovih oksida u ispušnim plinovima, grafikon na slici 34. Količina NO_X-a kod Euro 3 vozila je unutar granice propisane odgovarajućim emisijskim propisom, kod vozila s Euro 4 je veća za 86 %, a kod vozila s Euro 5 za 228 %, u odnosu na dopuštenu granicu s faktorom sukladnosti CF=2,1.
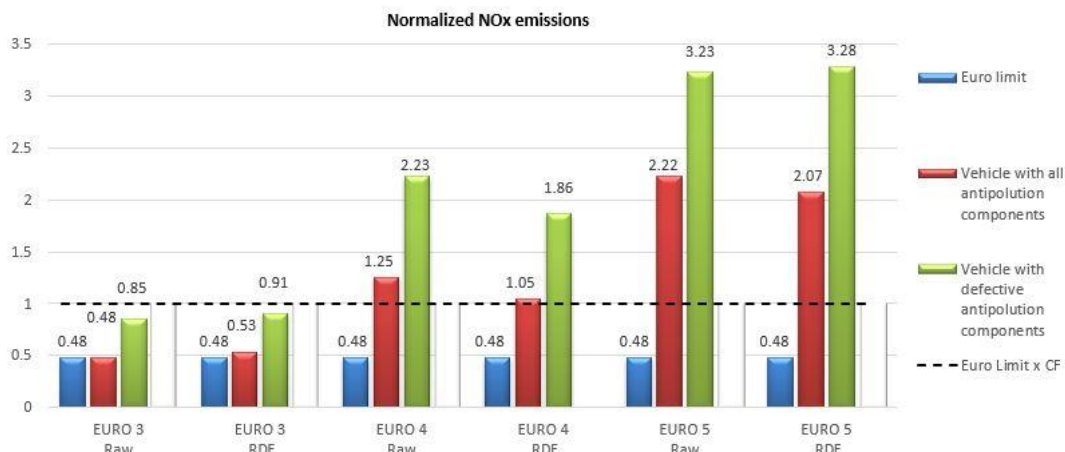
Slika 34. Usporedba jediničnih rezultata emisija NO_X-a u odnosu na granične vrijednosti za statistički standardizirane emisije prema RDE-u i neobrađeni podaci mjerenja [3].
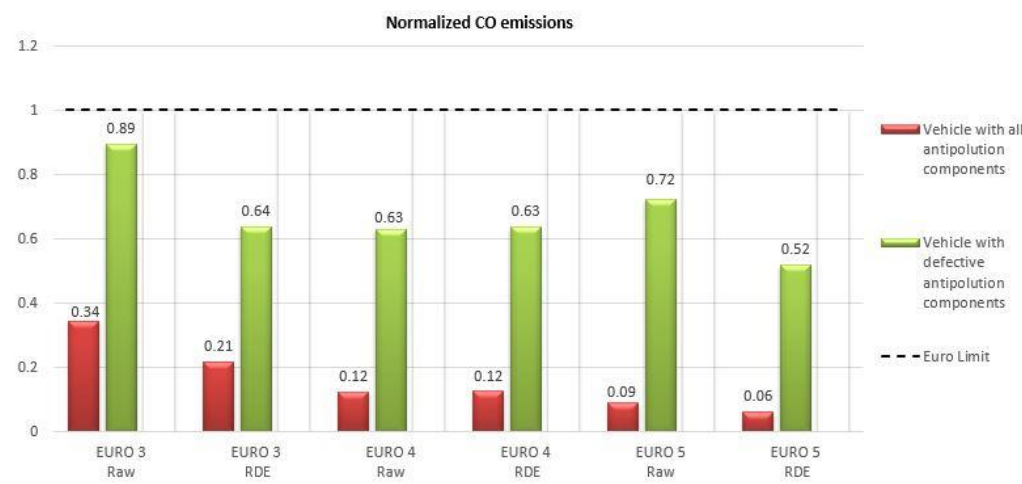
Slika 35. Usporedba jediničnih rezultata emisija CO u odnosu na granične vrijednosti za statistički standardizirane emisije prema RDE-u i neobrađeni podaci mjerenja [3].
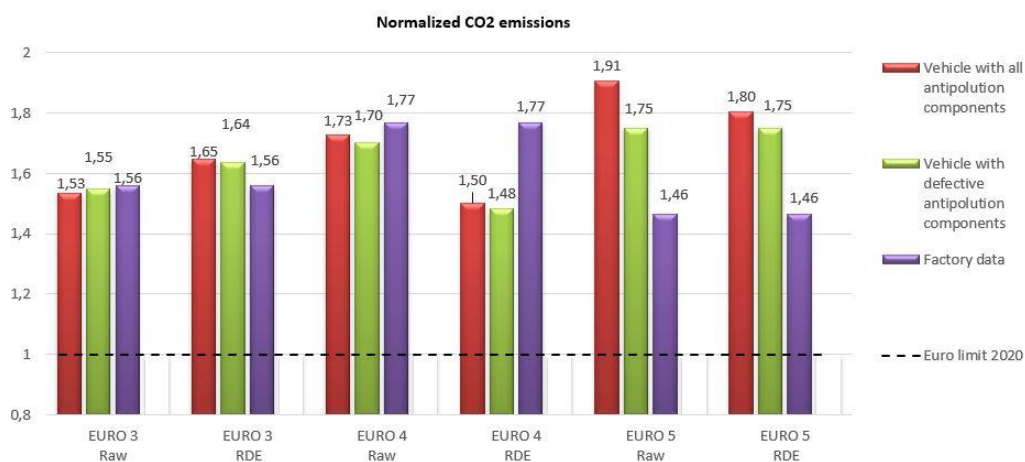
Slika 36. Usporedba jediničnih rezultata emisija CO_2 u odnosu na granične vrijednosti za statistički standardizirane emisije prema RDE-u i neobrađeni podaci mjerenja [3].

Veći značaj sustava za regulaciju emisija NO_X-a zabilježen kod novijih vozila, odnosno motora s višim emisijskim razinama, pripisuje se kvalitetnijim parametrima izgaranja s višim vršnim temperaturama i dobrom ispiranju cilindara koji pogoduju generiranju visokih koncentracija dušikovih oksida. Ovdje je za smanjenje emisija NO_X-a nužan rad s visokim koncentracijama recirkuliranih plinova u cilindru [43]. Količina CO_2 emisija i potrošnje goriva smanjila se neutralizacijom komponenti za kontrolu emisija kod svih ispitanih vozila, s tim da je zabilježen značajniji utjecaj kod Euro 5 vozila od oko 3 %, bez utjecaja regeneracije filtera čestica. Uzrok smanjenja potrošnje goriva je kvalitetnije izgaranje s višim vršnim temperaturama zbog izostanka EGR-a koji je kod strožih emisijskih standarda izraženiji, također su i veći povratni tlakovi katalitičkih pretvarača i finijih filtera čestica [56]. Za razliku od prosječnih normalnih uvjeta opterećenja, kod ekstremno niskih opterećenja zabilježena je do 10 % manja potrošnja goriva, odnosno CO_2 emisije ako je sustav recirkulacije ispravan. Ova se pojava može objasniti smanjenjem gubitaka izmjene radne tvari kod ispravnih sustava visokotlačnog EGR-a. Iz prethodno navedenog jasno je da je druga hipoteza uglavnom potvrđena s iznimkom CO emisija. CO emisije unatoč izostanku oksidacijskog katalizatora su unutar dozvoljenih granica, grafikon na slici 35. Iz navedenog proizlazi da nisu značajan problem kod vozila pokretanih dizelskim motorom unatoč značajnim povećanjem u odnosu na ispravna vozila. Kod Euro 5 vozila zabilježeno je povećanje od devet puta.

Detektiranje neispravnih ili uklonjenih komponenti za kontrolu emisija tijekom redovnih tehničkih pregleda predstavlja značajan problem jer ih najčešće nije moguće detektirati preko postojeće kontrole zabilježenih grešaka. Također mjerenja emisija u vožnji zbog visoke cijene i utroška vremena nisu opcija. Sva ispitana vozila normalno prolaze kontrolu tehničke ispravnosti unatoč neispravnim sustavima za kontrolu emisija. Predložena je i dokazana funkcionalnost koncepta na ispitivanim vozilima koja se temelji na mjerenjima u mirovanju s već postojećom opremom stanica za tehnički pregled, čime je potvrđena treća hipoteza ovog istraživanja.

Odsutnost ili neispravnost katalitičkog pretvarača moguće je dokazati povećanom koncentracijom CO i HC emisija. Izmjereno povećanje CO emisija u standardnoj vožnji kretalo

se između 200 % i 800 %, dok su koncentracije CO u praznom hodu porasle između 2,4 i 100 puta u odnosu na ispravna vozila, dijagram na slici 37.
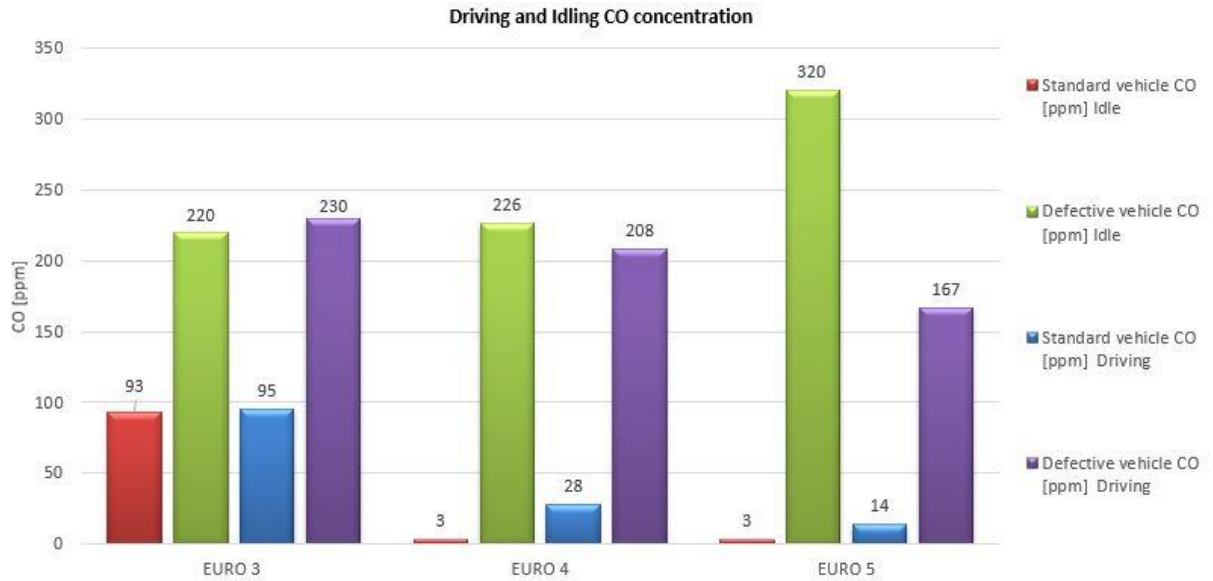
Slika 37. CO emisije u praznom hodu i u vožnji [3].

Na rezultate mjerenja CO i HC emisija u praznom hodu jako utječe temperatura oksidacijskog katalizatora [2]. Izmjerena ovisnost učinkovitosti oksidacijskih katalizatora o temperaturi prikazana je grafikonom na slici 38. Iz navedenog proizlazi da je potrebno osigurati njegovu povišenu temperaturu prethodnim radom na povišenoj brzini vrtnje i mogućom kontrolom preko OBD dijagnostičkog sučelja.
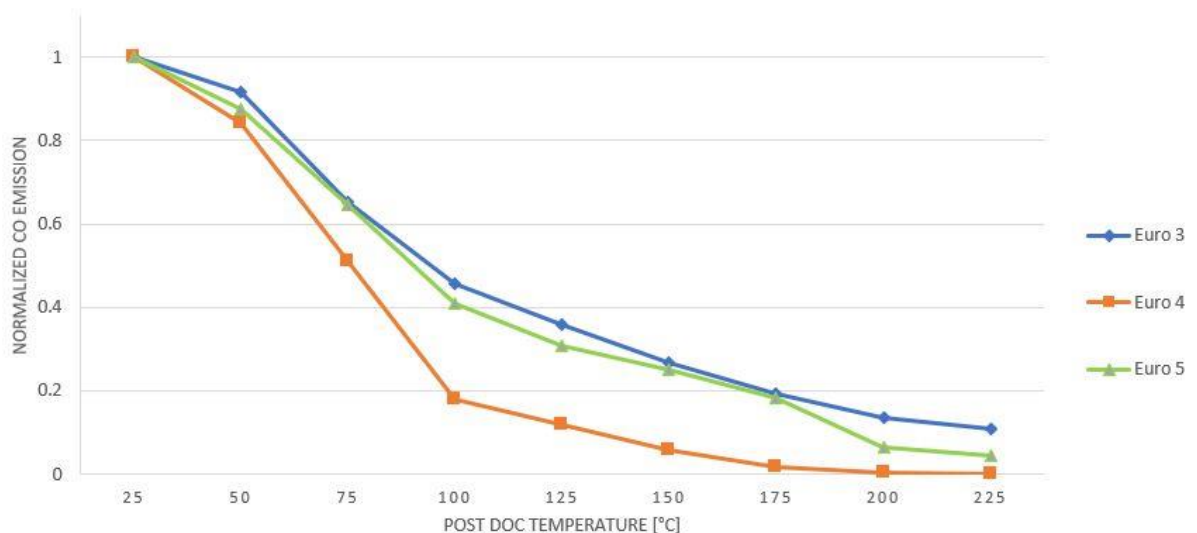
Slika 38. Učinkovitost oksidacijskog katalizatora u ovisnosti o temperaturi [3].

Dijagram na slici 39. prikazuje vezu između ispravnosti sustava recirkulacije ispušnih plinova EGR-a, tj. osnovnog sustava za kontrolu dušikovih oksida i omjera zraka i goriva ili pretička kisika, za vrijednosti u vožnji i za rad u praznom hodu. Prema rezultatima jedno od mogućih rješenja otkrivanja nepravilnosti je mjerenje omjera zraka i goriva.
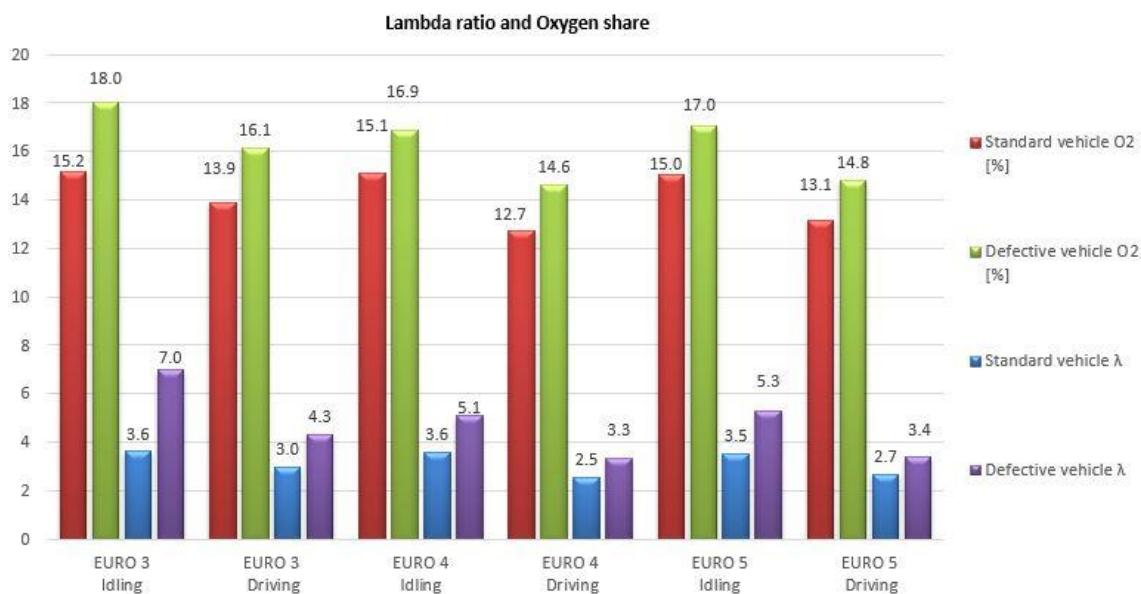
Slika 39. Pretičak kisika u vožnji i praznom hodu [3].

Izmjereni odnos zrak/gorivo u ispušnim plinovima pri praznom hodu kod vozila s neispravnim sustavom za recirkulaciju ispušnih plinova povećan je za 94 % kod Euro 3 vozila, 43 % za Euro 4 i 51 % za Euro 5 vozila.

Za uspješnu primjenu prethodno navedenih postupaka dijagnostike potrebno je napraviti tipsku bazu modela ponašanja koja pokriva većinu modela vozila. Iz prikazanog se vidi da je potrebno napraviti minimalno podjelu prema pripadajućem emisijskom propisu. Daljnje istraživanje potrebno je usmjeriti prema mogućnostima grupiranja podataka u odnosu na primijenjene tehnologije kontrole emisija, snage i tipove vozila u svrhu pojednostavljenja izrade tipske baze podataka.

3.2.2.   Predstavljanje modalnog emisijskog modela i modela potrošnje goriva hibridnog električnog vozila i primjena na ispitivano vozilo

Za formiranje emisijskog modela i modela potrošnje goriva HEV-a odabran je parametar trenutne pogonske snage odnosno specifične snage, čiji je analitički opis predstavljen u [104]. Odabran je zbog značajno bolje korelacije s emisijama i potrošnjom goriva u odnosu na ostale direktno mjerljive parametre iz literature i zbog mogućnosti povezivanja s energetskim tokovima HEV-a. Otpori vozila modelirani su polinomom drugog stupnja (3.5), čiji su koeficijenti određeni regresijskom analizom najmanjih kvadrata pomoću testa slobodnog usporavanja [129], iz čega proizlazi analitički opis (3.6)

$$f_0 + f_1 \cdot v + f_2 \cdot v^2 = m\frac{dv}{dt} \tag{3.5}$$

$$VSP = \frac{\frac{d}{dt}(KE + PE) + F_{roll} \cdot v + F_{aero} \cdot v}{m} = \frac{\frac{d}{dt}(KE + PE) + F_{res} \cdot v}{m}$$
$$= \frac{\frac{d}{dt}\left(\frac{1}{2}m \cdot v^2 + mgh\right) + (f_0 + f_1 \cdot v + f_2 \cdot v^2) \cdot v}{m} \tag{3.6}$$

Model je kreiran kinematičkim unatražnim pristupom koji polazi od krajnjih komponenti vozila, odnosno kotača koji zahtijevaju određeni moment da bi slijedile ciklus [17]. Ovakav pristup ne zahtijeva regulaciju u vidu povratne veze koja funkcionira samo u vremenskoj domeni. Nedostatak je „slijepo" praćenje ciklusa pa treba posebno voditi računa o odnosu maksimalnih performansi vozila u odnosu na zahtjeve ciklusa. Model se temelji na raspodijeli emisija unutar diskretnih raspona snage odnosno modalnih razreda. Polazna pretpostavka je da su odnosi količina prosječnih pojedinačnih emisija prema jediničnoj pogonskoj energiji približno jednak unutar promatranog raspona snage, bez obzira na vozni ciklus. Razvrstavanje u raspone vrši se prema granicama i uvjetima maksimalne odnosno minimalne snage pogona pojedinog raspone (3.7):

$$P_{c,j\ lower\ bound} <\quad P_{wheel} \leq P_{c,j\ upper\ bound} \tag{3.7}$$

Broj i raspored razreda preuzet je iz metode procjene emisija pomoću grupiranja snage. Definiranje granica razreda normalizacijom u ovisnosti o parametrima vozila je detaljnije

opisano u [3]. Slika 40. prikazuje vremenski udio, odnosno udio broja podataka, za provedenu testnu i za standardnu vožnju.
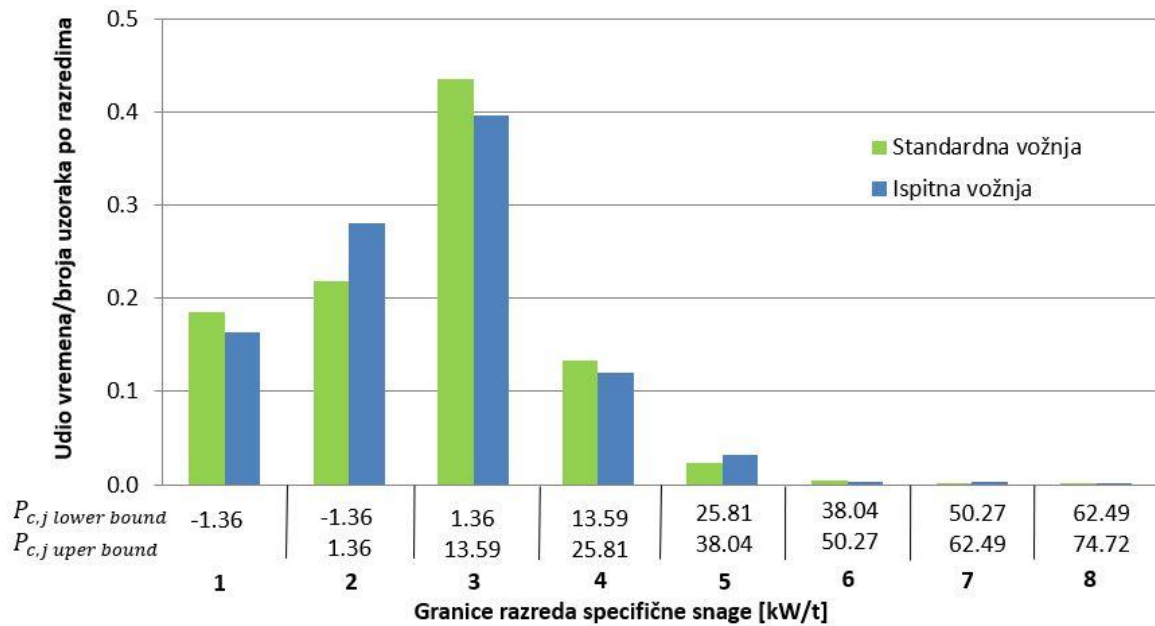
Slika 40. Granice razreda snage i udjeli u standardnoj vožnji.
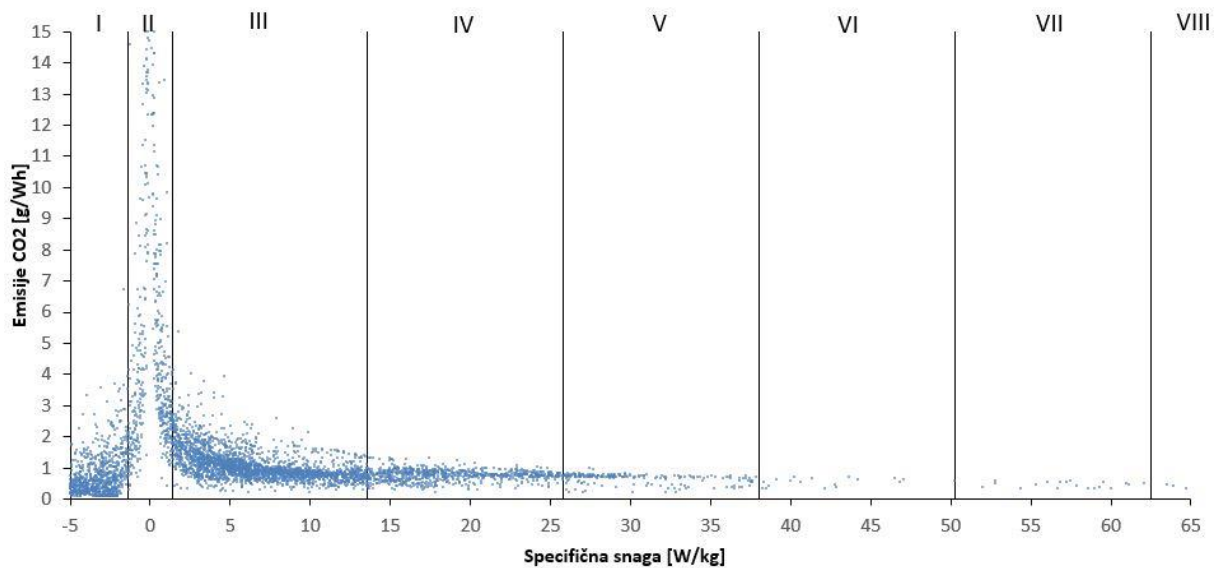
Slika 41. Izmjerene emisije CO_2 u razredima snage

Izmjereni podaci o specifičnim emisijama CO_2 raspoređeni u razrede snage su prikazani dijagramom na slici 41. Dodatno, teorijske postavke i matematički opis jedne krajnosti koja osigurava najtočniji opis, u kojoj broj razreda teži beskonačnosti, odnosno prelazak u područje kontinuirane varijable, predstavljene su i prilagođene modelu HEV-a u konferencijskom radu autora [130]. Emisije i potrošnja goriva *j*-tog raspona snage računaju se kao zbroj svih pomičnih

srednjih trenutnih vrijednosti masenog protoka $m_{x,j}$ pojedinačnih emisija x u vremenskom koraku k (3.8):

$$m_{x,j} = \sum_{all\ k\ in\ class\ j} m_{x,k} \tag{3.8}$$

Pomične srednje trenutne vrijednosti se definiraju u trosekundnom vremenskom intervalu sa frekvencijom $k=1\ s$. Izraz za pogonsku energiju j–tog raspona snage je definiran prema (3.9):

$$W_{tr,j} = m_{vehicle} \sum_{all\ k\ in\ class\ j} VSP_{tr,k} t_k \tag{3.9}$$

Zbog manje osjetljivosti odabrana je definicija po jedinici pogonske snage u odnosu na klasičnu VSP definiciju modalnih emisija preko uprosječenog protoka u jedinici vremena. Vrijednost pojedinačnih emisija po jedinici pogonske energije j-tog razreda jednaka je omjeru ukupne količine emisija razreda i njegove ukupne pogonske energije (3.10):

$$\dot{m}_{x,j} = \frac{m_{x,j}}{W_{tr,j}} = \frac{\sum_{all\ k\ in\ class\ j} m_{x,k}}{\sum_{all\ k\ in\ class\ j} P_{tr,k} t_k} = \frac{\sum_{all\ k\ in\ class\ j} m_{x,k}}{m_{vehicle} \sum_{all\ k\ in\ class\ j} VSP_{tr,k} t_k} \tag{3.10}$$

Ukupna količina emisija, odnosno potrošnja goriva, dobije se zbrajanjem emisija svih pojedinačnih razreda, odnosno produkta specifičnih emisija i pogonske energije koja dolazi iz motora s unutarnjim izgaranjem prema (3.11):

$$M_x = \sum_j m_{x,j} = \sum_j \dot{m}_{x,j} W_{ice,tr,j} \tag{3.11}$$

Prema predloženom dijagramu toka energije orijentiranom prema funkciji [121], slika 23. pogonska energija j-tog razreda hibridnog vozila koju generira motor s unutarnjim izgaranjem $W_{ice,tr,j}$ je definirana s (3.12):

$$W_{ice,tr,j} = w_{tr,j} + w_{mwa,j} - \gamma_j \eta_g \eta_{st} \eta_m \left(\alpha \eta_{gb}^2 \eta_f^2 W_{br} + \eta_{gb} \eta_f W_{s,mwa} \right) \tag{3.12}$$

Gdje je:

$w_{tr,j}$ - pogonska energija *j-tog* razreda,

$w_{mwa,j}$ - pozitivna energija pomaka radne točke MSUI-ja *j-tog* razreda,

γ_j -koeficijent upliva pohranjene energije *j-tog* razreda,

$\eta_m, \eta_g, \eta_{st}, \eta_{gb}$ i η_f- redom predstavljaju učinkovitosti električnog stroja u motornom i generatorskom režimu, učinkovitosti baterije, mjenjača i završnog prijenosa,

W_{br} - je ukupna energija potrošena na usporavanje vozila definirana prema (3.13),

$W_{s,mwa}$ - je ukupna spremljena energija generirana pozitivnim pomakom radne točke MSUI-ja koja je definirana s (3.14),

$P_{e,j} - P_j$ - je razlika srednje snage MSUI-ja i zahtjeva snage pogona *j-tog* razreda

$$W_{br} = \sum_j W_{br,j} \tag{3.13}$$

$$W_{s,mwa} = \sum_j T_{j,mwa}(P_{e,j} - P_j) \tag{3.14}$$

Potrebno je zadovoljiti uvjet energetske bilance (3.15) prema kojem se kompletna pogonska energija utroši na svladavanje otpora vozila, kočenje i promjenu potencijalne i kinetičke energije. Gdje su $w_{res,j}$ - otpori vozila; $w_{k,j}$ i $w_{p,j}$ - promjene u kinetičkoj i potencijalnoj energiji.

$$\sum_j w_{tr,j} = \sum_j W_{br,j} + w_{res,j} + w_{k,j} + w_{p,j} \tag{3.15}$$

Uvrštavanjem težinskih koeficijenata pripadajućih emisija A, B, C i D u općenitu funkciju cilja dobiva se konačna funkcija cilja (3.16).

$$\begin{aligned} J = \sum_j (\dot{A}m_{CO2,j} + \dot{B}m_{NOx,j} + \dot{C}m_{PN,j} + \dot{D}m_{CO,j}) \big[w_{tr,j} + W_{mwp,j} \\ - \gamma_j \eta_g \eta_{st} \eta_m (\alpha \eta_{gb}^2 \eta_f^2 W_{br} - \eta_{gb} \eta_f W_{s,mwa}) \big] \end{aligned} \tag{3.16}$$

U svrhu primjene predloženog modalnog emisijskog modela klasičnog i hibridnog vozila provedena je analiza tokova energije kompletnog vozila na testnoj ruti na osnovi izmjerenih podataka. Prema izrazu (3.15) je procijenjen potencijal regenerativne energije, dijagram na slici 42. Od ukupne energije goriva gotovo 30 % pretvara se u koristan mehanički rad predan na pogonske kotače vozila. Od toga, veći dio mehaničke energije utrošen je na otpore vozila 69 % i on je nepovratan, a ostatak od 31 % je potrošen na kočenje i djelomično ga je moguće vratiti u sustav korištenjem regenerativnog kočenja.
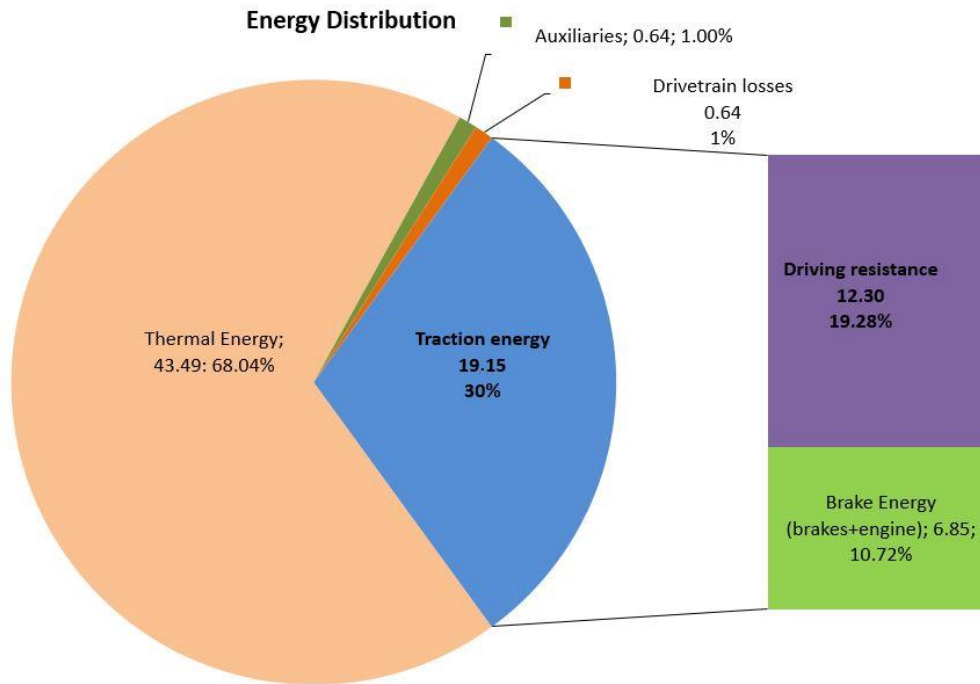
Slika 42. Raspodjela energije vozila u stvarnim uvjetima vožnje.

Nakon analize tokova energije napravljena je raspodjela količine emisija unutar pojedinih raspona pogonske snage i prikazana dijagramom na slici 43. Cilj je minimalizirati emisije NO_X-a prema funkciji cilja (3.17) uz zadovoljavanje uvjeta (3.15). U ovoj fazi istraživanja je korištena pojednostavljena funkcija cilja koja zanemaruje pomak radne točke MSUI-ja, te je $W_{s,mwa}=0$. Optimizacija je provedena permutacijom energetskih udjela i pripadajućih emisija pojedinih razreda kao i korištenjem regenerativne energije koje omogućava hibridni pogon, što grafički prikazuje slika 43.

$$J = A \sum_j \dot{m}_{NOx,j} \left[w_{tr,j} + W_{mwp,j} - \gamma_j \eta_g \eta_{st} \eta_m \left(\alpha \eta_{gb}^2 \eta_f^2 W_{br} \right) \right] \qquad (3.17)$$

Rezultat prema jednostavnoj strategiji koja preferira minimalizaciju NO_X emisija također je prikazan stupčastim dijagramom na slici 43. Stupci prikazuju energetske udjele i emisijske udjele odnosno udjele potrošnje goriva klasičnog vozila u standardnim uvjetima vožnje, neovisno da li su sa ispunom ili transparentni. Kod hibridnog vozila dio toka energije iz MSUI-ja je zamijenjen tokom energije iz spremnika i predstavljen je transparentnim stupcima. Ispunjeni dijelovi stupaca predstavljaju udjele toka energije iz MSUI-ja koji su odgovorni za emisije i potrošnju. U prva dva razreda snage, prvi sa samo negativnom snagom bez pozitivnog

energetskog udjela, i drugi s pozitivnim energetskim udjelom manjim od 0,5 % ukupne mehaničke energije, zajedno su odgovorni za više od 46 % emisija CO, gotovo 8 % emisija CO_2 i 5 % emisija NO_X-a. Optimizacija orijentirana prema bilo kojim emisijama eliminira 1. i 2. razred jer im je udio u pogonskoj energiji vrlo mali dok je količina emisija značajna. Optimizacija prema emisijama CO_2 preferirala bi više razrede zbog više učinkovitosti dok ona primijenjena, prema NO_X emisijama preferira razred 3. Razredi od 6 do 8 nemaju značajniji
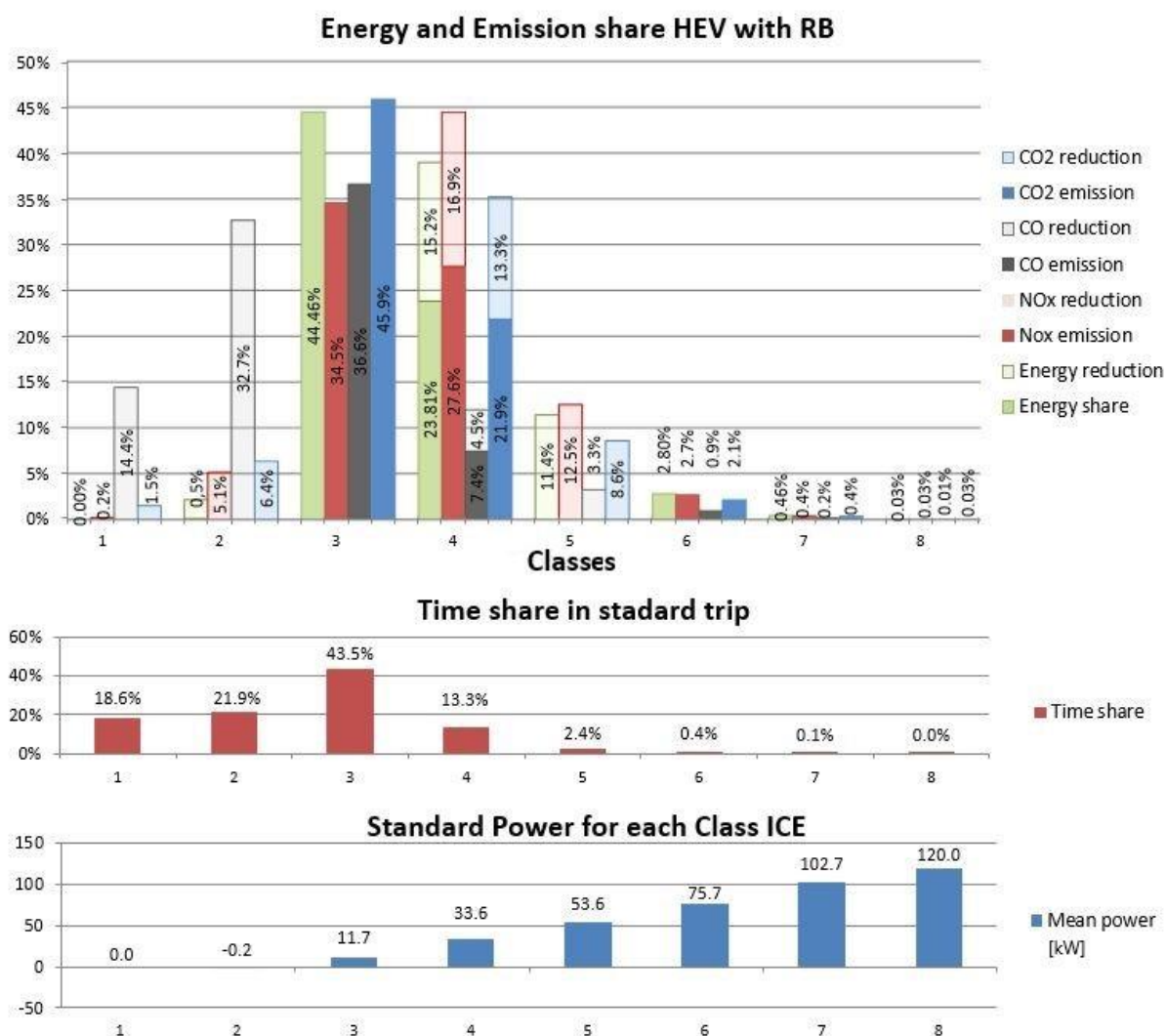
Slika 43. Raspodjela emisija i pogonske energije raspodijeljena prema rasponima snage [3].

energetski udio, a zahtijevaju pomicanje radne točke MSUI-ja tako da su ostali nepromijenjeni. Razred 5 je zbog relativno velikog udjela emisija NO_X-a u potpunosti zamijenjen spremljenom energijom, kao i dio razreda 4. Konačan rezultat na razini ciklusa predstavljen je grafički na slici 44. NO_X emisije reducirane su za gotovo 45 % u odnosu na početne vrijednosti, CO_2 i

potrošnja goriva reducirani su na 68 % početnih vrijednosti ili na 113g CO_2/km, dok su CO emisije dovedene na 50 % početne vrijednosti, odnosno na zanemariv iznos u odnosu na zakonsko ograničenje.
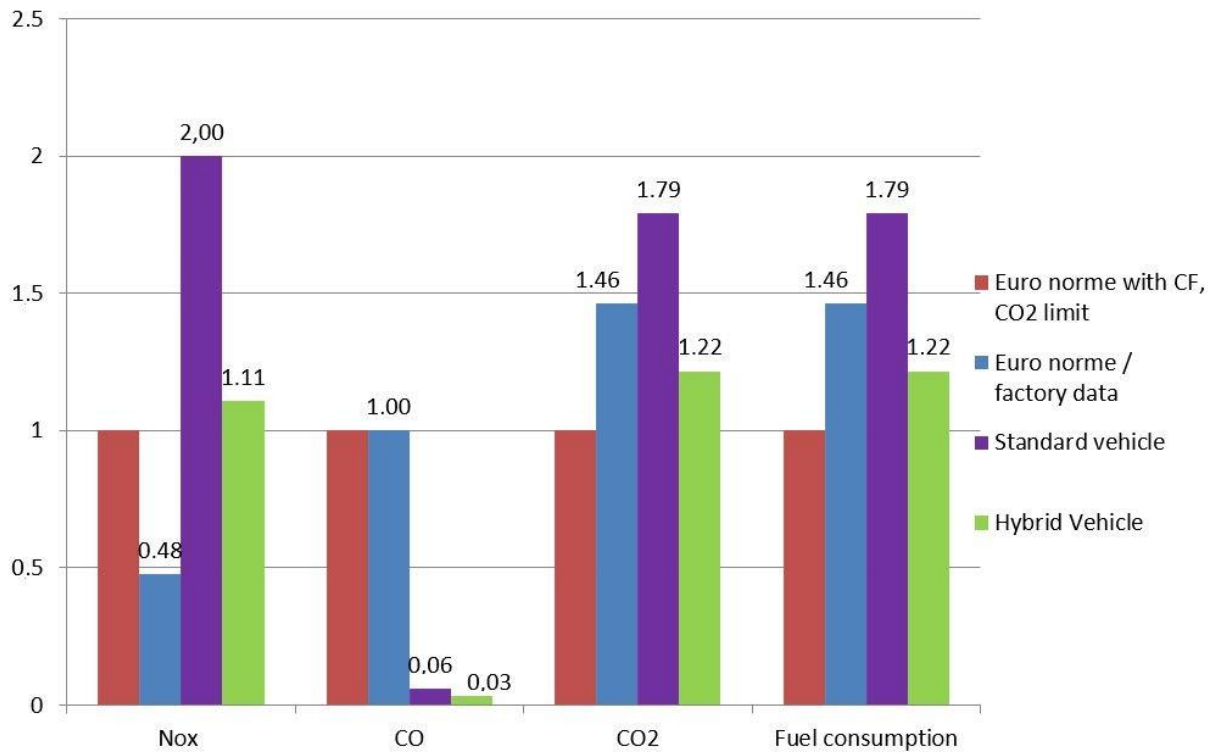
Slika 44. Usporedba emisija klasičnog i hibridnog pogona [3].

U radu je na osnovi modalne analize podataka o pogonskoj snazi, emisijama i potrošnji goriva, uz primjenu toka energije, formiran modalni emisijski model hibridnog vozila. Na predloženi model primijenjena je strategija upravljanja energijom temeljena na pravilima te su određeni maksimalni učinci hibridnog pogona u smislu redukcije emisija i potrošnje goriva. Ovime su potvrđene posljednje dvije hipoteze članka [3] koji čini doktorski rad, iako treba naglasiti da predstavljeni model nije uspoređen s eksperimentalnim rezultatima modeliranog hibridnog vozila niti s rezultatima poznatog modela, tako da je potrebno provesti njegovo vrednovanje u smislu točnosti predviđanja.

3.3. Validacija klasičnog i HEV modela na osnovi modalnih emisija i potrošnje goriva prema specifičnoj snazi

Nakon predstavljanja potpuno novog modela u [3] i detaljne analize obrađenih podataka utvrđeno je kako je u svrhu kvalitetnog vrednovanja modela potrebno koristiti znatno bolju opremu, prije svega analizatore plinova s kraćim vremenom odaziva. Potrebno je dokazati pretpostavku da predstavljeni model hibridnog vozila daje dovoljno dobre rezultate u vidu procjena, štetnih emisija, potrošnje goriva odnosno CO_2 emisija i pogonske energije u različitim ciklusima vožnje u usporedbi s referentnim modelom i uz primjenu jednake strategije upravljanja. S obzirom na tok energije i informacija, kontrolni model, prikazan na slici 45., formiran je unaprednim kvazistatičkim pristupom koji uključuje dinamiku samog vozila kroz PI regulator.
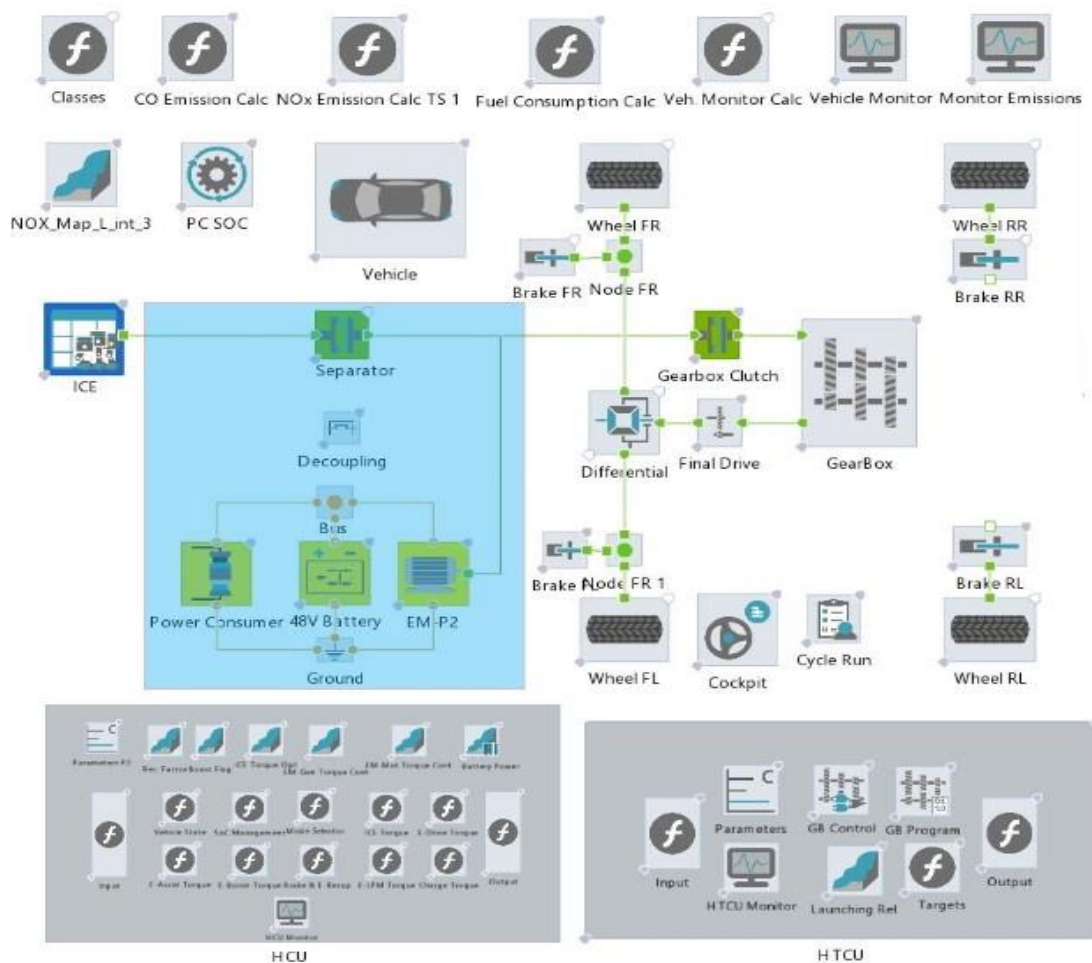
Slika 45. Shematski prikaz CruiseM modela.

Pojedini sklopovi opisani su karakterističnim fizikalnim veličinama dok se procjena emisija i potrošnje goriva oslanja na stacionarne pripadajuće mape motora s unutarnjim izgaranjem koji su generirani iz izmjerenih podataka na ispitnim valjcima. Emisije i potrošnja goriva mjerene su u stacionarnim radnim točkama kroz cijelo područje rada motora MSUI-ja. Slika 47. prikazuje ovisnost emisija NO_X-a o opterećenju i brzini vrtnje modeliranog MSUI-ja. Motorom upravlja kontrolna jedinica koja dobiva podatke iz svih sustava vozila te preko regulatora ostvaruje zadani ciklus. Detaljniji opis ostalih sustava koji utječu na dinamiku vožnje i kontrole rada modela vozila objašnjen je u radu [4]. Prijenosna oprema za mjerenje emisija AVL M.O.V.E instalirana je na ispitnom vozilu u svrhu mjerenja emisija onečišćujućih tvari i ugljikovog dioksida u stvarnim uvjetima vožnje te na ispitnim valjcima MAHA LPS 3000, slika 46.

Slika 46. Vozilo na ispitnim valjcima s ugrađenom mjernom opremom.
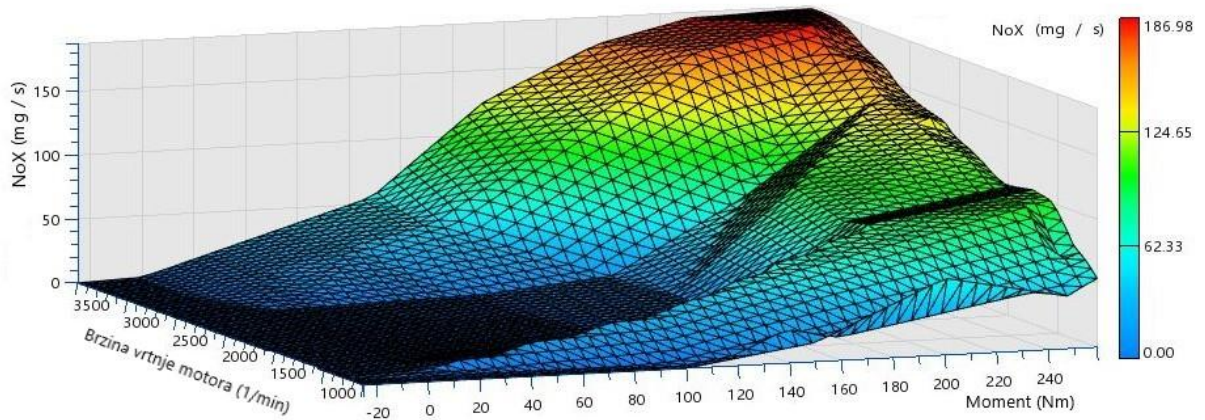
Slika 47. NO$_X$ emisijska mapa određena mjerenjem na ispitnim valjcima.

Mjerenja trenutne snage, potrošnje goriva i emisija bilježena su na ruti dugoj 87 km koja zadovoljava RDE kriterije mjerenja, sva su mjerenja izvedena prema proceduri RDE ispitivanja. Prikaz RDE rute i profil brzine prikazani su na slici 48.
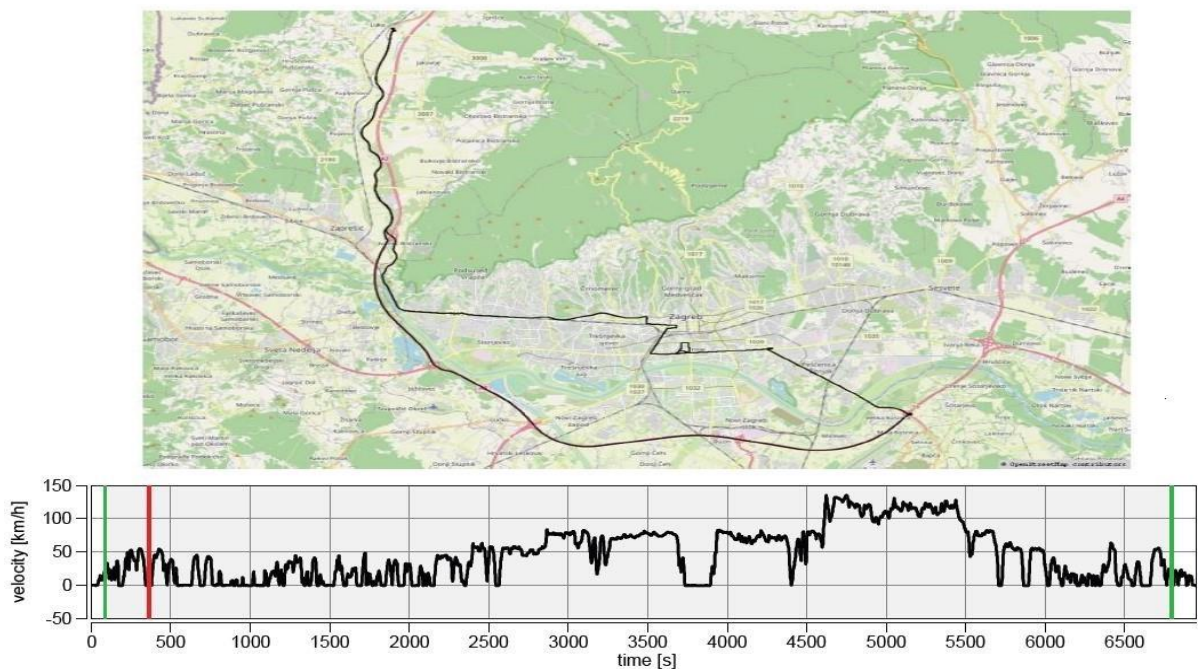
Slika 48. Testna ruta i profil brzine tijekom ispitivanja.

Testiranje je provedeno na cestama bez značajnije promjene nadmorske visine i u uvjetima umjerenog prometa, što je rezultiralo ujednačenijom vožnjom sa samo 16 % reverzibilne energije. Raspodjela emisija i pogonske energije prema razredima snage prikazana je na stupčastom grafikonu na slici 49, gdje su sve energetske vrijednosti prikazane u odnosu na

ukupnu pozitivnu vučnu energiju RDE ciklusa, dok su emisije prikazane kao postotak ukupnih emisija nastalih tijekom ciklusa.

Predstavljeni modalni model formiran je na osnovi podataka mjerenja u RDE ciklusu i analitike prikazane u prethodnom poglavlju, dok je Cruise M formiran na osnovi izmjerenih podataka na ispitnim valjcima i kalibriran u RDE ciklusu vožnje. Relevantni parametri za usporedbu VSP modela klasičnog vozila i kontrolnog CruiseM modela klasičnog vozila prikazani su u tablici 3.

Tablica 3. Relevantni pokazatelji usporedbe predstavljenog i kontrolnog modela.

Classic Vehicle	RDE Cycle			RDE (1/km)			Deviation			
	Measured	CruiseM	VSP	Measured	CruiseM	VSP	CruiseM	CruiseM (%)	VSP	VSP (%)
Distance (km)	86.21	86.63	86.21	1.000	1.005	1.000	0.005	0.48%	0.000	0.00%
Positive traction energy (kWh)	13.37	13.33	13.46	0.155	0.154	0.156	−0.035	0.22%	0.092	0.69%
Negative traction energy (kWh)	−2.14	−2.22	−2.27	−0.0248	−0.0256	−0.0263	−0.080	3.26%	−0.130	6.08%
CO_2 emission (g)	10540	10556	10540	122.2	121.9	122.2	16.259	−0.33%	0.000	0.00%
NO_x emission (mg)	39806	40051	39806	461.7	462.3	461.7	245.136	0.13%	0.000	0.00%
Consumption (kg)	3.366	3.371	3.366	0.039	0.039	0.039	0.005	−0.33%	0.000	0.00%

Prijeđeni put i emisije predloženog modalnog modela klasičnog vozila savršeno odgovaraju izmjerenim podacima jer je model nastao direktno iz tih parametara. Pozitivna i negativna vučna energija odstupaju od izmjerenih vrijednosti jer su određene integriranjem (3.6) na temelju trenutne specifične snage. Odstupanje prijeđenog puta CruiseM modela posljedica je unaprednog pristupa [17, 63], koji kontrolira brzinu pomoću PI regulatora. U ovom se pristupu ciklus vožnje ne prati savršeno jer uzima u obzir odziv sustava. Odstupanja pozitivne pogonske energije, udaljenosti, potrošnje goriva i emisije CO_2 unutar su 1 % od stvarnih vrijednosti, a što je prihvatljiv rezultat. Kalibracija regulatora povratne veze unaprednog modela izvršena je u RDE uvjetima što je utjecalo na smanjenje pogreške modela. Umjeren način vožnje na donjoj granici zahtijevane dinamike također je imao pozitivan utjecaj na rezultat CruiseM modela koji ne uključuje prijelazne pojave. Samo relativna negativna pogonska energija znatno odstupa između dva modela, dok je apsolutna devijacija mala zbog malog apsolutnog iznosa pogonske energije. Objašnjenje ovog odstupanja je jednako kao i kod odstupanja pozitivne energije.

Sljedeći korak bila je hibridizacija oba modela, modalnog i kontrolnog CruiseM modela u paralelnu hibridnu arhitekturu pod jednakim uvjetima. Oba hibridna modela testirana su i uspoređena u standardnim EU ciklusima: RDE, čiji je profil brzine identičan onome na kojem je izvršeno mjerenje, NEDC ciklus prema kojem je testno vozilo tipski odobreno i trenutno

važeći WLTC ciklus. Kontrolni model optimiziran je na temelju skupa jednostavnih pravila koja proizlaze iz globalne funkcije cilja (3.18). VSP model radi izvan vremenske domene tako da nema mogućnost optimizacije u stvarnom vremenu, ali se po istim pravilima mogu usporediti ova dva modela.

$$J = A \sum_j \dot{m}_{CO2,j} \left[w_{tr,j} + W_{mwp,j} - \gamma_j \eta_g \eta_{st} \eta_m \left(\alpha \eta_{gb}^2 \eta_f^2 W_{br} - \eta_{gb} \eta_f W_{s,mwa} \right) \right] \qquad (3.18)$$

Prikaz raspodjele emisija, potrošnje goriva i pogonske energije hibridnog modela u RDE ciklusu vožnje prikazan je stupčastim dijagramom na slici 49A. Funkcija cilja preferira samo minimum emisija CO_2, odnosno potrošnje goriva zanemarujući ostale štetne emisije tako što su faktori uz ostale *B=C=D=0*, stoga optimizacija preferira srednje i više razrede snage u kojima motor s unutarnjim izgaranjem radi učinkovitije. S druge strane, najviši razredi generiraju visoke emisije NO_X, koje u ovom slučaju nisu kažnjene jer nisu obuhvaćene funkcijom cilja. Ako usporedimo CruiseM model s novim pristupom, odstupanja prijeđenog puta su vrlo mala s najvećom vrijednosti od 0,69 % kod hibridnog vozila i RDE ciklusa. Uzroci odstupanja leže u različitim pristupima modeliranju, odnosno unaprednom pristupu kod kontrolnog modela [63]. Sve pozitivne pogonske energije imaju pozitivna odstupanja VSP modela između 0,35 % kod WLTP modela klasičnog vozila, do najviše 2,85 % kod RDE hibridnog modela. Odstupanja negativne pogonske energije su veća, do 8,38 % što je i očekivano jer je riječ o malim apsolutnim iznosima u odnosu na pozitivnu energiju tako da mnogo ne remete ukupan rezultat. Najbitniji element usporedbe dvaju modela su CO_2 emisije, prikazane na slici 50, i potrošnja goriva gdje je najveće odstupanje rezultata zabilježeno kod hibridnog modela vozila u uvjetima RDE ciklusa od 3,79 % i kod klasičnog nehibridnog modela vozila u WLTP uvjetima od 4,4 %. Sve ostale kombinacije ciklusa i modela daju odstupanja oko 1 % što pokazuje vjerodostojnost modela.
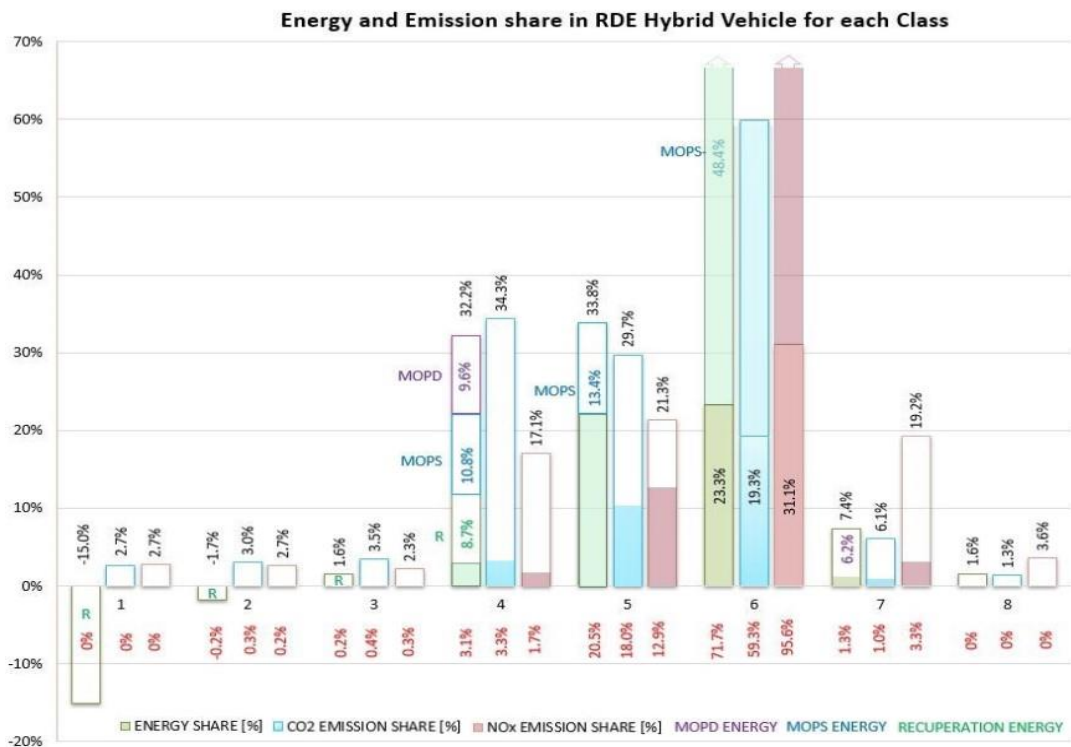
(**A**)

(**B**)
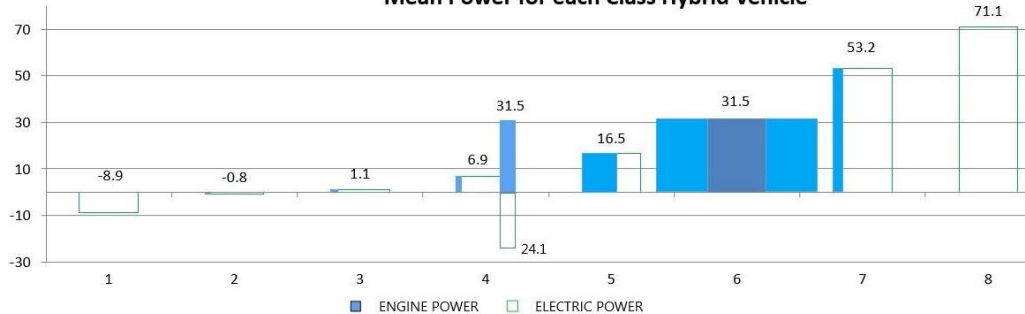
(**C**)

Slika 49. (A) Raspodjela energije i emisija VSP hibridnog modela u RDE uvjetima vožnje, (B) Vremenski udjeli razreda i (C) Prosječna snaga razreda.
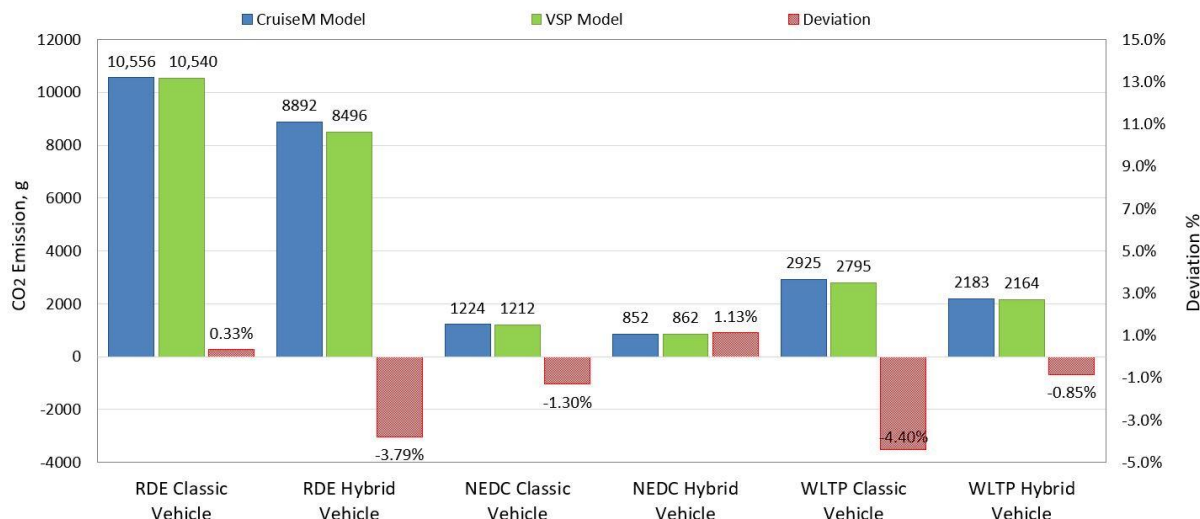
Slika 50. Usporedba predviđanja emisija CO_2 za različite modele i cikluse [4].

Što se tiče rezultata usporedbe emisija NO_X-a, odstupanja su nešto veća u usporedbi s emisijama CO_2 i potrošnjom goriva, slika 51. Najveća odstupanja emisija NO_X-a od 9,62 % pokazuju modeli hibridnog vozila u WLTP ciklusu, dok isti modeli u NEDC i RDE ciklusima pokazuju odstupanja nešto veća od 6 %. Modeli klasičnih vozila u uvjetima RDE, NEDC i WLTP razlikuju se redom za 0,13 %, 2,53 % i 6,07 %. Veća odstupanja ovih emisija su i očekivana, osobito u dinamičnijem WLTP ciklusu, između ostalog i zbog lošijih performansi CruiseM modela u predviđanju NO_X emisija kontroliranih EGR sustavom koji je jako osjetljiv na prijelazne pojave koje nisu opisane ovim modelom.
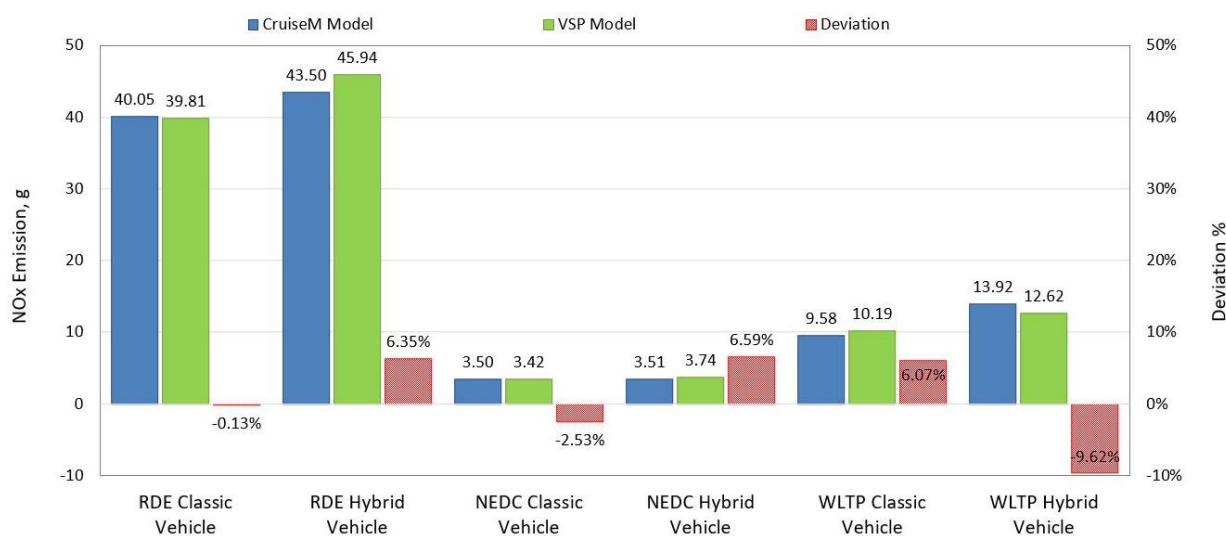
Slika 51. Usporedba predviđanja emisija NO_x-a za različite modele i cikluse [4].

Ako usporedimo dobivene rezultate predloženog modela s rezultatima korigiranih modela na osnovi VSP analize iz literature [116-118], ukupne pogreške u procjenama emisija i potrošnje goriva su znatno manje, od nekoliko postotaka do višestrukog iznosa. Zhai u [118] testira vlastiti modalni model HEV-a s visokim stupnjem hibridizacije, koji u odnosu na standardni VSP dodaje logiku paljenja i gašenja MSUI-ja. Relativna pogreška modela u različitim ciklusima vožnje je kod CO_2 emisija i potrošnje goriva od -3 % do -12 %, dok je kod NO_X emisija od -43 % do 98 % u različitim ciklusima vožnje. Duarte u [116] korigira klasični VSP model dobiven u RDE uvjetima s linearnim korekcijskim faktorima dobivenim na osnovi podataka tipskog odobrenja; relativna odstupanja CO_2 emisija i potrošnje goriva HEV-a su između -9,3 do 8,5 % za različita vozila. Mera u [117] uvodi korekcijske mape u VSP modele klasičnih vozila sa start/stop sustavom, značajno podiže točnost osnovnog VSP modela s odstupanjima CO_2 emisija i potrošnje goriva između 3,9 % i 12,5 % za različita vozila. Svrha usporedivih modela iz literature je isključivo predviđanje emisija modeliranog vozila u različitim uvjetima upotrebe replicirajući naučeno ponašanje. Povećanje stupnja hibridizacije HEV-a negativno utječe na točnost predviđanja emisija i potrošnje goriva jer razlikovanje više izvora energije postaje ključan dio modela [115]. Predloženi model replicira ponašanje u drugačijim uvjetima kroz naučenu strategiju upravljanja energijom, na koju je moguće naknadno utjecati sa svrhom optimizacije što mu omogućava upotrebu i u razvojnoj fazi. Uključivanje toka energije s osnovnim elementima pogona čini ga upotrebljivim i kod najviših stupnjeva hibridizacije, odnosno kod PHEV vozila.

4. PREGLED OBJAVLJENIH RADOVA NA KOJIMA SE TEMELJI DOPRINOS

U ovom poglavlju predstavljeni su sažeci objavljenih znanstvenih radova i doprinosi doktoranda svakom objavljenom radu.

4.1. Rad 1: Povećanje učinkovitosti izmjene radne tvari kod benzinskog motora pri djelomičnom opterećenju primjenom dvostrukog otvaranja ispušnih ventila

U ovom znanstvenom radu primarno je analiziran novi teoretski pristup povećanja učinkovitosti Ottovog motora, s direktnim ubrizgavanjem goriva u cilindar, smanjenjem gubitaka izmjene radnog medija kod djelomičnog opterećenja dodatnim otvaranjem ispušnih ventila u taktu kompresije. Rad predstavlja uvod u modeliranje motora s unutarnjim izgaranjem kao najsloženijeg dijela modela vozila. Istraživanje je provedeno na modelu motora u AVL-ovom programskom paketu Boost koji koristi 1D model usisnih i ispušnih sklopova motora te kvazidimenzionalni model za opise procesa unutar cilindra. Novina pristupa odnosi se na aktivno upravljanje dvostrukim otvaranjem ispušnim ventilima u svrhu smanjenja gubitaka izmjene radnog medija. Rezultati su pokazali višestruko povećanje učinkovitosti izmjene radne tvari jer je donja negativna petlja indikatorskog dijagrama svedena na minimalne vrijednosti, čime su gubici usisa svedeni na minimum. Održavanjem konstantnog srednjeg efektivnog tlaka, postavkama regulacije, površina gornje petlje je također smanjena za isti apsolutni iznos čime je posljedično smanjena potrošnja goriva. Modelom je dokazano povećanje učinkovitosti i smanjenje emisija CO_2 u područjima niskih opterećenja na razini Millerova i Atkinsonova ciklusa, koji su već u komercijalnoj upotrebi. Daljnje istraživanje koncepta ima smisla samo kod prednabijanih motora u vidu procjene mogućnosti korištenja pozitivnog rada predtlaka za vrijeme usisa. U odnosu na benzinski motor s fiksnom geometrijom usisa specifična potrošnja goriva u području promatranih niskih opterećenja između 2 i 4 bar srednjeg efektivnog tlaka je smanjena između 3,83 % i 4,23 %, a gubici izmjene plinova u cilindrima su smanjeni između 85 % i 87 %. Korišteni model primjeren je za istraživanja događaja vezanih za izmjene radne tvari, ali nedostatak modela u smislu točnosti je nemogućnost procjene utjecaja pristupa na promjene u učinkovitosti izgaranja zbog promjena u vrtloženju. Unatoč univerzalnosti i visokoj razini točnosti kod modeliranja motora, u pogledu procjene štetnih emisija vozila je upotreba CFD modela najčešće neprihvatljiva zbog svoje kompleksnosti.

4.1.1. Doktorandov doprinos radu

Doktorand je samostalno proveo numeričko prilagođavanje modela benzinskog motora za potrebe ispitivanja utjecaja promjene faze i vremena otvaranja ispušnih ventila za vrijeme takta kompresije na emisije odnosno potrošnju goriva. Izvršio je optimizaciju faze otvaranja i zatvaranja ispušnih ventila u svrhu minimalizacije potrošnje goriva te je proveo detaljnu analizu i usporedbu dobivenih podataka. U suradnji s mentorom i koautorom pripremio je rukopis za slanje u znanstveni časopis.

4.2.   Rad 2: Analiza sustava za redukciju emisija ispušnih plinova dizelskih motora

U ovom preglednom radu napravljena je napredna analiza svih poznatih sustava za kontrolu emisija s naglaskom na najproblematičnije NO_X emisije i emisije čestica. Obuhvaćeni su sustavi koji djeluju na emisije u samom mjestu nastanka kao i sustavi za naknadnu obradu ispušnih plinova. U svrhu razumijevanja složenih analitičkih i fizikalnih modela ponašanja obrađeni su učinci gotovo svih utjecajnih parametara na svaki pojedini sustav zasebno, kao i problematika predviđanja emisija kod učestalih hladnih startova čiji je problem izraženiji kod hibridnih vozila. Literatura je pokazala iznimno složeno predviđanje ponašanja i svakog pojedinog sustava na pojedine emisije, ali i nedostatak u području istraživanja zajedničkog djelovanja više sustava. Analizirani su problemi koji su se javljali pri korištenju pojedinih metoda za smanjenje emisija u određenim uvjetima rada motora. Objašnjen je utjecaj sustava kontrole emisija na parametre rada motora kao i na potrošnju goriva, reakcija na promjenu opterećenja i trajnost. Glavni zaključak odnosio se na potrebu za sustavnijim pristupom koji uključuje istodobno sve primijenjene sustave za kontrolu emisija zbog međusobnog djelovanja jednog na drugi. Dane su smjernice s procjenom kvalitete funkcionalnosti pojedinih tehnika u vidu usporedbe različitih rješenja cjelovitih sustava kontrole emisija s aspekta učinka na najutjecajnije emisije, potrošnju goriva, održavanje, veličinu i cijenu izvedbe kao i mogući načini postizanja određenih emisijskih propisa.

4.2.1. Doktorandov doprinos radu

Ovaj rad iniciran je potrebom za razumijevanjem složenih modela ponašanja sustava za kontrolu emisija vozila pogonjenih motorima s unutarnjim izgaranjem i opširnim pregledom literature iz tog područja. Doktorand je zajedno s koautorima pripremio rukopis na temelju sustavnog pregleda literature koji objedinjuje sve komercijalno dostupne sustave kontrole

emisija unutar jednog rada, bilo da je riječ o sustavima koji utječu na emisije na mjestu njihova nastanka ili o sustavima za naknadnu obradu emisija. Ovakav je pristup bio nužan za objašnjenje rada svakog cjelovitog sustava kontrole emisija čije je ponašanje osim pojedinačnim podsustavima određeno i složenim međusobnim utjecajima. Doktorand je napravio konceptualnu usporedbu mogućih kombinacija pojedinačnih sustava s aspekta učinka na najutjecajnije emisije, potrošnju goriva, održavanje, veličinu i cijenu izvedbe.

4.3. Rad 3: Analiza emisija dizelskih vozila u okolnostima kvara sustava za regulaciju emisija

Rad predstavlja nastavak istraživanja koje se odnosi na utjecaj zakazivanja pojedinih sustava i na predstavljanje metode procjene emisija vozila, a što je uža tema doktorskog rada. Eksperimentalno istraživanje provedeno na vozilima u dugotrajnoj eksploataciji s potpuno ispravnim sustavima kontrole emisija pokazuje značajna odstupanja u odnosu na dopuštene granične vrijednosti odgovarajućih emisijskih propisa. Odstupanja su vrlo slična očekivanim vrijednostima za nova vozila iz čega proizlazi da degradacija sustava kontrole ne predstavlja značajan problem. Analizirana su odstupanja pojedinih emisija i razlike u ponašanjima između različitih generacija vozila uz objašnjenje uzroka problema. Na vozilima sa simuliranim kvarovima rezultati mjerenja pokazali su višestruko povećanje štetnih emisija u slučajevima otkazivanja komponenti, odnosno sustava za njihovu kontrolu. Najveći su problem emisije NOX-a dok su emisije CO unatoč ogromnom povećanju ispod dozvoljenih granica i ne predstavljaju problem. Ukidanje pojedinih komponenti za kontrolu emisija uglavnom pozitivno utječe na ekonomičnost što je očekivano s obzirom na načine djelovanja objašnjene u [2]. Ustanovljena je samo iznimka kod izrazito niskih opterećenja gdje EGR sustav pridonosi smanjenju potrošnje goriva, što se može objasniti smanjenjem gubitaka izmjene radne tvari. Predloženi su i dokazani mogući modeli detektiranja kvarova DOC i EGR sustava u sklopu STP-a korištenjem trenutno postojeće opreme i dane su smjernice daljnjih istraživanja. Istraživanje je pokazalo da su novija vozila, koja zadovoljavaju novije emisijske propise, osjetljivija na kvarove komponenti za kontrolu emisija u odnosu na prethodne generacije. U ovom je radu na osnovi modalne analize i odgovarajućeg toka energije predložen novi model za predviđanje emisija i potrošnje goriva klasičnih i hibridnih vozila. Predloženi model primijenjen je na ispitivano vozilo s ispravnim sustavima kontrole emisija na osnovi zabilježenih podataka o emisijama, potrošnji goriva te energiji u stvarnim uvjetima upotrebe. Dodavanjem unutarnjih varijabli razvijeni model je moguće primijeniti na hibridni sustav pogona zbog mogućnosti razlikovanja pojedinih izvora energije. Pokazano je da se na model

može primijeniti jednostavna strategija upravljanja energijom temeljena na pravilima s ciljem optimizacije CO_2 emisija u uvjetima koji repliciraju stvarne uvjete upotrebe. Usporedbom fizikalne interpretacije pojedinih unutarnjih varijabli može se zaključiti da, za razliku od predloženog modela, postojeći modalni modeli nisu prihvatljivi kod najviših stupnjeva hibridizacije HEV-a. Dobiveni rezultati emisija i potrošnje goriva nisu uspoređeni s eksperimentalnim podacima, ali su unutar očekivanih vrijednosti.

4.3.1. Doktorandov doprinos radu

Doktorandovo istraživanje motivirano je problematikom predviđanja emisija u stvarnim uvjetima upotrebe klasičnih i hibridnih vozila i otkazivanja određenih sustava za kontrolu emisija čiji je rok trajanja u pravilu kraći od samog vozila. Izostanak kontrole ispravnosti i prisutnosti sustava za regulaciju emisija tijekom obaveznih redovnih pregleda uz visoku cijenu zamjene često rezultira nastavkom korištenja vozila bez njih. Doktorand je samostalno osmislio kompletan eksperiment te je uz pomoć mentora i kolega izradio i kalibrirao dio eksperimentalne opreme, a postojeći dio prilagodio i ugradio na sva ispitivana vozila. Izvršio je eksperimentalna mjerenja u cestovnim uvjetima upotrebe na ukupno šest vozila s potpuno ispravnim i neispravnim komponentama za kontrolu emisija. Također je proveo analizu izmjerenih rezultata te predstavio način kontrole izostanka odnosno neispravnosti pojedinih sustava s postojećom opremom STP-a. Doktorand je u radu predložio novi modalni model predviđanja emisija i potrošnje goriva vozila s naglaskom na hibridna vozila. Na jedno od ispitivanih vozila primijenio je predloženi model, na osnovi podataka izmjerenih u stvarnim uvjetima, upotrijebio je te analizirao dobivene podatke. Zajedno s mentorom i suradnicima pripremio je rukopis za slanje u časopis.

4.4. Rad 4: Novi model hibridnog vozila na osnovi analize emisija i potrošnje goriva prema specifičnoj snazi

U ovom izvornom znanstvenom radu izvršeno je vrednovanje novog razvijenog modela emisija i potrošnje goriva vozila s naglaskom na HEV. Model se temelji na modalnim emisijama i potrošnji goriva prema trenutnoj specifičnoj pogonskoj snazi vozila. Energetski tokovi opisani su fizikalnim modelima prema novom predloženom dijagramu toka energije temeljenom na funkcionalnim pojedinačnim tokovima HEV-a. Model se zasniva na stvarnim emisijama vozila, potrošnji goriva i energije koji su zabilježeni u stvarnim uvjetima vožnje prema pravilima Real Driving Emissions (RDE), koja su danas obvezni dio procesa tipskog

odobrenja vozila. Provedena je evaluacija novouvedenog modela u RDE, NEDC i WLTP ciklusu usporedbom rezultata sa standardnim, verificiranim modelom vozila koji je izrađen u AVL-ovu programskom paketu CruiseM. Na oba modela HEV-a primijenjena je ista strategija upravljanja energijom temeljena na nizu jednakih pravila. Pozitivne pogonske energije bilježe odstupanja između 0,35 % i 2,85 %. Najveće odstupanje u emisijama CO_2 zabilježeno je kod HEV modela u RDE ciklusu i kod nehibridnog modela u WLTP ciklusu od 3,79 % odnosno 4,4 %, sve ostale kombinacije ciklusa i vozila imale su odstupanja oko 1 % na razini kompletnog ciklusa. Očekivano, najveća relativna odstupanja zabilježena su za emisije NO_X od 0,13 % do 9,62 % za HEV u WLTP ciklusu. U usporedbi s postojećim emisijskim modelima i modelima potrošnje goriva HEV-a temeljenim na modalnim emisijama iz poglavlja 2, predstavljeni model HEV gotovo u svim segmentima pokazuje manju relativnu pogrešku procjene emisija i potrošnje goriva na razini kompletnog ciklusa.

4.4.1. Doktorandov doprinos radu

Doktorand je samostalno osmislio način provedbe istraživanja te je u suradnji s kolegama splitskog FESB-a i zagrebačkog FSB-a izvršio snimanje podataka na odabranom vozilu u RDE uvjetima vožnje i na ispitnim valjcima. Iz dobivenih podataka razvio je model klasičnog i hibridnog vozila temeljen na VSP analizi emisija i potrošnje goriva čije je teorijske osnove prikazao u radu. Zajedno sa suradnicima razvio je i verificirao kontrolni fizikalni model klasičnog i hibridnog električnog vozila u specijaliziranom AVL-ovu paketu CruiseM. Također je analizirao i usporedio rezultate predstavljenog modela s rezultatima kontrolnog modela istih vozila u RDE, NEDC i WLTC uvjetima korištenja vozila. Na kraju je zajedno s koautorima pripremio rukopis za slanje u znanstveni časopis.

5. ZAKLJUČAK

S obzirom na povećanje transportnih potreba s jedne strane i težnje za samoodrživosti s druge, neizbježno je okretanje prema tehnologijama koje značajno pridonose smanjenju štetnih emisija, a time i emisija stakleničkih plinova. S obzirom na zahtjeve nadolazećeg Euro 7 emisijskog propisa kao i planove o strožim ograničenjima CO_2 emisija, hibridna električna vozila postaju jedno od ključnih rješenja tranzicijskog perioda prema CO_2 neutralnim vozilima. Uz primjenu sintetičkih, CO_2 neutralnih goriva, hibridni pogonski sustavi će nakon tranzicijskog perioda, uz udio u standardnom cestovnom prometu, sigurno pronaći svoju primjenu u civilnim vozilima posebnih namjena, terenskim i vojnim vozilima bez obzira na stupanj elektrifikacije cestovnog prometa i na druge alternativne pogonske sustave.

Problemi vezani za štetne emisije, sustave za njihovu kontrolu i emisije CO_2 kod novih vozila, kao i u eksploataciji, ostat će jedan od budućih izazova, ali sa specifičnostima koje nose hibridni pogonski sustavi. Daljnji napredak u stupnju učinkovitosti ide primarno u dva osnovna smjera. Jedan se odnosi na povećanje učinkovitosti svih pojedinačnih sustava, prvenstveno motora s unutarnjim izgaranjem, dok se drugi odnosi na primjenu učinkovitih strategija upravljanja za koje su ključni kvalitetni modeli HEV-a. Značajno povećanje broja komponenti u odnosu na klasične pogonske sustave je neizbježno, što uz najmanje dva izvora energije predstavlja izazov u smislu modeliranja i procjene emisija kao i potrošnje goriva u stvarnim uvjetima upotrebe. U ovom radu analizirani su problemi vezani za učinkovitost i emisije u stvarnim uvjetima upotrebe kao i u trajnoj eksploataciji. Nadalje, razvijen je te verificiran modalni model emisija i potrošnje goriva hibridnog električnog vozila koji predstavlja značajan iskorak u odnosu na postojeće stanje.

U prvoj fazi istraživanja provedeno je testiranje novog koncepta povećanja učinkovitosti benzinskog motora smanjenjem gubitaka prilikom izmjene radne tvari, a koji se zasniva na dvostrukom otvaranju ispušnih ventila. Rezultati istraživanja pokazali su značajno smanjenje potrošnje goriva i CO_2 emisija kod niskih opterećenja čime je potvrđena osnovna hipoteza tog rada. Manji dobici na učinkovitosti u odnosu na očekivane vrijednosti objašnjeni su djelomičnim poništavanjem pozitivnog utjecaja zbog povećanih gubitaka topline. Primijenjeni model prikladan je za ispitivanje procesa u usisnom i ispušnom kolektoru, ali ne uzima u obzir utjecaj vrtloženja na kvalitetu izgaranja. Rezultati istraživanja koncepta na razini su Atkinsonova i Millerova ciklusa koji su ušli u serijsku primjenu. Daljnje ispitivanje koncepta kod atmosferskih motora u tom pogledu nema perspektivu, dok je područje prednabijanih motora i dalje aktualno. Istraživanje je pridonijelo razumijevanju kompleksnosti CFD modela

i jednim dijelom utjecalo na usmjeravanje daljnjeg istraživanja prema nužnosti razvoja jednostavnijih emisijskih modela MSUI-ja unutar modela hibridnih vozila.

Iz detaljne analize svih komercijalno dostupnih sustava za kontrolu emisija proizišli su zaključci koji su usmjerili istraživanje prema problemima ponašanja sustava kontrole emisija u eksploataciji i u stvarnim uvjetima upotrebe te u smjeru modeliranja emisija hibridnih vozila. Literatura iz ovog područja uglavnom obrađuje utjecajne faktore na pojedinačne podsustave iz čega proizlazi zaključak o potrebi istraživanja sustavnijim pristupom. Takav pristup podrazumijeva kompletan sustav regulacije emisija, odnosno istodobno promatranje svih primijenjenih podsustava zbog njihova jakog međusobnog utjecaja. Dane su smjernice s procjenom kvalitete funkcionalnosti pojedinih tehnika kao i mogući načini postizanja određenih emisijskih propisa. Napravljena je kvalitativna usporedba koncepata mogućih kombinacija pojedinačnih sustava s aspekta učinka na najutjecajnije emisije, potrošnju goriva, održavanje, veličinu i cijenu izvedbe.

Opširan pregled literature iz područja sustava za kontrolu emisija usmjerio je istraživanje na nekoliko područja koja su najveći izazovi za vozila pogonjena motorima s unutarnjim izgaranjem. Iako je problematika emisija u stvarnim uvjetima upotrebe široko istražena nakon „Diesel gate" afere, ispitivanja u stvarnim uvjetima nakon dužeg perioda eksploatacije su vrlo rijetka i obično se odnose na uska područja određenog sustava za kontrolu emisija. Provedeno ispitivanje na vozilima pokretanim dizelskim motorima s ispravnim sustavima za kontrolu emisija potvrđuje poznatu problematiku značajnog odstupanja emisija u stvarnim uvjetima upotrebe vozila u odnosu na zakonom propisane granične vrijednosti. Iznimka su samo emisije ugljikovog monoksida koje su daleko ispod graničnih vrijednosti. Unatoč tome što su u svrhu ispitivanja korištena ispravna rabljena vozila, s dugim periodom eksploatacije, rezultati mjerenja slični su očekivanim rezultatima za nova vozila. Može se zaključiti da promatrani sustavi za kontrolu emisija nisu podložni znatnijoj degradaciji pri čemu je najčešće dovoljno osigurati kvalitetnu kontrolu prisutnosti ili njihova potpunog zakazivanja.

Rezultati istraživanja na vozilima s neispravnim komponentama za kontrolu emisija pokazuju da emisije ispušnih plinova tih vozila višestruko premašuju granične vrijednosti, s tim da kvarovi sustava imaju znatno veće posljedice na vozilima s višim emisijskim propisima. I u ovom slučaju su iznimka CO emisije koje su, unatoč povećanju od gotovo deset puta u odnosu na vozila s ispravnim oksidacijskim katalizatorima, još uvijek ispod graničnih vrijednosti. Iz navedenog se može zaključiti da emisije ugljikovog monoksida nisu problem kod dizelskih vozila ni u jednom scenariju.

Predložen je koncept stacionarnog ispitivanja ispravnosti DOC i EGR sustava kontrole emisija dizelskih vozila u sklopu redovnog tehničkog pregleda vozila bez ulaganja u dodatnu opremu stanica za tehnički pregled. Funkcionalnost koncepta dokazana je na ispitivanim vozilima na način da se odsutnost ili zakazivanje sustava recirkulacije ispušnih plinova dokazuje smanjenim pretičkom kisika u ispušnim plinovima. Odsutnost dizelskog oksidacijskog katalizatora dokazuje se višestrukim povećanjem emisija CO u praznom hodu uz prethodno osiguravanje njegove radne temperature. Unatoč tome što sva ispitivana vozila pokazuju isti trend, uočena je značajna razlika ponašanja između vozila tipski odobrenih prema različitim emisijskim propisima, stoga je za primjenu predloženog koncepta potrebno izraditi tipsku bazu podataka koja obuhvaća sve karakteristične tipove vozila.

Na temelju zabilježenih podataka o emisijama, potrošnji goriva i pogonskoj energiji kreiran je novi emisijski model hibridnog električnog vozila. Jedan od najutjecajnijih uzroka slabe korelacije modalnih modela hibridnih vozila iz literature, odnosno nemogućnost primjene bilo kakve strategije upravljanja energijom između različitih izvora, riješen je implementacijom predloženog toka energije HEV-a. Dodavanjem dijagrama toka energije, koji uključuje unutarnje varijable, predstavljeni model se kao i korigirani modeli iz literature građom odmiče od klasične definicije VSP modela koji ovise isključivo o vanjskim varijablama, ali i dalje zadržava prednosti modalnih modela. Autori su u obrađenoj literaturi samo djelomično riješili ovaj problem primjenom osnovne logike uključivanja i isključivanja MSUI-ja, korekcijskim faktorima bez fizikalnog uporišta ili primjenom određenih dijelova emisijskih mapa MSUI-ja. Takva rješenja imaju za posljedicu značajno povećanje broja unutarnjih varijabli i vrlo složene postupke određivanja pojedinih parametara. Primijenjeni tok energije, orijentiran prema funkciji, omogućio je minimalno povećanje broja unutarnjih varijabli čime se bitno ne narušavaju osnovne prednosti modalnih modela. Definiranje modalnih emisija po jedinici pogonske energije smanjuje pogrešku rasipanja rezultata unutar jednog razreda i omogućava zapis funkcije cilja s jasnom fizikalnom interpretacijom. Predloženi model HEV-a preliminarno je testiran u identičnim uvjetima u kojima su vršena mjerenja tako da je primijenjena jednostavna strategija upravljanja energijom na temelju pravila, u svrhu minimalizacije CO_2 emisija odnosno potrošnje goriva.

Ustanovljena je osjetljivost modela na kvalitetu ulaznih podataka, posebice u području modalnih razreda manje učestalosti, gdje tromost analizatora uzrokuje usrednjavanje sa susjednim razredima. Iz navedenog proizlazi da je za kvalitetan postupak vrednovanja modela potrebno osigurati opremu s visokom dinamikom analize ispušnih plinova. Značajna prednost

predloženog modela u odnosu na kontrolni je daleko jednostavnije praćenje zadanih pravila zbog višestruko većeg broja varijabli i rada u vremenskoj domeni kontrolnog modela. Manja zabilježena odstupanja prijeđenog puta posljedica su različitih pristupa modeliranju kod uspoređenih modela, odnosno upotrebe PID regulatora kod unaprednog modela. Najveća zabilježena odstupanja CO_2 emisija i potrošnje goriva od 3,8 % zabilježena su kod HEV-a u RDE ciklusu i odstupanja od 4,4 % za klasično vozilo u WLTP ciklusu. Sve ostale kombinacije vozila i ciklusa pokazuju bolja predviđanja s oko 1 % pogreške, što pokazuje vjerodostojnost modela. Predloženi model pokazuje nešto lošije rezultate kao i veće rasipanje u predviđanju NO_X emisija, gdje su najveća odstupanje od 9,6 % zabilježena kod modela HEV-a u WLTP ciklusu. Veće odstupanje emisija NO_X-a je očekivano zbog značajnijeg utjecaja tranzijenata i njihove loše interpretacije kod kontrolnog modela, ali i zbog EGR-a kao osnovnog sustava kontrole emisija NO_X-a, čije ponašanje nije potpuno definirano trenutnom radnom točkom. Predstavljeni model pokazuje dobre rezultate i u području klasičnih vozila u kojima i konvencionalni VSP modeli pokazuju dobra svojstva. Najveću prednost razvijeni model pokazuje kod hibridnih vozila gdje klasični VSP modeli pokazuju značajne manjkavosti u pogledu točnosti predviđanja, dok korigirani modalni modeli imaju velik stupanj složenosti sa značajno većom pogreškom. Osnovna svrha usporedivih modela iz literature je isključivo predviđanje emisija modeliranog vozila u različitim uvjetima upotrebe, kopirajući strategiju izvornog vozila. Viši stupnjevi hibridizacije HEV-a smanjuju točnost predviđanja emisija i potrošnje goriva jer razlikovanje više izvora energije postaje ključan dio modela. Predloženi model ima mogućnost kopiranja ponašanja u drugačijim uvjetima kroz naučenu strategiju upravljanja energijom, na koju je moguće naknadno utjecati u svrhu optimizacije što mu omogućava upotrebu i u razvojnoj fazi. Primjena varijabli koje opisuju unutarnje tokove energije s osnovnim elementima pogona čini ga upotrebljivim i kod najviših stupnjeva hibridizacije, odnosno kod PHEV vozila. Složeni klasični fizikalni modeli zahtijevaju velike vještine i složene algoritme da bi ostvarili stvarne funkcije cilja. Također, problem klasičnih fizikalnih modela je zbog ogromnog broja varijabli i parametara vrlo složen postupak optimizacije i često zapinjanje u lokalnim minimuma bez pronalaska globalno optimalnog rješenja. U konačnici postoji i mogućnost korištenja predloženog modela kao kontrolnog mehanizma ili mehanizma procjene kvalitete primijenjene strategije kod konvencionalnih fizikalnih modela.

5.1.   Smjernice za daljnja istraživanja

Tijekom a i nakon provedenih istraživanja došlo se do novih znanstvenih spoznaja koje bi trebalo istražiti u svrhu daljnjeg poboljšanja predstavljenih modela. Na razvoj modela utjecalo je znatno šire područje istraživanja od same problematike modeliranja i korištenja modalnih modela. Široko područje istraživanja je rezultiralo značajno drugačijim pristupom od do sada korištenih tehnika primijenjenih na području istraživanja.

Predstavljeni model samo u određenoj mjeri obuhvaća dinamičko ponašanje u obliku usrednjavanja rezultata, što u predstavljenim uvjetima osrednje dinamike vožnje bez znatnije promjene elevacije dobro aproksimira stvarno stanje modeliranog vozila. Model ne obuhvaća hladne startove koji u odnosu na hibridna vozila s vanjskim izvorom električne energije imaju daleko veći značaj nego kod klasičnih vozila. Nešto slabije predviđanje emisija NO_X-a uzrokovano je utjecajnim faktorima koji nisu obuhvaćeni trenutnom radnom točkom MSUI-ja nego prije svega i smjerom i brzinom dolaska do te radne točke. Općenito svi sustavi kontrole emisija temeljeni na katalitičkom učinku jako ovise o temperaturama unutar samih sustava na koje utječe niz događaja. Ove je utjecaje fizikalnim modelima vrlo teško opisati, a kod modalnih modela isti su potpuno zanemareni. Proširenje modela na višedimenzionalno područje, uključivanjem dodatnih varijabli, poput temperature motora donekle bi riješilo probleme predviđanja emisija kod hladnog starta. Međutim ovakav pristup nije najkvalitetnije rješenje zbog slabe korelacije s parametrima rada sustava kontrole emisija kao i gomilanja unutarnjih varijabli koje su teško predvidive izvana. U svrhu rješavanja prethodno opisanih problema predlaže se daljnje istraživanje proširenog modela s dva utjecajna modula opisana isključivo vanjskim ili postojećim unutarnjim varijablama:

- utjecaj gradijenta snage koji korigira izrazito dinamička ponašanja svih sustava čije ponašanje nije dovoljno dobro opisano trenutnom radnom točkom, a jako ovise o brzini i smjeru dostizanja te točke (EGR, omjer zraka i goriva, kut paljenja…)

- utjecaj povijesti događaja, odnosno povijesti snage, koji korigira spore, ali jako utjecajne promjene sustava kontrole emisija koji obično izraženo ovise o temperaturama (SCR, oksidacijski i redukcijski katalizatori i sl.), kao i sustave koji zahtijevaju periodične regeneracije (DPF, GPF, LNT i sl.)

Predloženi se model, kao i klasični VSP modeli, temelji na raspodjeli emisija unutar diskretnih raspona snage odnosno modalnih razreda. Broj i raspored razreda uglavnom su preuzeti iz metode procjene emisija pomoću grupiranja snage pri čemu nije izvršena analiza

njihova utjecaja na točnost rezultata predviđanja. Za razliku od metode grupiranja snage, u literaturi se u VSP analizi uglavnom koriste rasporedi razreda s konstantnim rasponima jednake širine. U svrhu optimizacije i postizanja određene točnosti potrebno je istražiti utjecaj broja, kao i raspored raspona snage na točnost predviđanja te odrediti njihove optimalne vrijednosti. Potrebno je istražiti utjecaj i svrhovitost uvođenja kontinuirane varijable na točnost predviđanja emisija i potrošnje goriva u odnosu na standardnu VSP definiciju.

LITERATURA

[1]   A. Kozina, G. Radica, and S. Nižetić, "Increasing engine efficiency at part load with the exhaust valve control: a simplified modelling approach," *International Journal of Exergy,* vol. 26, no. 1-2, pp. 131-153, 2018.

[2]   A. Kozina, G. Radica, and S. Nižetić, "Analysis of methods towards reduction of harmful pollutants from diesel engines," *Journal of Cleaner Production,* vol. 262, p. 121105, 2020.

[3]   A. Kozina, G. Radica, and S. Nižetić, "Emission Analysis of Diesel Vehicles in Circumstances of Emission Regulation System Failure: A Case Study," *Journal of Energy Resources Technology,* vol. 144, no. 8, 2022.

[4]   A. Kozina, T. Vidović, G. Radica, and A. Vučetić, "A New Vehicle-Specific Power Model for the Estimation of Hybrid Vehicle Emissions," *Energies,* vol. 16, no. 24, p. 8094, 2023.

[5]   "Regulation (EU) 2023/851 of the European Parliament and of the Council of 19 April 2023 amending Regulation (EU) 2019/631 as regards strengthening the CO2 emission performance standards for new passenger cars and new light commercial vehicles in line with the Union's increased climate ambition (Text with EEA relevance)." https://eur-lex.europa.eu/eli/reg/2023/851 (accessed May 10, 2024).

[6]   B. Mali, A. Shrestha, A. Chapagain, R. Bishwokarma, P. Kumar, and F. Gonzalez-Longatt, "Challenges in the penetration of electric vehicles in developing countries with a focus on Nepal," *Renewable Energy Focus,* vol. 40, pp. 1-12, 2022/03/01/ 2022, doi: https://doi.org/10.1016/j.ref.2021.11.003.

[7]   T. Fleischer, "Transport and sustainability, with special regard to the EU Transport White Paper of 2011," *Institute for World Economics of the Hungarian Academy of Sciences Working Papers,* 2011.

[8]   P. Mock and S. Díaz, "Pathways to decarbonization: the European passenger car market in the years 2021–2035," *communications,* vol. 49, pp. 847129-848102, 2021.

[9]   T. Takaishi, A. Numata, R. Nakano, and K. Sakaguchi. "Approach to high efficiency diesel and gas engines." https://www.mhi.co.jp/technology/review/pdf/e451/e451021.pdf (accessed June 19, 2024).

[10]   "Proposal for a REGULATION OF THE EUROPEAN PARLIAMENT AND OF THE COUNCIL on type-approval of motor vehicles and engines and of systems, components and separate technical units intended for such vehicles, with respect to their emissions and battery durability (Euro 7) and repealing Regulations (EC) No 715/2007 and (EC) No 595/2009." https://eur-lex.europa.eu/legal-content/EN/TXT/?uri=CELEX%3A52022PC0586 (accessed June 19, 2024).

[11]   "Commission proposes new Euro 7 standards to reduce pollutant emissions from vehicles and improve air quality." https://ec.europa.eu/commission/presscorner/detail/en/ip_22_6495 (accessed 19 June, 2024).

[12]   Z. C. Samaras *et al.*, "A European regulatory perspective towards a Euro 7 proposal," *SAE International Journal of Advances and Current Practices in Mobility,* vol. 5, no. 2022-37-0032, pp. 998-1011, 2022.

[13]   W. Zhuang *et al.*, "A survey of powertrain configuration studies on hybrid electric vehicles," *Applied Energy,* vol. 262, p. 114553, 2020.

[14] S. S. Ravi, J. Mazumder, J. Sun, C. Brace, and J. W. Turner, "Techno-Economic assessment of synthetic E-Fuels derived from atmospheric CO2 and green hydrogen," *Energy Conversion and Management,* vol. 291, p. 117271, 2023.

[15] A. Vučetić *et al.*, "Real Driving Emission from Vehicle Fuelled by Petrol and Liquefied Petroleum Gas (LPG)," *Cognitive Sustainability,* vol. 1, no. 4, 2022.

[16] U. K. Medževeprytė, R. Makaras, V. Lukoševičius, and S. Kilikevičius, "Application and Efficiency of a Series-Hybrid Drive for Agricultural Use Based on a Modified Version of the World Harmonized Transient Cycle," *Energies,* vol. 16, no. 14, p. 5379, 2023.

[17] W. Enang and C. Bannister, "Modelling and control of hybrid electric vehicles (A comprehensive review)," *Renewable and Sustainable Energy Reviews,* vol. 74, pp. 1210-1239, 2017.

[18] İ. A. Reşitoğlu, K. Altinişik, and A. Keskin, "The pollutant emissions from diesel-engine vehicles and exhaust aftertreatment systems," *Clean Technologies and Environmental Policy,* vol. 17, no. 1, pp. 15-27, 2015.

[19] P. Lakshminarayanan, Y. V. Aghav, and Y. Shi, *Modelling diesel combustion*. Springer, 2010.

[20] M. Perin and T. Achek, "Lean burn engines," SAE Technical Paper, 0148-7191, 2013.

[21] A. K. Agarwal, D. Kumar, N. Sharma, and U. Sonawane, *Engine Modeling and Simulation*. Springer, 2022.

[22] D. Kihas and M. R. Uchanski, "Engine-Out NOx models for on-ECU implementation: A brief overview," 2015.

[23] J. Ma, F. Xu, K. Huang, and R. Huang, "Improvement on the linear and nonlinear auto-regressive model for predicting the NOx emission of diesel engine," *Neurocomputing,* vol. 207, pp. 150-164, 2016.

[24] A. N. Bhatt and N. Shrivastava, "Application of artificial neural network for internal combustion engines: a state of the art review," *Archives of Computational Methods in Engineering,* vol. 29, no. 2, pp. 897-919, 2022.

[25] H. Omidvarborna, A. Kumar, and D.-S. Kim, "Recent studies on soot modeling for diesel combustion," *Renewable and Sustainable Energy Reviews,* vol. 48, pp. 635-647, 2015.

[26] S. Daido, Y. Kodama, T. Inohara, N. Ohyama, and T. Sugiyama, "Analysis of soot accumulation inside diesel engines," *JSAE review,* vol. 21, no. 3, pp. 303-308, 2000.

[27] J. B. Heywood, *Internal combustion engine fundamentals*. McGraw-Hill Education, 2018.

[28] E. Jiaqiang *et al.*, "Soot formation mechanism of modern automobile engines and methods of reducing soot emissions: A review," *Fuel Processing Technology,* vol. 235, p. 107373, 2022.

[29] Ö. L. Gülder and D. R. Snelling, "Influence of nitrogen dilution and flame temperature on soot formation in diffusion flames," *Combustion and flame,* vol. 92, no. 1-2, pp. 115-124, 1993.

[30] D. Du, R. Axelbaum, and C. K. Law, "Soot formation in strained diffusion flames with gaseous additives," *Combustion and flame,* vol. 102, no. 1-2, pp. 11-20, 1995.

[31] R. Zhang and S. Kook, "Influence of fuel injection timing and pressure on in-flame soot particles in an automotive-size diesel engine," *Environmental science & technology,* vol. 48, no. 14, pp. 8243-8250, 2014.

[32] Z. Han, A. Uludogan, G. J. Hampson, and R. D. Reitz, "Mechanism of soot and NOx emission reduction using multiple-injection in a diesel engine," *SAE transactions,* pp. 837-852, 1996.

[33]   H. Hiroyasu and T. Kadota, "Models for combustion and formation of nitric oxide and soot in direct injection diesel engines," *SAE transactions,* pp. 513-526, 1976.

[34]   J. Nagle and R. Strickland-Constable, "Oxidation of carbon between 1000–2000 C," in *Proceedings of the fifth conference on carbon*, 1962: Elsevier, pp. 154-164.

[35]   F. Tao, S. Srinivas, R. D. Reitz, and D. E. Foster, "Comparison of three soot models applied to multi-dimensional diesel combustion simulations," *JSME International Journal Series B Fluids and Thermal Engineering,* vol. 48, no. 4, pp. 671-678, 2005.

[36]   F. Perini, E. Mattarelli, and F. Paltrinieri, "Development and validation of predictive emissions schemes for quasi-dimensional combustion models," SAE Technical paper, 0148-7191, 2010.

[37]   A. Onorati, G. Ferrari, and G. D'Errico, "1D unsteady flows with chemical reactions in the exhaust duct-system of SI engines: predictions and experiments," *SAE Transactions,* pp. 738-752, 2001.

[38]   H. Shen, T. Shamim, and S. Sengupta, "An investigation of catalytic converter performances during cold starts," SAE Technical Paper, 0148-7191, 1999.

[39]   S. Chan and D. Hoang, "Modeling of catalytic conversion of CO/HC in gasoline exhaust at engine cold-start," SAE Technical Paper, 0148-7191, 1999.

[40]   G. D'Errico, G. Ferrari, A. Onorati, and T. Cerri, "Modeling the pollutant emissions from a SI engine," *SAE Transactions,* pp. 1-11, 2002.

[41]   H. S. Sorathia, P. P. Rahhod, and A. S. Sorathiya, "Effect of Exhaust gas recirculation (EGR) on NOx emission from CI engine. A review study," *Int J Adv Eng Res Studies,* vol. 3, pp. 223-227, 2012.

[42]   K. Mollenhauer, H. Tschöke, and K. G. Johnson, *Handbook of diesel engines*. Springer Berlin, 2010.

[43]   P. R. Ghodke and J. G. Suryavanshi, "Review of Advanced EGR and Breathing Systems for High Performance and Low Emission HSDI Diesel Engine," *Int. J. Mod. Eng. Res.,* vol. 2, no. 5, pp. 3138-3142, 2012.

[44]   Y. Park and C. Bae, "Experimental study on the effects of high/low pressure EGR proportion in a passenger car diesel engine," *Applied Energy,* vol. 133, pp. 308-316, 2014.

[45]   S. Reifarth, "EGR-systems for diesel engines," 2010.

[46]   B. Pereda-Ayo and J. R. González-Velasco, "NOx storage and reduction for diesel engine exhaust aftertreatment," *Diesel Engine-Combustion, Emissions and Condition Monitoring,* 2013.

[47]   C. D. DiGiulio *et al.*, "NH3 formation over a lean NOX trap (LNT) system: Effects of lean/rich cycle timing and temperature," *Applied Catalysis B: Environmental,* vol. 147, pp. 698-710, 2014.

[48]   T. Maunula, "Combination of LNT and SCR for NOx reduction in passenger car applications," *Combustion Engines,* vol. 53, 2014.

[49]   H. Sinzenich and K. Wehler, "Selective Catalytic Reduction: Exhaust aftertreatment for reducing nitrogen oxide emissions," *MTU Friedrichshafen GmbH,* 2014.

[50]   M. Nesbit *et al.*, "The Differences between the EU and US Legislation on Emissions in the Automotive Sector," 2016.

[51]   B. Amon and G. Keefe, "On-Road Demonstration of NOx Emission Control for Heavy-Duty Diesel Trucks using SINOx™ Urea SCR technology-Long-term Experience and Measurement Results," SAE Technical Paper, 0148-7191, 2001.

[52]   L. Lietti, I. Nova, and P. Forzatti, "Role of ammonia in the reduction by hydrogen of NOx stored over Pt–Ba/Al2O3 lean NOx trap catalysts," *Journal of catalysis,* vol. 257, no. 2, pp. 270-282, 2008.

[53]   J. H. Kwak, R. G. Tonkyn, D. H. Kim, J. Szanyi, and C. H. Peden, "Excellent activity and selectivity of Cu-SSZ-13 in the selective catalytic reduction of NOx with NH3," *Journal of Catalysis,* vol. 275, no. 2, pp. 187-190, 2010.

[54]   M. Koebel, M. Elsener, and M. Kleemann, "Urea-SCR: a promising technique to reduce NOx emissions from automotive diesel engines," *Catalysis today,* vol. 59, no. 3-4, pp. 335-345, 2000.

[55]   B. T. Johnson, "Diesel engine emissions and their control," *Platinum Metals Review,* vol. 52, no. 1, pp. 23-37, 2008.

[56]   A.-M. Stamatellou and A. Stamatelos, "Overview of Diesel particulate filter systems sizing approaches," *Applied Thermal Engineering,* vol. 121, pp. 537-546, 2017.

[57]   Y. Quan-shun, T. Jian-wei, G. Yun-Shan, H. Li-jun, and P. Zi-hang, "Application of diesel particulate filter on in-use on-road vehicles," *Energy Procedia,* vol. 105, pp. 1730-1736, 2017.

[58]   B. Guan, R. Zhan, H. Lin, and Z. Huang, "Review of the state-of-the-art of exhaust particulate filter technology in internal combustion engines," *Journal of environmental management,* vol. 154, pp. 225-258, 2015.

[59]   O. M. Govardhan, "Fundamentals and classification of hybrid electric vehicles," *International Journal of Engineering and Techniques,* vol. 3, no. 5, pp. 194-198, 2017.

[60]   W. Liu, *Introduction to hybrid vehicle system modeling and control*. John Wiley & Sons, 2013.

[61]   D. S. Cardoso, P. O. Fael, and A. Espírito-Santo, "A review of micro and mild hybrid systems," *Energy reports,* vol. 6, pp. 385-390, 2020.

[62]   F. Zhang, L. Wang, S. Coskun, H. Pang, Y. Cui, and J. Xi, "Energy management strategies for hybrid electric vehicles: Review, classification, comparison, and outlook," *Energies,* vol. 13, no. 13, p. 3352, 2020.

[63]   S. Onori, L. Serrao, and G. Rizzoni, *Hybrid electric vehicles: Energy management strategies*. Springer, 2016.

[64]   K. Ç. Bayindir, M. A. Gözüküçük, and A. Teke, "A comprehensive overview of hybrid electric vehicle: Powertrain configurations, powertrain control techniques and electronic control units," *Energy conversion and Management,* vol. 52, no. 2, pp. 1305-1313, 2011.

[65]   K. V. Singh, H. O. Bansal, and D. Singh, "A comprehensive review on hybrid electric vehicles: architectures and components," *Journal of Modern Transportation,* vol. 27, no. 2, pp. 77-107, 2019.

[66]   L. Wang, Y. Cui, F. Zhang, and G. Li, "Architectures of planetary hybrid powertrain system: review, classification and comparison," *Energies,* vol. 13, no. 2, p. 329, 2020.

[67]   J. Meisel, W. Shabbir, and S. A. Evangelou, "Evaluation of the through-the-road architecture for plug-in hybrid electric vehicle powertrains," in *2013 IEEE International Electric Vehicle Conference (IEVC)*, 2013: IEEE, pp. 1-5.

[68]   S. Zulkifli, S. Mohd, N. Saad, and A. Aziz, "Split-parallel through-the-road hybrid electric vehicle: Operation, power flow and control modes," in *2015 IEEE Transportation Electrification Conference and Expo (ITEC)*, 2015: IEEE, pp. 1-7.

[69]   C. Chan, "The state of the art of electric and hybrid vehicles," *Proceedings of the IEEE,* vol. 90, no. 2, pp. 247-275, 2002.

[70]   M. Mądziel, "Vehicle emission models and traffic simulators: a review," *Energies,* vol. 16, no. 9, p. 3941, 2023.

[71]   B. Othman, G. De Nunzio, D. Di Domenico, and C. Canudas-de-Wit, "Ecological traffic management: A review of the modeling and control strategies for improving environmental sustainability of road transportation," *Annual Reviews in Control,* vol. 48, pp. 292-311, 2019.

[72] K. Ahn, H. Rakha, A. Trani, and M. Van Aerde, "Estimating vehicle fuel consumption and emissions based on instantaneous speed and acceleration levels," *Journal of transportation engineering,* vol. 128, no. 2, pp. 182-190, 2002.

[73] H. Eichlsederr, S. Hausberger, M. Rexeis, M. Zallinger, and R. Luz, "Emission Factors from the Model PHEM for the HBEFA Version 3," 2009.

[74] G. Scora and M. Barth, "Comprehensive modal emissions model (cmem), version 3.01," *User guide. Centre for environmental research and technology. University of California, Riverside,* vol. 1070, p. 1580, 2006.

[75] B. Degraeuwe and M. Weiss, "Does the New European Driving Cycle (NEDC) really fail to capture the NOX emissions of diesel cars in Europe?," *Environmental Pollution,* vol. 222, pp. 234-241, 2017.

[76] L. I. Panis, S. Broekx, and R. Liu, "Modelling instantaneous traffic emission and the influence of traffic speed limits," *Science of the total environment,* vol. 371, no. 1-3, pp. 270-285, 2006.

[77] C. C. Chan, A. Bouscayrol, and K. Chen, "Electric, hybrid, and fuel-cell vehicles: Architectures and modeling," *IEEE transactions on vehicular technology,* vol. 59, no. 2, pp. 589-598, 2009.

[78] K. B. Wipke, M. R. Cuddy, and S. D. Burch, "ADVISOR 2.1: A user-friendly advanced powertrain simulation using a combined backward/forward approach," *IEEE transactions on vehicular technology,* vol. 48, no. 6, pp. 1751-1761, 1999.

[79] J. Liu and H. Peng, "Modeling and control of a power-split hybrid vehicle," *IEEE transactions on control systems technology,* vol. 16, no. 6, pp. 1242-1251, 2008.

[80] S. Bogosyan, M. Gokasan, and D. J. Goering, "A novel model validation and estimation approach for hybrid serial electric vehicles," *IEEE Transactions on Vehicular Technology,* vol. 56, no. 4, pp. 1485-1497, 2007.

[81] F. Chiara, J. Wang, C. B. Patil, M.-F. Hsieh, and F. Yan, "Development and experimental validation of a control-oriented Diesel engine model for fuel consumption and brake torque predictions," *Mathematical and Computer Modelling of Dynamical Systems,* vol. 17, no. 3, pp. 261-277, 2011.

[82] L. Pelkmans, P. Debal, T. Hood, G. Hauser, and M.-R. Delgado, "Development of a simulation tool to calculate fuel consumption and emissions of vehicles operating in dynamic conditions," SAE Technical Paper, 0148-7191, 2004.

[83] M. Zhou and H. Jin, "Development of a transient fuel consumption model," *Transportation Research Part D: Transport and Environment,* vol. 51, pp. 82-93, 2017.

[84] M. Lindgren, "A transient fuel consumption model for non-road mobile machinery," *Biosystems Engineering,* vol. 91, no. 2, pp. 139-147, 2005.

[85] W. Lei, H. Chen, and L. Lu, "Microscopic emission and fuel consumption modeling for light-duty vehicles using portable emission measurement system data," *World Academy of Science, Engineering and Technology,* vol. 66, pp. 918-925, 2010.

[86] M. Pettiti, L. Pilo, and F. Millo, "Development of a new mean value model for the analysis of turbolag phenomena in automotive diesel engines," *SAE Transactions,* pp. 822-833, 2007.

[87] M. Barth *et al.*, "The development of a comprehensive modal emissions model," *NCHRP Web-only document,* vol. 122, pp. 25-11, 2000.

[88] M. V. E. Simulator, "User guide," *ANSYS Inc. URL http://www.ansys.com,* 2009.

[89] D. W. Gao, C. Mi, and A. Emadi, "Modeling and simulation of electric and hybrid vehicles," *Proceedings of the IEEE,* vol. 95, no. 4, pp. 729-745, 2007.

[90] T. Markel *et al.*, "ADVISOR: a systems analysis tool for advanced vehicle modeling," *Journal of power sources,* vol. 110, no. 2, pp. 255-266, 2002.

[91]   G. Liao, T. Weber, and D. Pfaff, "Modelling and analysis of powertrain hybridization on all-wheel-drive sport utility vehicles," *Proceedings of the Institution of Mechanical Engineers, Part D: Journal of Automobile Engineering,* vol. 218, no. 10, pp. 1125-1134, 2004.

[92]   H. T. Arat, B. Tanc, N. Yonet, and E. Baltacioglu, "Comparative Simulation Analyses on Eenergy flow chatacteristic of different HEV configurations," *16th International Conference on Clean Energy (ICCE-2018), 9-11 May 2018, Famagusta, N. Cyprus*.

[93]   K. Chen, A. Bouscayrol, A. Berthon, P. Delarue, D. Hissel, and R. Trigui, "Global modeling of different vehicles," *IEEE Vehicular Technology Magazine,* vol. 4, no. 2, pp. 80-89, 2009.

[94]   A. Shukla, "Modelling and simulation of hybrid electric vehicles," Department of Mechanical Engineering, Imperial College London, 2012.

[95]   X. Li and S. S. Williamson, "Efficiency and suitability analyses of varied drive train architectures for plug-in hybrid electric vehicle (PHEV) applications," in *2008 IEEE Vehicle Power and Propulsion Conference*, 2008: IEEE, pp. 1-6.

[96]   B. Wahono, W. B. Santoso, and A. Nur, "Analysis of range extender electric vehicle performance using vehicle simulator," *Energy Procedia,* vol. 68, pp. 409-418, 2015.

[97]   I. Mahalec, Z. Lulić, and D. Kozarac, "Motori s unutarnjim izgaranjem," *Fakultet strojarstva i brodogradnje, Zagreb,* 2010.

[98]   A. Kozina, "Procjena emisija, modeliranje i upravljanje sustavima pogona hibridnih električnih vozila," *Fakultet elektrotehnike, strojarstva i brodogradnje, Split,* Kvalifikacijski doktorski ispit 2022.

[99]   D.-D. Tran, M. Vafaeipour, M. El Baghdadi, R. Barrero, J. Van Mierlo, and O. Hegazy, "Thorough state-of-the-art analysis of electric and hybrid vehicle powertrains: Topologies and integrated energy management strategies," *Renewable and Sustainable Energy Reviews,* vol. 119, p. 109596, 2020.

[100] M. Sabri, K. A. Danapalasingam, and M. F. Rahmat, "A review on hybrid electric vehicles architecture and energy management strategies," *Renewable and Sustainable Energy Reviews,* vol. 53, pp. 1433-1442, 2016.

[101] F. R. Salmasi, "Control strategies for hybrid electric vehicles: Evolution, classification, comparison, and future trends," *IEEE Transactions on vehicular technology,* vol. 56, no. 5, pp. 2393-2404, 2007.

[102] P. Zhang, F. Yan, and C. Du, "A comprehensive analysis of energy management strategies for hybrid electric vehicles based on bibliometrics," *Renewable and Sustainable Energy Reviews,* vol. 48, pp. 88-104, 2015.

[103] A. M. Ali and D. Söffker, "Towards optimal power management of hybrid electric vehicles in real-time: A review on methods, challenges, and state-of-the-art solutions," *Energies,* vol. 11, no. 3, p. 476, 2018.

[104] J. L. Jimenez-Palacios, "Understanding and quantifying motor vehicle emissions with vehicle specific power and TILDAS remote sensing," *Massachusetts Institute of Technology,* 1998.

[105] H. Watson, E. Milkins, M. Preston, C. Chittleborough, and B. Alimoradian, "Predicting fuel consumption and emissions - transferring chassis dynamometer results to real driving conditions," *SAE Transactions,* pp. 188-211, 1983.

[106] D. Bowyer, R. Akçelik, and D. Biggs, "Guide to fuel consumption analyses for urban traffic management," 1984: Australian Road Research Board.

[107] G. Song and L. Yu, "Characteristics of low-speed vehicle-specific power distributions on urban restricted-access roadways in Beijing," *Transportation research record,* vol. 2233, no. 1, pp. 90-98, 2011.

[108] H. Zhai, H. C. Frey, N. M. Rouphail, G. A. Goncalves, and T. L. Farias, "Comparison of flexible fuel vehicle and life-cycle fuel consumption and emissions of selected pollutants and greenhouse gases for ethanol 85 versus gasoline," *Journal of the Air & Waste Management Association,* vol. 59, no. 8, pp. 912-924, 2009.

[109] H. C. Frey, N. M. Rouphail, H. Zhai, T. L. Farias, and G. A. Gonçalves, "Comparing real world fuel consumption for diesel and hydrogen fueled transit buses and implication for emissions," *Transportation Research Part D: Transport and Environment,* vol. 12, no. 4, pp. 281-291, 2007.

[110] Q. Yu, T. Li, and H. Li, "Improving urban bus emission and fuel consumption modeling by incorporating passenger load factor for real world driving," *Applied Energy,* vol. 161, pp. 101-111, 2016.

[111] H. Wang, L. Fu, Y. Zhou, and H. Li, "Modelling of the fuel consumption for passenger cars regarding driving characteristics," *Transportation Research Part D: Transport and Environment,* vol. 13, no. 7, pp. 479-482, 2008.

[112] X. Zhou, J. Huang, W. Lv, and D. Li, "Fuel consumption estimates based on driving pattern recognition," in *2013 IEEE International Conference on Green Computing and Communications and IEEE Internet of Things and IEEE Cyber, Physical and Social Computing*, 2013: IEEE, pp. 496-503.

[113] M. Campino, N. Henriques, and G. Duarte, "Energy Assessment of a Plug-in Hybrid Vehicle Propulsion Management System," *KnE Engineering,* pp. 833–845, 2020.

[114] G. Duarte, R. A. Varella, G. Gonçalves, and T. Farias, "Effect of battery state of charge on fuel use and pollutant emissions of a full hybrid electric light duty vehicle," *Journal of Power Sources,* vol. 246, pp. 377-386, 2014.

[115] W. Wang *et al.*, "A new vehicle specific power method based on internally observable variables: Application to CO2 emission assessment for a hybrid electric vehicle," *Energy Conversion and Management,* vol. 286, p. 117050, 2023.

[116] G. O. Duarte, G. A. Gonçalves, P. C. Baptista, and T. L. Farias, "Establishing bonds between vehicle certification data and real-world vehicle fuel consumption–a vehicle specific power approach," *Energy Conversion and Management,* vol. 92, pp. 251-265, 2015.

[117] Z. Mera, R. Varella, P. Baptista, G. Duarte, and F. Rosero, "Including engine data for energy and pollutants assessment into the vehicle specific power methodology," *Applied Energy,* vol. 311, p. 118690, 2022.

[118] H. Zhai, H. C. Frey, and N. M. Rouphail, "Development of a modal emissions model for a hybrid electric vehicle," *Transportation Research Part D: Transport and Environment,* vol. 16, no. 6, pp. 444-450, 2011.

[119] X. Zeng, Q. Qian, H. Chen, D. Song, and G. Li, "A unified quantitative analysis of fuel economy for hybrid electric vehicles based on energy flow," *Journal of cleaner production,* vol. 292, p. 126040, 2021.

[120] T. Katrašnik, "Analytical framework for analyzing the energy conversion efficiency of different hybrid electric vehicle topologies," *Energy Conversion and Management,* vol. 50, no. 8, pp. 1924-1938, 2009.

[121] A. Kozina, G. Radica, and S. Nižetić, "Hybrid Vehicles Emissions Assessment," in *2021 6th International Conference on Smart and Sustainable Technologies (SpliTech)*, 2021: IEEE, pp. 1-5.

[122] J. Anderson, "Expectations for actual Euro 6 vehicle emissions," ed: Concawe-Ricardo, 2018.

[123] J. Demuynck, D. Bosteels, M. De Paepe, C. Favre, J. May, and S. Verhelst, "Recommendations for the new WLTP cycle based on an analysis of vehicle emission measurements on NEDC and CADC," *Energy Policy,* vol. 49, pp. 234-242, 2012.

[124] N. Hooftman, M. Messagie, J. Van Mierlo, and T. Coosemans, "A review of the European passenger car regulations–Real driving emissions vs local air quality," *Renewable and Sustainable Energy Reviews,* vol. 86, pp. 1-21, 2018.

[125] S. Kwon, Y. Park, J. Park, J. Kim, K.-H. Choi, and J.-S. Cha, "Characteristics of on-road NOx emissions from Euro 6 light-duty diesel vehicles using a portable emissions measurement system," *Science of the Total Environment,* vol. 576, pp. 70-77, 2017.

[126] R. O'Driscoll, M. E. Stettler, N. Molden, T. Oxley, and H. M. ApSimon, "Real world CO2 and NOx emissions from 149 Euro 5 and 6 diesel, gasoline and hybrid passenger cars," *Science of the total environment,* vol. 621, pp. 282-290, 2018.

[127] (2016). *COMMISSION REGULATION (EU) 2016/427; amending Regulation (EC) No 692/2008 as regards emissions from light passenger and commercial vehicles (Euro 6).*

[128] R. A. Varella, G. Duarte, P. Baptista, L. Sousa, and P. M. Villafuerte, "Comparison of data analysis methods for European real driving emissions regulation," SAE Technical Paper, 0148-7191, 2017.

[129] I. Preda, D. Covaciu, and G. Ciolan, "Coast down test–theoretical and experimental approach," presented at the CONAT 2010 - International Automotive Congress, 2010. [Online]. Available: http://hdl.handle.net/123456789/7.

[130] A. Kozina, T. Vidović, G. Radica, and S. Nižetić, "Emission and efficiency estimation of hybrid powertrains with continuous Vehicle Specific Power analysis," in *2022 7th International Conference on Smart and Sustainable Technologies (SpliTech)*, 2022: IEEE, pp. 1-5.

PRILOG A

Naslov rada: Increasing engine efficiency at part load with the exhaust valve control: a simplified modelling approach

Autori: Ante Kozina, Gojmir Radica, Sandro Nižetić

Sažetak: In this study, a new, innovative system based on variable regulation of the exhaust valves in the spark ignited engine was described and analysed. The efficiency of standard spark ignited engines decreases during partial load compared to full load, due to increased losses in the exchange of working medium, precisely, loss of suction. The simplified model of the new system has been developed and a comparison was made between the standard engine, regulated with a valve on the intake system, and an engine that is regulated by dual opening of the exhaust valves. Research was carried out on the model of a four cylinder Otto engine with direct injection into the cylinder. The main results showed a significant improvement over the standard engine with a fixed intake geometry. Specific consumption is reduced between 3.83% and 4.23%, and losses of cylinder gases exchange have decreased between 85% and 87%.

Increasing engine efficiency at part load with the exhaust valve control: a simplified modelling approach

A. Kozina and G. Radica*

Faculty of Electrical Engineering,
Mechanical Engineering and Naval Architecture,
Department of Heat Engines,
University of Split,
Split, 21000, Croatia
Email: antekozina2@gmail.com
Email: goradica@fesb.hr
*Corresponding author

S. Nižetić

LTEF-Laboratory for Thermodynamics and Energy Efficiency,
Faculty of Electrical Engineering,
Mechanical Engineering and Naval Architecture,
University of Split,
Split, 21000, Croatia
Email: snizetic@fesb.hr

Abstract: In this study, a new, innovative system based on variable regulation of the exhaust valves in the spark ignited engine was described and analysed. The efficiency of standard spark ignited engines decreases during partial load compared to full load, due to increased losses in the exchange of working medium, precisely, loss of suction. The simplified model of the new system has been developed and a comparison was made between the standard engine, regulated with a valve on the intake system, and an engine that is regulated by dual opening of the exhaust valves. Research was carried out on the model of a four cylinder Otto engine with direct injection into the cylinder. The main results showed a significant improvement over the standard engine with a fixed intake geometry. Specific consumption is reduced between 3.83% and 4.23%, and losses of cylinder gases exchange have decreased between 85% and 87%.

Keywords: engine efficiency; exhaust valve control; cylinder gas exchange; gasoline engine.

Reference to this paper should be made as follows: Kozina, A., Radica, G. and Nižetić, S. (2018) 'Increasing engine efficiency at part load with the exhaust valve control: a simplified modelling approach', *Int. J. Exergy*, Vol. 26, Nos. 1/2, pp.131–153.

Biographical notes: Ante Kozina is a PhD student at Faculty of Electrical Engineering, Mechanical Engineering and Naval Architecture (FESB) at University of Split (Croatia), has a Master's degree in Mechanical Engineering and Bachelor degree in Electrical Engineering. His research interest is in energy efficiency and optimisation of heat engines. He worked as a Head of

Design Department for five years at company Tromont, responsible for railway and military industry projects. Currently, he is Head of Design Department at company Espera.

Gojmir Radica, PhD, is a Full Professor at the Faculty of Electrical Engineering, Mechanical Engineering and Naval Architecture (FESB) at University of Split (Croatia). He has years-long experience in heat engines, acquiring of new technology in engine diagnostic and optimisation, energy efficiency, marine engineering, cogeneration and hybrid systems. He served as Head of Department of Mechanical Engineering and Naval Architecture at Faculty of FESB. Currently he is Head of Laboratory for heat engines and chair for Heat Engines at University of Split.

Sandro Nižetić is an Associate Professor at the Faculty of Electrical Engineering, Mechanical Engineering and Naval Architecture (FESB) at University of Split (Croatia). He has experience in theoretical and applied thermodynamics, HVAC systems, energy efficiency in buildings, rational usage of energy, utilisation of renewable energy sources, and more than 15 years of the teaching experience. He served as the Vice Dean for the research at faculty of FESB and also as the deputy minister in the Croatian government. He is Head of the Laboratory for Thermodynamics and Energy Efficiency (LTEF-Laboratory) at University of Split.

1 Introduction

According to the European vehicle market statistic (Peter, 2012), GDI engines are mostly used in the automotive industry to run passenger and light commercial vehicles and general gasoline engines (Figure 1). Growing public awareness of the needs for environmental protection, as well as the recent increases in crude oil prices, are the strongest drivers for the recent developments in the internal combustion engine technology in the last 15 years (EUROPEAN VEHICLE MARKET STATISTICS, 2016/17 ICCT-Figure 1). Gasoline engines in the European market lost 20% of the stake of road vehicles in favour of diesel engines (Figure 2). According to Cygnar and Sendyka (2013), diesel engines, in terms of conventional efficiency, reached almost maximum while the development of petrol engines is only now in full swing (Pesiridis et al., 2015). The main disadvantage of gasoline engines, compared to diesel, is the control of the suctioned working fluid to maintain an approximately constant ratio of air and fuel. This control is achieved by throttling the intake air which causes under pressure in the cylinder during the suction stroke. According to Cygnar and Sendyka (2013), and Raju and Hithaish (2014), the greatest progress in controlling the working fluid flow was achieved by applying variable-valve timing and the transition to direct fuel injection into the cylinder instead of the intake port. Variable valve timing is a technique at high-speed Otto-cycle engines that have been successfully used for over 20 years, and in the past few years has also been used in diesel engines (Bonatesta et al., 2016; Fontana and Galloni,

2009; Lee et al., 2010; Xie et al., 2014; Pournazeri et al., 2017). Theoretical concepts and principles of work exist dating back from the beginning of the last century. Their use has been limited by the development of technology and management mechanisms for valve timing. In the beginning, there was control of the valve timing, then valve lifting (usually in two steps). In the early 2000s, continuous control of phase and lifting have been used, which enables full control of the engine load without the use of a separate throttle valve at the inlet.

The effects of variable valve timing strategy on the gas exchange process and performance of a 4-valve direct injection HCCI engine were computationally investigated using a 1D fluid-dynamic engine cycle simulation code. A non-typical intake valve strategy was examined; whereby the intake valves were assumed to be independently actuated with the same valve-lift profile but at different timings. Using such an intake valves strategy, the obtained results showed that the operating range of the exhaust-valve-timing within which the HCCI combustion can be facilitated and maintained becomes much wider than that of the typical intake valve-timing case (Mahrous et al., 2009).

The influence of continuously variable valve timing of the intake valves in the operation of hydrogen-powered engines is analysed (Verhelst et al., 2010). Results show that it is possible to optimise the applied control strategy by using variable valve timing as a means to increase the range of both the qualitative and quantitative load control methods,

The latest generation of engines used electrohydraulic valve train that allows them almost unlimited possibilities such as phase adjustment, strokes and shape of the valve opening curve etc. (Radica, 2008). Most of the currently used strategies for valve control are based on the Atkinson cycle, which involves the later closure of the intake valves, or the Miller cycle that involves the early closure of the intake valve relative to the Otto cycle. Regarding the loss reduction during the interchange of the working fluids, Atkinson cycle has an advantage, compared to the standard Otto cycle, because a portion of the gas mixture is returned into the intake manifold during the extended time of the opening valve. In Atkinson cycle the mean pressure in the cylinder during the intake stroke increases resulting in reduced intake losses. The advantage of Miller cycle is as intake of mixture or air is shorter, due to the early closure of intake valve and therefore there is less need for damping. The previous results are causing the higher mean effective pressure in the cylinder during the intake (Knop and Mattioli, 2015). There are other solutions for reducing the loss in suction, that are based on the lean combustion process by Çelik and Özdalyan (2010). As it is not possible to achieve stable combustion in a homogeneous lean gas mixture, stratified injection has been applied which allows locally rich mixture that burns stably. Rich mixture appears usually near sources of sparks. Stratified injection is limited to a low medium pressure in the cylinder and a lower speed range because those parameters increase the swirl and layered mixture of fuel and gas (Cygnar and Sendyka, 2013). According to Crolla (2009), the specific fuel gasoline consumption at full load is between 250 g/kWh and 300 g/kWh, thus, there is room for investigation and possible progress.

The main objective of this research was to develop a simplified model of the gasoline engine regulated by the dual opening of the exhaust valves, and to compare it with the standard gasoline engine. The general idea is to reduce losses incurred through changes to the working media and to increase the efficiency of high-speed gasoline internal

combustion engines with direct injection of fuel into the cylinder GDI (eng. Gasoline Direct Injection).

In this study, a new approach to the above issues is described, which is based on a dual opening of the exhaust valves. The valves are opened by default in the exhaust cycle, then again in the compression stroke. In this regard, dropping the excess air that is trapped in the cylinder could be due to the removal of the intake restrictor or its reduced activity. Excluding damping intake reduces losses during suction phase, which have a large share of the losses incurred during the gas exchange process for petrol engines at part load. As most of the time automotive engines work in the load range of less than 50%, the efficiency of the petroleum car engines at part load is more important than efficiency at full load. The effect of technologies on brake specific fuel consumption (BSFC) at low load according to Analysis and Strategic Solution Concepts on Powertrain System Level is shown in Figure 1. The distribution of losses in the internal combustion engine is shown in Figure 2.

Figure 1 Specific fuel consumption for different technologies at 2 bar BMEP (see online version for colours)
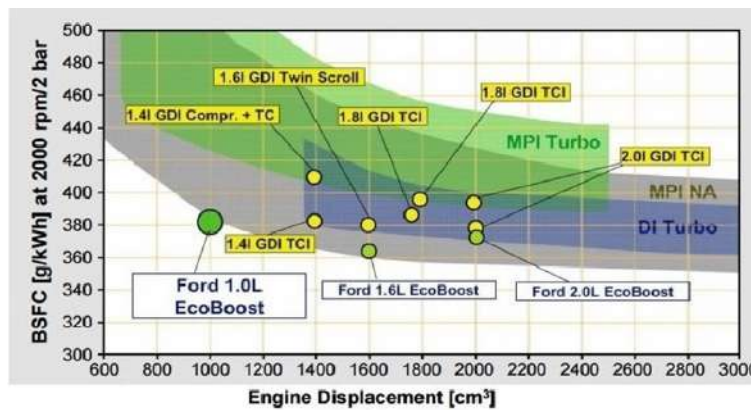
Source: Schoppe et al. (2012)

Figure 2 Distribution losses in an internal combustion engine
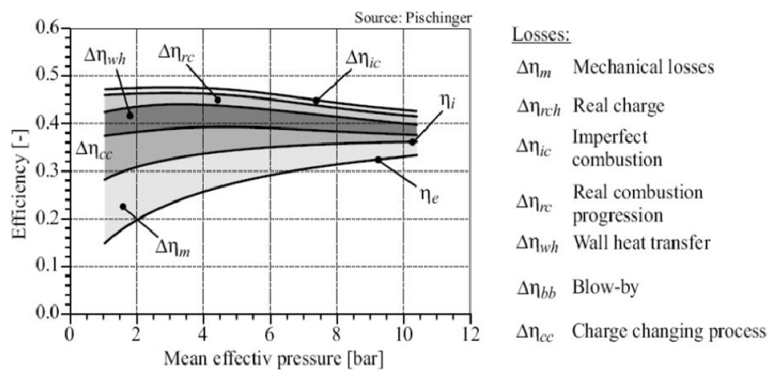
Source: Sorusbay (2016)

2 Elaboration of the simplified modelling approach and applied methodology

For the purpose of this research the model of the four-stroke, sixteen valves, four-cylinder petroleum engine was used with features presented in Table 1.

Table 1   Engine main parameters

Displacement	2000 cm^3
Stroke/Piston	86 mm/86 mm
Compression ratio	10.5

It is necessary to inject the fuel after the release of excess gas during the compression stroke, thus this system can only work in conjunction with direct fuel injection into the cylinder. For the modelling of combustion, single Vibe function was used (Sorusbay, 2016; Ghojel, 2010), and for modelling heat transfer, Woschni model was used. Control of the engine power is derived with control valve R3 (Figure 3) which is controlled by measuring the mean effective cylinder pressure at first cylinder.

For a model that simulates the engine with dual opening exhausts, complete control of the exhaust valve (phase, lift and shape of the curve) is assumed. The simulation of three possible models was considered:

- with the dual opening of the exhaust valve

- with the opening of one exhaust valve in the exhaust stroke and the other in the compression stroke

- with separate valves that represent another opening in the compression stroke.

The first model represents the real conditions, but the disadvantage is the interaction of the exhaust gas with excess gases that are emitted during the compression stroke, and therefore need another additional step of optimising the exhaust pipe. The second model also the conventional way as in reality at low loads only a single exhaust valve opens in the exhaust cycle while the second opening is during the compression cycle. This model is less susceptible to the influence of the geometry of the exhaust pipes than the first model. The third model describes an optimised exhaust system, where the exhaust valves open twice, as in the first model but the difference is that another opening has been provided with separate valves and equal geometrical characteristics. This model was chosen because of the simplicity and uniformity of the performance of all cylinders, without additional steps of optimising the geometry of the exhaust pipe (Figure 3).

During research, a comparison of conventional direct fuel injection petrol engines was made with the same characteristics equipped engine but with a system for the double opening of the exhaust valve. For the purpose of this experiment AVL – BOOST module was utilised which uses the quasi-dimensional model (QD) to simulate processes inside the cylinder and one-dimensional model (1D) to simulate the intake and exhaust. Parameters of load and engine speed have been selected, according to NEDC cycle by Barlow and McCrae (2009): speed 2000 RPM and, Brake Mean Effective Pressure) BMEP at: 2 bar, 3 bar and 4 bar corrected for the standard model and for DVA model. All tested working point of simulated engine are shown in Table 2. First of all, the

ignition angle was optimised to maximum efficiency for a standard engine at 2000 RPM and BMEP 3 bar. The best result was achieved for the ignition angle −10 BTDC (Figure 4). The timing of intake and exhaust valves was fixed. Intake cam phase has a significant effect on the observed performance and needs to be well defined and optimised according to the maximum power in the upper-speed range (Figure 5).

Figure 3 Schematic diagram of the engine with dual opening exhaust valves (DVA model) in the software package AVL-Boost (see online version for colours)
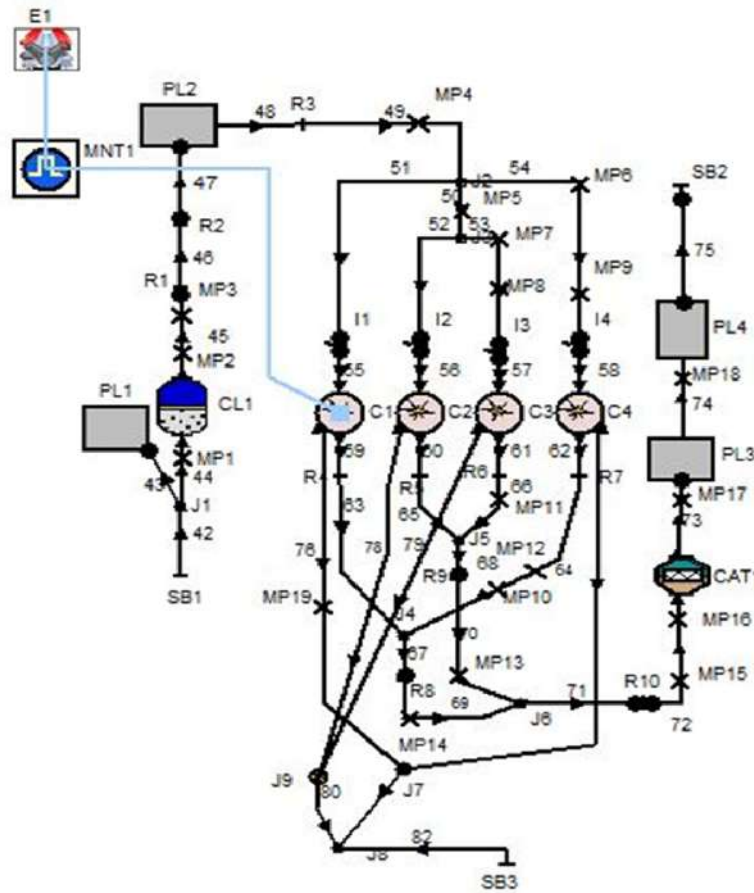
Table 2   Comparison of simulated engine

Model		Max BMEP	Standard_2B	Standard_3B	Standard_4B	DVA_2B	DVA_3B	DVA_4B
RPM	1/min	5000	2000	2000	2000	2000	2000	2000
BMEP	bar	11.4	2	3	4	2	3	4
FMEP	bar	2	0.94	0.94	0.94	0.94	0.94	0.94
Geometric compression ratio	1	10.5	10.5	10.5				

Figure 4 Indicated specific fuel consumption ISFCE in function of start of combustion angle SOC (see online version for colours)
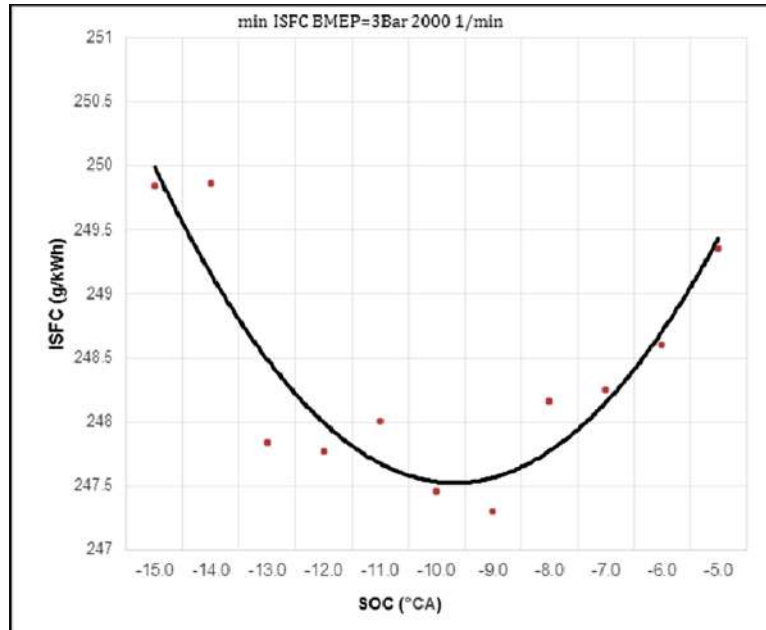
Figure 5 The dependence of the maximum mean indicated pressure on changing the angle of maximum strokes MOP (see online version for colours)
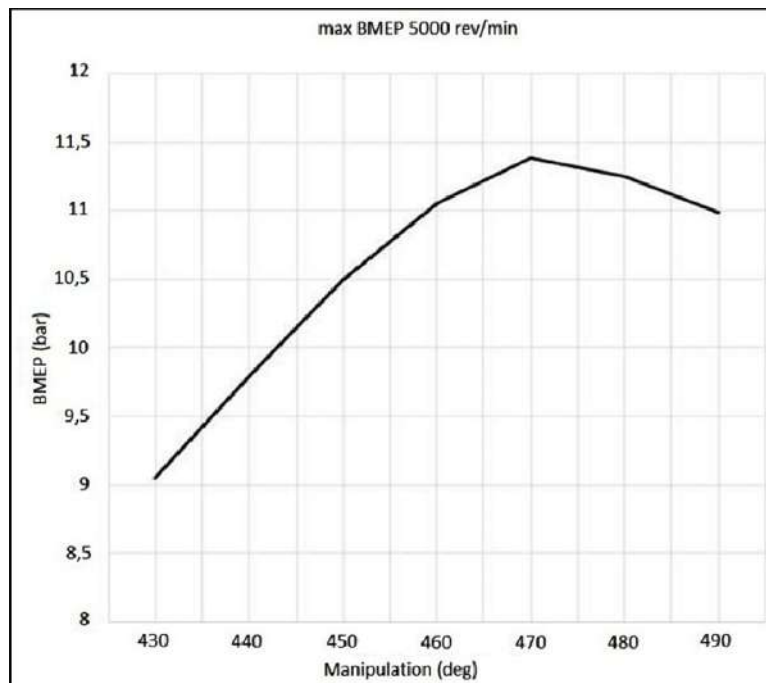
2.1   Standard engine model

The most important engine parameters that will be observed are indicated mean effective pressure-high pressure (IMEP-hp) which is the mean effective pressure in the cylinder during the compression and expansion stroke, and mean pressure in the cylinder during the induction and exhaust stroke pumping mean effective pressure (PMEP). The ratio of these two pressures IMEP-hp/PMEP is correlated to the engine efficiency and is also called gas exchange efficiency. Indicated efficiency represents the efficiency of chemical energy conversion, of fuel into mechanical energy, before mechanical friction losses friction mean effective pressure (FMEP).

Correlation of losses and efficiency of the gas exchange is best seen in the P-V diagram. The red line in Figures 6 and 7 shows a P-V diagram of the first cylinder of baseline engine at 2000 rpm and mean effective pressure BMEP=3bar, the second line shows the pressure in the same cylinder at the same rpm's with the full open throttle (free intake), i.e., the full load. Each of these lines closes two loops, the upper loop represents the useful work (IMEP-hp) and the lower loop, the work that needs to be done for cylinder gas exchange (PMEP). Wide open throttle allows for the pressure in the cylinder, during the intake stroke, to be a little less than atmospheric, so work required to induct fresh air is at a minimum. The pressure in the cylinder during the intake stroke may be slightly above atmospheric pressure as a result of well-timed pressure wave i.e., intake geometry. Thus higher volumetric efficiency is achieved. The cylinder pressure during the exhaust stroke are similar in both cases, and it is possible to achieve pressures slightly below atmospheric given that the exhaust geometry is favourable for the observed engine work parameters. As stated above, it is evident that for changes in PMEP it is enough to observe the indicated pressures only during the suction stroke.

Figure 6   p-V diagram of standard engine (see online version for colours)
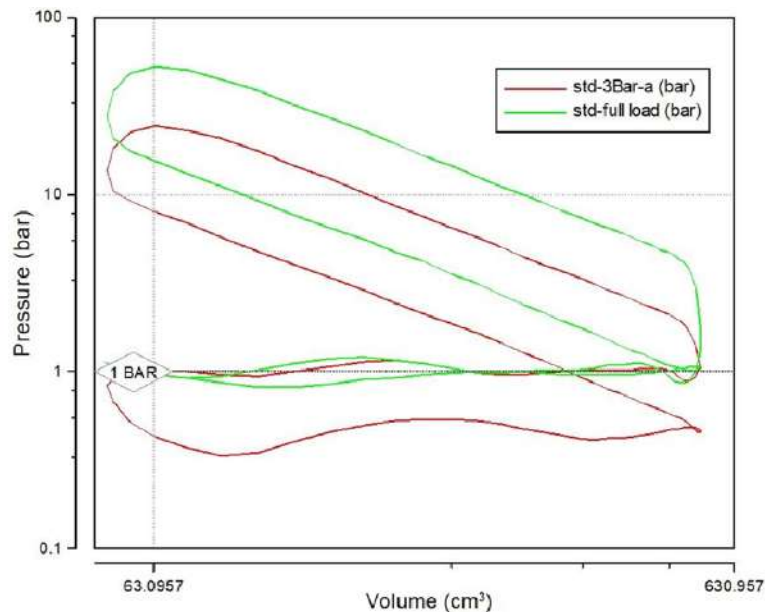
Figure 7   P-V diagram of standard engine in log-log scale (see online version for colours)
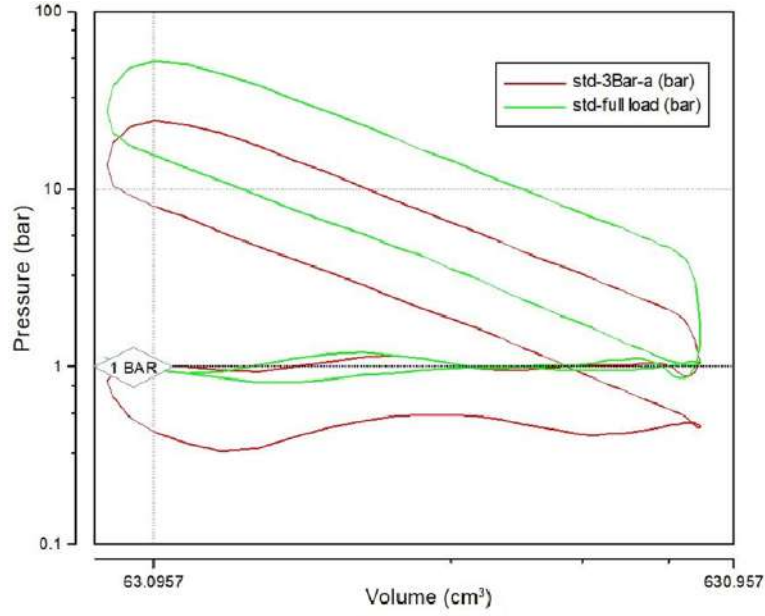
The indicated specific fuel consumption can be obtained as follows:

$$\text{ISFC}_1 = \frac{m_t \cdot \eta_c}{P_i}; \; m_t\text{-Total amount of injected fuel} \tag{1}$$

and

$$\text{ISFC}_2 = \frac{m_c \cdot \eta_c}{P_i}; \; m_c\text{-Amount of cylinder combusted fuel} \tag{2}$$

and

$$\text{IMEP} = \frac{1}{V_d} \int_{CD} p_c \cdot \mathrm{d}v; \; \text{IMEP}_{hp} = \frac{1}{V_d} \int_{-180}^{180} p_c \cdot \mathrm{d}v \tag{3}$$

and

$$\text{PMEP} = \frac{1}{V_d} \int_{180}^{540} p_c \cdot \mathrm{d}v. \tag{4}$$

2.2   *Engine model with double exhaust valves actuation (DVA)*

The indicated engine efficiency can be determined as the ratio of mean indicated effective pressure during the compression stroke and combustion, and mean effective pressure during cylinder gas exchange:

$\eta_i \approx \text{IMEP}_{hp}/\text{PMEP}$

$$\eta_i = \frac{\int_{CD} p_c \cdot dv}{m_f \cdot h_d} = \frac{\frac{1}{Vc} Vc \int_{CD} p_c \cdot dv}{m_f \cdot h_d} = \frac{V_c \cdot IMEP}{m_f \cdot H_d} \tag{5}$$

$$\eta_i = \frac{V_c}{H_d} \cdot \frac{IMEP}{m_f}; \tag{6}$$

$$IMEP = IMEP_{hp} + PMEP \tag{7}$$

$$\eta_i = \frac{V_c}{H_d}\left(\frac{PMEP}{m_f} + \frac{IMEP_{hp}}{m_f} \right) \tag{8}$$

$$= \frac{V_c}{H_d} \cdot \frac{IMEP_{hp}}{m_f}\left(\frac{PMEP}{IMEP_{hp}} + 1 \right); \frac{V_c}{H_d} \cdot \frac{IMEP_{hp}}{m_f} = \eta_{hp} \tag{9}$$

$$\eta_i = \eta_{hp}\left(1 - \frac{|PMEP|}{IMEP_{hp}} \right); PMEP \le 0; \tag{10}$$

$$\eta_{ex} = \frac{1}{k_{ex}} = \frac{|PMEP|}{IMEP_{hp}}; \eta_i = \eta_{hp}\left(1 - \frac{1}{k_{ex}} \right). \tag{11}$$

During part load, IMEP is decreasing and PMEP is increasing which means that both parts of the equation are decreasing efficiency. As IMEP-hp is directly related to IMEP and cannot be changed independently, the only option is to change the PMEP part of the equation. PMEP comprises of PMEP-i (intake part) and PMEP-e (exhaust part):

$$PMEP = PMEP_e + PMEP_i. \tag{12}$$

Since PMEP-e is approximately constant (not taking into account the effect of the geometry of the exhaust pipes), regardless of the load, thus PMEP-i has to be changed. The aim of this simulation is to determinate the impact of double valve actuation on PMEP-i and its effect on the overall efficiency of the engine. With the application of double valve actuation, the efficiency at partial load is increased due to more air entering the cylinder during the induction stroke, which leads to an increase in the mean pressure in the intake manifold and lowers intake losses. The system needs to be tuned to achieve the maximum pressure in the intake manifold (minimal impact of the R3 restrictor) while maintaining specific mean effective pressure BMEP. Valve lift characteristics of the DVA exhaust valve, are shown in Figure 8. The initial opening angle at the beginning of the compression stroke of the DVA valve is 540 BTDC, and initial closing angle of the DVA valve is 670 BTDC. The valve must be closed before the start of the fuel injection into the cylinder; otherwise, a certain amount of fuel will leak through DVA valves in the exhaust pipe, and thus, increase the specific consumption. The optimising of the lowest specific consumption ISCF is done by two variables, the shift in the opening angle of the DVA valve valve opening shift (VOS), and the shift of the closing angle of the DVA valve valve closing shift (VCS) for each observed load. 24 working points were selected for each of the load, in the range from -30 to +20 degrees for closing shift and from -50 to +20 degrees for the opening of the DVA valve.

Figure 8 Dependence of valve lift on crankshaft angle (VOS = 0, VCS = 0)
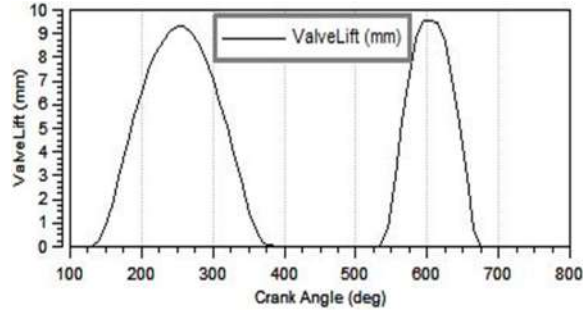
Figure 9 P-V diagrams of standard engine in log-log scale for observed loads (see online version for colours)
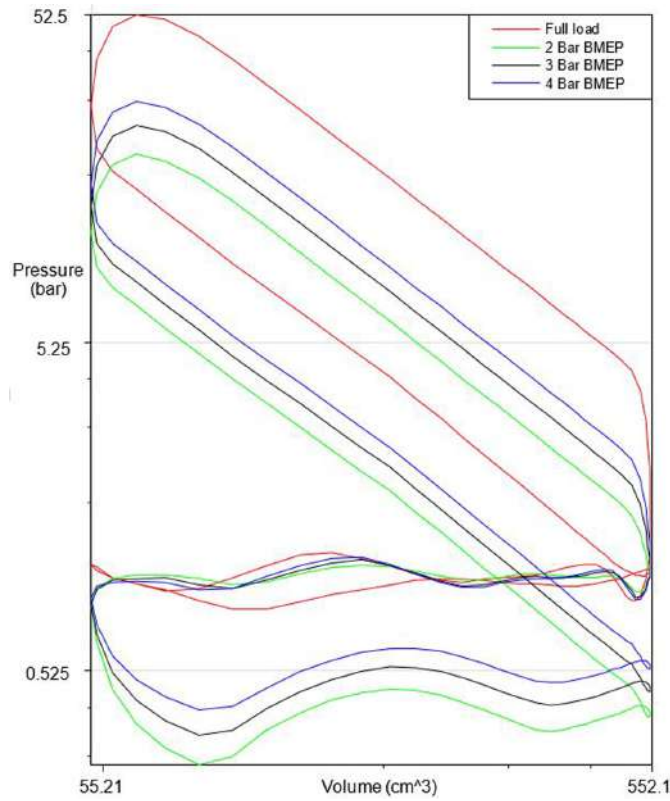

3 Results and discussion

3.1 Standard engine

Comparing the results for the baseline engine at full load with the results at about 20, 30 and 40% load, we see that the efficiency of the engine decreases significantly with a reduction in the load (Table 3). While at full load, the work required to exchange the

cylinder gases is minimal, at 2 bar of BMEP mean effective pressure of the cylinder gases exchange PMEP increases 8-fold and this causes the increase of the specific consumption by 23% compared to the full load. The table shows that the losses of the cylinder gases exchange increase only due to an increase in the intake losses, while the exhaust losses are almost constant throughout the load range, within the 3%. Figure 9.shows the comparison of the indicated pressures at full load (9.5 bar) and part-load (2, 3 and 4 bar) for a standard engine at 2000 rpm. Figure 10 shows a comparison of specific fuel consumption for 2, 3 and 4 bar BMEP loads, and shows that transient changes are caused by the imperfect transmission characteristic of the engine load regulation system.

Table 3   Characteristics of standard engine for various BMEP

		Standard full load	*Standard 2B*		*Standard 3B*		*Standard 4B*	
		Amount	*Amount*	*% Differences to full load*	*Amount*	*% Differences to full load*	*Amount*	*% Differences to full load*
Engine RPM	1/min	2000	2000	0.00	2000	0.00	2000	0.00
BMEP	bar	*9.50*	*2.00*	*78.95*	*3.00*	*68.42*	*4.00*	*57.89*
FMEP	bar	0.94	0.94	0.00	0.94	0.00	0.94	0.00
IMEP-hp	bar	10.59	3.57	66.29	4.49	57.60	5.42	58.82
PMEP	bar	*−0.08*	*−0.63*	*−740.00*	*−0.55*	*−633.33*	*−0.48*	*540.00*
PMEP-i	bar	*0.96*	*0.39*	*59.38*	*0.46*	*52.08*	*0.53*	*44.79*
PMEP-e	bar	−1.04	−1.01	2.88	−1.01	−2.88	−1.01	−2.88
The point of maximum intake valve lift MOPi	°CA	470.00	470.00	0.00	470.00	0.00	470.00	0.00
The effective compression ratio	_	10.50	10.50	0.00	10.50	0.00	10.50	0.00
Mean intake manifold pressure	bar	1.00	0.55	45.24	0.47	−52.76	0.40	−60.28
BSFC	g/kWh	242.20	397.10	−63.96	333.10	37.53	300.10	23.91
ISFC	*g/kWh*	*220.40*	*271.30*	*−23.09*	*254.20*	*15.34*	*243.30*	*10.39*
Effective efficiency	_	0.341	0.208	39.00	0.248	−27.27	0.275	−19.35
Indicated efficiency	_	0.375	0.305	18.67	0.326	−13.07	0.339	−9.60
Maximum cylinder pressure	bar	52.5	19.7	62.48	24.2	−53.90	28.7	−45.33

Figure 10 Specific fuel consumption changes before steady state (see online version for colours)
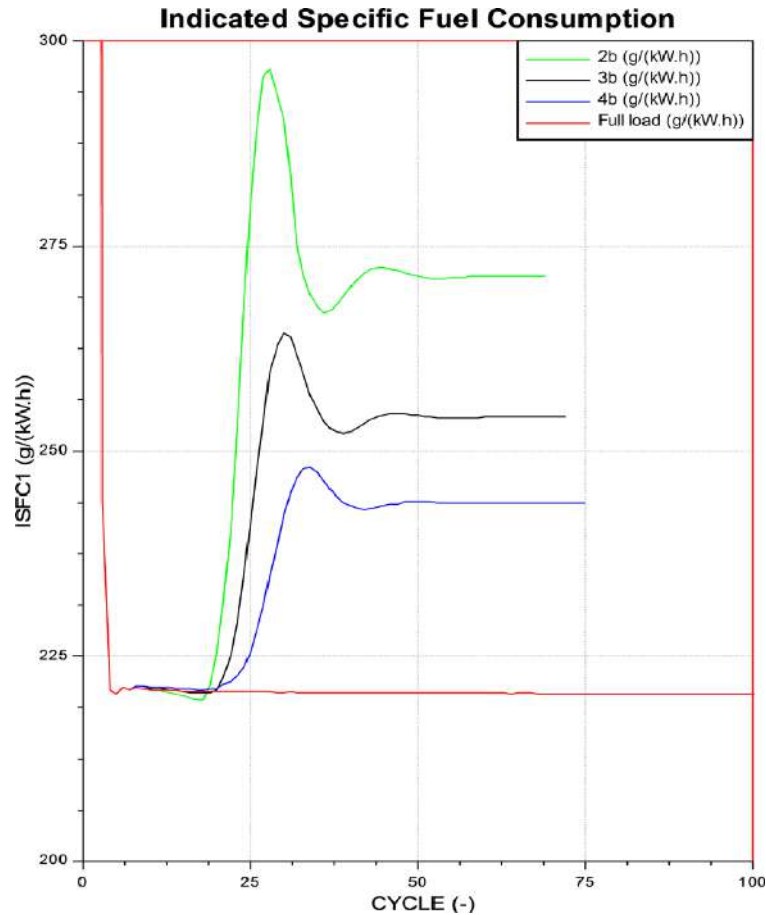
3.2   DVA engine

For each of the observed load the optimal opening and closing angle of the DVA valve is determined, in order to achieve the minimum specific consumption.

Figures 11–13 show a trend of specific indicated fuel consumption ISFC1, and Figures 14–16 indicated fuel consumption ISFC2 to VOS and VCS variables.

If we isolate VOS and observe only variable VCS we can see that the area of the minimum specific consumption is within the observed range. To the left of the minimum ISFCE is an area where consumption is growing due to small amounts of the gases exiting through DVA valves, so the need for restriction at the intake is greater. Right from the minimum is an area in which there is an excessive discharge of gases in the exhaust system, and a decline in BMEP below the desired value with a completely free intake. If we compare diagram ISFC1 with ISFC2 we can see that the left side of the diagrams is almost identical, and that the right side of the ISCF2 diagram is shifted to the right i.e., ISFC1 specific consumption is growing faster. This is due to the late closing of the DVA valve (higher values of VCS) after the start of fuel injection. This leads to the loss of a certain amount of fuel and a decrease in the efficiency. It is also evident that in all the

observed loads the best results are achieved with the lowest values of VOS ie. the early opening of the DVA valve. Here the gases flow in the opposite direction from the exhaust manifold in the cylinder because the DVA valve opens before the bottom dead canter, i.e., in the induction stroke. An explanation for the reduced consumption due to the early opening of the DVA valve is the return of hot air from the exhaust pipe, so the cylinder has less air with the same volume. However, the exact return of gases in the cylinder causes a gap in relation to the real engine, because return gases in the model engine are clean air, and in the real engine they are mixture of exhaust gas and air, so VOS should be limited to the area in which the return gases have no significant impact on the simulation results. For these reasons the optimisation of the shift in the DVA valve openings is restricted only to positive angles regardless of load, variable VOS can be fixed at 0 degrees. After eliminating VOS the only remaining variable is VCS, which enables finding the minimum of the function of the specific consumption more accurate and/or quicker. Figures 17–19 show dependents of the specific consumption on the DVA closing valve shift for the 2, 3 and 4 bar BMEP loads. In line with expectations, the value of the optimal closing angle of the DVA valve decreases with the increasing of load, because a higher amount of cylinder gases needs to be retained at higher loads. Table 4 shows typical data for optimal VCS angles, BMEP = 2 bar VCS = –7°KS; BMEP = 3 bar VCS = 0°KS i BMEP = 4 bar VCS = +7°KS.

Figure 11 Dependence of ISFC1 on VOS and VCS shift for 2 bar BMEP (see online version for colours)
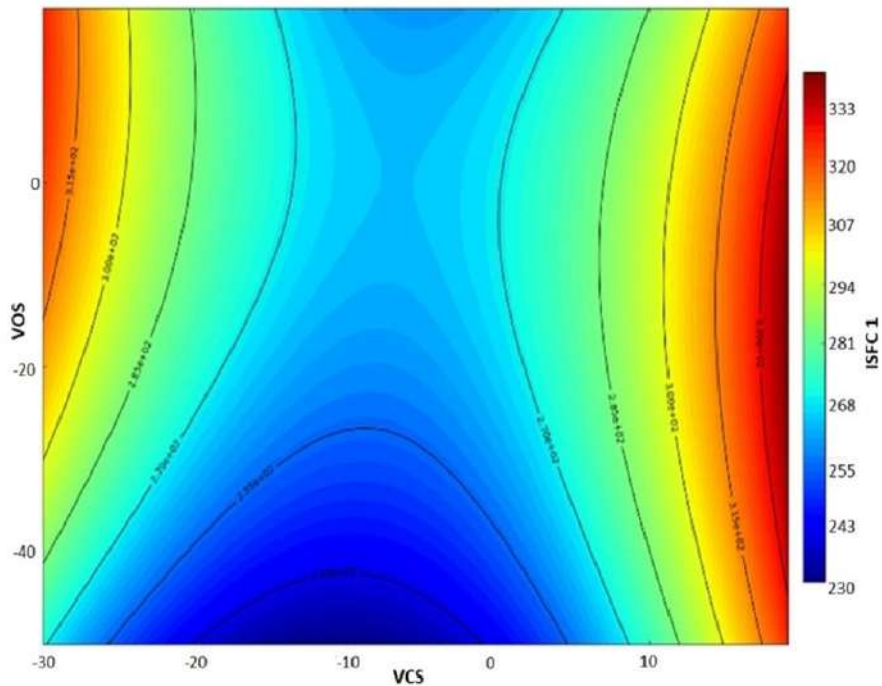
Figure 12 Dependence of ISFC2 on VOS and VCS shift for 2 bar BMEP (see online version for colours)
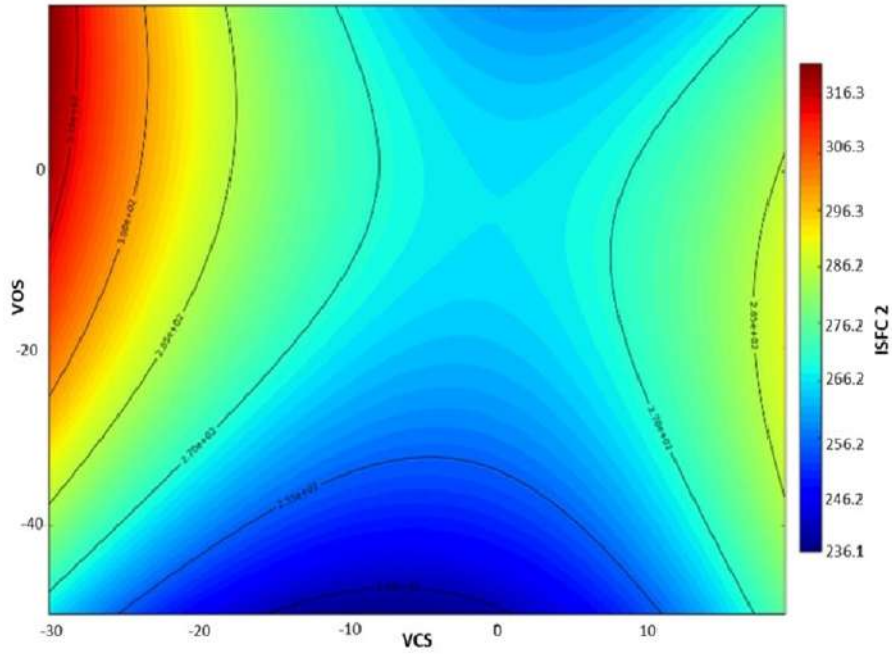
Figure 13 Dependence of ISFC1 on VOS and VCS shift for 3 bar BMEP (see online version for colours)
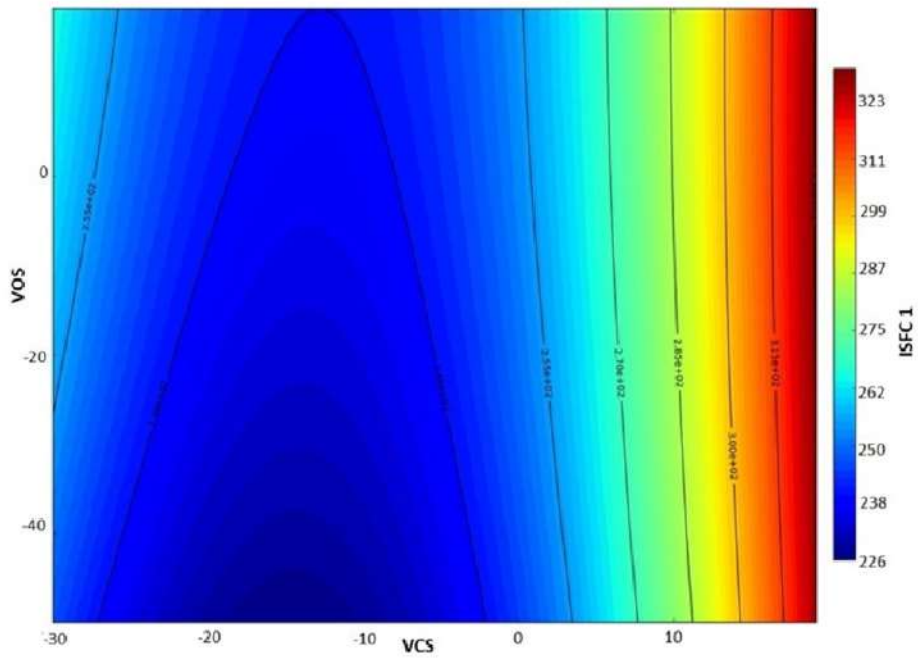
Figure 14 Dependence of ISFC2 on VOS and VCS shift for 3 bar BMEP (see online version
        for colours)
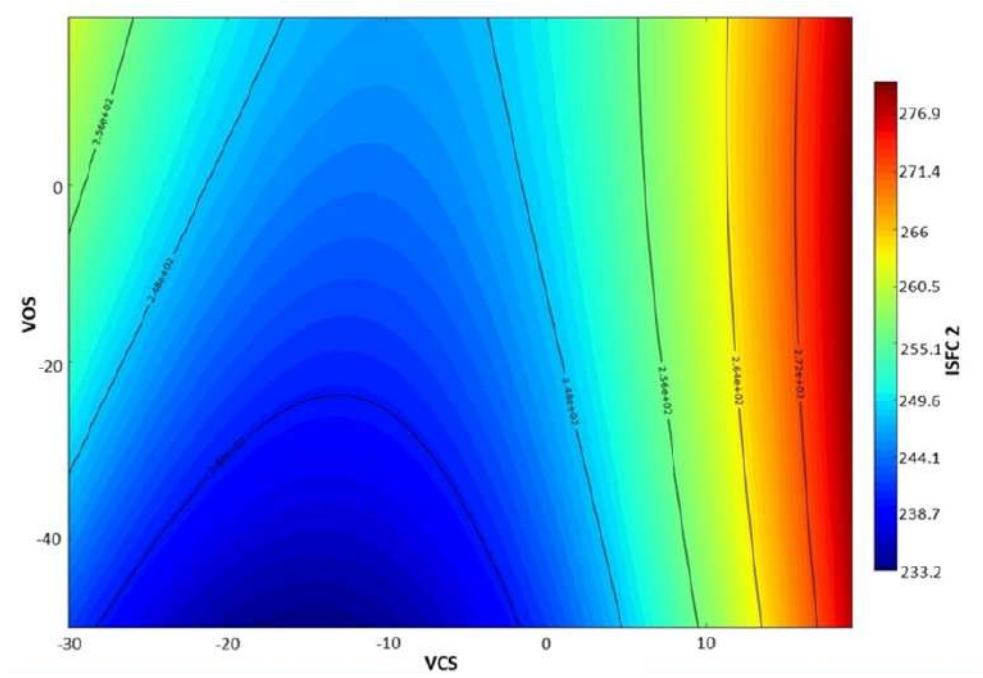
Figure 15 Dependence of ISFC1 on VOS and VCS shift for 4 bar BMEP (see online version
        for colours)
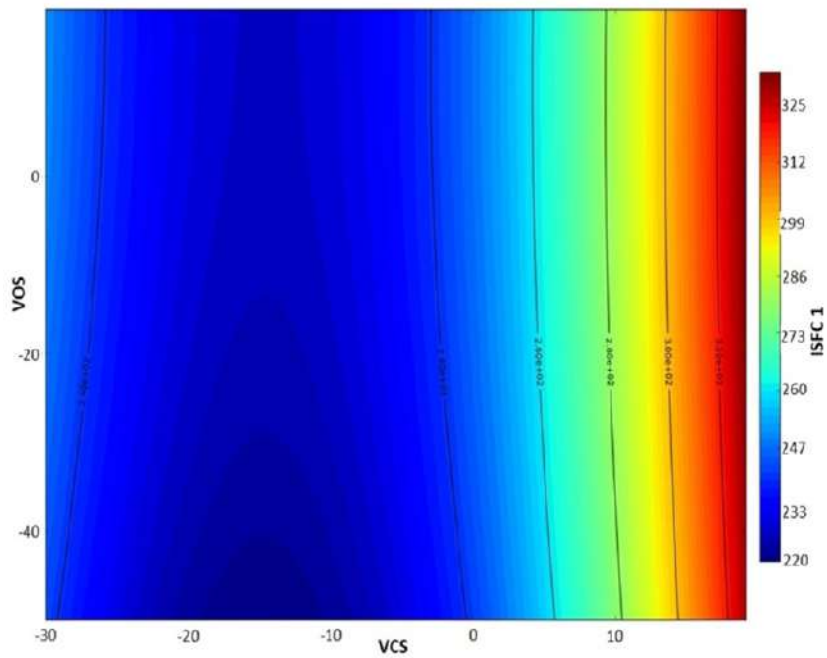
Figure 16 Dependence of ISFC2 on VOS and VCS shift for 4 bar BMEP (see online version for colours)

Figure 17 Dependence of ISFC on DVA valve closing shift (°CA) at load of 2 bar BMEP (see online version for colours)

Figure 18 Dependence of ISFC on DVA valve closing shift (°CA) at load of 3 bar BMEP
(see online version for colours)

Figure 19 Dependence of ISFC on DVA valve closing shift (°CA) at load of 4 bar BMEP
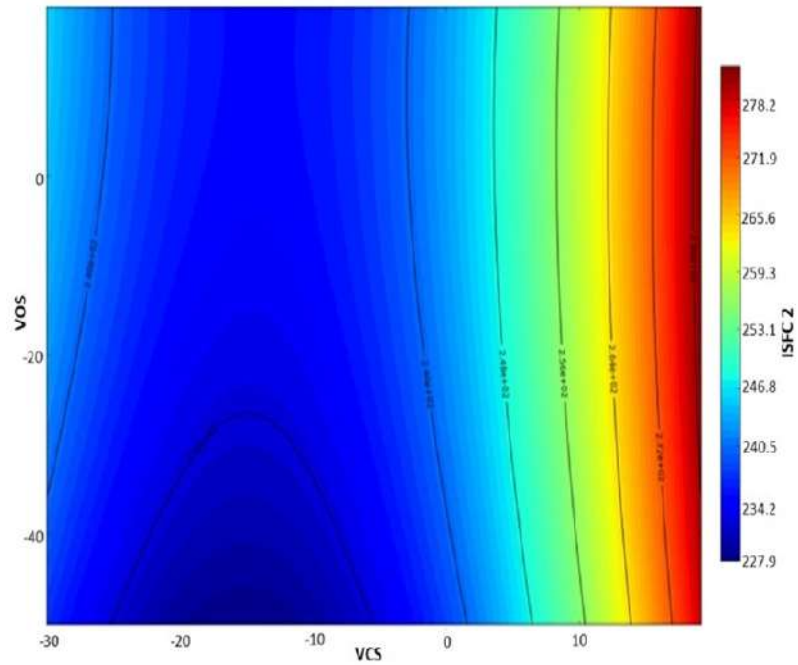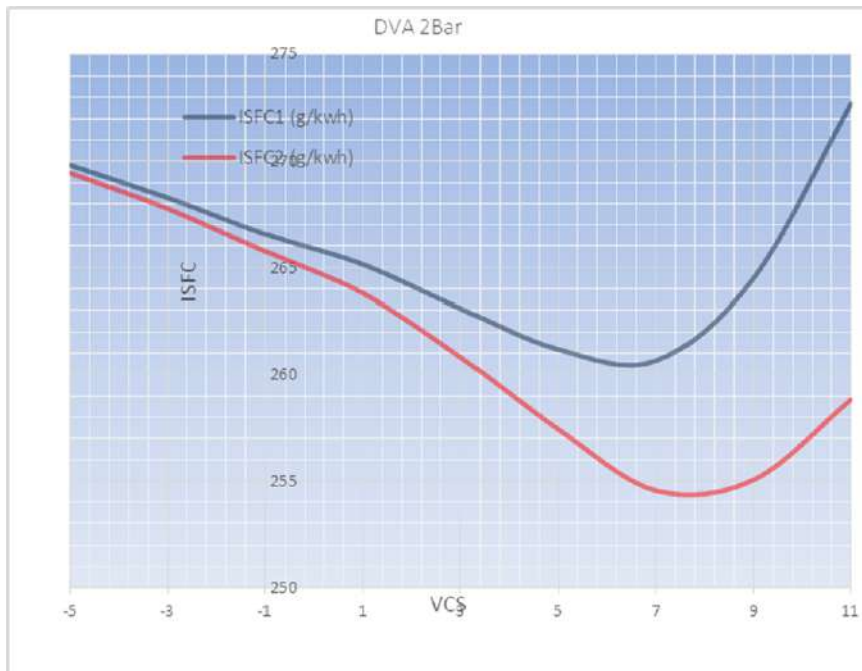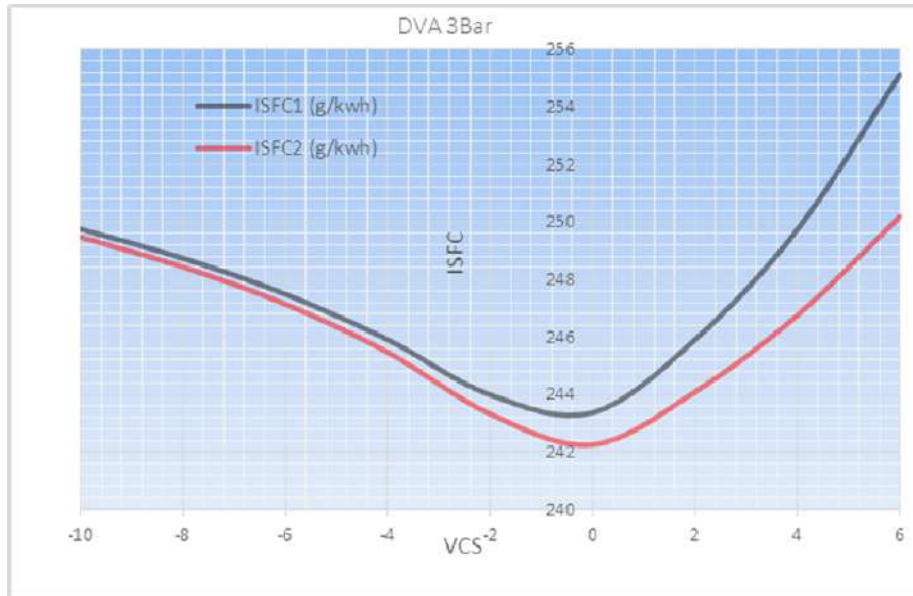(see online version for colours)
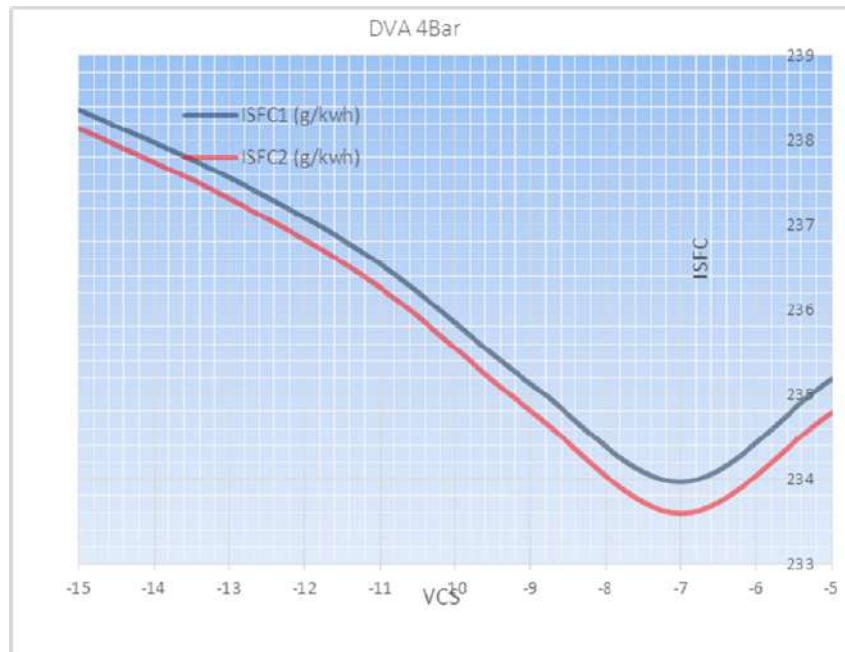
Table 4 Characteristics of DVA engine for observed loads

		Full load	DVA 2B		DVA 3B		DVA 4B	
		Amount	*Amount*	*% Differences to full load*	*Amount*	*% Differences to full load*	*Amount*	*% Differences to full load*
Engine RPM	1/min	2000	2000	0.00	2000	0.00	2000	0.00
BMEP	*bar*	*9.50*	*2.00*	*−78.95*	*3.00*	*−68.42*	*4.00*	*−57.89*
FMEP	bar	0.94	0.94	0.00	0.94	0.00	0.94	0.00
IMEP-hp	bar	10.59	3.01	−71.58	3.98	−62.42	4.98	−52.97
PMEP	*bar*	*−0.08*	*−0.08*	*6.67*	*−0.07*	*−4.00*	*0.07*	*−194.67*
PMEP-i	*bar*	*0.96*	*0.94*	*−2.60*	*0.94*	*−2.08*	*0.94*	*−2.08*
PMEP-e	bar	−1.04	−1.02	−2.21	1.01	−197.12	1.01	−197.12
VCS	°CA		7.00		0.00		−7.00	
DVA-VC	°CA		672.00		665.00		658.00	
Effective compression ratio	_	10.50	5.21	−50.43	4.78	−54.52	4.09	−61.08
Mean pressure in inlet receiver	bar	1.00	0.97	−2.71	0.97	−2.71	0.98	−1.71
BSFC	g/kWh	242.20	382.88	58.08	320.21	32.21	289.36	19.47
ISFC	*g/kWh*	*220.40*	*260.65*	*18.26*	*243.44*	*10.45*	*233.98*	*6.16*
Effective efficiency	_	0.341	0.216	−36.66	0.258	−24.34	0.286	−16.13
Indicated efficiency	_	0.375	0.325	−13.33	0.342	−8.80	0.354	−5.60
Maximum cylinder pressure	bar	52.5	16.04	−69.45	20.25	−61.43	24.71	−52.93

3.3 Comparison of obtained results of DVA and standard engine

All the analyses of different systems are conducted by AVL BOOST simulation software. Table 5 shows a results comparison obtained by simulating a standard and DVA petroleum engine. One can see a significant increase in the efficiency of the cylinder gases exchange, which is a consequence of the reduction of losses during the induction stroke due to restricting the inlet manifold during partial load. The highest specific consumption on a standard engine is at the lowest load as a result of significant losses of cylinder gases exchange. Therefore the biggest gain is expected in this area of work of DVA engine relative to the standard engine. According to the results, a slightly higher gain was achieved for the 3 bar of BMEP than 2 bar, as a result of other parameters that affect the overall efficiency such as intake and exhaust systems geometry. Specific consumption is to reduce between 3.83% and 4.23%, and losses of cylinder gases exchange have decreased to between 85% and 87%. It is also interesting that the maximum cylinder pressures are lower from between 13.9% and 18.6% compared to the

standard engine, primarily from the standpoint of ecology and durability of the engine. The lower value of maximum pressures is the result of a lower mean indicated pressure required during the compression and combustion (lower losses = lower power required for equal work) and lower starting temperature of the compression due to the cooling effect of the air which does not participate in combustion but passes through the cylinder.

Table 5   Comparison of obtained results of DVA and standard engine for observed loads

		Standard 2B	Standard 3B	Standard 4B	DVA 2B		DVA 3B		DVA 4B	
		Amount	Amount	Amount	Amount	% Difference to standard	Amount	% Difference to standard	Amount	% Difference to standard
Engine RPM	1/min	2000	2000	2000	2000		2000		2000	
BMEP	bar	2	3	4	2.00	0.00%	3.00	0.00%	4.00	0.00%
FMEP	bar	0.94	0.94	0.94	0.94	0.00%	0.94	0.00%	0.94	0.00%
IMEP-hp	*bar*	*3.57*	*4.49*	*5.42*	*3.01*	*−15.69%*	*3.98*	*−11.36%*	*4.98*	*−8.12%*
PMEP	*bar*	*−0.63*	*−0.55*	*−0.48*	*−0.08*	*−87.30%*	*−0.07*	*−86.91%*	*−0.07*	*−85.21%*
PMEP-i	*bar*	*0.39*	*0.46*	*0.53*	*0.94*	*139.74%*	*0.94*	*104.35%*	*0.94*	*77.36%*
PMEP-e	bar	−1.01	−1.01	−1.01	−1.02	0.69%	−1.01	0.00%	−1.01	0.00%
IMEP-hp/ PMEP		*5.67*	*8.16*	*11.29*	*37.63*	*563.97%*	*55.28*	*577.12%*	*70.14*	*521.17%*
VCS	°CA				7.00		0.00		−7.00	
DVA-VC	°CA				672.00		665.00		658.00	
Effective compression ratio	_	10.5	10.5	10.5	5.21	−50.43%	4.78	−54.52%	4.09	−61.08%
Mean pressure in cylinder	Bar	0.55	0.47	0.4	0.97	76.36%	0.97	106.38%	0.98	145.00%
BSFC	g/kWh	397.1	333.1	300.1	382.88	−3.58%	320.21	−3.87%	289.36	−3.58%
_	_	_	_	_	_	_	_	_	_	_
Effective efficiency	_	0.208	0.248	0.275	0.216	3.85%	0.258	4.03%	0.286	4.00%
Indicated efficiency	_	*0.305*	*0.326*	*0.339*	*0.325*	*6.56%*	*0.342*	*4.91%*	*0.354*	*4.42%*
Maximum cylinder pressure	bar	19.7	24.2	28.7	16.04	−18.58%	20.25	−16.32%	24.71	−13.90%

4   Further consideration

In this study, a new innovative concept of controlling the workflow of the IC engine was introduced. The initial idea for the application of this concept has arisen from boosted engines. In atmospheric engines, pressure limit in the cylinder is approximately

atmospheric pressure, while in the boosted engines the limit is the boost pressure. Therefore we have available a larger area to increase efficiency and not only to decrease losses during the intake, but it is also possible to get positive work using the energy of compressed air. The above-mentioned effects are not part of this study due to the greater amount of elements that should be studied in depth, such as the characteristics of the mechanical and turbocharged compressors, which will be a good foundation for future research. Particularly interesting is the combination of the DVA approach with turbocharger and divided exhaust, due to the reduced pressure in the 'other" exhaust pipe which would be used for DVA outlet gases. From the previously obtained data, although we used simplified modelling approach, we have seen that the efficiency of the described approach increases with earlier opening of the DVA valve, but that data has been excluded due to exhaust gases returning into the cylinder, i.e., exhaust gas recirculation EGR. The study could be extended to determine the point of minimum specific consumption with EGR included. As this method (DVA) does not exclude so far known solutions to the cylinder gases exchange problem during induction, for example, VVT and fuel stratified injection FSI, and there is a possibility for a research of a combination of these methods. Further investigation of the same issues needs to be done by using 3D CFD analysis, taking into account the effects of DVA method to turbulence, mixing of fuel-air and combustion.

5   Conclusions

This study deals with increasing the efficiency of the petrol engine at part load in a completely new approach, with an additional opening of the exhaust valve. Test results show a significant improvement over the standard engine, with a fixed intake and exhaust geometry. The simplified model of the new system which has been developed and a comparison was made between the standard engine, regulated with a valve on the intake system, and an engine which is regulated by the dual opening of the exhaust valves. All the analyses of different systems are conducted by AVL BOOST simulation software. The research was carried out on the model of a four-cylinder Otto engine with direct injection into the cylinder. The main results showed a significant improvement over the standard engine with a fixed intake and exhaust geometry. Specific consumption is reduced between 3.83% and 4.23%, and losses of cylinder gases exchange have decreased between 85% and 87%. A significant increase in the efficiency of the cylinder gases exchange is obtained, which is a consequence of the reduction of losses during the induction stroke due to restricting in the inlet manifold during partial load. The highest specific consumption on a standard engine is at the lowest load as a result of significant losses of cylinder gases exchange. Therefore the biggest gain is expected in this area of work of DVA engine relative to the standard engine. According to the results, a slightly higher gain was achieved for the 3 bar of BMEP than 2 bars, as a result of other parameters that affect the overall efficiency such as intake and exhaust systems geometry.

The largest gains of DVA approach are at the lowest loads and were achieved by minimising the cylinder gas exchange losses by reducing the effects of intake restriction or a complete removal of the effects of intake restriction, which led to an increase of pressure in the cylinder during the induction stroke to approximately atmospheric pressure, so the work needed to overcome the losses during induction is minimal. The functional deficiency of this approach is the expensive implementation of the valve train

and functionality only in combination with a direct injection into the cylinder under high pressure, the implementation of which is also complex. Application of the fuel stratified injection enables stable combustion in a poor mixture, and thereby reduces the intake losses at partial loads.

References

Barlow, L. and McCrae, B. (2009) *A Reference Book of Driving Cycle for Use in the Measurement of Road Vehicle Emissions*, TRL Limited, Crowthorne House, Nine Mile Ride Wokingham, Berkshire RG40 3GA, UK.

Bonatesta, F., Altamore, G., Kalsi, J. and Cary, M. (2016) 'Fuel economy analysis of part-load variable camshaft timing strategies in two modern small-capacity spark ignition engines', *Applied Energy*, Vol. 164, pp.475–491.

Çelik and Özdalyan (2010) *Gasoline Direct Injection*, Intech, Karabuk University, Engineering Faculty, Turkey.

Crolla, D.A (2009) *Automotive Engineering – Powertrain Chassis System and Vehicle Body*, Elsevier Inc., Linacre House, Jordan Hill, Oxford OX2 8DP, UK.

Cygnar, M. and Sendyka, B. (2013) *Stratified Charge Combustion in a Spark-Ignition*, Intech, Cracow University of Technology, Poland.

EUROPEAN VEHICLE MARKET STATISTICS (2016/17) http://www.theicct.org/sites/default/files/publications/ICCT_Pocketbook_2016.pdf

Fontana, G. and Galloni, E. (2009) 'Variable valve timing for fuel economy improvement in a small spark-ignition engine', *Applied Energy*, Vol. 86, pp.96–105.

Ghojel, J. (2010) 'Review of the development and applications of the Wiebe function', *International Journal of Engine Research*, Monash University, Australia.

Knop, V. and Mattioli, L. (2015) 'An Analysis of limits for part load efficiency improvement with VVA devices', *Energy Conversion and Management, Research Gate*, IFP Energies nouvelles, 1 et 4 avenue de Bois-Préau, 92852 Rueil-Malmaison, France.

Lee, D., Jiang, L., Yilmaz, H. and Stefanopoulou, A.G. (2010) 'Preliminary results on optimal variable valve timing and spark timing control via extremum seeking', 5th IFAC Symposium on Mechatronic Systems, Marriott Boston Cambridge, Cambridge, MA, USA, 13–15 September.

Mahrous, A-F.M., Potrzebowski, A., Wyszynski, M.L., Xu, H.M., Tsolakis, A. and Luszcz, P. (2009) 'A modelling study into the effects of variable valve timing on the gas exchange process and performance of a 4-valve DI homogeneous charge compression ignition (HCCI) engine', *Energy Conversion and Management*, Vol. 50, pp.393–398.

Pesiridis, A., Barber, M. and Cairns, A. (2015) 'A comparison of variable valve strategies at part load for throttled and un-throttled SI engine configurations', *International Journal of Automotive Engineering and Technologies*, Brunel University, London, UK.

Peter, M. (2012) *European Vehicle Market Statistic*, http://www.theicct.org/sites/default/files/publications/Pocketbook_2012_opt.pdf

Pournazeri, M., Khajepour, A. and Huan, Y. (2017) 'Development of a new fully flexible hydraulic variable valve actuation system for engines using rotary spool valves', *Mechatronics*, Vol. 46.

Radica, G. (2008) 'Expert system for diagnosis and optimisation of marine diesel engines', *Strojarstvo*, pp.105–116.

Raju, T.B. and Hithaish, D. (2014) 'A review on gasoline direct injection system', *International Journal of Research in Aeronautical and Mechanical Engineering*, Department of Mechanical Engineering, R V College of Engineering, Bangalore, India.

Schoppe, D., Zhang, H., Kapphan, F. and Schmidtm C. (2012) *Analysis and Strategic Solution Concepts on Powertrain System Level, Continental Automotive*, Continental, Regensburg, Germany.

Sorusbay, C. (2016) *Spark Ignition Engine Combustion*, Istambul Technical University, Ayazağa Yerleşkesi, Maslak –34469 İstanbul.

Verhelst, S., Demuynck, J., Sierens, R. and Huyskens, P. (2010) 'Impact of variable valve timing on power, emissions and backfire of a bi-fuel hydrogen/gasoline engine', *International Journal of Hydrogen Energy*, Vol. 35, pp.4399–4408.

Xie, H., Song, K. and He, Y. (2014) 'A hybrid disturbance rejection control solution for variable valve timing system of gasoline engines', *ISA Transactions*, Vol. 53, pp.889–898.

Nomenclature

DVA	Double valve actuation
NEDC	New European driving cycle
BMEP	Break mean effective pressure
BTDC	Before top dead centre
ISFC	Indicated specific fuel consumption
VOS	Valve open shift
VCS	Valve closing shift
FMEP	Friction mean effective pressure
PMEP	Pumping mean effective pressure
SOC	Start of combustion

PRILOG B

Naslov rada: Analysis of methods towards reduction of harmful pollutants from diesel engines

Autori: Ante Kozina, Gojmir Radica, Sandro Nižetić

Izvornik: *Journal of cleaner production*

Broj izdanja, stranice, godina: Vol. 262, p. 121105, 2020

Vrsta rada: pregledni znanstveni

Izvorni jezik: engleski

Ključne riječi: diesel engines; emissions; nitrogen oxides; soot particles; catalysts
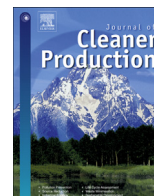
Sažetak: Internal combustion engines will be the main power for the vessels, heavy duty vehicles and thermoelectric plants in the future as it is nowadays. Finding the way to reduce environmental impact and to produce cleaner energy is the main task of engine manufacturers. In this paper, different methods and systems of diesel emission control are analyzed, especially exhaust gas recirculation (EGR) techniques that regulate emissions during their formation as well as exhaust after treatment techniques which reduce already generated harmful emissions based on the catalytic effect of precious metals, various catalytic converters and particle filtering (DPF). The problems of divergence with existing emission norms and ways of fulfilling them are also explained. The mechanism of exhaust gas formation and their connection with engine parameters were thoroughly analyzed. Problems that occurred when using individual methods for reducing emissions in specific working conditions of engines were explained. The impact of emission control systems on engine performance parameters such as fuel consumption, CO_2 emissions, load reaction and durability were explored. The experiments were performed based on failed studies of important parts within an emission control system. It was shown that only a systematic approach of solving diesel exhaust emissions with the use of advanced technologies will retain their importance and enable truly cleaner engines which will not only satisfy but well below the allowed emission norms.

Analysis of methods towards reduction of harmful pollutants from diesel engines

Ante Kozina [a], Gojmir Radica [a, *], Sandro Nižetić [b]

[a] *Department for Thermal Machines, Faculty of Electrical Engineering, Mechanical Engineering and Naval Architecture, University of Split, Rudjera Boskovica 32, 21000, Split, Croatia*
[b] *LTEF- Laboratory for Thermodynamics and Energy Efficiency, Faculty of Electrical Engineering, Mechanical Engineering and Naval Architecture, University of Split, Rudjera Boskovica 32, 21000, Split, Croatia*

ABSTRACT

Internal combustion engines will be the main power for the vessels, heavy duty vehicles and thermo-electric plants in the future as it is nowadays. Finding the way to reduce environmental impact and to produce cleaner energy is the main task of engine manufacturers. In this paper, different methods and systems of diesel emission control are analyzed, especially exhaust gas recirculation (EGR) techniques that regulate emissions during their formation as well as exhaust after treatment techniques which reduce already generated harmful emissions based on the catalytic effect of precious metals, various catalytic converters and particle filtering (DPF). The problems of divergence with existing emission norms and ways of fulfilling them are also explained. The mechanism of exhaust gas formation and their connection with engine parameters were thoroughly analyzed. Problems that occurred when using in-dividual methods for reducing emissions in specific working conditions of engines were explained. The impact of emission control systems on engine performance parameters such as fuel consumption, CO_2 emissions, load reaction and durability were explored. The experiments were performed based on failed studies of important parts within an emission control system. It was shown that only a systematic approach of solving diesel exhaust emissions with the use of advanced technologies will retain their importance and enable truly cleaner engines which will not only satisfy but well below the allowed emission norms.

1. Introduction

The constant growth of needs for internal combustion engines as the main source of propulsion in maritime and road traffic as well as for most of heavy duty machines, and the desire to reduce the total amount of greenhouse gas emissions, primarily CO_2, have set two new goals for manufacturers: to increase efficiency as the main requirement for the market, and reduce emission gas pollution, as an environmental sustainability requirement. On the other side, they are major issues with limited resources, efficiency of energy conversion systems and necessity for the smart based approach, Nižetić et al. (2019). Understanding the behavior of pollutant emissions from heavy-duty diesel engines that pose a major threat to environment and human health, facilitate the formulation of traffic-related policy measures to mitigate the adverse effects, Cheng et al. (2019). In order to fulfill the vehicle requirements of Euro 6d and at the same time increase the efficiency of engines, internal combustion engines (ICE) are becoming ever more complex with an increasing number of control systems. Complex control systems are making engines more versatile in aspects of engine load and speed that can lead to the reduction of pollution and fuel consumption. The main drawbacks of such systems are by nature their high price of production and maintenance, also the requirements for monitoring emission gases which are becoming more complex in order to create a basis for car type approval and to monitor the function of all parts during exploitation. Authors such as O'Driscol et al. (2018), Hooftman et al. (2018), Pouresmaeili et al. (2018) and Kerbachi et al. (2017) have dealt with the above-mentioned problems that create a divergence between emissions and controlled by law to type approval vehicles and emissions for everyday usage. Nesbit et al. (2016) also address the issue of disagreement with actual and homologated emissions, and the scandals associated with them, comparing the homologation

conditions in Europe with the homologation conditions in America. From an economical point of view, a vehicle driven with a diesel engine have a 20–30% lower fuel consumption due to its higher energetic value per litre and higher efficiency. From an ecological point of view, a vehicle driven with a diesel engine has a lower emission of carbon dioxide CO_2, hydrocarbon HC and carbon monoxide CO, while the soot emission PM and NO_x emission are higher, despite a complex refinement process. Burning 1 kg of diesel fuel produced approximately 3.1 kg of CO_2 and 1.3 kg of H_2O. Despite the fact that the same energy equivalent of gasoline fuel produces about 8% less CO_2 emissions, due to the significantly greater efficiency, the average diesel car in Europe typically emits about 17% less CO_2 than a similar conventional gasoline car within the same vehicle segment, Diaz et al. (2017). Aside from carbon dioxide and water, the burning of fuel within an engine also generates around 1% of harmful gases Resitoglu et al. (2015). Fig. 1 shows a pie chart where the chemical compound of carbon and oxide are generally called NO_x, emission particles PM, unburned hydrocarbon HC, carbon monoxide CO and other less represented gases. Along with the mentioned harmful gases, the amount of carbon dioxide is also considered, which does not pose a direct threat to people, however, it is considered to be a greenhouse gas that causes global warming problems. The goal of the Kyoto protocol was to reduce the overall emissions of CO_2 by the end 2008 in all economic sectors by 8% compared to 1990. According to the author Santos et al. (2017), road traffic generates around 20% of overall CO_2 emissions out of which 15% is made out of passenger cars and light commercial vehicles. There has been a target of 130 g/km since 2015, which is applied for the EU fleet-wide emission of new passenger cars. The emission target for 2021 regarding new cars will be 95 g/km and in that case, car manufacturers will pay penalties of 95€ for every extra gram produced by vehicles.

The increasingly stringent emission requirements and introduction of more realistic methods of type approval testing, the WLTP cycle combined with real-world RDE testing, demand from manufacturers to develop their strategy in two possible manners: the rapid development of even more efficient internal combustion engines along with emission reduction or the development of alternative propulsion systems. The use of alternative fuels, most commonly bio fuels and blend fuels is becoming more prevalent due to their availability and classification as a renewable energy source, therefore the environmental aspect of the use of such fuels
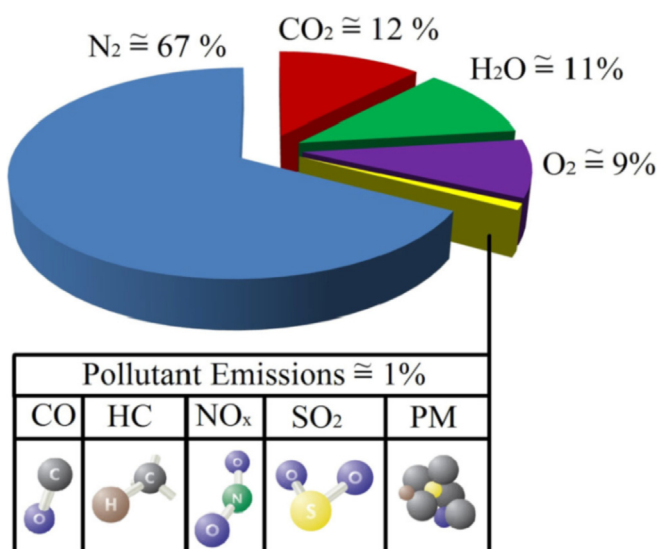
should be taken into account, i.e. their specificity in terms of influencing the amount of harmful emissions. According to Nabi et al. (2019) and Zhang et al. (2019), quality blends of available bio fuels contribute to a significant reduction in CO and PM emissions, but increase NOx emissions with a minimal decrease in performance compared to standard diesel fuels. Cleaner environments and economical sustainability can be achieved with compression ignition engine that use tire pyrolysis diesel blends doped with nano additives as a fuel, Kumaravel et al. (2019). To reduce gaseous emissions such as CO, CO_2, NO, NO_x, and HC in internal combustion engines and to recover some of the wasted energy trough an exhaust the thermoelectric generation could be a solution Ramirez et al. (2019). Since the introduction of the first environmental emission standards, one of the biggest issues with diesel engines has been the emissions of nitrogen oxides and particulate matter emissions. After two decades of intensive diesel engine development in the direction of successful consumption reduction and thus CO_2 emissions, there has only been a marginal satisfaction regarding harmful emissions Chen et al. (2014), followed by numerous emission scandals, of which Dieselgate marked the turning point in the direction of the further development of environmental standards, Brand (2016). Euro 6d standards for passenger cars and light commercial vehicles have a completely different approach to measuring type approval emissions, while the emission limit values have remained virtually unchanged compared to earlier Euro 6 norms (except for temporary compliance factors) Hooftman et al. (2018). This approach will push the development of an emission control system at the forefront of engine development for two significant reasons caused by significantly higher loads during type-approval testing. The first is the multiple increases in harmful emissions that should be brought to the originally set limits, and the second reason is the wide range of loads that systems operating in relatively narrow temperature ranges need to adapt. High sensitivity to fluctuations in exhaust gas temperatures is most pronounced in after treatment systems, the most significant being Lean NOx trap and Selective Catalytic Reduction. DiGiulio et al. (2014) deals with the effect of exhaust temperatures on the optimum regeneration duration and on the conversion efficiency of NOx emissions with LNT catalytic converters. Qi et al. (2003) study the behaviour of catalysts of different materials at low exhaust gas temperatures. Miller (2015) studies the effect of different ammonia/NOx ratios, the conversion efficiency and the release of ammonia into the atmosphere depending on the exhaust gas temperature. According to DiGiulio et al. (2014) the optimum temperature range for using the LNT + SCR combination is between 300 and 450 °C. On the other hand, high temperatures have a negative effect on the durability of the exhaust after treatment system as it causes thermal aging. Manula et al. (2014) among others study the influence of high temperatures such as 800 °C on the operation of LNT-SCR catalysts from different materials. A normal regeneration of the DPF filter occurs at temperatures of about 650 °C, while regeneration from heavily saturated filters over 10 g results in an uncontrolled regeneration with temperatures above 1000 °C, which reduce efficiency or may permanently damage the filter and downstream elements, Zhan et al. (2006). In the literature used, authors most often address a narrower area related to one or more parts of exhaust after treatment systems or deal with emission regulations. This paper will cover the increasingly more available techniques that control exhaust emissions of engines which normally operate in the area of a lean mix, primarily diesel engines, to explain the influencing factors and mechanisms of emission generation.

The main objective of this paper is to make a more systematic approach to the issue of emissions, to integrate all the influencing factors on the exhaust emissions of the mentioned engines, and to link

Fig. 1. Diesel engine pollutant emissions, Resitoglu et al. (2015).

them to the legislation on emissions, i.e. to link the causes and background of today's problems with consequences, as well as to provide guidelines for the further development of the diesel exhaust control system, as part of a complete system with the focus being on mobile applications. To achieve this objective, a wide range of research works has to be analyse such as: environmental impacts, emission formation mechanisms, emission control systems as well as the issue with homologation process for determining actual emission. A detail explanation of the overall system and process will allow experts in these fields of science, an insight into related topics and a broader view with clear development direction.

The paper deals first with the mechanisms of emission formation and their impact on the environment. Understanding these mechanisms and the influencing factors, results in conclusion how to control harmful emissions. Most of the work is related to control emissions with the emphasis on NOx and soot particle. First the exhaust gas recirculation EGR system and then the various exhaust after treatment systems have been addressed. The emphasis is placed on particulate filters and catalytic converters to reduce the most problematic pollutants of diesel engines, soot particles and NOx, respectively. A separate chapter deals with management and optimization strategies to achieve the desired results of emission reduction. Issues related to homologation process, emission regulations and their monitoring and enforcement are included in this paper as well. Finally, the results were quantified, the suggestions how to meet existing standards is established and direction for future development of emission control systems were proposed.

This comprehensive approach will enable a better understanding of the overall problem of exhaust emissions and hopefully lead to truly, not artificially, cleaner and more environmentally friendly diesel-powered vehicles and machines.

2. Exhaust gas toxic emissions

All organic origin fuels are basically a mixture of different hydrocarbons. In an ideal controlled thermodynamic process with an ideal combustion process, the engine would have carbon dioxide and water as a by-product. However, the fuel composition is not perfect, aside from carbon and hydrogen, there are also impurities, one of them being sulfur within diesel fuel that is being reduced due to newer engine regulation requirements. Under real conditions, engines generate a variety of undesirable emission products with a harmful environmental impact. The amount of such generated emissions depends on a number of conditions (faulty air/fuel ratio, bad ignition angle, tumble and swirl motion within the combustion chamber) and those are: nitrogen and oxide compounds that are
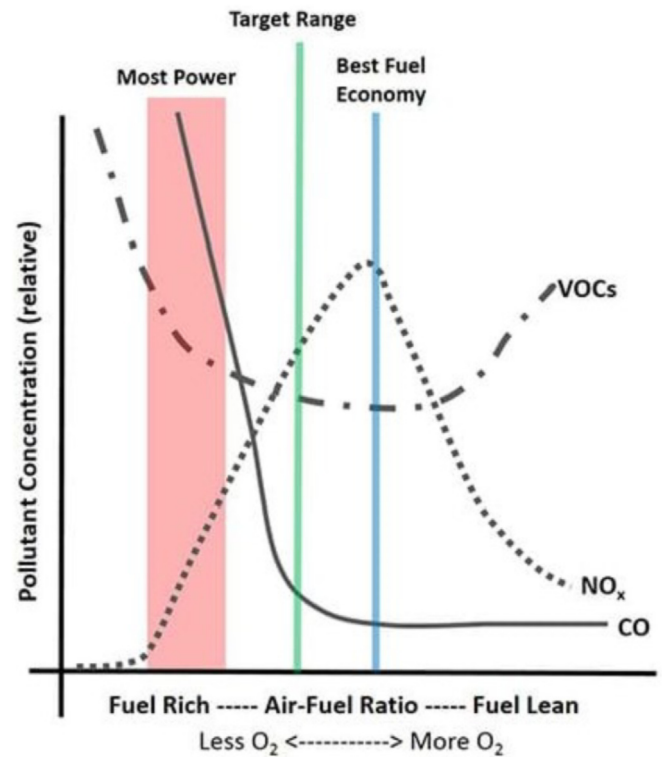
Fig. 3. Emission formation in function of fuel/air ratio Emission control systems, teachengineering.

generally called NO_x, PM particles, unburned hydrocarbon HC, carbon monoxide CO, lead salts, polyaromatic hydrocarbons, sulfur oxides, ketone aldehydes and olefins. The most harmful of them all are HC, CO, NO_x and soot particles PM according to Resitogul et al. (2015). If diesel engines were compared without any emission control systems, in terms of harmful emissions, then they are much cleaner than gasoline enginesair-quality but petrol engines combined with three-way catalysts are three times more "eco-friendly" than diesel engines.

2.1. Hydrocarbons HC

Hydrocarbons are made out of a number of chemical compounds such as alkenes and aromatic hydrocarbons. Therefore,

Fig. 2. Oxygen excess and combustion temperature influence on NO_x formation, Perin and Okoniewski (2013).

their impact on people and environment depends solely on their compound. The general name for such compounds is Volatile Organic Compounds (VOCs) or Total Hydro Carbons (THC). According to Inekwe et al. (2017) and Sorathia et al. (2012) The most important factor responsible for the formation of hydrocarbons is insufficient temperature which occurs in some parts of the combustion chamber, usually near the cylinder w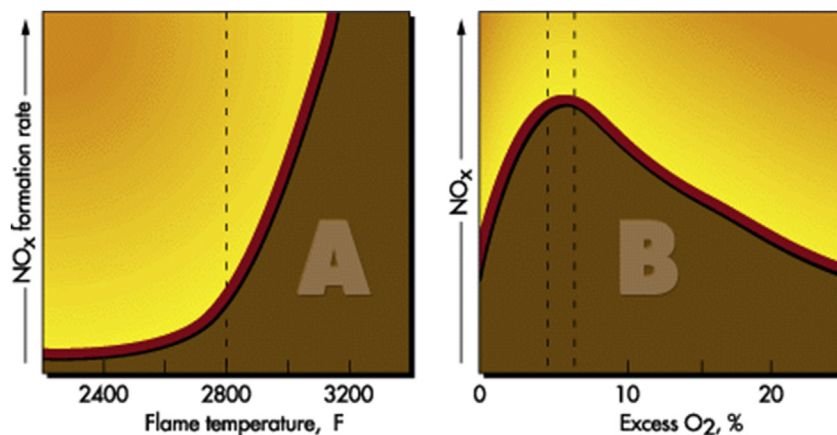all. At medium load, diesel engines generate a small amount of THC, usually the THC is generated at low loads due to higher air flow. A lean mixture causes low flame propagation speed in the combustion chamber, and combustion sometimes may not occur. Fast load changes, large bore openings on injectors and the uneven injecting of fuel may also cause the increase of THC emissions. According to Resitoglu et al. (2015), THC emissions in the exhaust collector continue to react with the air flow in the exhaust as long as the temperature is above 600 °C. Bhandarkar et al. (2013) conducted research about internal combustion engine emissions and their effect on human health. According to the research, most hydrocarbons are not directly harmful to human health at concentrations found in the ambient air. However, through different reactions in the troposphere, they play an important role in forming NO_2 and ozone O_3 which are dangerous for people and the environment. Non methane hydrocarbons react and form secondary air pollution. Engines also emit toxic hydrocarbons including benzene, aldehydes and polyaromatic hydrocarbons PAH. Emissions of benzene, toluene and acids are characteristic for gasoline engines while emissions from poly aromatic hydrocarbons are more expressed with diesel engines.

2.2. Carbon monoxide CO

Carbon monoxide is a result of incomplete combustion and usually forms in certain parts of the combustion chamber where the mixture of fuel and air is rich, also CO can be formed in a very lean but still combustible fuel air mixtures. Since diesel engines work with a richer air flow, CO emissions are relatively small. According to Inekwe et al. (2017), the causes of carbon monoxide are: too rich mixture, insufficient turbulence and too large droplets of fuel within the combustion chamber. Carbon monoxide is dangerous for human health and in higher concentrations even deadly. Carbon monoxide binds to hemoglobin in the same places as oxygen but 150−300 times greater which causes the drop of oxygen levels in human blood and can have deadly consequences. People who are exposed to a concentration of CO above 9 ppm can have permanent damage to cognitive functions. The time period for CO to convert to CO_2 in the atmosphere is quite slow and can last from 2 to 5 months.

2.3. Soot particles PM (particulate matter)

Soot particles are usually associated with diesel powered vehicles. Emission particles are usually the size of 0.04 μm−1 μm, and their wide range size agglomerates. They are formed from unburned fuel that becomes solid in some parts of the combustion chamber where it is under the influence of medium temperatures. Despite numerous researches, Diesel emission particles form complex aerosols are neither physical nor chemical properties. Their impact on human health are not fully understood. Particle emissions from diesel engines usually imply soot particles, as the usual soot proportion is over 50% that is seen as black smoke. The rest of particles are usually unburned fuel, oil for lubrication, metal particles and sulfur compounds, Srivastava and Agarwal (2008), Majewski W.A. (2019). Aside from diesel engines, gasoline engines also emit soot particles but in lower quantities. Port fuel injection petrol engines have considerably lower PM emissions, than engines with direct cylinder injection. The problem with the high amount of

soot particles that are emitted from diesel (and gasoline engines with direct injection) engines is solved by installing DPF filters. There is a high interest for researching the reduction of emission particles due to their posing danger to human health. Aerosols within the atmosphere also have an effect on the absorption of sunlight. A typical example are soot particles which have a direct effect on sunlight absorption and scattering Srivastava et al. (2008). Aside from NO_x emissions, the reduction of particulate matter emissions is one of the main pollution problems regarding modern diesel engines.

2.4. NO_x emission

Nitrogen oxide emissions are currently the biggest issue with diesel engines. Although NO_x emissions are higher than in petrol engines, these emissions can easily be removed using a three-way catalyst. Nitrogen and oxygen do not react together at room temperature but at higher temperatures, they create oxides such as NO, NO_2, N_2O, N_2O_3 and N_2O_5 which are all called NO_x. High combustion temperatures, oxygen excess and their duration are solely responsible for NO_x emission formation, as illustrated in Fig. 2. If the combustion process was to be observed, it is easy to notice a correlation between high efficiency combustion, which favors low consumption, the reduction of CO_2 and harmful emissions such as CO, THC and PM. The only exception is higher NO_x emissions. If the goal was to decrease NO_x emissions, it would be necessary to decrease the combustion temperatures within the cylinders but lowering combustion temperatures also leads to a decrease of engine efficiency and consequently increase in fuel consumption. Fig. 3 illustrates the influence of air/fuel ratio on various emission formations. The most significant nitrogen oxides are NO_2 and NO, about 90% of NO_x emissions are in the form of NO, but NO_2 has a considerably higher toxicity in the aspect of photochemical effects. Under the influence of sunlight radiation, it breaks up into NO plus highly reactive O, which react with a molecule of oxygen O_2 creating ozone O_3. In normal conditions, NO would soon after the breakup recombine into NO_2 but due to the presence of hydrocarbons, the reaction is slowed down, Pardiwala (2011), Sillman (1999), Gerrett explain how the ozone with a complex chemical mechanism combined with air moisture creates a substance such as a fog, which is called smog. The nitrogen oxides react with the moisture, ammonia and other compounds forming a vapor of nitrogen acid with fine particles. These particles easily penetrate into fragile lung tissue and this process leads to numerous lung diseases.

3. Emission control systems

The main reason why diesel engine development is growing fast is due to stricter requirements for emission gas control and the need for lower fuel consumption. The development is based on improvements to existing systems, invention and implementation of new technologies. The further consideration only includes systems whose primary purpose is the reduction of harmful emissions, with the focus being on particulate matters and NO_x emissions.

3.1. Exhaust gas recirculation (EGR)

Exhaust gas recirculation is the most common technology for reducing the emissions of NO_x in internal combustion engines. The main difference between EGR and after treatment systems is that the EGR reduces the formation of NO_x emissions during combustion while other systems reduce the amount of already generated NO_x emissions. The main principle is simple, part of emission gases is returned back into the intake system where it is mixed with fresh air and reduce the amount of oxygen within the cylinder. Lower

oxygen excess reduces the possibility of chemical reactions of oxygen and nitrogen and consequently NO_x formation, Fig. 2A. Recirculated gases decrease peak combustion temperatures, inside the combustion chamber, required to form NO_x emissions, Fig. 2B Sorathia et al. (2012). Lower peak combustion temperatures are due to the slowdown of combustion and higher heat capacity relative to fresh air. Aside from using EGR technology as a method of reducing NO_x emissions, this system is used in petrol engines for reducing losses during intake strokes and reducing the possibility of developing detonations during combustion strokes. The EGR effect can also be performed internally within the combustion chamber itself with a suitable exhaust valve phase. Standard HP (High Pressure) EGRs have been used for a few decades as the main system to reduce NO_x emissions in diesel engines.

These systems use a part of exhaust gases from the exhaust manifold upstream of the turbocharger if it exists, and leads it into the intake manifold through the EGR cooler, where it is mixed with fresh air. With the main goal of improving the performance and efficiency LP (Low Pressure), EGR is introduced. In the LP, EGR exhaust gases are collected at low pressures of the exhaust system, downstream of the turbocharger and DPF filter, driven into intake upstream of the compressor, through a low pressure cooler. Both configurations of HP and LP EGR can be used independently or together, Fig. 4. According to Sorathia et al. (2012), the presence of exhaust gases in the amount of 15% in the cylinders reduces the amount of NO_x by 80%. Aside the impact of NO_x emissions, EGR also has an impact on HC, CO and PM, Fig. 5 illustrates the effect of the EGR rate on the PM, NO_x, HC and CO. Emission results are given from a Euro 2 truck engine at a low load of 10% with fuel injection 6° before TDC (Top Dead Center). According to Wenmig et al. (2017), an EGR rate less than 43% has no great effect on the engine performance, while the fuel consumption significantly increases above 37% of EGR. Rudrabhate et al. (2017) present a similar result, but only observe a useful range of EGR rates, up to 60%.

The results of the study show that the effect of EGR on NO_x emission reductions is most pronounced at low loads, that is, in the NEDC test cycle, a decrease of 85% is measured, while at medium loads at constant speed, it decreases to 75% under normal load conditions while with variable loads the EGR efficiency under NO_x reduction is below 50%. A slight increase of fuel consumption is noted during normal driving conditions at medium loads while at low loads, a drop of 15% in fuel consumption is noticed with EGR systems on. A lower fuel consumption is the result of the mean effective pressure reduction during exhaust strokes. Ghodke et al. (2012) conducted a thermodynamic comparison between HP and LP EGR systems at various constant and transient loads. They observed Brake Specific Fuel Consumption (BSFC), loses during

Fig. 4. LP and HP EGR configuration, greencarcongress.

exchange working medium and oxygen excess or air fuel ratio. As all the observed values depend on the flow and pressure of gases in the intake and exhaust manifold which are regulated by variable geometry turbochargers, the results are presented and explained on the compressor maps in Fig. 6. Fig. 6 illustrates how HP EGR moves the compressor's operating point, at a low engine load BMEP = 2 bar, towards a lower compressor efficiency and reduced airflow (left side) with a low turbocharger speed.

Fig. 7 illustrates the impact of the variable geometry turbocharger's blade position and EGR HP/LP ratio from 0 to 100% at medium engine load with medium engine speeds BMEP = 12 bar n = 2500 °/min with 30% EGR to the compressor behavior. Increasing LP/HP EGR ratio increases the mass flow rate through the turbine and compressor with a constant amount of EGR, the gas flow rate through the turbine is increased so that the turbocharger works at higher speed and efficiency. EGR cooling enables lower compressor operating pressures, with the same mass flow rate, with more opened turbine blades, illustrated with red arrows in Fig. 7.

Park (2014) conducted an experimental research on high speed diesel engines at constant partial load and measure specific fuel consumption, NO_x emissions and combustion characteristics in relation to LP/HP EGR. According to them, the increase in relation to LP/HP has a positive impact on fuel consumption and NO_x emissions as illustrated in Fig. 8. Furthermore, Ghotke et al. (2012) describes the behavior of HP/LP EGR in transient loads. Fig. 9 illustrates the response time of the engine with transient loads, from a low load of 2 bar to medium load of 9 bar BMEP. It can be seen that the amount of EGR at LP barely effects the engine response time, LP EGR achieves better results for euro 4 standards and higher.

Advantages of LP EGR are achieved with lower temperatures of exhaust recirculated gases, which are cooled in the low-pressure cooler and intercooler together with fresh air that causes lower temperatures within the cylinder and reduces NO_x emissions with an equal flow of recirculated gases. The second advantage is that hot gases are not taken before passing through the turbocharger which causes the energy of the gases that pass through the turbine to be much higher. This is rather important in low loads where the overall gas energy is rather low while EGR is most efficient in this field of operation, Park et al. (2014), Reifarth et al. (2010). It has a positive effect on engine response time at transient load and this is important for the engines used on road vehicles, especially for passenger cars where comfort is of utmost importance. The third advantage is referred to cleaner EGR gases which are taken downstream of the DPF filter and makes them much cleaner from soot keeping in the whole intake system. This is on the other hand the biggest drawback of the HP EGR system. Most failures are caused by soot depositions building up in EGR valve, coolers and connecting lines. Soot deposition on EGR valves can cause them to always be slightly opened. At higher loads, the EGR should be fully closed to secure the right amount of air flow. This causes a chain reaction, a low fresh air flow rate causes a higher amount of soot being generated at exhaust which causes even more soot deposition on the EGR valve, intake manifold and valves that can cause serious engine failure. The disadvantages of LP-EGR compared to HP-EGR are the inertness or slower response of EGR concentration at transient load. Load changes require changes to the EGR rate, which make the path of recirculated gases to cylinder much longer. Longer time is needed for changes in EGR concentration. The second drawback is the corrosive atmosphere from the exhaust gases that pass through the complete inlet system which is the most sensitive part of the compressor. In LP EGR, gases are taken after DPF and are driven to the intake system right before the compressor, the pressure is almost the same as the atmospheric pressure at both sides. Because of this, sometimes it is necessary to
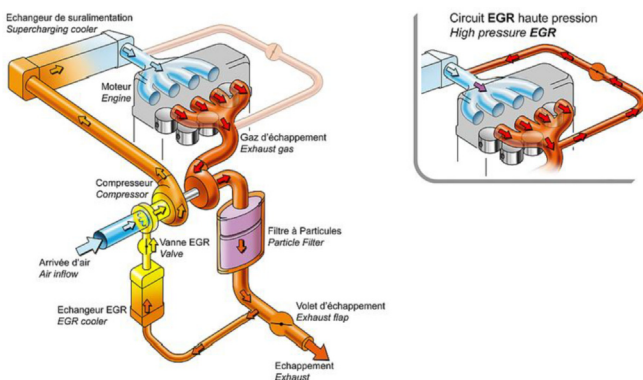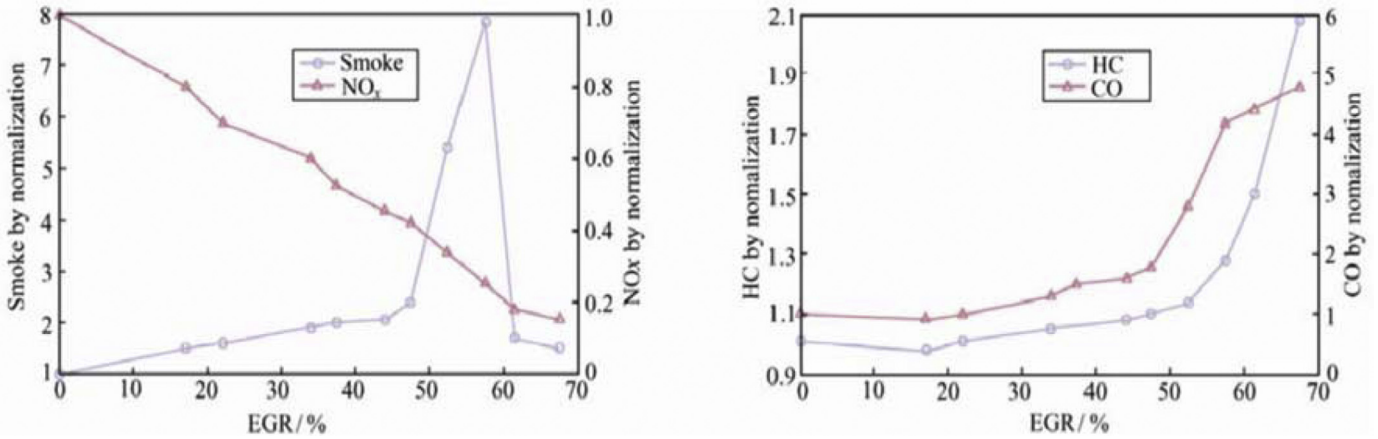
Fig. 5. Effect of EGR rate on NO$_x$, PM, HC and CO emissions, Wenming et al. (2017).
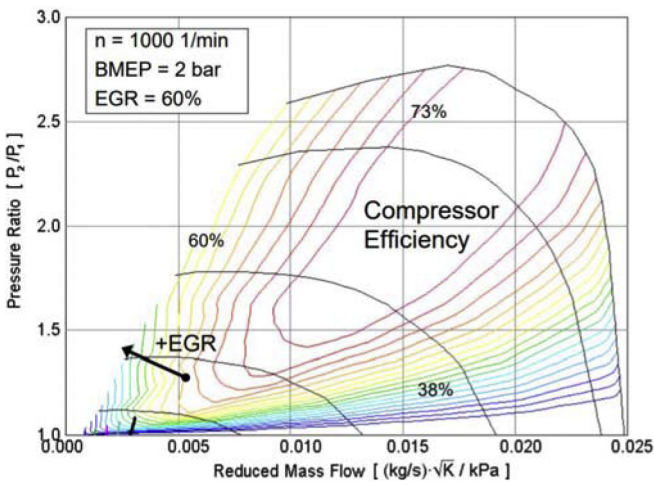
Fig. 6. HP EGR influence of compressor map, Ghodke et al. (2012).
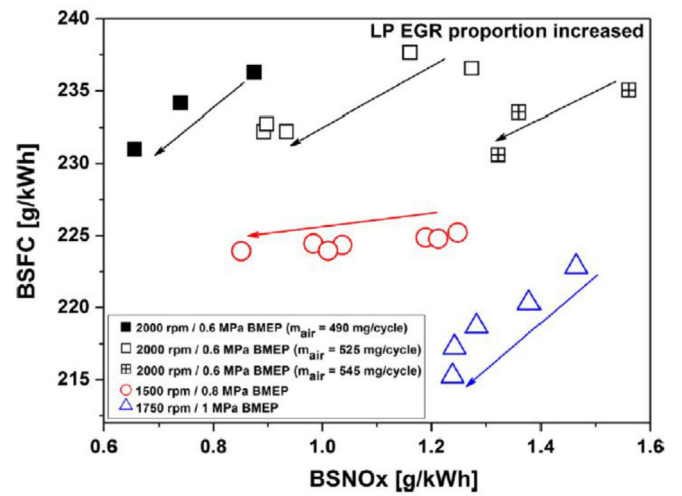
Fig. 8. BSFC and NO$_x$ emission in function of LP EGR, Park et al. (2014).
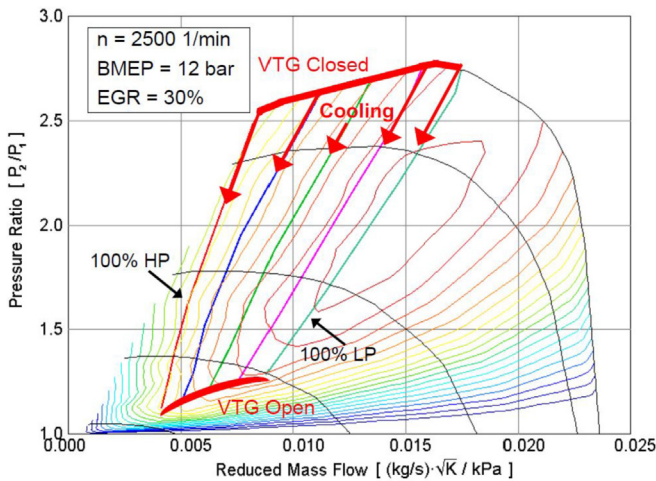
Fig. 7. Influence of VGT and LP/HP ratio to compressor map, Ghodke et al. (2012).
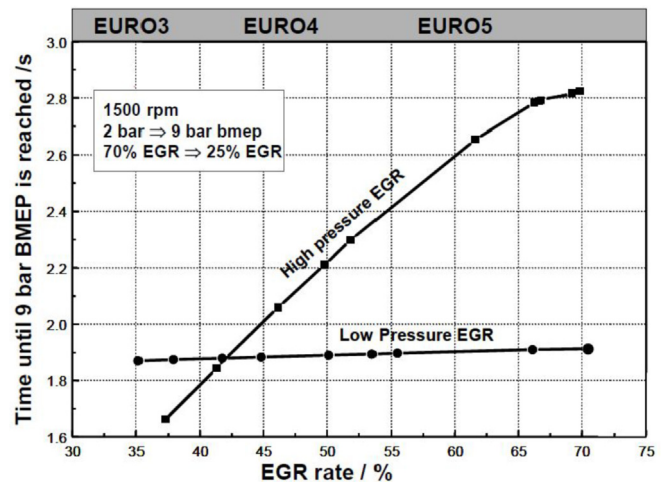
Fig. 9. Engine response at different Euro norms for HP and LP EGR, Park et al. (2014).

install a restriction in the exhaust line which has a negative impact on the engine fuel consumption, Reifarth et al. (2010), With the

entry of Euro 6d, which includes the WLTP cycle and RDE testing, the high-pressure HP EGR loses its importance due to limited or no

effect at increased load, but will continue to be used solely in combination with other systems for limiting the NO_x low-load emissions, especially when combined with a low-pressure LP EGR system. LP EGR shows better performance than HP EGR separately, and especially in combination with HP EGR. Despite its limited performance when compared to most exhaust after treatment systems, its lower cost and ability to combine with all after treatment systems ensures further applications.

3.2. Exhaust after treatment systems

3.2.1. Catalytic converters - catalysts

Catalytic converters are devices that are used for decreasing the toxicity levels of exhaust gases in internal combustion engines. This device provides chemical reaction conditions in which toxic combustion by-products are converted into less toxic or completely non-toxic chemical compounds. Standard catalysts, oxidation, reduction and three-way catalysts, have been successfully used for many years, and their technologies have already reached their pinnacle, so only the principles of operation, shortcomings and limitations of using in combination with diesel and modern gasoline engines will be briefly explained. According to the type of reaction, they are divided into:

1. Oxidation catalysts (oxidation of CO and HC)
2. Reducing catalysts (reduction of NO_x)

The wide application of catalysts started in the 70s in the USA when the Environmental Protection Agency EPA had issued a law requiring all vehicles manufactured as of 1975 to comply with regulations in order to lower overall emissions, the required reductions of HC are 87%, 82% in CO_2 and 24% in NO_x when compared to the emission law of the 60s, Garrett et al. (2009). Two-way catalysts, which reduced carbon monoxide and hydrocarbon emissions were first used. By 1978, GM had developed the first three-way catalyst consisting of an oxidation and reduction bed to reduce NO_x emissions.

3.2.1.1. Two-way catalyst.
Oxidizing catalysts reduce the amount of unburned hydrocarbons and carbon monoxide; this is accomplished by passing them over a platinum or palladium film as a catalyst accelerates the reaction.

$$HC+O_2 \rightarrow CO_2+H_2O \tag{1}$$

$$2CO+O_2 \rightarrow CO_2 \tag{2}$$

This type of catalytic converters has a wide application with diesel engines DOC (Diesel Oxidation Catalyst) but are more helpful

as a support-system combined with DPF filters, because the CO and HC emissions from diesel engines are not high. Based on the author's conducted studies on the effect of defective components of emission control systems, it was concluded that Euro 3 and most of Euro 4 engines can satisfy CO and HC limits without the help of oxidation catalysts. The DOC catalyst converter is explained in chapter 3.2. Diesel Particle Filter.

3.2.1.2. Reduction catalyst.
A reduction catalytic converter reduces the amounts of nitrogen oxide in the exhaust. It can be installed as a separate unit, but also with the addition of the oxidation catalyst, which should be installed downstream. It works efficiently only when the engine operates in a rich or stoichiometric mixture as free oxygen slows the desirable chemical reaction down. Structurally, it is very like an oxidation catalyst, the difference is mainly in the catalytic material, and the basic principle is that hot exhaust gases pass over the catalyst film within the honeycomb structure, which accelerates the NO_x decomposition to nitrogen and oxygen, according to the chemical reaction (3).

$$2NO \rightarrow O_2+N_2 \tag{3}$$

3.2.1.3. TWC three way catalyst.
This has been the most commonly used catalyst for many years, its greatest advantage is that the carbon monoxide oxidation, hydrocarbon oxidation and nitrogen oxide reduction occur simultaneously. The noble metal, palladium Pd or rhodium Rh are most commonly used as active catalyst elements. Palladium is particularly interesting because of its low cost, good selectivity and activity in the oxidation of hydrocarbons, Rhodium is widely used as it is the most effective catalyst for the
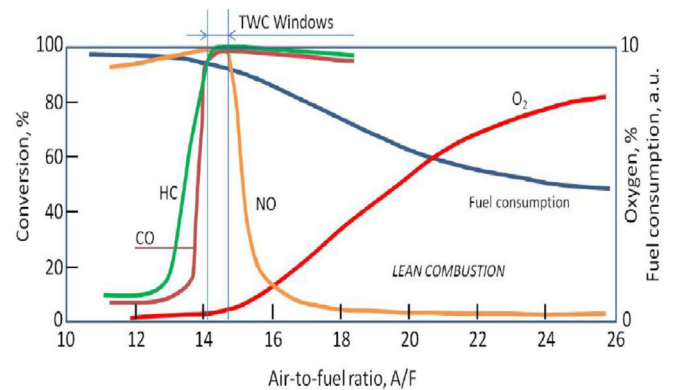

Fig. 11. TWC operating window, Pereda-Ayo et al. (2013).

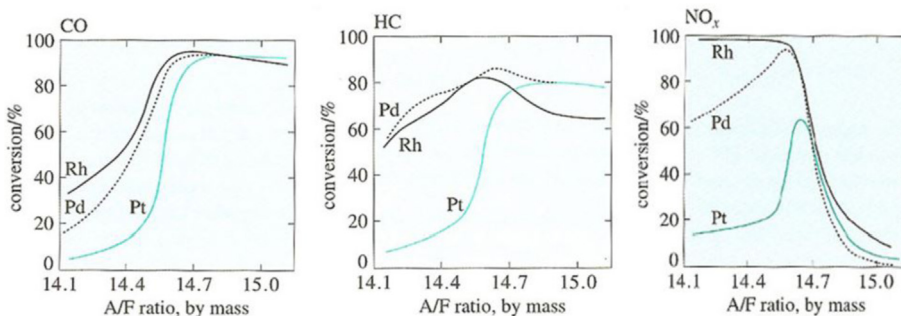**Fig. 10.** Efficiency of different catalysts on CO, HC and NO_x reduction in function of AFR, Mollenhauer and Tschoeke (2010).
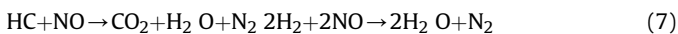
reduction of nitrogen compounds, Pardiwala et al. (2011).

Fig. 10 shows the impact of the Air/Fuel Ratio on the performance of rhodium, palladium and platinum as catalysts for CO, HC, and NO_x reduction. Temperature has a strong influence on the efficiency of TWC catalysts, only temperatures above 600 °C have a full effect. The high operating temperatures of this type of catalyst determine its position within the exhaust system and it has to be installed as close as possible to the exhaust manifold. The chemical reactions of this converter are very complex, most importantly shown in Equations (4)–(9). In addition to the oxidation and reduction reactions, water and water vapor react as well.
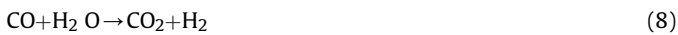
Oxidation:

$$HC + O_2 \rightarrow CO_2 + H_2O \tag{4}$$

$$2CO + O_2 \rightarrow CO_2 \tag{5}$$

Reduction:

$$2CO + 2NO \rightarrow 2CO_2 + 2N_2 \tag{6}$$

$$HC + NO \rightarrow CO_2 + H_2O + N_2 \quad 2H_2 + 2NO \rightarrow 2H_2O + N_2 \tag{7}$$

Reactions with water and vapor

$$CO + H_2O \rightarrow CO_2 + H_2 \tag{8}$$

$$HC + H_2O \rightarrow CO_2 + H_2 \tag{9}$$

In order to archive full converter potential, it is necessary to ensure that they operate in a narrow Air/Fuel Ratio Fig. 11, this is achieved by the introduction of feedback control, and measuring the oxygen excess in the exhaust by a lambda probe. The biggest drawback of TWC is its narrow operating range, i.e. the impossibility of continuous operation in lean mode, as the NO_x reduction catalyst. TWC catalysts have the ability to operate in lean mode for a short time, approximately 1 min, by storing nitrogen oxides and reducing them during rich or stoichiometric periods, so that this converter completely fulfills its function in combination with standard gasoline PFI engines, Pereda-Ayo et al. (2013). As diesel engines typically operate at high Air/Fuel Ratios, this type of catalyst is useless for the reduction of NO_x emissions. A similar situation is also with the latest

generation of petrol engines with direct stratified fuel injection in the cylinder which also operate in lean mode at low load, Raju et al. (2014), Kumaravel et al. (2014).

3.2.1.4. Catalytic converter with NO_x in lean mixture conditions LNT (lean NOx trap). LNT catalytic converters, in some literature named NSR (NO_x Storage Reduction) which is also used by Pereda-ayo et al. (2013). LNT catalytic converters consist of oxidizing catalysts, adsorbers which temporary store NO_2 under lean conditions and reduce the catalyst. Constructively speaking, it is similar to standard three-way catalysts, in addition to the adsorber which is made of alkali or alkaline earth metals. Due to its ability to work in lean conditions, it is suitable for diesel and petrol lean burn engines.

During the lean period, the platinum oxidized NO to NO/NO_2 mixture, alkali or alkali-earth oxide adsorbed NO_x, creates nitrates and nitrites, this is called "storing phase" Fig. 12. When the adsorber is saturated, under lean conditions, it has to be exposed for a short time to a rich mixture which delivers reducing components CO, HC and H_2. During the rich mixture, the LNT releases and reduces its stored nitrogen oxide with the presences of catalysis, this period is also called "regeneration phase". Manula et al. (2014) states that the regeneration phase in passenger car engines lasts for about 2−5 s at intervals of 1−3 min, which causes an increase in fuel consumption by 10%.

DiGiulio et al. (2014) conducted a test on commercial LNT converters in passenger cars and observed the impact of temperature and regeneration time to the catalyst performance. The same author states that temperatures between 350 °C and 400 °C are the optimal working temperatures which achieve a high conversion level of 95% and above in intervals of 180 s regardless of regeneration duration. With the temperature below 300 °C, NO_x reduction is a slow chemical process which leads to a longer regeneration time with lower concentrations of rich fuel mixtures. At temperatures, above 450 °C, the situation is exactly the opposite, the release and reduction of NO_x is a fast process which gives better results with a shorter rich period using a richer fuel mixture, Fig. 13. The drop in efficiency at high temperatures is caused by an unbalanced reduction process and a decrease in NO_x storage capacity. Thermal aging and sulfur contamination are the two main factors which lead to a drop in the performance of LNT catalysts. The mechanics that lead to sulfur contamination during a poor mixture is similar to that of NO_x storing. During the lean mixture period, LNT adsorbs SO_2 in the same way as NO_x, as sulfates are more stable than nitrates, regenerations are not completed and over time, block the formation of nitride, and hence reduce the efficiency of LNT catalysts. After sulfur contamination, it is necessary to carry out the desulfurization process of the NO_x storage unit. Complete desulfurization requires significantly higher temperatures than normal operating ones, above 650 °C in rich mixture, there is a thermal aging problem that this converter is prone to Mollenhauer and Tschoeke (2010) and Choi et al. (2007) investigated the impact of various amounts of sulfur to the LNT catalyst performance. They compare the efficiency of catalysts that are exposed to exhaust gases without sulfur and exhaust gases with a sulfur concentration of 20 ppm, and 300 ppm of NO_x in various intervals. After only 4 h of exposure, with a corresponding 3.4 g of sulfur per a 1 L of catalyst, the NO_x concentration at the converter outlet was 30−40 ppm, and the efficiency dropped below 90%, while the same catalyst under the same conditions but without sulfur contamination had an efficiency close to 100%. After 1 h of the desulfurization process at 700 °C, the efficiency of the converter is returned to normal. From all of this, it is clearly seen that the LNT catalysts are sensitive to sulfur and that solely relies on the sulfur content in the fuel which means that it is necessary to use a higher quality of fuel in vehicles equipped with LNT catalysts. A great advantage of LNT
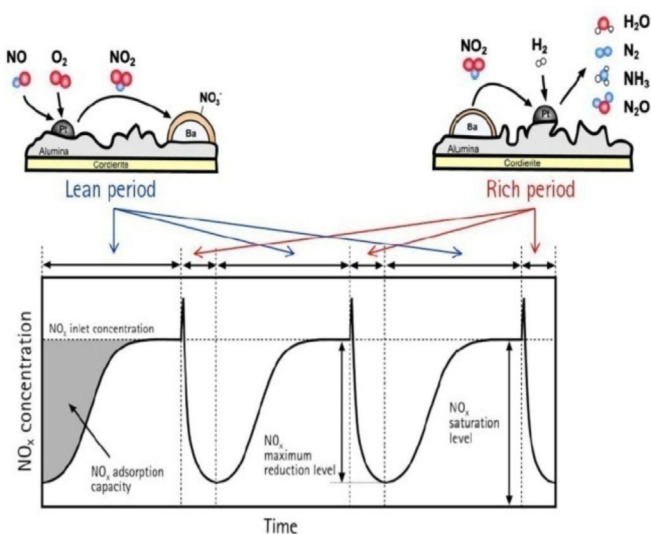

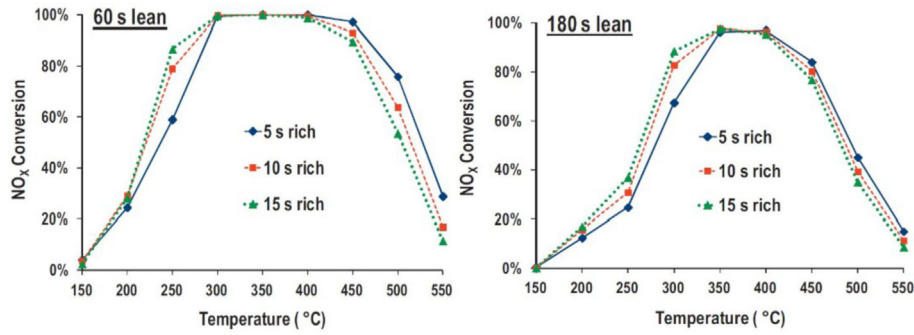**Fig. 12.** NO_x storage and reduction, Pereda-Ayo et al. (2013).

Fig. 13. NOx conversion rate in LNT for 60s and 180s lean period, DiGiulio et al. (2014).

technology is that converters with all additional elements take up relatively small space, at a reasonable price, high efficiency between 70 and 90% in most driving conditions, Nesbit et al. (2016). The drawback of these LNT systems is the requirement of occasional rich mixtures i.e. need to use additional fuel for the regeneration process. According to Yang et al. (2015), cars equipped with LNT converters show a weakness in lab testing with the new WLTP cycle, while still keeping up to the requirements of the NEDC cycle. So far, this has shown more results in adjusting vehicle emissions to the satisfaction of the NEDC cycle, to reduce the negative impact on economy under real conditions of use, than the real weakness of this type of catalyst. Despite the drawbacks, the future application of LNT catalysts is guaranteed with a lower cost and less space required for accommodation than other exhaust after treatment systems.

3.2.1.5. Selective Catalytic Reduction. SCR technology combines active control and a catalytic converter which reduces NO_x by adding an external reducing reagent, which is usually a urea-based liquid, known in Europe as Ad Blue, a solution consisting of very pure urea in de-ionized water in the amount of 32.5%, Sinzenich et al. (2011). It is held in a special tank that refills, usually like refueling, or is only intended to be refilled during service intervals. A schematic of the complete system is shown in Fig. 14. The amount of fluid is dosed very precisely with a metering device operated by a separate ECU control unit and the fluid is piped to a nozzle which injects fluid into the catalyst. Typical chemical reactions occurring

within a SCR converter under appropriate conditions are, Busca et al. (1998):

$$4NH_3 + 2NO_2 + O_2 \rightarrow 3N_2 + 6H_2O \qquad (10)$$

$$4NH_3 + 6NO \rightarrow 5N_2 + 6H_2O \qquad (11)$$

The SCR converter achieves a NO_x conversion rate of between 80 and 95% under normal using conditions, which is why this
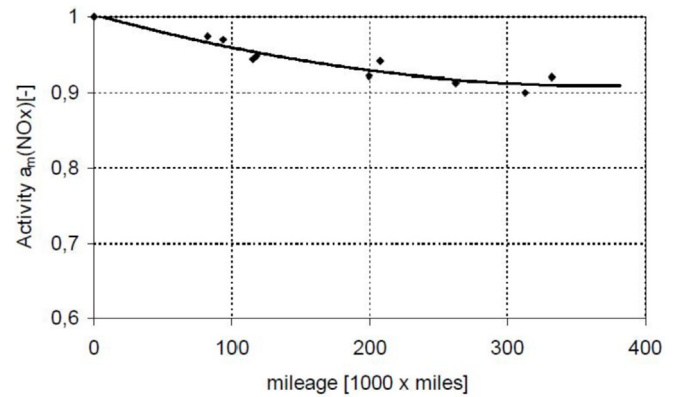

Fig. 15. Performance drop of HD SCR system with $TiO_2-V_2O_5$ converter, Amon et al. (2001).
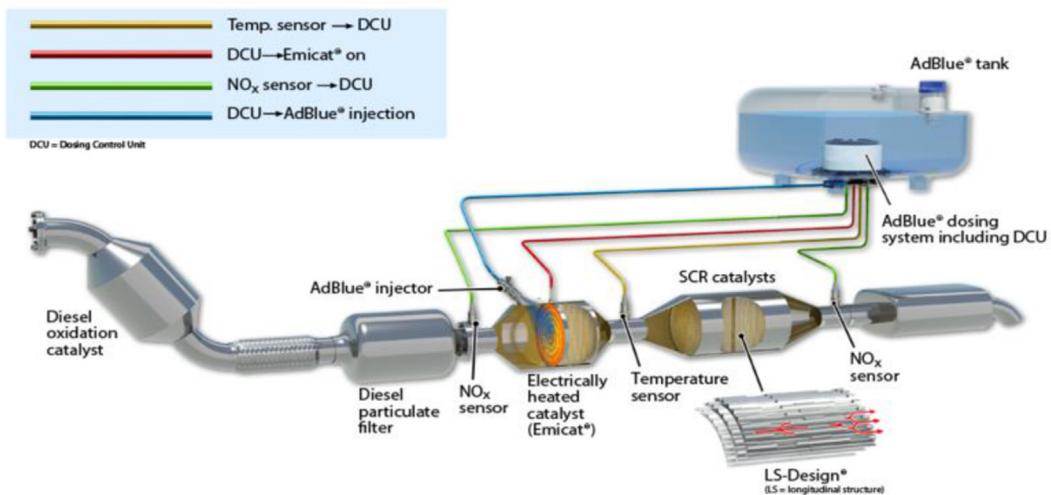

Fig. 14. Schematic representation of SCR catalytic converter components, Vitesco Technologies (2018).

technology sets standards in the degradation of NO_x emissions in lean air-fuel ratio conditions Nesbit et al. (2016). Amon et al. (2001) did research on truck engines, which are at a relatively early stage in the development of SCR truck engine technology. They did it by measuring and comparing real-world results (over 6 M km in total) and test bench results.

The measurements show the high stability of the SCR converter, Fig. 15, at 500,000 km the NO_x conversion efficiency is over 90% of the efficiency of the new SCR converter. A spectrometric analysis showed very small variations in physical and chemical properties after a prolonged use of the SCR converter. The measurements show an average NO_x conversion efficiency of 70% in real-world truck condition tests, the bench data showed very similar results. The urea consumption during the test program was 4.1% and 5.5%, respectively, compared to fuel consumption. The main disadvantages of SCR catalysts are the operating efficiency in narrow temperature ranges since they operate efficiently at temperatures above 190 °C, large additional space that takes up all the components of this converter and the extra fluid that needs to be replenished Lietti et al. (2008). Kwak et al. (2010) compared three zeolite SCR catalysts, Cu-ZSN-5, Cu-beta and Cu-SSZ-13, in a temperature range of 150—550 °C in a gas mixture with 350 ppm NO, 350 ppm NH_3, 14% O_2, 2% H_2O with a balance of N_2. All three catalysts exhibit weaknesses at temperatures below 200 °C, and their efficiency also decrease at elevated temperatures, Cu-SSZ-13 showing the least sensitivity to temperature rises above the optimum operating range, Fig. 16. The decrease in efficiency at high temperatures is due to the formation of NO_2 and N_2O by a chemical reaction between the ammonia and free oxygen.

SCR catalytic converters are often exposed to very high temperatures above 650 °C, for example, due to the burning of soot particles in the DPF filter located upstream of the SCR. According to Gao et al. (2013), Cu-SSZ-13 does not have such superior characteristics of NO_x conversion at high temperatures compared to other catalysts, but has a higher resistance to thermal aging and exposure to high temperatures. The same author conducts thermal aging research on four different commercial Cu-zeolite converters at 800 °C with a 10% water steam for 16 h.
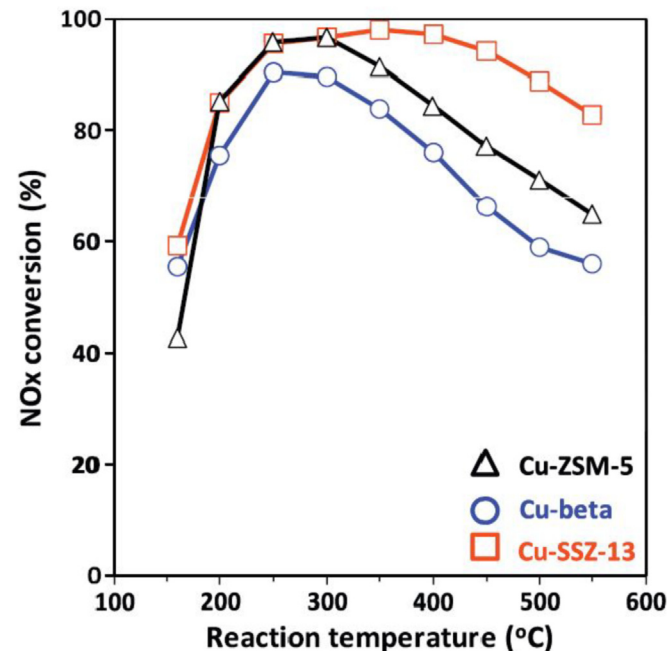

Fig. 17. Properties of commercial SCR converters after aging treatment, Gao et al. (2013).

All four catalysts have an efficiency of over 90% regarding a certain temperature range, after the aging treatment, the NO_x conversion efficiency decreases with all catalytic converters, with Cu—Y completely losing its catalytic properties, Fig. 17. Qi et al. (2003) examined three different catalysts, manganese oxide, manganese-cerium, and iron-manganese on a zeolite substrate at low SCR temperatures between 80 and 180 °C. The tests were performed with a gas mixture of 1000 ppm NO, 1000 ppm NH_3, 2% O_2, 2.5% H_2O and He for the balance. The manganese oxide catalyst performs best at low temperatures, with an efficiency of about 90% already at 140 °C. The same author examines the effect of the presence of sulfur in the exhaust gases on the efficiency of the converter by exposing it to the above-mentioned gas mixture with the addition of 100 ppm SO_2. After 5 h of SO_2 exposure, the efficiency of the SCR catalyst drops to 80%, but soon after the SO_2 exposure ceases, the catalyst returns to its original state, Fig. 18.

Unlike the laboratory testing of Kwak et al. (2010) and Qi et al. (2003) where ammonia was injected directly into the hot gas stream, under real conditions of SCR, ammonia usage is obtained with the decomposition of the urea mixture. After 32% of the urea is injected into the hot gas stream of the diesel engine upstream of the SCR converter, it decomposes according to reactions (12) and

Fig. 16. Temperature dependence of NO_x conversion for different catalytic materials, Kwak et al. (2010).

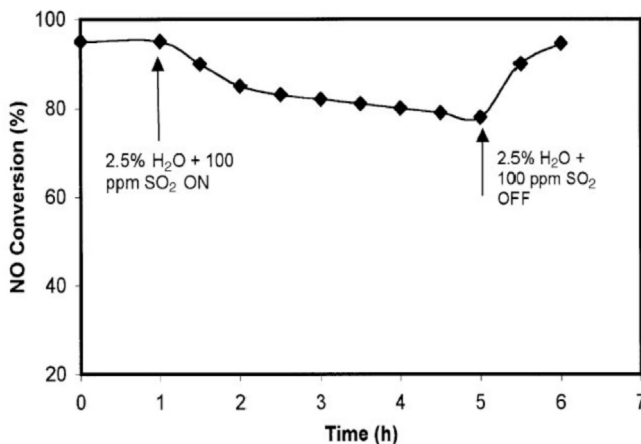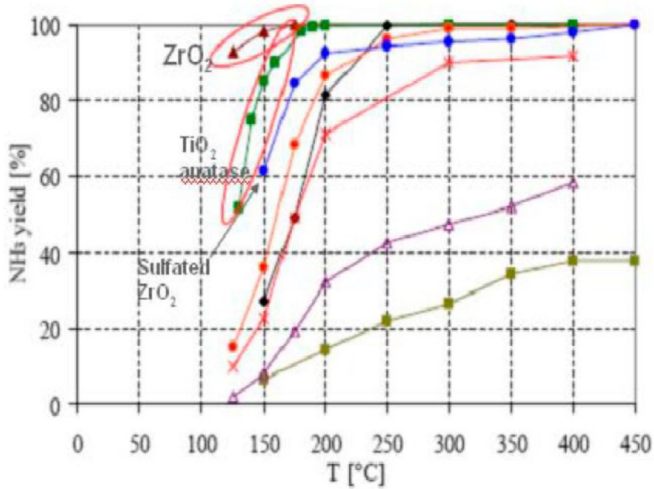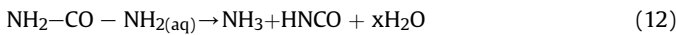**Fig. 18.** Dependence of NO_x conversion rate on exposure time to gas mixture with 100 ppm SO_2, Qi et al. (2003).

Fig. 19. Influence of temperature on decomposition of urea for different catalyst materials, Johnson et al. (2008).

Fig. 21. Relationship between NO_x conversion, NH3 leakage and NH3/NO_x ratio, Miller (2015).

(13) to ammonia and CO_2:

$$NH_2-CO-NH_{2(aq)} \rightarrow NH_3 + HNCO + xH_2O \qquad (12)$$

After which isocyanic acid (HNCO) reacts with water:

$$HNCO + H_2O \rightarrow NH_3 + CO_2 \qquad (13)$$

These chemical reactions require elevated temperatures. Eichelbaum et al. (2010) studied the decomposition of urea into ammonia using various catalysts which shift thermalizes temperatures from 290 to 200 °C and the decomposition temperatures of solid products from 370 to 290 °C and reduce the formation of solid residues in the range of 200 to 300 °C. Solid residues are formed with the decomposition of the urea, having a negative effect on the SCR, since their decomposition requires temperatures above 600 °C. Fig. 19 shows how temperature affects the urea decomposition of certain materials used as catalysts, Johnson et al. (2008).

The problem of poor performance at low-temperature exhaust gases, which occurs when driving at low loads and after cold starts, in addition to poor SCR performance, is caused by the urea decomposition problems described above. This problem can be partially solved by injecting AdBlue fluid into the electrically preheated urea decomposition catalyst as in Fig. 14. Koebel et al. (2000) addressed the problems of SCR application on vehicle engines, among others, they studied the impact of NO_2/NO ratio on NO_x conversion

efficiency. This effect is most pronounced when operating in a low temperature range. SCR efficiency measurements were performed on a coated converter in a temperature range from 150 to 450 °C with a ratio of NO_2/NO = 1 and with pure NO. Measurements show that the NO_2/NO ratio have a strong influence on the efficiency of SCR, especially at lower temperatures, Fig. 20. At 200 °C and 10 ppm NH_3, SCR with pure NO has an efficiency of 21% and with a ratio of 1:1, its conversion efficiency increases up to 93%. The usual total proportion of NO_2 in the nitrogen oxides of diesel exhausts is only 5−10%. This proportion is increased by the use of a high-quality platinum oxidation catalyst, which does not completely solve the problem of low temperature conversion since it also needs elevated temperatures to efficiently convert the NO to NO_2.

Another problem with the use of the SCR catalytic converter is the leakage of excess ammonia and its discharge into the environment. The high concentrations of ammonia at the output of the SCR are due to the use of too few SCR converters, the uneven distribution of ammonia within the SCR converter, and the large values of stoichiometric ratio ANR (Ammonia NO_x Ratio) $\alpha = NH_3/NO_x$, Koebel et al. (2000), which ensure a better NO_x conversion. On the other hand, a small ANR ratio reduces or abolishes ammonia leakage but the effect on the NO_x conversion is negative. The relationship between NO_x conversion and ammonia leakage depending on the NH3/NO_x ratio is shown in Fig. 21. Miller (2015). Due to the wide range of exhaust temperatures and the dependence of the ammonia absorption capacity within the SCR on temperature, urea dosing is a very complex procedure. The highest quality, but also the most

Fig. 20. Efficiency of SCR with pure NO and mixture of NO_2/NO 1: 1 Koebel et al. (2000).

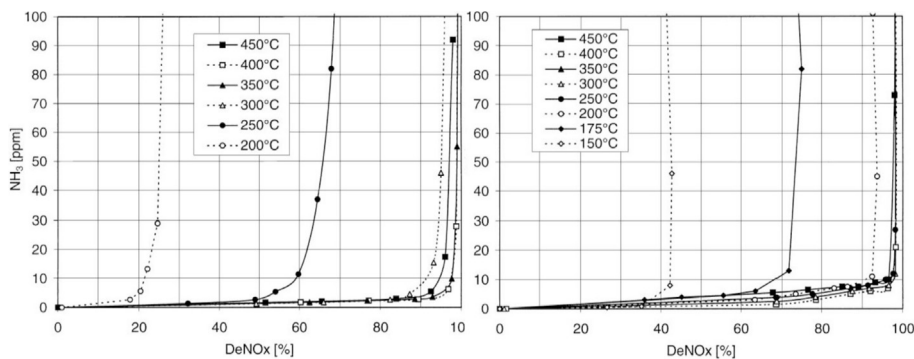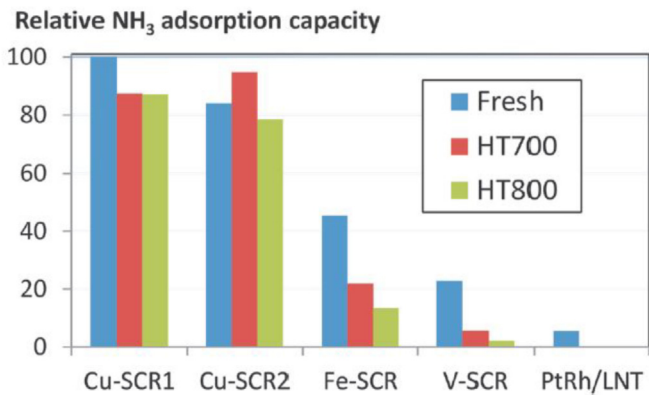**Fig. 22.** Ammonia adsorption capacity for new SCR converters at 200 °C and after hydrothermal aging at 700 and 800 °C for 20 h, Manula et al. (2014).

Fig. 24. Different configurations of LNT-SCR catalytic converters, Wittka et al. (2015).

Fig. 25. Comparison of single LNT and combination with passive SCR, Manula et al. (2014).

expensive solution of ammonia leakage is the installation of an Ammonia Slip Catalyst (ASC catalytic converter), downstream of the SCR. ASC allows the operation of SCR-s with a relatively high ANR, i.e., in the area of high NO_x conversion, and the excess ammonia decomposes into water and nitrogen. Despite the fact that anything above 15 ppm of ammonia causes a foul odor and leads to irritation of the eyes and respiratory system, Euro standards for passenger cars and heavy-duty vehicles still do not limit the amount of ammonia in the exhaust gases. In spite of high costs and all the difficulties that the SCR brings, it still finds great use in reducing NO_x emissions, primarily because of its high efficiency that allows better engine settings, with less EGR or completely without exhaust gas recirculation. It has been used with most truck engines after the introduction of the Euro 4 standard, and is increasingly entering the upper and middle-class passenger car and light commercial vehicle sector, especially to meet the Euro 6d standard.

3.2.1.6. LNT + SCR catalytic converter. This converter combines LNT and SCR technology, LNT enables ammonia synthesis during the regeneration phase, there is an SCR downstream of the LNT converter that stores ammonia and uses it to reduce NO_x so that the combination of LNT + SCR converter combines the advantages and eliminates most of the disadvantages of both converters separately. A high conversion rate is achieved by SCR, while LNT can operate at a lower conversion rate, so there is no need for a large amount of precious metals and no additional reagent is required (AdBlue), Zheng et al. (2014). This technology is more acceptable for lower- and middle-class passenger cars because it requires less space, no AdBlue tanks, dispensers and piping, and shows better
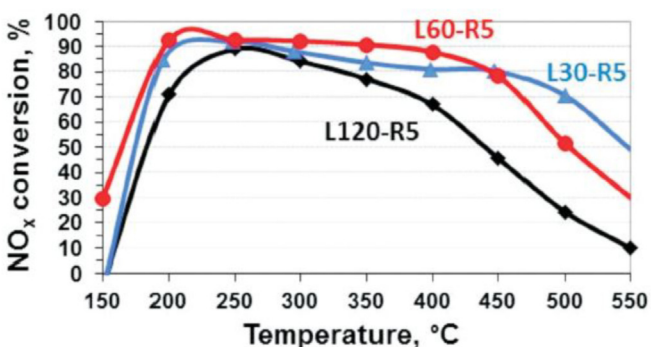

Fig. 23. Efficiency of NO_x conversion for different durations with lean mixture, Manula et al. (2014).
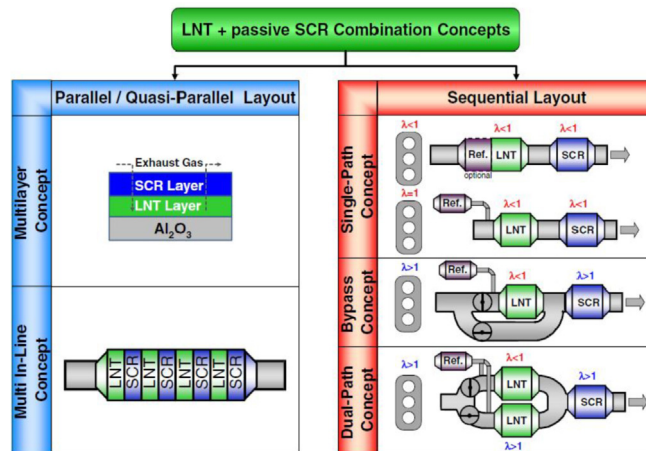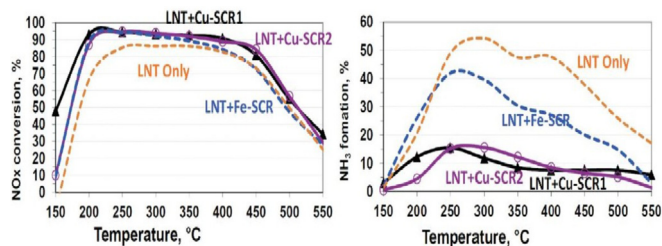
performance than LNT individually. According to Wittka et al. (2015), the combination of LNT and passive SCR (without the external addition of ammonia) works most effectively at temperatures between 200 and 300 °C, achieving almost 100% efficiency at 250 °C. In an individual LNT, the regeneration period with a rich mixture causes a significant increase in CO, HC, PM and ammonia concentrations in the exhaust gases. All of these quantities can be regulated in the duration of the rich and lean mixture period. It is common for LNTs not to complete the regeneration process completely during the rich period, thus avoiding the leakage of reducing components (HC and CO) and NH_3. The installation of the SCR catalytic converter downstream of the LNT enables complete regeneration and better utilization of the LNT, because the ammonia generated during this period is absorbed by the SCR. As LNT-SCR systems are typically used in passenger cars and light commercial vehicles where exhaust gas temperatures are expected to be in a range of 100−250 °C, the characteristics of the LNT-SCR system should be adjusted to lower operating temperatures. On the other hand, there is a need to use materials that are resistant to thermal aging due to the high temperatures that occur during DPF filter regeneration (above 700 °C). In this configuration, the SCR will almost always work with pure NO without the presence of NO_2, because complete NO_2, which is formed partly in the engine, partly in the DOC converter or catalyzed DPF, will consume LNT. Manula et al. (2014) compared the effect of different types of SCRs under low temperature conditions with pure NO. The best results are shown with copper and iron-based catalysts and have the best NO conversion both before and after hydrothermal aging treatment (800 °C/20 h). SCR catalytic converters in such configurations also have a tendency of losing their ammonia adsorption capacity, which is why they cannot store sufficient ammonia during the

regeneration phase, it would be necessary for SCR reactions during the lean mixture period. Copper-based catalysts best retain the adsorption capacity after aging, Fig. 22.

The overall efficiency (LNT + SCR) of NO_x conversions is directly influenced by the duration and frequency of the lean and rich mixture. The lean-rich timing also correlates to fuel economy, shorter rich periods and longer lean periods lead to better fuel economy, so it is necessary to find the optimum. Manula et al. (2014) conducted an experiment with copper-based DOC/LNT + SCR with different durations (30−120s) of lean mixture l = 1.41, with a NO_x concentration of 500 ppm and time rich mixture 5s with l = 0.86 with NO_x concentration of 1500 ppm in laboratory conditions.

The longest rich time, 120s, gives the worst NO_x conversion results, especially at elevated temperatures where the adsorption of NH_3 in SCR becomes a limiting factor, Fig. 23. A short period of poor mixture of 30s compared to 60s brings no improvement; it even has a slightly negative effect, since not enough ammonia is generated to effectively operate the SCR. From the foregoing, it can be seen that even with this type of catalytic converter, tuning the operating parameters is a major challenge, especially in the conditions of variable engine loads.

Wittka et al. (2015) carried out research on different LNT-SCR configurations and the best NO_x conversion results when considering an increased fuel consumption is given for engine-independent regeneration configurations, the bypass or dual-path concept in Fig. 24 because of better fuel utilization during LNT regeneration. In the standard configuration, 10−45% of the extra consumed fuel is used as a reducing agent, while this ratio increases to between 50 and 65% in the system with bypass and reforming unit. The LNT-SCR combination for equal total converter volume achieves, at lower exhaust temperatures, better nitrogen oxide conversion results than the LNT individually. At elevated temperatures, the conversion efficiency is approximately the same and very little depends on the choice of catalytic converter active substance, but the benefit is the reduced ammonia release to the environment by 3−5 times. Fig. 25 shows the comparison of LNTs individually and in combination with SCR.

3.2.2. Diesel Particle Filter

Besides NO_x, one of the main goals of the development of modern diesel engines is the reduction of soot emissions. The basic element for reducing particulate emissions is the Diesel Particulate Filter DPF, which is a mechanical filter that stops particulate matter from the exhaust, including solid carbon (soot) and fine particles, while the rest of the exhaust gases pass through the filter. After a certain period of use, the filter is saturated. The degree of DPF contamination is estimated, as with standard mechanical filters, on
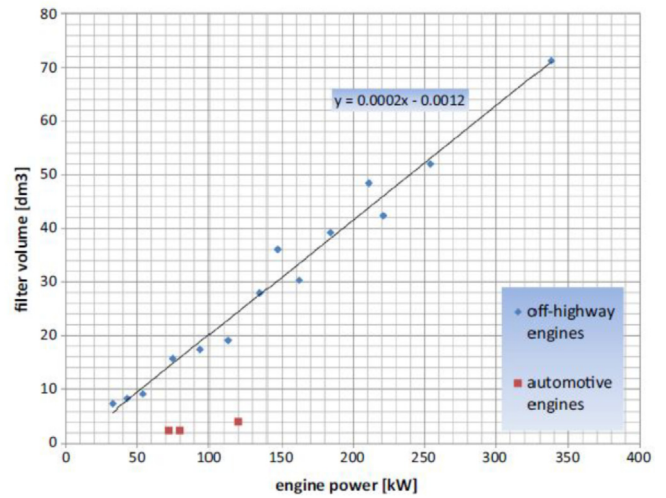
Fig. 27. vol ratio of DPF filters to maximum engine power, Stamatellou et al. (2017).
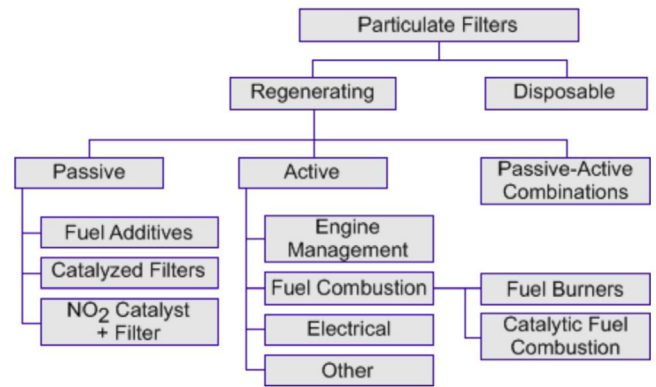
Fig. 28. Classification of DPF systems by regeneration, Majewski (2015)

the differential pressure between the inlet and outlet of the filter. An increase in back pressure leads to a decrease in effective pressure according to relation (14). The drop in mean effective pressure is related to the drop in torque or power. To ensure the desired performance, we must compensate the loss which requires additional fuel. According to Stamatello et al. (2017), an increase in back pressure of 200 mbar leads to an increase in specific consumption by approximately 2%.
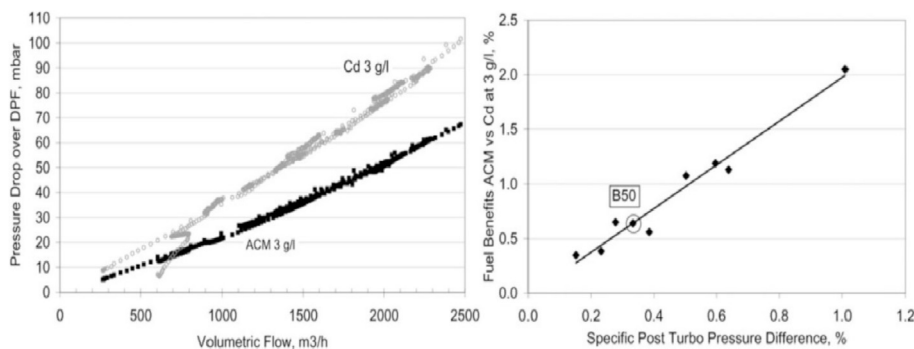
Fig. 26. Comparison of pressure drops and relative consumption of ACM and Cd DPF, Mikulić et al. (2010).

Fig. 29. Reactivity of O_2 and NO_2 as function of temperature, Gorsmann et al. (2005).

Fig. 31. Comparison of DPF filters (non-catalyzed DPF, CSF, CRT, and CCRT) and their back-pressure behaviors in low exhaust gas temperatures T < 270 °C, Gorsmann et al. (2005).

Fig. 30. Oxidation rate of diesel particles by oxygen as function of temperature, Majewski (2005).

$$W_{cycle} = \oint pdV + (p_{in} + p_{ex}) \times V_d \qquad (14)$$

The back pressure of the saturated DPF increases rapidly with the accumulated mass of particles in the filter channels. The pressure drop on the DPF depends on the saturation, the gas flow, the geometric characteristics of the filter and the filter materials. Monolithic filter walls are usually made of special porous materials, and the most commonly used ones in mobile applications are: Cordierite (Cd, 2MgO*2Al$_2$O$_3$*5SiO$_2$), Silicon Carbide (SiC), Acicular Mullite (ACM, Al$_2$SiO$_5$), Aluminum Titanate (AT, Al$_2$TiO) and metal alloy foam (Alloy Foam AF). Mikulic et al. (2010) addressed the impact of DPF back pressure on the increased fuel consumption of an HD truck diesel engine with two different DPFs. The results show that filters of the same design, of equal wall thickness, of equal volume, give different back pressure. The ACM-built filter provides a significantly lower pressure drop, especially at higher flow rates, than the cordierite filter, thus saving on fuel economy.

Fig. 26a and b show the results of the pressure drop at the DPF on flow for Cd and ACM, and the relative savings on fuel consumption compared to the difference in pressure drop between Cd and ACM DPF according to BMEP (Break Mean Effective Pressure). Under load conditions according to the ESC (European Stationary Cycle), the gains in consumption by using an ACM filter instead of

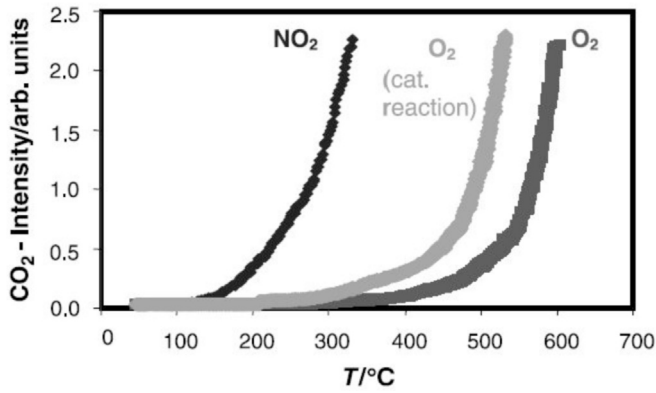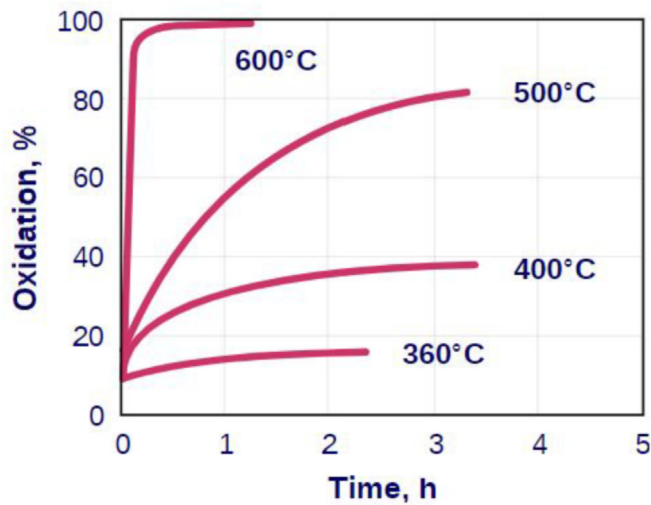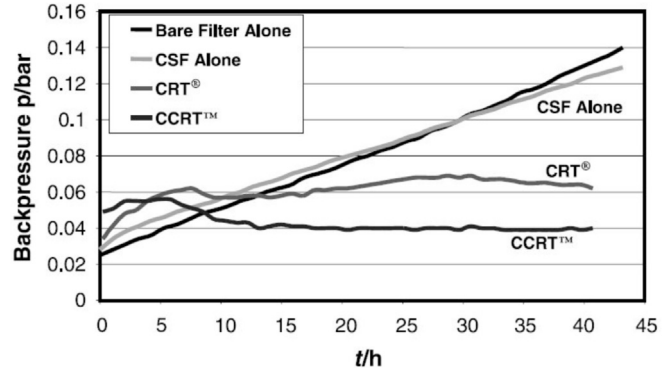the standard factory-installed Cd, ranges between 0.4 and 2%. Stamatellou et al. (2017) addressed the problems of sizing DPF filters with an emphasis on stable applications where filters are in most cases oversized as opposed to moving applications where filters are well dimensioned. Reducing the size of the DPF while maintaining the maximum allowable backpressures declared by the manufacturer generally has a positive effect on the filter behavior during the regeneration phase due to the faster heating of the filter. According to Stamatellou et al. (2017), the filter volume should not exceed twice the working volume of the engine. Fig. 27 shows the ratio of the DPF filter sizes to the maximum engine power for automotive engines and for off-highway engines, as well as for stable applications, construction machinery, marine propulsion, etc.

Particle filtering efficiency is influenced by its mechanical properties; most of all pore sizes and cell counts. Maunula et al. (2007) compared filters with different mechanical properties in a standard EDC cycle for vehicle type approval. Filters with 90 cpsi (cells per square inch) and a mean pore size of 37 μm has an efficiency of between 87 and 92%, while a filter with 200 cpsi and a mean pore size of 25 μm has an efficiency of between 98 and 99.5%. Filters with relatively large pore sizes are suitable for retrofit, i.e. subsequent installation to less demanding applications, where the benefit is that the ash passes through them and extends their life. Modern vehicle engines use filters with pore sizes between 10 and 25 μm in order to meet stringent type approval regulations which achieve efficiencies above 98%. Filter saturation occurs, if the exhaust temperatures are not high enough to maintain self-cleaning (auto-regeneration). After the filter is saturated with soot particles to a predefined limit, the particles must be removed, i.e. the filter should be regenerated. In addition to soot particles, the filter retains ash particles that cannot be removed by regeneration, so filter service is required.

There are also disposable DPF filters that are replaced after saturation, but these are special-purpose filters and are not commonly used. The classification of filter systems with regeneration methods are shown in Fig. 28. There are three modes of regeneration: passive, active and combined. Passive regeneration solves the problem of filter saturation by reducing the combustion temperature of the particles to a temperature reached under normal operating conditions without the need for additional energy consumption, while active regeneration raises the exhaust gas temperature to the point where soot particles begin to oxidize. In diesel exhaust, there are only two gases which are suitable for soot oxidation, oxygen and nitrogen dioxide and both play an important role in the regeneration process, this role depends on the reactivity
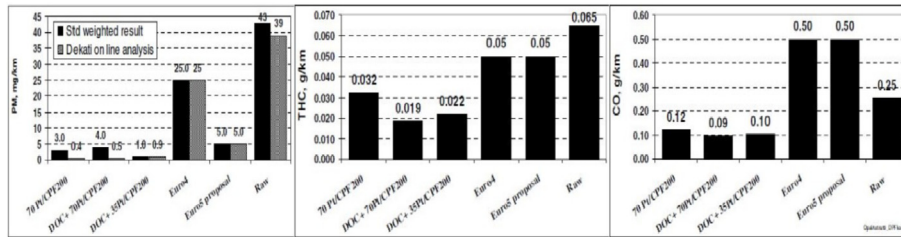
Fig. 32. NEDC passenger car emissions with different DPF catalyzed combinations, Maunula et al. (2007).

and amount of those gases. The amount of oxygen in the exhaust of a diesel engine is approximately 2−3 orders of magnitude larger than the amount of NO_2, but the NO_2 is more active at lower temperatures. The difference in reactivity between NO_2 and O_2 as an oxidation agent for soot is shown in Fig. 29.

3.2.2.1. Passive regeneration. Passive regeneration can reduce the combustion particle temperature in several ways:

1. By adding additives that lower the inflammation point of the particles - FBC (Fuel Borne Catalyst-assisted)
2. Oxidation by oxygen
3. Particulate combustion using NO_2

The use of additives to lower the oxidation temperature is one of the most effective methods for regenerating DPF filters. The FBC is precisely dosed into the fuel, kept in a special tank that is usually refilled during regular service. The principle is to incorporate a catalyst particle about 10 nm in diameter into the soot particles and deposit them in the filter. The advantage over a catalyst film DPF is the large number of contact points and contact surface with soot particles throughout the volume. Thus, this type of regeneration has the ability to regenerate faster than catalyzed DPF. FBC decreases the regeneration temperature from over 600 °C to about 350 °C and accelerates reaction, making regeneration faster and more complete. Quan-shun et al. (2016) measured emissions before and after the DPF filter with and without the DOC option on bus motors under real driving conditions and on a test table. The FBC method with additive addition was used for regeneration. The results of NO_2 reduction measurements under all conditions show similar results, decreasing to about 44% relative to input values, while the reduction of other nitrogen oxides is negligible. The particle filtering efficiency ranged between 95 and 99%. Oxidation by excess O_2 in the exhaust gases at lower temperatures is generally a slow reaction and DPF regeneration is incomplete, Fig. 30. Temperatures above 600-650 °C are required to achieve complete combustion of soot particles, which rarely occurs under normal operating conditions. A significant acceleration of the reaction is achieved with a catalyzed DPF, which accelerates the reaction between the carbon in the particles and free oxygen in the exhaust gases. The DPF with this type of primary oxidation is rarely used because of the need for a relatively large catalytic converter with a large amount of expensive precious metals. Particulate combustion with NO_2 is a particularly interesting regeneration method for most HD applications because of the usual exhaust gas temperature between 200 and 300 °C, and is used in addition to active regeneration for passenger cars and light commercial vehicles. Chemical reactions are described with Eq. (15)−(17). Fig. 31.

$$2NO+O_2 \rightarrow 2NO_2 \tag{15}$$

$$NO_2+C \rightarrow NO+CO \tag{16}$$

$$NO_2+C \rightarrow N_2 + CO_2 \tag{17}$$

As the NO_2 concentration in diesel engines is only 5−20% of the total nitrogen oxides and the rest is mostly NO, a DOC (Diesel Oxidation Catalyst) is usually placed upstream of the DPF, which accelerates the NO oxidation reaction in NO_2, equation (16). DOC is a catalytic converter consisting of a substrate that can be ceramic or metal with a surface area of several m^2. To increase the surface, usual metal oxide (e.g. Al_2O_3) wash coats are used and coated with catalytic materials (usually platinum). The typical amount of catalyst applied is 0.1−10 g/dm^3, Gorsmann et al. (2005). In addition to NO oxidation, DOC is also used to oxidize the unburnt HC hydrocarbons and CO carbon monoxide. There are several commercial systems based on NO_2 regeneration:

- CRT (Continuously Regenerating Trap) = DOC + DPF,
- CSF (Catalyzed Soot Filter) or CPF (Catalyzed Particulate Filter) = catalyzed DPF and
- CCRT (Catalyzed continuously Regenerating Trap) = DOC + CSF

It can be seen from equations (16) and (17) that DPF with CRT regeneration reduces the amount of NO_x harmful emissions. For CSF filters, the oxidation of HC, CO and NO takes place inside the filter itself. NO_2 is formed inside the filter duct and collides with the soot particles that oxidize to CO_2 and NO_2 and is reduced to NO which travels further through the duct and is oxidized with excess oxygen, and these reactions are repeated all the way through the duct. The CCRT system allows the highest utilization of NO_2 in soot regeneration. The advantage of CSF is its compactness, while CRT is the least sensitive to ash accumulation (which cannot be removed by regeneration). Gorsmann et al. (2005) observed the behavior of different filters with or without passive regeneration under low exhaust temperature conditions, Fig. 32. The pressure drop of the filters is related to the accumulated soot. Therefore, changes in the pressure drop are related to the ability to regenerate.

Maunula et al. (2007) studied the behavior of different types of DPFs, with varying amounts of precious metals, with a volume of 2.4 dm^3 with 200cpsi on a Euro 4 passenger car under NEDC (New European Driving Cycle) conditions, where the exhaust temperatures were generally between 100 and 300 °C. The CCRT system combines the properties of CRT and CSF, which enables better utilization of NO_x for the combustion of soot particles. It shows better properties than CRT and CSF individually and in cases where a smaller amount of precious catalytic materials is used in the filter compartment, Fig. 32. The possible leakage of unused NO_2 is resolved by the proper selection of precious metal amounts and their distribution. These properties are particularly pronounced at low loads with low exhaust temperatures at low NO_x concentrations. The biggest advantage of passive regeneration is the operation of the DPF system within a safe temperature range without the risk of individual component destruction, while the disadvantage is the limited use in cold applications with low loads, as well as the high initial cost of systems that allow this type of regeneration.

3.2.2.2. Active regeneration. When DPF filters are used in operating conditions of low exhaust gas temperatures or in conditions where temperatures sufficient for passive regeneration occur rarely, active DPF regeneration must be ensured. This approach is based on the activation of regeneration by raising the temperature of the particles trapped in the filter using an external energy source. If there is a sufficient amount of NO_x in the exhaust gas, it is sufficient to raise the temperature to that sufficient to burn the soot particles with NO_2, which is approximately 300 °C. If the NO_2 amount is low, the filter can only be regenerated by oxygen excess. For this type of oxidation, the exhaust gas should be raised to about 550−600 °C. There are two possible sources of energy: fuel or electricity. In the case of fuel usage, there are also two basic ways, injecting the fuel into the exhaust gases in the exhaust manifold or post injection with late combustion stroke. For large systems, separate burners are still used to regenerate DPF filters. Late or subsequent injection of fuel into the cylinder is the most common used method because of its low cost, where only software changes are required most of the time. The disadvantage is a small amount of unburned fuel that ends up in the crankcase and dilutes the oil, which requires more frequent service intervals. With HD applications, it is more common to apply fuel injection to the exhaust manifold for DPF regeneration due to longer intervals between engine oil changes, Guan et al. (2015). The purpose of the additional or delayed injection is to provide sufficient hydrocarbons that do not burn in the engine to gain useful work but oxidize in the DOC catalytic converter and raise the exhaust gas temperatures high enough to oxidize the soot particles. The use of electricity as a heat source to raise the exhaust gas temperature is rarely used and involves the installation of an electric heater in front of the DPF filter inlet. In addition to energy consumption (electricity and fuel), the temperature of the exhaust gases can also be affected by the air path control which implies the control of fresh air and exhaust gas flow. This type of control involves regulating the amount of exhaust gas recirculation via the EGR valve, regulating the amount of fresh air, the boost pressure through the throttle valve, variable geometry of the VGT, and bypassing the EGR cooler. Moraal et al. (2004) and Guan et al. (2015) thoroughly described the problems, modes, and constraints in managing an engine system for DPF regeneration. One of the main disadvantages of active regeneration are very high temperatures downstream the DOC, therefore all the exhaust components should be resistant to high temperatures especially DPF. Regeneration in very large soot accumulations are particularly

dangerous, because in high temperatures and sufficient oxygen conditions, soot burns very quickly and can raise the temperature to above 900 °C despite the activated high temperature protection, which can cause permanent damage to the DPF. A critical temperature rise occurs if the filter load is above 8−10 g/L, Maunula et al. (2007). According to the same author, the temperatures of active regeneration in low PM load do not exceed 650-700 °C, while the pressure drop in 2 min of regeneration drops from 200 mbar to 50 mbar. Zhan et al. (2006) dealt with various causes of uncontrolled DPF regeneration, in addition to regeneration with high filter loading, the uneven distribution of soot and the reduction of exhaust gas flow during regeneration (idling) are also a problem. The movement of temperatures during regeneration with a high filter load of 10.1 g/L is shown in Fig. 33. Although the temperatures at the inlet of the filter are within normal limits, 650 °C for a start and 550 °C for maintaining a regeneration, the bed temperatures are outside the permissible limits, up to 1100 °C, which can cause permanent damage.

Active regeneration due to the need for additional heating has an impact on increasing the consumption by 2−3%, while in the case of passive regeneration this influence is reduced by about 80%, Guan et al. (2015). The use of active oxygen regeneration is very widespread, in almost all engines equipped with DPF filters, while in low-temperature applications it is the only possible choice.

4. Emission control strategy

Advanced diesel engine technologies such as common rail injections, variable geometry or staged turbochargers, variable valve management and complex exhaust after treatment systems described in the previous chapters allow efficient engine operation, but many degrees of freedom simultaneously increase the number of possible solutions and make it difficult to find optimal management strategies. The challenges facing modern engines are meeting the demands of power, quick response to changing loads, high efficiency and durability as user demands and meeting environmental standards as a type approval demand. Engine optimization is performed in several steps: initial calibration, steady-state optimization, transient load optimization, and finally optimization to the type approval cycle (most often adapted to the test cycle), Grahn (2013) addressed the problems of modelling and optimizing diesel engine control systems. The optimization of engines to meet older standards, euro 1 and 2, focused on steady-state optimization, with euro 3 and 4 standards, the emphasis was on cycle optimization, due to the large discrepancies between the type approval NEDC test cycle and real driving conditions. With the Euro 5 and Euro 6a, the manufacturers of passenger cars and light commercial vehicles have resorted to a greater use of proven and relatively inexpensive HP exhaust gas recirculation methods in order to avoid using expensive exhaust after treatment components, for the reasons explained earlier in the EGR section, and with the additional increase in back pressure due to DPF, it had an effect on the significantly slower response to load changes, so the emphasis was not only on optimization by cycle but also on the optimization of transient loads. A new WLTP (Worldwide Harmonized Light Vehicle Cycle) was introduced after the Dieselgate emission scandal, which is more similar to real driving conditions as well as emission control under real driving conditions using PEMS (Portable Emission Measurement System), which should minimize the need for optimization according to the approval cycle. It should be emphasized that the optimal engine management strategy depends not only on the engine, but also on the complete vehicle used, in the case of passenger and light commercial vehicles. If the same engine, with all the necessary emission control systems, is installed in a heavier vehicle, it will normally operate at higher loads during the standard
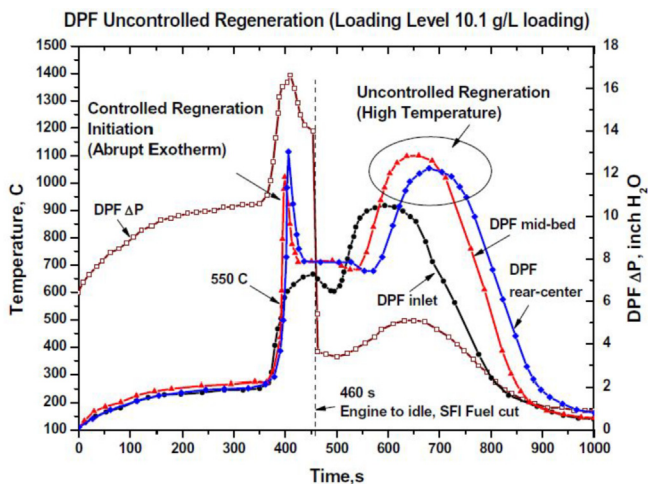

Fig. 33. DPF temperature movement in uncontrolled regeneration, loaded with 10.1 g/L, Zhan et al. (2006).

test cycle, but also in everyday use. It therefore follows that the optimum engine settings in one model of vehicle will not be optimal for that same engine fitted to an another vehicle model. For trucks and stationary applications, the situation is simpler because the emission limit values are given per kWh of delivered mechanical energy to the flywheel. Engine settings to meet customer and environmental requirements often differ, but not always. The best examples are the engine settings that give the minimum of particulate emissions PM, carbon monoxide CO and hydrocarbons HC which mostly match with the low consumption settings. The additional requirements for even lower level mentioned pollutants require the use of oxidation catalysts for CO, HC and DPF for PM emissions, which slightly increase fuel consumption. On the other hand, any reduction in NO_x emissions, whether influenced in the cylinder during combustion or after treatment of gases, has a negative impact on the fuel economy. With regard to NO_x emissions, the situation is further worsened by the fact that the reduction of NO_x emissions during combustion leads to an increase in HC, CO and especially PM emissions. According to a detailed analysis of existing technologies, a diagram was developed, Fig. 34 that clearly shows in principle ways how to achieve type approval standards with the different technologies. Lines 1, 2 and 3 represent the engine technologies in the narrow sense, without any emission control systems. The position and shape of the lines is conditioned by the degree of engine development, which depends on different applied technologies of injection, turbo charging, swirl and tumble in the combustion chamber, working medium exchange, compression ratio, etc.

Line 1 represents the engine with the highest level of development, while the position of points P1, P2 and P3 is determined by the current engine settings, i.e. settings of injection angle, precharge pressure, swirl intensity, valve opening and closing angles, etc. For example, movement from point P1 in direction of point P3 can be achieved by early main fuel injection which allows for a better mixing of the fuel with the air before ignition, which avoids the conditions for soot formation, with the inevitable increase in NO_x emissions, Fig. 35. While soot is formed in the region of moderate combustion temperatures and locally rich mixtures, NO_x emissions occur under high temperature conditions and leaner mixtures, Meloni et al. (2013). An earlier injection causes the maximum temperatures and pressures to rise, which favours nitrogen oxidation but increases engine efficiency. It is obvious that even the engine with the highest level of development represented by Line 1 cannot meet the stringent environmental requirements without additional systems.

Fig. 34 shows how different Euro norms can be achieved using different emission control systems and technologies. The Euro 4
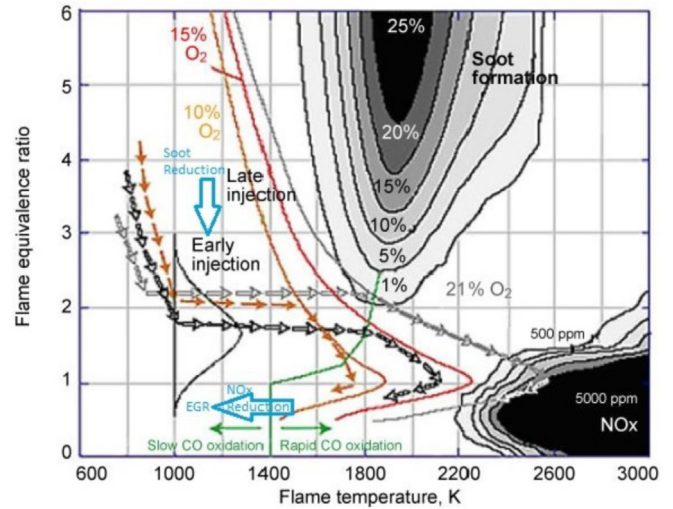

Fig. 34. Effect of different emission control technologies to achieve different Euro norms.

Fig. 35. Conditions for soot particle formation and NO_x emissions, Johnson (2008).

standard can be achieved from the starting point P1, which is a compromise between NO_x emissions on the one hand and PM and consumption on the other. EGR reduces NO_x but increases PM slightly and then DPF solves the particle problem. Another way is by starting with point P2, which is no longer a compromise but point of low fuel consumption with a large amount of NO_x, the NO_x emissions are reduced by the SCR catalyst and then the particles are reduced by the DPF filter. The second method allows significantly lower fuel consumption, due to a starting point in the area of low consumption and low soot particle emission, thus increasing the interval between DPF regenerations, further reducing consumption. The disadvantages of this approach are the high initial cost of the SCR system, as well as the cost of maintenance, reagent consumption and taking up a relatively large space, so it is not suitable for smaller vehicles. The emission control techniques and systems explained earlier provide manufacturers with several possible ways to meet the required standards. Most often, combinations of different techniques give the best results in terms of emission limitation and fuel consumption, while the required space and particularly the cost of the system are a limiting factor for the use of better solutions.

5. Discussion

This paper analyses techniques and systems whose primary purpose is to regulate or reduce the harmful emissions of diesel engines. In addition to analysing individual systems, the effect of different system combinations is explained, without those future standards, they cannot be fulfilled. So far the dominant NO_x emission reduction technique for passenger and light commercial vehicles, a high-pressure HP-EGR exhaust recirculation could only satisfy Euro 6b under laboratory test conditions according to the outdated NEDC type-approval cycle. With the introduction of Euro 6d, which includes a new WLTP homologation cycle with real-world RDE testing, HP EGR becomes insufficient but will be used in the future in combination with other systems, especially in combination with LP-EGR. LP-EGR delivers promising results, and because of its lower cost and less space usage, makes it suitable for applications in smaller vehicles compared to exhaust after treatment systems. A compact design makes LNT technology interesting in the use of passenger cars, but its efficiency limitation is between 60 and 70% in normal driving conditions, with an unavoidable increase in consumption due to periodical operation in rich mode and
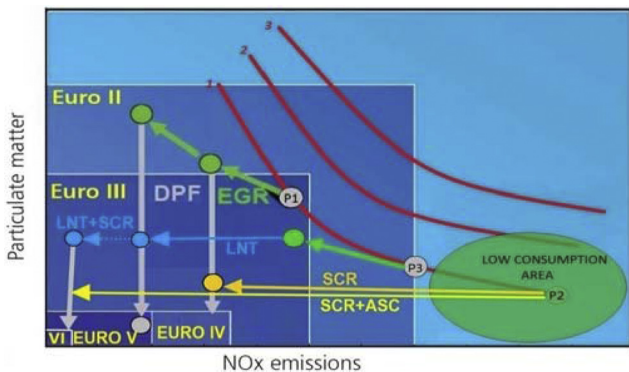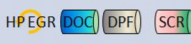
in areas with low fuel quality with an additional problem in sulfur sensitivity. The Selective Catalytic Reaction System (SCR) gives the best results and sets standards in terms of NO_x conversion efficiency, over 90% over a certain temperature range with the addition of an ASC catalytic converter that prevents ammonia leakage. Its use is limited to larger vehicles due to the complex delivery and dosing system of ammonia and the space that it occupies. The need to refill the AdBlue fluid which increases costs by about 2% over fuel is not negligible. Another problem is the fact that their efficiency drops sharply below 150-200 °C, depending on the type of converter used. This disadvantage is mitigated by engine downsizing in which the operating range is shifted to higher exhaust gas operating temperatures or by additional heating that requires additional energy consumption. The current state of the art, LNT + passive SCR gives very good results as the ammonia required for NO_x reduction is generated in the LNT while operating in rich mixture mode so that the whole system does not require large space for accommodation. There has not been a rapid turn in heavy duty (HD) engines due to well-defined standards where emission limits are given per kWh of mechanical works regarding the engine instead of per traveled kilometer in passenger cars. Thus, for the control of NO_x emissions, SCR technology remains at the centre of application, benefiting from the operation of the exhaust gas engine in the mid-temperature range. Further development will focus on extending the scope of action to low temperature applications and further optimizing the system. Since the introduction of Euro 4 for trucks and Euro 5 standards for passenger and light commercial vehicles powered by diesel engines, DPF filters have become mandatory elements for reducing particulate matter in the exhaust. By introducing direct fuel injection, gasoline engines also emit more particulate matter than allowed, so particulate filters should become an integral part of vehicles powered by gasoline engines. Techniques for regulating soot particle emissions are further developed and optimized for DPF filter technologies, especially in the field of regeneration, which includes catalytic DPF filters with continuous CCRT regeneration through control of active regeneration parameters. When designing and optimizing the engine emission control systems of a vehicle, their effect should be considered on the transient response that directly affects driving comfort As a rule, all

after treatment systems increase the exhaust back pressure, which causes a drop in the turbocharger performance, while the EGR (especially HP-EGR) situation is even more complicated as it takes some of the gas from the turbocharger and further reduces its rotational speed, which increases the response time during transient load. Several problems caused by modern diesel emission control systems such as slow load responses, cold applications in engine partial loads and inefficient regeneration, can be effectively resolved with hybrid powertrains. Hybrid powertrains allow the internal combustion engine to operate in optimal load range in which emission control systems are highly efficient. Diesel hybrid vehicle emissions are not suitable discussed in the existing literature where future research work should be directed in that specific research field. The main question is if it is possible to meet the latest euro norms in certain applications using a hybrid drive without an expensive SCR system? The use of a combination of diesel-electric hybrid propulsion is expected to significantly reduce CO_2 emissions, toxic emissions and fuel consumption. Problems with reducing toxic emissions can occur after a longer engine stand still period, i.e. after a semi-cold start, which is especially pronounced in plug-in hybrids. Research on the impact of cold and semi-cold start-ups on the amount of emissions, as well as the ways in which catalytic converters are rapidly heated and the effect of rapid heating on consumption, should certainly be carried out. Due to the intensive development of the emission control system in recent years, more intensively than ever before in the history of engine development, in which the automotive industry invests enormous resources, there is no gap between published studies and the current state of the art in this field. One could even say that it is publicly available literature in some segments lags behind the techniques used, as the automotive industry keeps some of its knowledge secret. The authors are mainly concerned with individual technics for emission control, however, as such, i.e. independently, they are not applicable. These systems can be useful only as a part of a complete emission control system incorporated in the power train. The articles such as written by Grahn (2013), and Asprion et al. (2014) dealing with the interrelationships of different techniques, i.e. the optimization of a complete engine, which includes exhaust gas treatment techniques, are rare. This topic has

Table 1
Diesel emission concepts comparison.

Technical solution	Emissions						Packaging	Maintenance	Costs	Comments
	NOx	PM/PN	CO2	NH3	CO	THC				
HP EGR Cooled HP EGR DOC DPF	BASELINE									Pure NOx reduction potential. Commonly used up to Euro 6b. Failed in RDE.
High EGR combustion HP/LP EGR DOC DPF	⊕	○	○	○	○	○○⊖	⊖	○○⊖	⊖	Insufficient NOx reduction potential for future euro norms. Possible HEV application in smaller vehicles.
Lean NOx Trap System HP EGR DOC DPF LNT	⊕⊕	○	⊖	⊖	○	○	○○⊖	○○⊖	○○⊖	Suitable for smaller vehicles. Sensitive to sulfur content in fuel. NOx reduction potential affects fuel consumption.
SCR System HP EGR DOC DPF SCR	⊕⊕⊕	○	⊕	○○⊖	○	○	○○○⊖	○○⊖	○○○⊖	Very robust and large system. Suitable for hihgly and midium loaded engine in large vehicles.
Close-coupled SCR/ASC System HP EGR DOC DPF SCR ASC	⊕⊕⊕⊕	○	⊕⊕	○	○	○	○○○⊖	○○⊖	○○○○⊖	Very efficient NOx reduction system also suitable for low loaded engine. Able to meet all future standards of harmful emissions, especially in combination with HEV

⊕ -better than baseline   ○ -same as baseline
⊖ -worse than baseline   ○ -same as baseline, fully satisfied requirements

recently been a particularly interesting but also challenging area because of the large amount and complexity of exhaust gas control techniques described in this paper. Table 1 shows a comparison of commonly used technical solutions in terms of conversion efficiency, production cost, size and maintenance of diesel engine emission control systems. Further variations are possible using different individual systems (e.g. catalyzed DPF), within the technical solutions presented, as well as combinations thereof (e.g. SCRF = SCR + DPF). Increasing the complexity of propulsion systems will undoubtedly lead to more environmentally friendly vehicles, with utmost importance on durability and quality of all installed components.

6. Conclusion

In this paper, a comprehensive study of diesel emission control systems with an emphasis on NO_x and PM emissions was conducted with the aim of meeting the latest emission regulations and development of cleaner diesel engines. CO and HC emissions in modern diesel engines are negligible compared to the equivalent gasoline engines, those emissions even could be met without catalyst. The largest amount of these emissions occurs during cold starts, so the only room for further progress is the fast heating of the exhaust system. Well-known NO_x control techniques such as HP-EGR remain in use, but because of their low efficiency, below 50%, in realistic conditions, only as ancillary systems. HP-EGR techniques has a very small impact on increasing consumption and CO_2 emissions, but due to the low NO_x conversion efficiency, it requires initial engine settings that significantly increase fuel consumption or CO_2 emissions by more than 10%. Further improvement of the LP EGR system is possible through innovative technical solutions, such as a separate compressor or part thereof, which would allow the exhaust gas to be separated from the clean air and accurately dosed with a faster response. Better solutions are LP EGR and various exhaust after treatment systems LNTs, SCRs or combinations of them under certain conditions have efficiencies near 100%. The advantage of LNT is its compact and simpler design, while SCR in real conditions shows slightly better results in terms of NO_x reduction (more than 90%) and fuel consumption, but with an additional reagent cost of about 2% compared to fuel costs. LNTs increase consumption and CO_2 emissions up to 10%, while the impact of SCR on them is negligible. Further development should be directed towards low-temperature applications which will be especially pronounced in start-stop mode in hybrid vehicles. Particulate emissions are successfully handled with fine DPF filters through a very high efficiency of above 95% so that the particulate emissions from the diesel engine become minor compared to the emissions caused by other vehicle components, wear of the brake pads, tires, etc. Further development is required in the field of regeneration and back pressure reduction, which leads to a consumption rise between 5 and 10%. In order to make engines truly (not apparently as in the past) cleaner and more environmentally friendly, it is necessary to get a wider picture of the engine with all systems and parameters that regulate the exhaust composition and also to consider powertrain requirements as well as applicable standards. Particular attention should be put on the diagnostics of each component during exploitation. The malfunction of components will have a far more pronounced effect on the harmful emission leakage than in the past. Increasing the complexity of modern exhaust systems with a more systematic approach to powertrain design and emission control management will enable it to meet stringent emission regulations and make the diesel engine cleaner and nearly zero-emission powertrain in terms of harmful emissions, as internal combustion engines is and will be the main power for marine and heavy duty applications.

Declaration of competing interest

The authors declare that they have no known competing financial interests or personal relationships that could have appeared to influence the work reported in this paper.

CRediT authorship contribution statement

Ante Kozina: Conceptualization, Data curation, Formal analysis, Investigation, Methodology, Validation, Visualization, Writing - original draft, Writing - review & editing. **Gojmir Radica:** Project administration, Conceptualization, Resources, Investigation, Methodology, Validation, Visualization, Writing - original draft, Writing - review & editing. **Sandro Nižetić:** Supervision, Methodology, Validation, Visualization, Writing - original draft, Writing - review & editing.

References

Web source. air-quality.org.uk/26.php. Accessed, October 24, 2019.

Amon, B., Keefe, G., 2001. On-road demonstration of NO_x emission control for heavy-duty diesel trucks using SINOx™ urea SCR technology — long-term experience and measurement results. SAE Technical Paper 2001-01-1931. https://doi.org/10.4271/2001-01-1931.

Asprion, J., Chinellato, O., Guzzellat, L., 2014. Optimal control of diesel engines: numerical methods, applications, and experimental validation. Article ID 286538. https://doi.org/10.1155/2014/286538.

Bhandarkar, S., 2013. Vehicular pollution, their effect on human health and mitigation measures. Veh. Eng. (VE) 1 (2).

Brand, C., 2016. Beyond 'Dieselgate': implications of unaccounted and future air pollutant emissions and energy use for cars in the United Kingdom. Energy Pol. 97, 1—12. https://doi.org/10.1016/j.enpol.2016.06.036.

Busca, G., Lietti, l., Ramis, G., Berti, F., 1998. Chemical and mechanistic aspects of the selective catalytic reduction of NO_x by ammonia over oxide catalytic : a review. Appl. Catal. B Environ. 18, 1—36.

Chen, Y., Borken-Kleefeld, J., 2014. Real-driving emissions from cars and light commercial vehicles e Results from 13 years remote sensing at Zurich/CH. Atmos. Environ. 88, 157—164. https://doi.org/10.1016/j.atmosenv.2014.01.040.

Cheng, S., Zhang, Z., Peng, P., Yang, Z., Lu, F., 2019. Spatiotemporal evolution pattern detection for heavy-duty diesel truck emissions using trajectory mining: a case study of Tianjin, China. J. Clean. Prod. 244 https://doi.org/10.1016/j.jclepro.2019.118654.

Choi, J.S., Partridge, W.P., Daw, C.S., 2007. Sulfur impact on NO_x storage, oxygen storage, and ammonia breakthrough during cycle lean/rich operation of a commercial lean NO_x trap. Appl. Catal. B: Environ. 77, 145—156. Science Direct.

Díaz, S., Miller, J., Mock, P., Minjares, R., Anenberg, S., Meszler, D., 2017. Shifting Gears: the Effects of a Future Decline in Diesel Market Share on Tailpipe CO_2 and NO_x Emissions in Europe. The International Council on Clean Transportation.

DiGiulio, C.D., Pihl, J.A., Choi, J.-S., Parks, J.E., Lance, M.J., Toops, T.J., Amirisis, M.D., 2014. NH3 formation over a lean NO_x trap (LNT) system: effects of lean/rich cycle timing and temperature. Appl. Catal. B Environ. 147, 698—710.

Eichelbaum, M., Farrauto, R.J., Castaldi, M.J., 2010. The impact of urea on the performance of metal exchanged zeolitas for the selective catalytic reduction of NO_x. Appl. Catal. B Environ. 97, 90—97.

Gao, F., Kwak, J.H., Szanyi, J., Peden, C.H.F., 2013. Current Understanding of Cu-Exchanged Chabazite Molecular Sieve for Use as Commercial Diesel Engine DeNOx Catalysts, vol 56. Springer, Top in Catalyst, pp. 1441—1459. https://doi.org/10.1007/s11244-013-0145-8.

Ghodke, P.R., Suryavanshi, J.G., 2012. Review of advanced EGR and breathing systems for high performance and low emission HSDI diesel engine. Int. J. Mod. Eng. Res. (IJMER) 2 (5), 3138—3142. ISSN: 2249-6645.

Gorsmann, C., 2005. Catalytic coatings for active and passive diesel particulate filter regeneration. Monatshefte fur Chemie 136, 91—105. https://doi.org/10.1007/s00706-004-0261-z.

Grahn, M., 2013. Model-Based Diesel Engine Management System Optimization, Thesis for the Degree of Doctor of Philosophy. Department of Signals and Systems Chalmers University of Technology. ISBN 978-91-7385-909-7.

Garrett T. K., Newton K., Steels W., 2009. Emissions control.Crolla D. A. (eds), Automotive Engineering Powertrain Chassis System and Vehicle Body, (Chapter 3).1. 53-73.

Web source. greencarcongress.com/2011/04/dci130-20110414.html. Accessed, October 28, 2019.

Guan, B., Zhan, R., Lin, H., Huang, Z., 2015. Review of the state-of-the-art of exhaust particulate filter technology in internal combustion engines. J. Environ. Manag. 154, 225—258. https://doi.org/10.1016/j.jenvman.2015.02.027.

Hooftman, N., Messagie, M., Mierloi, V.J., Coosemans, T., 2018. A review of the European passenger car regulations — real driving emissions vs local air quality. Renew. Sustain. Energy Rev. 86, 1—21.

Inekwe, G., Ajav, E.A., 2017. An investigation into the exhaust emissions from tractors operating under different field conditions. In: Proceeding of 18 International Conference and 38 Annual General Meetings of the Nigerian Institution of Agricultural Engineers (NIAE) (Umudike, Nigeria).

Johnson, T., 2008. Diesel engine emissions and their control, corning environmental technologies. Platin. Met. Rev.. 52, 23–37. https://doi.org/10.1595/147106708X248750.

Johnson, T.V., 2008. Diesel Emission Control in Review. SAE International, World Congress Detroit, Michigan. April 14-17.

Kerbachi, R., Chikhi, S., Boughedaoui, M., 2017. Development of real exhaust emission from passenger cars I Algeria by using on-board measurement. Energy Procedia 136, 388–393.

Koebel, M., Elsener, M., Kloemann, M., 2000. Urea-SCR : a promising technique to reduce NO_x emissions from automotive diesel engines. Catal. Today 59, 335–345.

Kumaravel, K., Saravanan, G.G., Premanand, B., 2014. Experimental studies on the Comparison of static fuel injection characteristics of fuel injectors used in GDI engine. Int. J. Adv. Sci. Tech. Res. 1 (4) https://doi.org/10.1016/j.jclepro.2019.118128.

Kumaravel, S.T., Murugesan, A., Vijayakumar, C., Thenmozhi, M., 2019. Enhancing the fuel properties of tyre oil diesel blends by doping nano additives for green environments. J. Clean. Prod. 244 https://doi.org/10.1016/j.jclepro.2019.118128.

Kwak, J.H., Tonkyn, R.G., Kim, D.H., Szany, J., Peden, C.H.F., 2010. Excellent activity and selectivity of Cu-SSZ-13 in the selective catalytic reduction of NO_x with NH3. J. Catal. 275, 187–190.

Lietti, L., Nova, I., Pio, Forzatti, 2008. Role of ammonia in the reduction by hydrogen of NO_x stored over Pt-Ba/AL2 O3 lean NO_x trap catalysts. J. Catal. 257, 270–282.

Majewski, W.A., 2005. Diesel Filter Regeneration. DieselNet. https://dieselnet.com/tech/dpf_regen.php. (Accessed 28 October 2019).

Majewski, W.A., 2015. Diesel Filter Systems. DieselNet. https://dieselnet.com/tech/dpf_sys.php. (Accessed 28 October 2019).

Majewski, W.A., 2019. Exhaust Particulate Matter. DieselNet. https://dieselnet.com/tech/dpm.php. (Accessed 28 October 2019).

Maunula, T., 2014. Combination of LNT and SCR for NO_x reduction in passenger car applications. Combust. Engines 157 (2), 60–67. ISSN 2300-9896.

Maunula, T., Matilainen, P., Louhelainen, M., Juvonen, P., Kinnunen, T., 2007. Catalyzed Particulate Filters for Mobile Diesel Applications. SAE International Fuels & Emissions Conference Cape Town. South Africa January 23-25, 2007, ISSN 0148-7191.

Meloni, R., Naso, V., 2013. An insight into the effect of advanced injection strategies on pollutant emissions of a heavy-duty diesel engine. Energies- Energies 6, 4331–4351. https://doi.org/10.3390/en6094331.

Mikulic, I., Zhan, R., Eakle, S., 2010. Dependence of fuel consumption on engine backpressure generated by a DPF. SAE Int. https://doi.org/10.4271/2010-01-0535.

Miller, A., 2015. SCR and Advanced Ammonia Slip Catalyst. Johnson Matthey R&D.

Mollenhauer, K., Tschoeke, H. (Eds.), 2010, 4. Springer-Verlag Berlin Heidelberg, Part. https://doi.org/10.1007/978-3-540-89083-6.

Moraal, P.E., Yacoub, Y., Christen, U., Carberry, B., 2004. Diesel particulate filter regeneration: control or calibration?. In: IFAC Proceedings, 37, pp. 349–353. https://doi.org/10.1016/S1474-6670(17)30368-3.

Nabi, M.N., Rahman, S.M.A., Bodisco, T.A., Rasul, M.G., Ritovski, Z.D., Brown, R.J., 2019. Assessment of the use of a novel series of oxygenated fuels for a turbocharged diesel engine. J. Clean. Prod. 217, 549–558. https://doi.org/10.1016/j.jclepro.2019.01.249.

Nesbit, M., Fergusson, M., Colsa, A., Ohlendorf, J., Hayes, C., Paquel, K., Schweitzer, J-p., 2016. Comparative Study on the Differences between the Eu and Us Legislation on Emissions in the Automotive Sector. Policy Department A: Economic and Scientific Policy. Web source. europarl.europa.eu/supporting-analyses.

Nižetić, S., Djilali, N., Papadopoulos, A., Rodrigues, J.J.P.C., 2019. Smart technologies for promotion of energy efficiency, utilization of sustainable resources and waste management. J. Clean. Prod. 231, 565–591.

O'Driscol, R., Stettler, M., Molden, N., Oxley, T., Apsimon, H.M., 2018. Real world CO_2 and NO_x emissions from 149 Euro 5 and 6 diesel, gasoline and hybrid passenger cars. Sci. Total Environ. 621, 282–290.

Pardiwala, J.M., Patel, F., Patel, S., 2011. Review Paper on Catalytic Converter for Automotive Exhaust Emission. Institute of technology, Nirma university, Ahmedabad.

Park, Y., Bae, C., 2014. Experimental study on the effects of high/low pressure EGR proportion in a passenger car diesel engine. Appl. Energy 133, 308–316.

Pereda-Ayo, B., Gonzalez-Velasco, J.R., 2013. NO_x Storage and Reduction for Diesel Engine Exhaust Aftertreatment. InTech. https://doi.org/10.5772/55729.

Perin, Marcio, Okoniewski, Thiago, 2013. SAE tehnical paper series. https://doi.org/10.4271/2013-36-0402.

Pouresmaeili, M.A., Aghayan, I., Taghizadeh, S.A., 2018. Development of Mashhad driving cycle for passenger car to model vehicle exhaust emissions calibrated using on-board measurements. Sustain. Cities Soc. 36, 12–20. https://doi.org/10.1016/j.scs.2017.09.034.

Qi, G., Yang, R.T., Chang, R., 2003. Low-temperature SCR of NO with NH3 over USY-supported manganese oxide-based catalysts. Catal. Lett. 87, 67–71.

Quan-shun, Y., Jian-wei, T., Yun-shan, G., Li-jun, H., Zi-hang, P., 2016. Application of diesel particulate filter on in-use on-road vehicles. Energy Procedia 105, 1730–1736. https://doi.org/10.1016/j.egypro.2017.03.496.

Raju, T.B., Hithaish, D., 2014. International journal of research in aeronautical and mechanical engineering. Int. J. Res. Aeronaut. Mech. Eng. 2, 224–231.

Ramírez, R., Gutiérrez, A.S., Eras, J.J.C., Valencia, K., Forero, J.D., 2019. Evaluation of the energy recovery potential of thermoelectric generators in diesel engines. J. Clean. Prod. 241 https://doi.org/10.1016/j.jclepro.2019.118412.

Reifarth, S., 2010. EGR-systems for Diesel Engines. KTH Industrial Engineering and Management. ISSN 1400-1179, ISRN/KTH/MMK/R-10/01-SE.

Resitoglu, I.A., Altinisik, K., Keskin, A., 2015. The Pollutant Emissions from Diesel-Engine Vehicles and Exhaust Aftertreatment Systems, vol 17. Springer, Clean Technologies and Environmental Policy, pp. 15–27, 10.107/s.10098-014-0793-9.

Rudrabhate, S.D., Chaitanya, S.V., 2017. Comparison between EGR & SCR technologies. In: International Conference on Ideas, Impact and Innovation in Mechanical Engineering, 5, pp. 856–861.

Santos, G., 2017. Road transport and CO_2 emissions : what are the challenges? Transport Pol. 59, 71–74.

Sillman, S., 1999. The relation between ozone, NO_x and hydrocarbons in urban and polluted rural environments, Pergamon. Atmos. Environ. 33, 1821–1845.

Sinzenich, H., Wehler, K., Muller, R., 2011. Exhaust Aftertreatment for Reducing Nitrogen Oxide Emissions. MTU. Web source. tougher-whatever-the-conditions.com/fileadmin/fm-dam/mtu-bauma/MTU_White_Paper_SCR_EN.pdf.

Sorathia, H.S., Rahhod, P.P., Sorathiya, A.S., 2012. Effect of exhaust gas recirculation (EGR) on NO_x emission from C.I. engines, Technical journals. IJAERS 1, 223–227.

Srivastava, D.K., Agarwal, A.K., 2008. Particulate matter emissions from single cylinder diesel engine : effect of engine load on size and number distribution. SAE Int. 2008.

Stamatellou, A.-M., Stamatelos, A., 2017. Overview of Diesel particulate filter systems sizing approaches. Appl. Therm. Eng. 121, 537–546.

TeachEngineering. Hands on activity: combustion and air quality. Web source. teachengineering.org/activities/view/cub_airquality_lesson01_activity2. Accessed, October 28, 2019.

Web source. emitec.com/en/technology/product-applications/e-scrr, 2018. Vitesco Technologies Emitec. Accessed, October 28, 2019.

Wenming, C., Xianghn, L., Xing, Y., 2017. Influence of exhaust gas recirculation on low-load diesel engine performance. Wuhan Univ. J. Nat. Sci. 22, 443–448. https://doi.org/10.1007/s11859-017-1270-1.

Wittka, T., Holderbaum, B., Dittmann, P., Pischinger, S., 2015. Experimental investigation of combined LNT + SCR diesel exhaust aftertreatment. Emiss. Control Sci. Technol. 1, 167–182. https://doi.org/10.1007/s40825-015-0012-0. Springer.

Yang, L., Franco, V., Campestrini, A., German, J., Mock, P., 2015. NO_x Control Tehnologies for Euro 6 Diesel Passenger Cars. ICCT.

SAE Technical paper series Zhan, R., Huang, Y., Khair, M., 2006. Methodologies to Control DPF Uncontrolled Regenerations. 2006 SAE World Congress Detroit, Michigan. April 3-6.

Zhang, Y., Lou, D., Hu, Z., Tan, P., 2019. Particle number, size distribution, carbons, polycyclic aromatic hydrocarbons and inorganic ions of exhaust particles from a diesel bus fueled with biodiesel blends. J. Clean. Prod. 225, 627–636. https://doi.org/10.1016/j.jclepro.2019.03.344.

Zheng, Y., Liu, Y., Harold, M.P., Luss, D., 2014. LNT-SCR dual-layer catalysts optimized for lean NO_x reduction by H2 and CO. Appl. Catal. B Environ. 148–149, 311–321.

PRILOG C

Naslov rada: Emission Analysis of Diesel Vehicles in Circumstances of Emission Regulation System Failure: A Case Study

Autori: Ante Kozina, Gojmir Radica, Sandro Nižetić

Sažetak: Despite the development of other propulsion systems, the internal combustion engines will continue to be an essential element of vehicle propulsion on the road, as the sole source of propulsion or in the hybrid drives. The main challenge for the regulatory bodies is to find suitable strategies to ensure the lowest possible impact on the environment, for new and in use vehicles. This research gives an insight into the issue related to the disproportion of exhaust emissions of diesel-powered vehicles under the conditions of real, in use, vehicle operation with respect to the approved values. Emissions measurements were performed on 6 different passenger vehicles homologated according to Euro emission standards, with correct and faulty emission control systems. The results obtained show significant increases in defective vehicle's NO_X emissions from 58.2% for Euro 5 vehicles to 78.2% for Euro 4 vehicles and increases of 86% and 227% respectively, compared to the approved values with Conformity Factor 2.1, CO emissions are increased in the fault case from 197% for Euro3 to 780% for Euro 5. A guideline is given for the emission control system with respect to its accuracy. The brief analysis of the hybrid powertrain was also elaborated as a future replacement for conventional ICE units, contributing greatly to a cleaner environment. The proposed novel hybrid energy management strategy which included only regenerative braking, has given a promising result; NO_X emissions are reduced by 45%, consumption and CO_2 emissions by 44% and CO emissions by 31%.

Emission Analysis of Diesel Vehicles in Circumstances of Emission Regulation System Failure: A Case Study

Ante Kozina
Department for Thermal Machines,
University of Split, FESB,
Rudjera Boskovica 32,
Split 21000, Croatia
e-mail: akozina@mechtron.hr

Gojmir Radica[1]
Department for Thermal Machines,
University of Split, FESB,
Rudjera Boskovica 32,
Split 21000, Croatia
e-mail: goradica@fesb.hr

Sandro Nižetić
Laboratory for Thermodynamics and Energy
Efficiency,
University of Split, FESB,
Rudjera Boskovica 32,
Split 21000, Croatia
e-mail: snizetic@fesb.hr

Despite the development of other propulsion systems, the internal combustion engines will continue to be an essential element of vehicle propulsion on the road, as the sole source of propulsion or in the hybrid drives. The main challenge for the regulatory bodies is to find suitable strategies to ensure the lowest possible impact on the environment, for new and in use vehicles. This research gives an insight into the issue related to the disproportion of exhaust emissions of diesel-powered vehicles under the conditions of real, in use, vehicle operation with respect to the approved values. Emissions measurements were performed on six different passenger vehicles homologated according to Euro emission standards, with correct and faulty emission control systems. The results obtained show significant increases in defective vehicle's NO_x emissions from 58.2% for Euro 5 vehicles to 78.2% for Euro 4 vehicles and increases of 86% and 227%, respectively, compared to the approved values with Conformity Factor 2.1, CO emissions are increased in the fault case from 197% for Euro 3 to 780% for Euro 5. A guideline is given for the emission control system with respect to its accuracy. The brief analysis of the hybrid powertrain was also elaborated as a future replacement for conventional ICE units, contributing greatly to a cleaner environment. The proposed novel hybrid energy management strategy which included only regenerative braking has given a promising result; NO_x emissions are reduced by 45%, consumption and CO_2 emissions by 44% and CO emissions by 31%.
[DOI: 10.1115/1.4053070]

Keywords: diesel vehicle emissions, impact of faulty antipollution components, energy systems analysis, hybrid propulsion assessment

1 Introduction

The constant growth of transport needs for more efficient powertrains is setting two basic goals for manufacturers: to increase efficiency as the main user requirement and to reduce emissions as an environmental sustainability requirement. To achieve these goals, it is necessary to find a compromise that includes a collaboration of different technical professions and addressing the issues of limited energy sources as well as invention of the alternative energy concepts such as proposed in Ref. [1]. The efficiency of energy conversion systems and the need for a smart systems approach was discussed in Ref. [2], indicating an importance of the cleaner aspect in technological developments. Despite the European Union's efforts to reduce emissions, as requested in Directive 2008/50/EC, according to reports in Ref. [3], no significant progress has been made, from which it can be concluded that the plans are not ambitious enough or there is a discrepancy between the legal and actual emission levels. In urban area, the most influential factors on air quality is undoubtedly traffic, and researchers across the world invest a lot of efforts to find the way how to reduce pollutant from vehicles [4]. According to the EC Statistical pocketbook (2016), cars and trucks are responsible for 23% of CO_2 emissions, while 88% of that is accounted for by passenger and light delivery vehicles. To comply with increasingly imposed environmental regulations and at the same time increase efficiency, IC engines are becoming more and more complex and equipped with more demanding control systems. The electronic control systems enables wide range of engine operating options over a wide load and speed range, providing additional opportunities to reduce fuel consumption and exhaust emissions. Previous leads to higher production and maintenance costs and offers great possibilities for manipulating exhaust data. To avoid tampering, additional methods of emission measurement are needed for homologation of new cars and monitoring the correctness of all systems during the operation [5]. For the above reasons, there is a discrepancy between the permitted emissions for which vehicles are homologated and the actual emissions that occur during vehicle exploitation [6]. The Dieselgate affair was the trigger to start investigating longstanding suspicions of a discrepancy between actual and officially measured (homologation) emissions [7]. This leads to the rejection of the old and outdated NEDC (New European) Driving Cycle [8] and the introduction of a new, much more reliable standard WLTP cycle (World-harmonized Light-duty Test Procedure), which requires emissions measurements according to Real Driving Emissions (RDE). This is now established as a standard process in homologation [3]. According to the latest study by Ref. [9], the ADAC test was performed on 13 diesel vehicles, with most of European passenger vehicle manufacturers represented. All of them complied with the current homologation standard Euro 6d temp, in force from 1 September 2019. Interesting fact coming from this test is that petrol engine emissions are now higher than those from diesel engines. It can be noted that harmful emissions of diesel engines can be effectively neutralized, of course at an appropriate cost [10].

The actions for further reduction of CO_2 emissions by the conventional route are very limited, while very promising results are given by the hybrid powertrains of Ref. [11], and in particular, the use of CO_2 neutral or bio-diesel fuels [12]. According to

---

Ref. [13], Reactivity Controlled Compression Ignition (RCCI) in combination with the use of appropriate ratios of mineral diesel and methanol significantly reduces PM and NO_x and increases Brake Thermal Efficiency (BTE), and Ref. [14] performs experiments also with RCCI and shows that it is possible to meet the EURO 6 norm in a wide range of loads without aftertreatment systems with increasing thermal efficiency, while Ref. [15] shows that port injection of E100 or E85 reduces NO_x emissions but achieves lower thermal efficiency compared to standard SI engine. There are numerous authors dealing with emissions from new, i.e., fully correct, cars, and light commercial vehicles [16], and other passenger vehicles [17], but not with vehicles from real-world operating conditions.

The question remains what is the situation with vehicle emissions in operating conditions and in particular after the projected lifetime of the exhaust reduction and aftertreatment system. In this part, American and European approaches to homologation differ the most, i.e., mainly in the in-use testing. EPA is authorized to take any vehicle out of service and test it within the standard vehicle life of 241,000 km in the US. The standard testing is performed at 16,000 and 80,000 km on an actual vehicle, while European law prescribes the duration of emission limitation components 160,000 km and proving is done with a test engine on a test bench. In the US, the EPA can impose a fine on the manufacturer for the non-compliant vehicle, while in Europe, the responsibility is transferred to the Member State where the vehicle is approved, i.e., there is no uniform penalty system as indicated in the work [18]. Part of the responsibility for emission controlling lies with the inspection bodies during periodical technical inspection, which are required to carry out a visual inspection, and opacity test for diesel vehicles or a check of the volume content of carbon monoxide, total hydrocarbons and the lambda ratio for gasoline engines. Mentioned type of the inspection is adequate for vehicle exploitation inside of the warranty period, as all defective parts are usually replaced with OEM components similar to those of the initial installation. The only exception is in the cases where manufacturers "allow" modifications to the driver software without losing warranty on the drive assembly.

Problems with exhaust emissions occur after a failure of the emission control system that occurs outside the warranty period, and the reason is that more expensive original parts. Namely, the DPF system, EGR system, and catalytic converters such as DOC (Diesel Catalytic Converter), SCR system (Selective Catalytic Reduction), LNT (Lean NO_x Trap), etc. are replaced by spare parts of the questionable quality. Moreover, the performance or cheaper "permanent" solutions are resorted to so that the components are completely discarded, or their function is extinguished. Mentioned problems are the most pronounced in developing countries where the number of newly registered used vehicles exceeds the number of newly registered new vehicles. As vehicles covered by the Dieselgate affair do not meet the applicable standards on exhaust emissions or NO_x from the time of their production, i.e., do not meet the type-approval according to the NEDC cycle, they should not be used in public transport for instance. As a possible solution to the problem, the manufacturer has offered an update of the software that manages the engine, the purpose of which is to reduce NO_x emissions to the legally permitted level. This approach generates two new problems, the first is that there is no state body that monitors the number of vehicles that have not updated the disputed software, and thus, there is no statutory penalty for such vehicles. The second issue is the negative impact of the new software on the vehicle performance and the durability of components, especially of those components that affect emissions. The modes of action and effects of individual components or systems for reducing emissions are known, and they have been discussed in the literature mostly under the laboratory conditions [19]. Laboratory experiments on the effects of cooled EGR [20] and high/low pressure EGR proportion in a passenger car diesel engine have been investigated and a review of EGR systems for high performance and low emission diesel engine was provided

[21,22]. The disadvantages of previous research is that it has not been conducted in real conditions of exploitation. To assess the actual effects, it is necessary to perform measurements on the vehicle under normal driving conditions during the entire lifecycle period. On road measurements of diesel vehicle emissions by remote sensing on a large sample showed that the dirtiest 10% vehicles emitted much higher levels of harmful emissions than the rest 90% vehicles [23].

The main objective of this research was to define the real effects of the absence or use of inadequate components affecting exhaust emissions under real driving conditions. The paper is a continuation of research [24], whose upgraded measurements were used as a source of some of the input data. The novel solution approach for controlling the above described components was proposed to reduce total harmful emissions (CO, HC, NO_x) from diesel vehicles. The main goal of the control proposal is to isolate a small share of vehicles with defective anti-pollution components during the standard periodical technical inspection, which have a majority share in certain emissions. In addition, novel method which will simplify the assessment of hybrid powertrain performance and emissions has been introduced. Hybrid powertrains in addition to electric ones represent a future replacement for existing propulsion units.

2 Experiment

2.1 Route and Tested Vehicles. The emission measurements were carried out on six diesel-powered passenger cars approved for Euro 3, Euro 4, and Euro 5 emission norms. One vehicle was equipped with the correct emission reduction systems (all antipollution components are within factory tolerances), the other vehicle was missing some of the relevant parts for emission reduction. As the main goal of the work is to compare vehicle emissions with correct and incorrect exhaust gas treatment systems, the tests were performed under similar conditions, in the late afternoon to avoid excessive traffic jams with outside temperature deviation of $\pm 5\,°C$ between comparable tests and relative humidity deviation of $\pm 15\%$ RH. All tests were started with a fully warmed engine. The vehicle performance characteristics are shown in Table 1. The tests were performed for all test vehicles on the defined route as shown in Fig. 1. The specific route was chosen to impose and secure quite different driving conditions, including urban, interurban, and highway driving. Different driving styles were applied, from low power driving to maximum power.

2.2 Measurement Methods. Two methods have been approved by the European Commission to estimate the real-world emissions as part of the September 2019 type-approval procedure, namely Power Binning and Moving Average Window [3]. Both methods have their advantages and disadvantages depending on the test conditions. CO_2 and NO_x values were compared for both methods which deviate for vehicles powered by CI engines by 13% and 3%, respectively [25].

The Power Binning method was chosen with certain deviations and related to the measuring equipment, due to the use of data to determine the possibility of hybrid powertrain or the potential of regenerative braking and displacement of the working area of the IC drive engine. The determination of emissions by this method is based on an estimate obtained by normalizing the distribution of the standard power frequency, and which implies that measurement and recording are done in real road driving circumstances under normal conditions, i.e., loads and driving modes. The measurement includes driving on the open road, highway, and city driving in approximately equal proportions. From all relevant data, three-second mean values are calculated to reduce the effect of timing between mass flow and output power on the drive wheels according to Eqs. (1)–(3). The k is the step of the moving values and i is the time-step from the current test data.

Table 1 Characteristics of the tested cars

No	Year of production	Total distance traveled	Emission standard	Engine displacement	Engine power HP/kW	Antipollution system	Fuel type	Mass
1	2004	391000	Euro3	1.9	115/77	DOC, EGR	D	1390
2	2004	236000	Euro3	1.9	115/77 170/125	No DOC, EGR off, Remap	D	1390
3	2005	171000	Euro4	1.9	150/110	DOC, EGR	D	1395
4	2005	171000	Euro4	1.9	150/110 200/147	No DOC, EGR off, Remap	D	1395
5	2010	293000	Euro5	2.0	170/125	DOC, EGR, DPF	D	1515
6	2010	293000	Euro5	2.0	170/125	No DOC, EGR off, no DPF	D	1515

$$m_{gas,3s,k} = \frac{\sum_{i=k}^{k+3} m_{gas,i}}{3} \qquad (1)$$

$$P_{w,3s,k} = \frac{\sum_{i=k}^{k+3} P_{w,i}}{3} \qquad (2)$$

$$v_{3s,k} = \frac{\sum_{i=k}^{k+3} v_i}{3} \qquad (3)$$

City driving means an average three-second speed of up to 60 km/h, extra-urban driving between 60 and 90 km/h, and highway driving means a speed above 90 km/h. The total driving time was between 90 and 120 min, the minimum distance for all types of driving, urban, suburban, and highway, was 16 km. Table 2 shows the power classes in the function of time share, to be valid for any personal and light commercial vehicle. Column $P_{c,norm}$ is denormalized by multiplying with P_{drive}, respectively,

$$P_{cj}[kW] = P_{c\ norm} \times P_{drive} \qquad (4)$$

P_{drive} is the actual power on the wheels at the reference speed, $v_{ref} = 70$ km/h and reference acceleration
$a_{ref} = 0.45$ m/s^2
TM is the calculated mass of the vehicle as follows,

$$P_{drive} = \frac{v_{ref}}{3,6} \times (f_0 + f_1 \times v_{ref} + f_2 \times v_{ref}^2 + TM_{NEDC} \times a_{ref} \times 0.001) \qquad (5)$$

The drag coefficients of the vehicle f_0, f_1, and f_2 from Eq. (6) were determined by least-squares regression analysis using the Coast Down test [26]. The measurement was performed on a flat road with the smallest possible height difference and the influence of wind, which are compensated by the repetition of free deceleration in both directions. The calculated mass of the vehicle TM is obtained by summing the mass of the empty vehicle, a number of persons, fuel, and equipment with the addition of 3% which
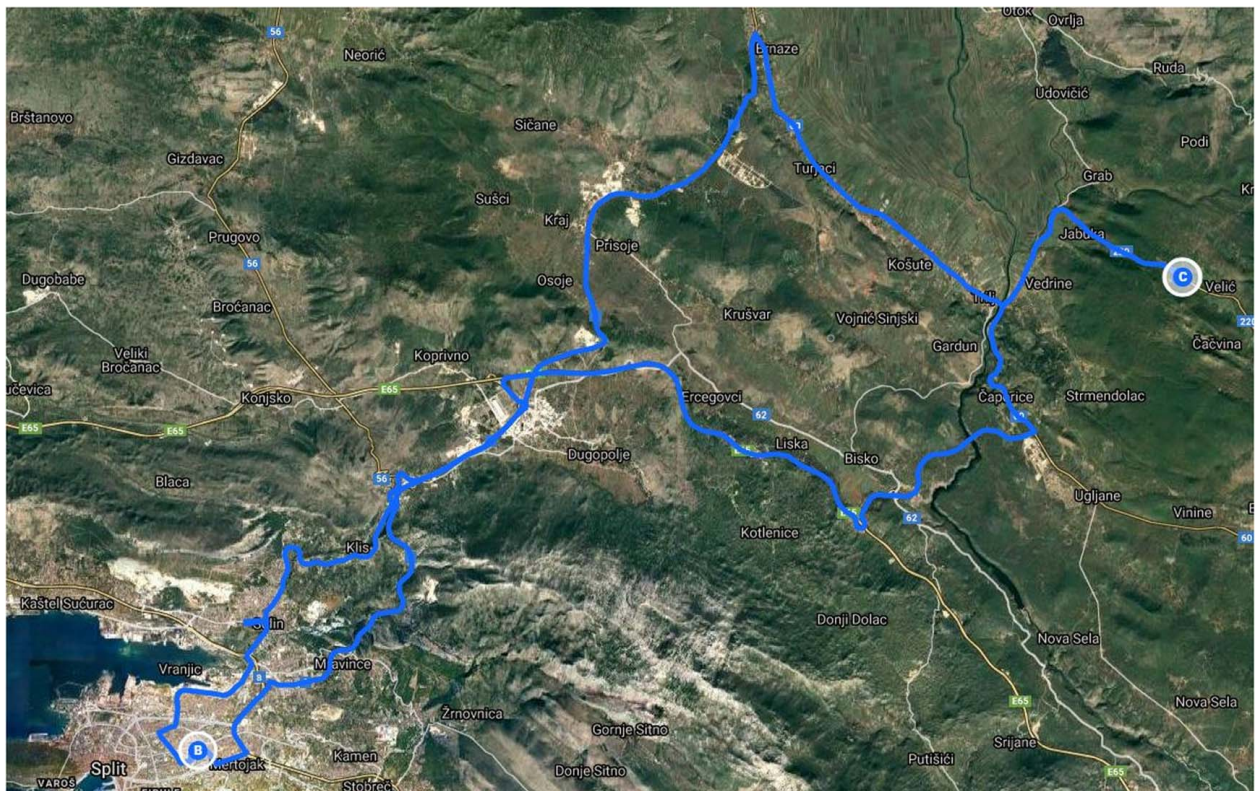

Fig. 1 Sketch of the road map of the selected test route, Google Maps (2020)

Table 2 Normalized standard power for driving (EU) 2016/427 (2016)

Power class no	$P_{c,norm,j}$ From >	$P_{c,norm,j}$ To <=	Total trip Time share, $t_{c,j}$
1		−0.1	18.5611%
2	−0.1	0.1	21.8580%
3	0.1	1	43.45%
4	1	1.9	13.2690%
5	1.9	2.8	2.3767%
6	2.8	3.7	0.4232%
7	3.7	4.6	0.0511%
8	4.6	5.5	0.0024%
9	5.5		0.0003%

represents the moment of inertia, respectively.

$$f_0 + f_1 \times v + f_2 \times v^2 = TM \frac{dv}{dt} \tag{6}$$

The highest power class considered in Table 1 is 90% of the declared maximum engine power of the vehicle. The time shares of all excluded classes are added to the highest remaining class. The average of the mean mass emission value classified in each power class on the drive wheels is calculated from the expression:

$$\bar{m}_{gas,j} = \frac{\sum_{all\ k\ in\ class_j} \times m_{gas,3s,k}}{counts_j} \tag{7}$$

$$\bar{v}_j = \frac{\sum_{all\ in\ class_j} \times v_{3s,k}}{counts_j} \tag{8}$$

The average values of each power class on the drive wheels are multiplied by the time fraction $t_{c,j}$ for each class in Table 1, and they were added to obtain a weighted average value for each parameter according to the following relations,

$$\bar{m}_{gas} = \sum_{j=1}^{9} m_{gas,j} \times t_{c,j} \tag{9}$$

$$\bar{v} = \sum_{j=1}^{9} m_j \times t_{c,j} \tag{10}$$

The aim was to obtain values related to the distance, i.e., the average amount of exhaust emissions per km traveled. This is obtained by dividing the mass flow of each gas at standard power frequencies with the average speed and standard power frequencies according to Eq. (11),

$$M_{w,gas,d} = 1000 \frac{\bar{m}_{gas} \times 3600}{\bar{v}} \tag{11}$$

A detailed description of the method of checking the dynamic conditions of Power binning in Commission Regulation (EU) 2016/427 (2016) [27].

2.3 Measuring Equipment. The following data has to be collected to determine the exhaust emission amount: wheels power, speed, exhaust gases mass flow and composition, distance, altitude, and time. To measure the composition of exhaust gases, an exhaust gas analyzer MRU Vario Plus was used. The measuring principle is based on the electrochemical effect for measuring O_2, NO, NO_2, and SO_2. For the measurement of CO and CO_2, an infrared spectrometry method was used. The analyzer is calibrated at an authorized service center earlier, and zeroing was performed before the measurement itself. The Pitot tube was used for velocity measurements and temperature measuring the probe Pt100 (Fig. 2). Calibration of the Pittot together with the measuring tube was performed in the laboratory for fluid mechanics. The power at the drive wheels was determined as the product of angular velocity and torque. Torque was measured by attaching strain gauges to the drive shaft via the dual-channel wireless transmitter Lord Microstrain's SGLink. The other parameters such as altitude, distance, and speed were acquired and recorded via On-Board Diagnostic (OBD) communication directly from the ECU of the vehicle (Fig. 2). Since the geometrical characteristics of the drive shaft on which the strain gauges are mounted were not known, the torque measurement system was calibrated. The velocity was acquired by the drive wheel and a GPS signal was used for correction. All measuring instruments have been securely mounted on the vehicle to avoid any influence on the measurement results. It is also necessary to warm the vehicle engine to the operating temperature and to warm the analyzer from the main power supply. Measuring accuracy is shown in Table 3.

2.4 Measurements. First, the resistances were determined with free deceleration tests for each vehicle. After the free deceleration tests, an emission test is performed on the mentioned route. The emissions of nitrogen oxides NO and NO_2 (which together make up NO_x), carbon dioxide CO_2, carbon monoxide CO and emissions of sulfur oxide SO_2 were obtained. The data from the analyzer was coupled with the data received from GPS and OBD, and the wheel's torque data from the driveshaft. The complexity of processing the results obtained by measuring emissions was increased due to the need for time adjustment of volumes, flows, and temperatures from MRU devices due to the different response times of different sensors. The first measurements, which included THC emissions, showed

Fig. 2 Measuring equipment installed on the vehicle: Torque and power measurement device, gas analyzer, Pitot connection, and OBD connection

Table 3 Measuring accuracy

Measured component	Sensor	Measuring range	Accuracy
O_2	Electrochemical	0–21%	±2% absolute
CO	Electrochemical	0–10,000 ppm	±10 ppm or ±5% reading
NO	Electrochemical	0–500 ppm	±5 ppm or ±5% reading
NO_2	Electrochemical	0–1000 ppm	±5 ppm or ±5% reading
SO_2	Electrochemical	0–5000 ppm	±10 ppm or ±5% reading
H_2S	Electrochemical	0–500 ppm	±5 ppm or ±5% reading
H_2	Electrochemical	0–2%	±0,05% or ±5% reading
CO	NDIR	0–30,000 ppm	±40 ppm or ±5% reading
CO_2	NDIR	0–20%	±0,6% or ±5% reading
Flow	Pitot	1–100 m/s	±1 m/s
Pressure	Piezoresistive	±100 hPa	±0.03 mBar or ±5% reading
Exhaust out temperature	Thermocouple	0–650 °C	±1 °C or ±2% reading
Torque	Strain Gauge	±1000 Nm	±4%
Speed	GPS/OBD	0–255 km/h	±1%
Distance	GPS/OBD		±1%

that they do not differ significantly from CO emissions in terms of concentration, time of occurrence, and Euro norms, so due to the aforementioned low concentration of these gases in modern diesel engines, THC measurements were abandoned. High-quality diesel fuels with ultra-low sulfur content were used, so sulfur oxide emissions were not performed due to the negligible concentration.

3 Results and Discussion

3.1 Emission Analysis. A vehicle with the functional all antipollution components of exhaust emission system shows a considerable deviation of NO_x and CO_2 emissions with respect to the legally prescribed emissions. Within the permissible limits are CO emissions because the engine operates with a lean mixture, combustion is optimized by ECU unit and oxidation catalysts are fitted. A large discrepancy in NO_x emissions relative to permitted data is due to outdated NEDC standards [8]. It has already been mentioned that the preliminary measurements of SO_2 emissions have shown almost negligible values due to the high purity low sulfur fuels. The normalized NO_x, CO, CO_2 emissions, and fuel consumption are shown in Figs. 3–6. For each pollutant, there are two representations, one obtained according to the RDE power binning method, and the second diagram includes only recorded data, i.e., raw data which are obtained by dividing the total amount of emissions by the total distance traveled.

In Fig. 3, the measured NO_x emissions of vehicles with all regular antipollution components and vehicles with defective antipollution components are compared to the applicable Euro norm and then multiplied by the current valid Conformity factor 2.1. while Table 4 shows absolute values. It is apparent that despite the further NO_x reduction in newer emission standards, there has been no real reduction compared to the older standards, in fact, NO_x levels have increased under real driving conditions. The NO_x emissions only for the vehicles of Euro 3 standard are within the limit, and there are 53% for fully correct vehicles and 91% for defective vehicles of the prescribed limit multiplied by CF. When there are failures in the control systems of EGR or and DPF, the amounts of nitrogen oxides in the exhaust gasses increase significantly because the absence of recirculated exhaust gases raises the peak combustion temperatures [21], and the removal of DPF, to a lesser extent causes the absence of soot oxidation with NO [5]. The NO_x emissions for correct and defective Euro 4 vehicles are 5% and 86%, respectively, and for Euro 5 vehicles 107% and 227% higher than the prescribed limit multiplied by CF. The NO_x emissions reduction system is particularly important for newer vehicles, as higher cylinder temperatures and good cylinder scavenging favor the formation of high concentrations of nitrogen oxides. To reduce NO_x emissions, it is necessary to work with high concentrations of recirculated gasses in the cylinder.

The situation is much more favorable for the CO emissions regarding the vehicles with correct emission control systems or
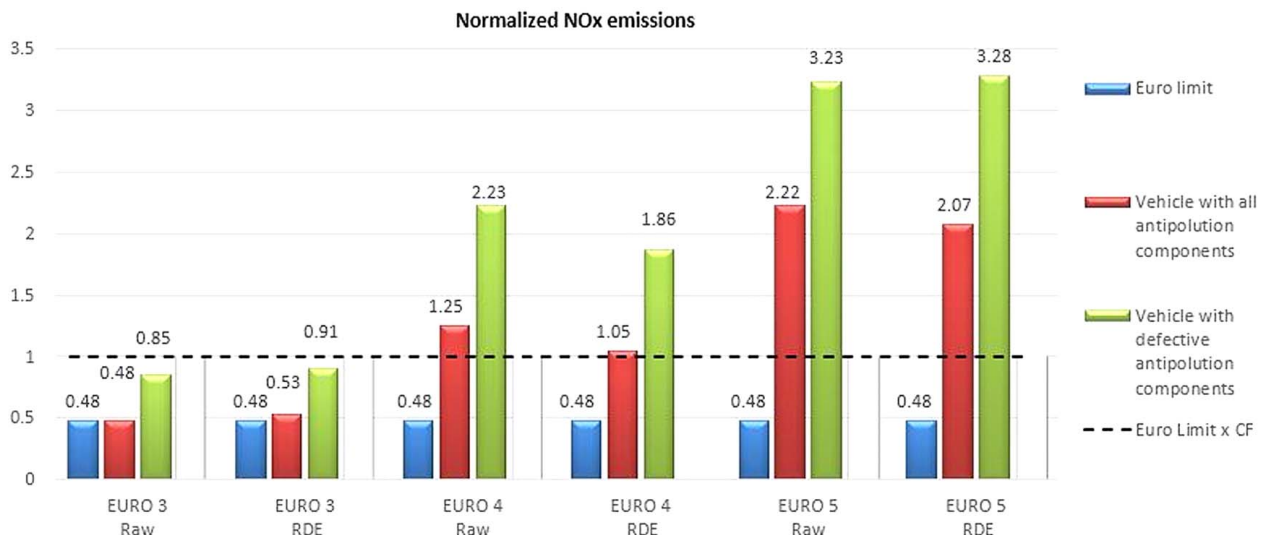

Fig. 3 NO$_x$ emission rate and comparison with corresponding norm statistically processed data according to power binning and raw unprocessed measurement data
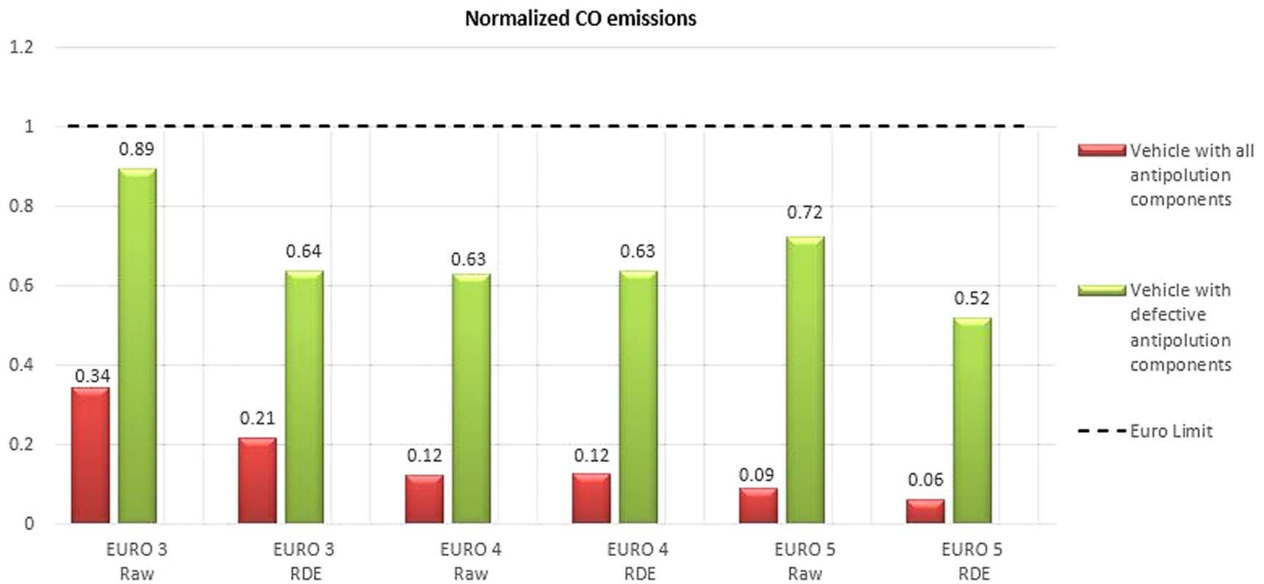
Fig. 4 CO emission rate and comparison with corresponding norm; statistically processed data according to power binning and raw unprocessed measurement data

even without an oxidation catalyst CO, they have emissions within the legal limits. Table 5 shows absolute values of CO emissions, and Fig. 4. shows normalized CO values with regard to euro limits, carbon monoxide increases three times for Euro 3, more than five times for Euro 4, and even 8.7 times for a Euro 5 vehicle in relation to the correct vehicle. It follows that the upper limits of CO emissions are not set too ambitiously, which should be considered when drafting the next Euro standard.

The declared CO_2 emissions, shown in Table 6 and Fig. 5, and fuel consumption, shown in Table 7 and Fig. 6, for older Euro 3 cars show only minimal deviations of nearly 5% higher, for euro 4 nearly 18% higher from the results obtained by measurements under the real driving conditions. For Euro 5 vehicles, this deviation is significant, more than 23% higher CO_2 emissions and consumption than is factory declared. The absence of an emission control system has only a small impact on fuel consumption and CO_2 emissions, and for all tested vehicles, it causes a slight decrease in

consumption or CO_2 emissions up to 3%. The reduction in CO_2 emissions is attributed to the reduction in backpressure in the absence of DPF filters and DOC catalysts [28,29], which is especially pronounced at low loads [30] to which a large share belongs. Measurements of emissions at constant speeds, i.e., constant loads, have shown that removal of the exhaust gas recirculation system even increases CO_2 and fuel consumption, by up to 10% at very low loads, only up to about 15% of maximum load, due to increased backpressure which increases gas flow through the exhaust system. At higher loads, mentioned effect exceeds the effect of lowering the combustion temperature by the EGR gasses in the cylinder, causing an increase in fuel consumption [22]. From 2020, the value of 95 g/km CO_2 is the basis for calculating the penalty for car manufacturing companies as shown as the limit in Fig. 6. The emission target of fleet-average CO_2 emission of 95 g/km has to be fully met by each manufacturer by 2021; otherwise, they would be penalized.
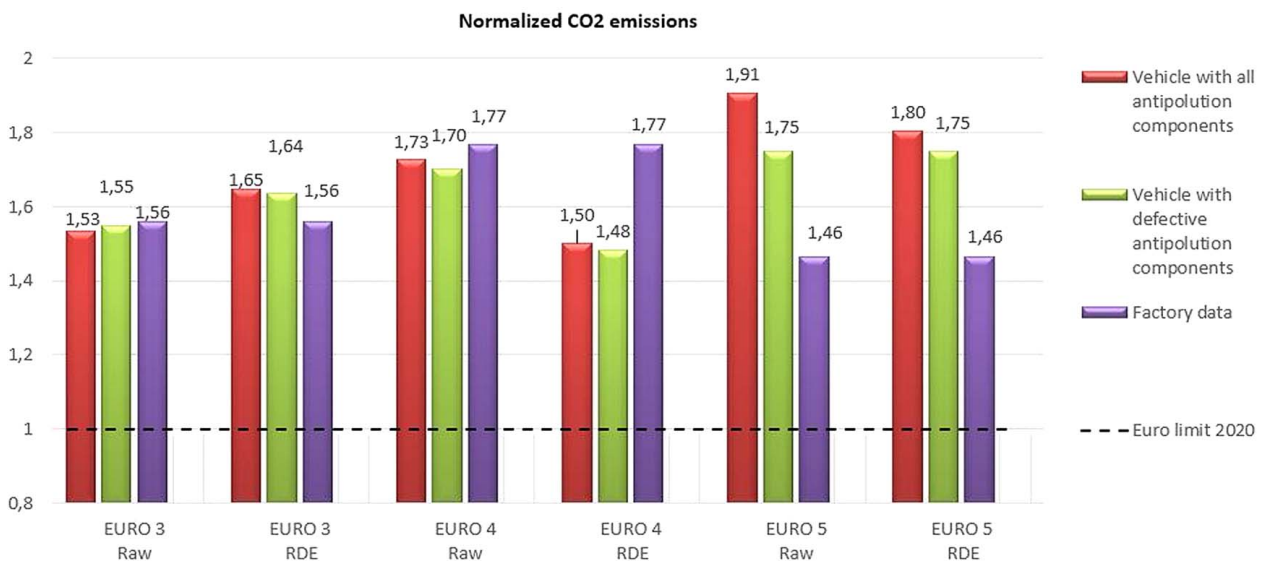

Fig. 5 CO_2 emission rate and comparison with corresponding norm and statistically processed data according to power binning and raw unprocessed measurement data
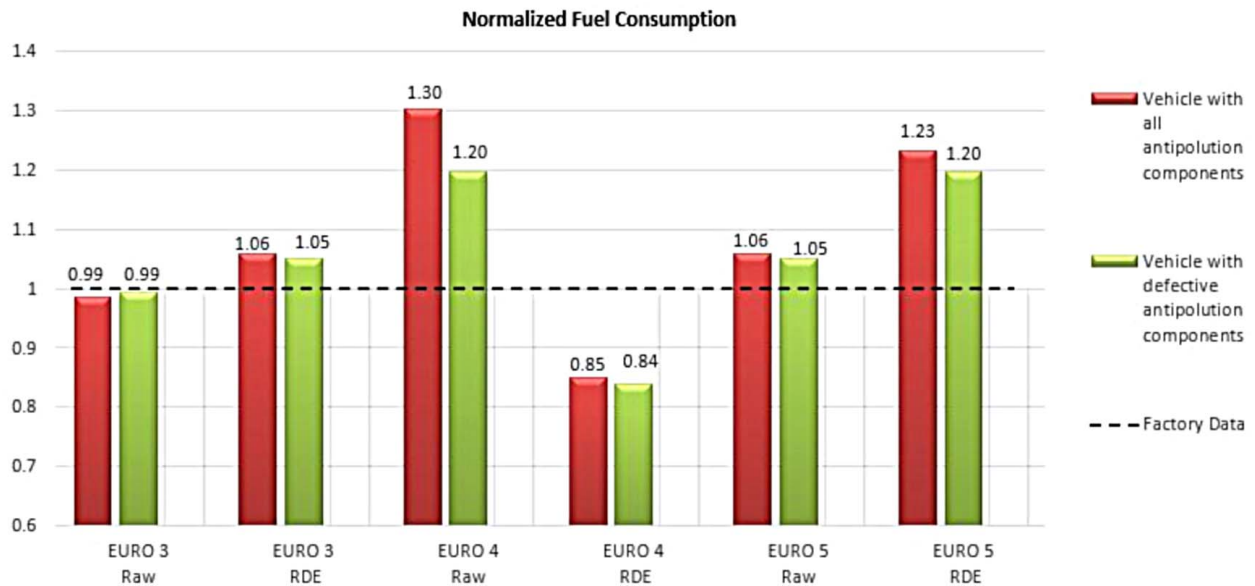
Fig. 6 Fuel consumption and comparison with declared data; statistically processed data according to power binning and; raw unprocessed measurement data

3.2 Antipollution Components Defect Detection. From the emissions analysis obtained, it can be concluded that the vehicles emit more than the legally permissible emissions, even with a proper emission control system. These deviations are expected due to the old homologation standard [8]. During operation, when a defective emission control system usually must be repaired with non-original spare parts or even some components are excluded, the situation worsens. The missing part cannot be noticed during the periodical technical inspection, so the solution is to perform additional measurements of the exhaust gas composition to avoid the previously mentioned case. The defective catalyst can be detected by a high concentration of HC or CO, where the values of CO during normal operation range from three to nine times higher emissions. Measuring exhaust emissions, especially while driving, is a very complex procedure and not practical to perform in a periodical vehicle inspection. In order to determine the deficiencies in the catalytic converters, it is not necessary to measure the number of exhaust emissions, i.e., it is sufficient to measure the concentrations of CO or HC gasses at a stationary vehicle. The bar graph in Fig. 8 shows the average carbon monoxide concentrations in the exhaust gasses under driving conditions and when the engine is idling. From Fig. 8, it can be seen that the increase in CO emission concentration is even more pronounced when the vehicle is idling than when it is driving, which allows more accurate detection of the catalytic converter failure. At idle, an average increase in CO emissions of 2.4 times for Euro 3, 75 times for Euro 4, and even 107 times for Euro 5 vehicles was found when the diesel oxidation

catalyst DOC failed. The reason for the higher efficiency of the catalytic converter, when idling compared to driving, is due to the fact that the engine produces a constant amount of carbon monoxide emissions when idling. During normal driving, there are significant variations in the concentrations emitted by the engine. These concentrations increase particularly during high power demands, i.e., heavy acceleration, so that catalytic converters cannot oxidize such a large amount of carbon monoxide in a short time due to oversaturation, regardless of the favorable operating temperature range. It should also be noted how important it is to check the exhaust gas temperature during the detection of catalytic converter malfunction at idle. If the test is performed with a cold engine, it may give a false negative result because the oxidation catalyst operates inefficiently at low temperatures and concentrations are increased by cold cylinder walls and cylinder heads [5]. The dependence of the concentration of carbon monoxide emissions in the exhaust gasses of the vehicle on the temperature of the DOC catalytic converter is shown in Fig. 7. The blue line represents the vehicle with Euro 3 standard, red Euro 4, and green Euro 5. For a valid measurement, it is necessary to maintain the DOC in the appropriate temperature range which can be achieved by elevated engine speed. For passenger vehicle engines, the speed should be kept above 3000 rpm for one to several minutes.

The proper EGR system in conjunction with the air–fuel ratio is shown in Fig. 8. The increase of the lambda air–fuel ratio was measured by 94% in Euro 3, 43% in Euro 4, and 51% in Euro 5 with defective EGR systems. Measuring the air–fuel ratio could be a solution to detect EGR system failure, as it is indicated by a

Table 4 NO_x emission rate, statistically processed data according to power binning and raw unprocessed measurement data

NO_x emissions (mg/km)	EURO 3		EURO 4		EURO 5	
	RAW	RDE	RAW	RDE	RAW	RDE
Euro limit	500		250		180	
Euro limit × CF	1050		525		378	
Vehicle with all antipollution components	502	552	656	549	841	784
Vehicle with defective antipollution components	889	954	1169	978	1221	1240

Table 5 CO emission rate, statistically processed data according to power binning and raw unprocessed measurement data

CO emissions (mg/km)	EURO 3		EURO 4		EURO 5	
	RAW	RDE	RAW	RDE	RAW	RDE
Euro limit	660		500		500	
Vehicle with all antipollution components	225	141	61	62	44	29
Vehicle with defective antipollution components	590	419	314	317	361	258

Table 6 CO₂ emission rate, statistically processed data according to power binning and raw unprocessed measurement data

CO₂ emissions (g/km)	EURO 3		EURO 4		EURO 5	
	RAW	RDE	RAW	RDE	RAW	RDE
Euro limit 2020	95		95		95	
Factory data	148		168		139	
Vehicle with all antipollution components	146	157	164	143	181	171
Vehicle with defective antipollution components	147	156	162	141	166	166

Table 7 Fuel consumption, statistically processed data according to power binning and raw unprocessed measurement data

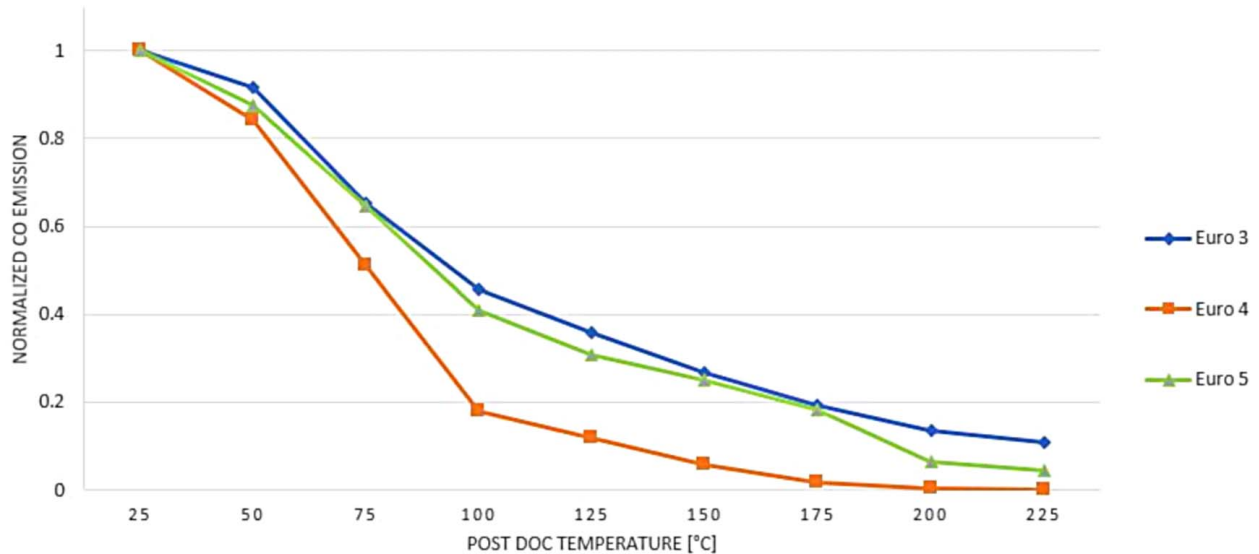| Fuel consumption (l/100 km)	EURO 3		EURO 4		EURO 5	
	RAW	RDE	RAW	RDE	RAW	RDE
Factory data	5.61		6.36		5.27	
vehicle with all antipollution components	5.52	5.93	6.21	5.40	6.86	6.49
Vehicle with defective antipollution components	5.57	5.89	6.13	5.33	6.30	6.30

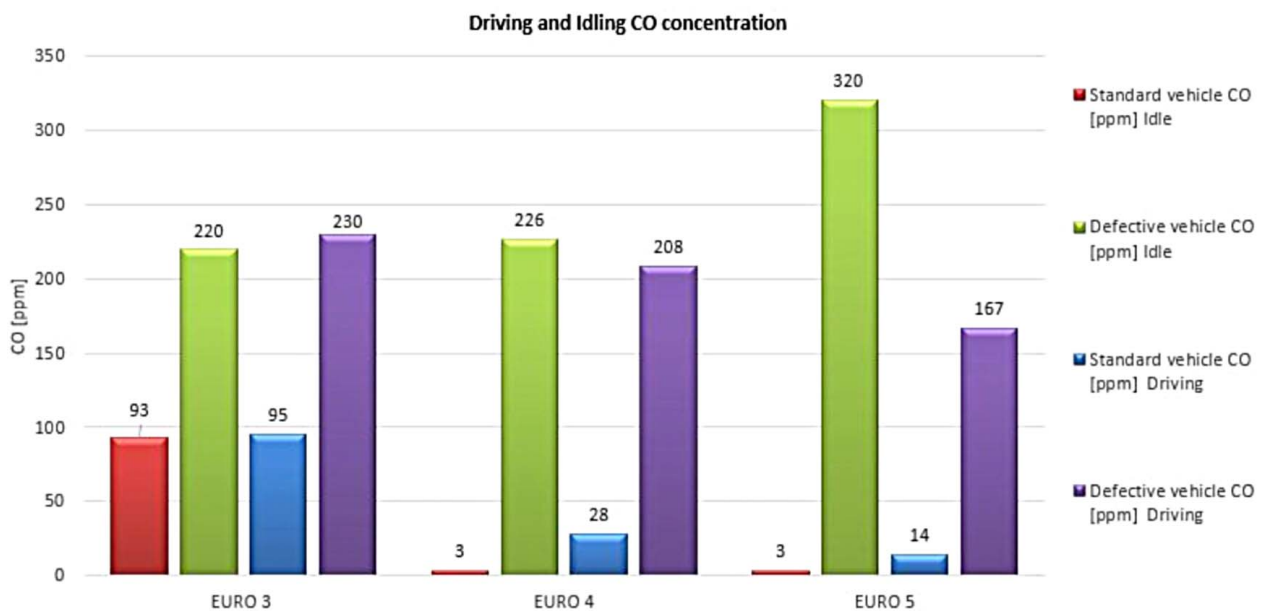Fig. 7 Temperature-dependent CO conversion efficiency

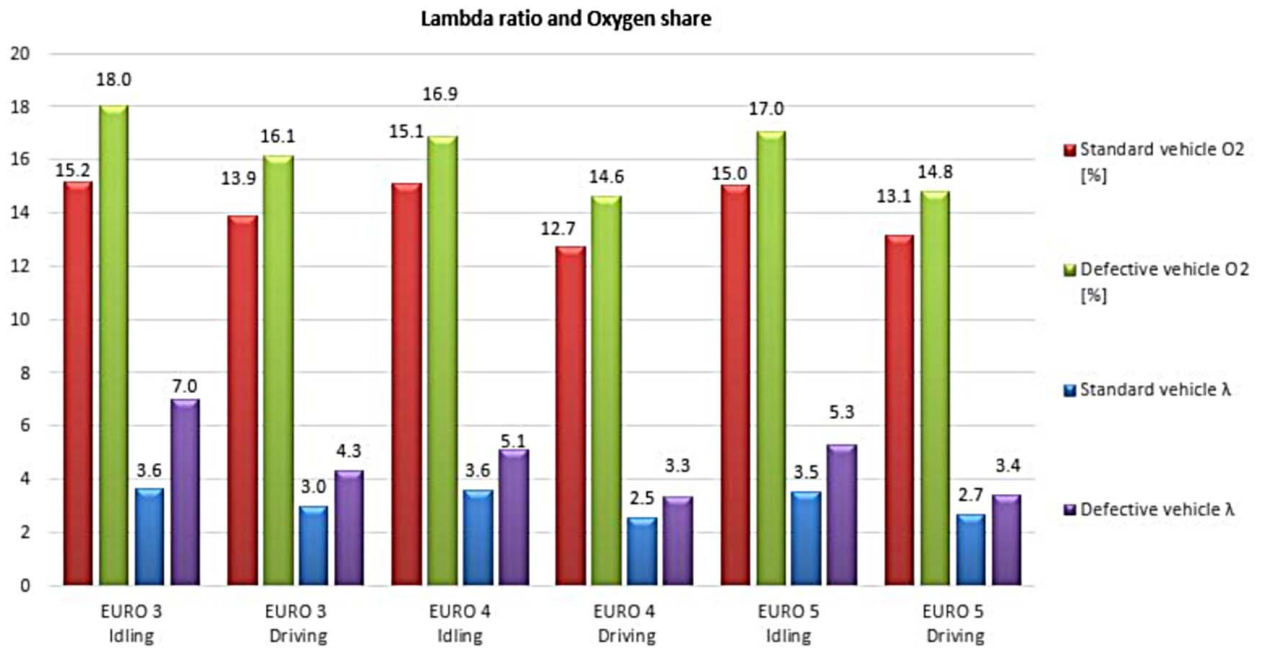Fig. 8 CO emissions: during drive and at idling

Fig. 9 Oxygen excess during drive and at idling

significant increase in the excess air. The usual procedure for testing the technical correctness of vehicles with gasoline engines includes the measurement of the ratio of air and fuel, as well as the measurement of carbon monoxide concentration. There is no need to make additional investments in new equipment, but only to implement appropriate procedures. Mentioned procedures would be based on the measurements described above and ranges within which the concentrations of carbon monoxide and excess air should be prescribed for each generation of a vehicle relative to the relevant standards (Fig. 9).
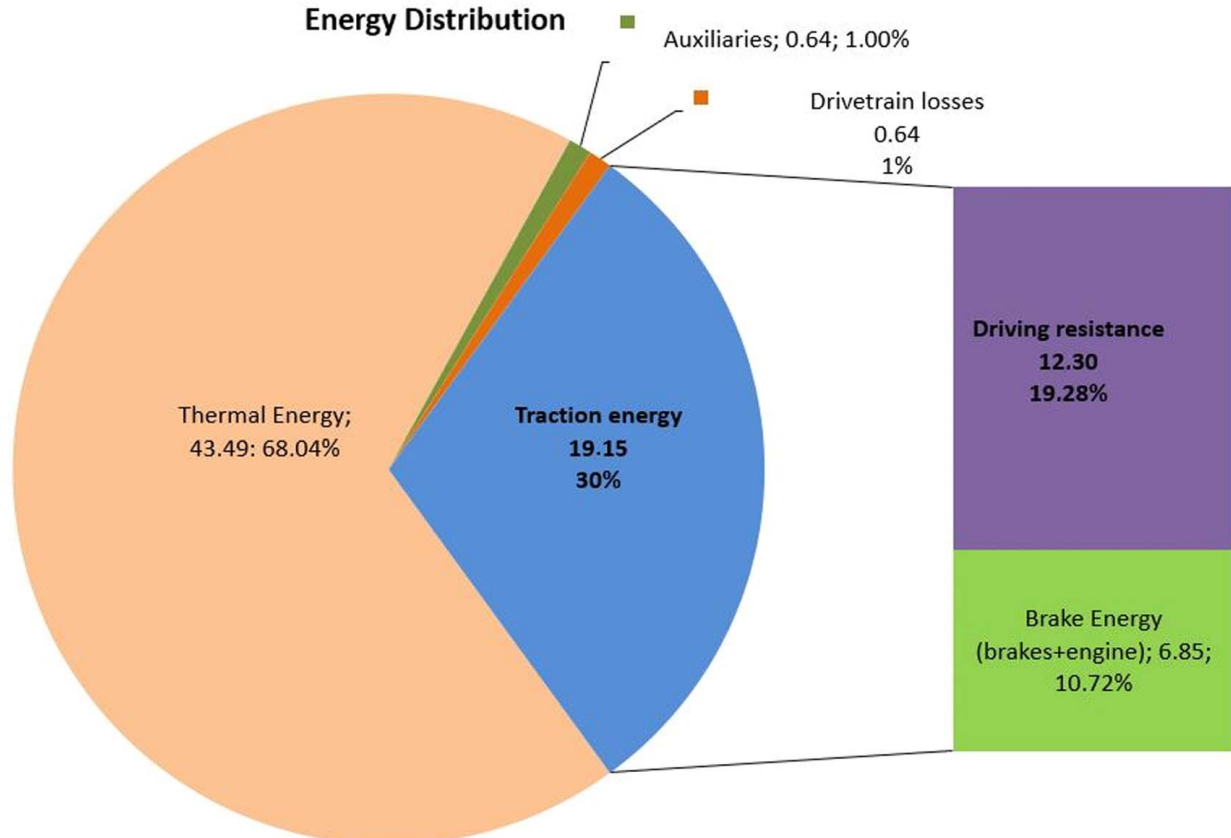

Fig. 10 Energy distribution in real driving operation

3.3 Analysis of Energy Flows, Hybrid Powertrain and Impact on Emissions. Despite the high efficiency of the diesel engine, its use in vehicle propulsion in the classical sense is limited mainly by exhaust emissions and most manufacturers will switch to hybrid propulsion systems from the Euro-7 standard [31]. For vehicle number 5 with Euro-5 standard and all correct exhaust emission control systems, the energy flow in real driving conditions was analyzed according to Fig. 10. With respect to the total fuel energy about 30% is converted into usable mechanical work, which is delivered to the vehicle's drive wheels. Most of the mechanical energy is spent on vehicle drag (64%) and is irreversible, while the remainder is spent on braking (36%), whether engine or friction braking. The part of mechanical energy wasted on braking, 36%, i.e., 6.85 kWh per 100 km, can be converted into useful energy instead of being converted into heat by conventional braking. The easiest way to use the braking energy is to convert it into electricity due to the simplicity of the system and the high-efficiency conversion. If the regenerative energy conversion factor wheel to wheel is being introduced, i.e., $\xi = 0.8$ [26,32], then, the hybrid powertrain has 5.48 kWh/100 km of additional mechanical energy. It is now necessary to determine how this energy should be managed. The simple strategy used herein is based on minimizing the most problematic emissions, in this case, NO_x. In addition to using regenerative braking energy, the hybrid drive has the ability to shift the operating point of the internal combustion engine, which provides additional benefits in terms of further reducing emissions and increasing fuel economy [33], but this topic goes beyond scope of the research in this work.

After the analysis of the energy flows, the distribution of emissions within each power range is made with the Power Binning method and shown in Fig. 11. The first power class has only negative power with no positive energy contribution, and the second power class has a positive energy contribution of less than 0.5% of the total mechanical energy. The first two power classes together account for over 46% of the CO emissions, almost 8% of the CO_2 emissions and 5% of the NO_x emissions. It is obvious that the previously mentioned two classes must be eliminated as their share of mechanical energy is very small while the amount of emissions is significant. Over 90% of all remaining emissions are in power classes 3, 4, and 5, so further analysis is reduced to these three classes. As the share of all emission types of class 3 is lower than the share of mechanical energy, and especially, the share of NO_x emissions, this power class is favorable. The higher power classes are obviously more favorable in terms of CO_2 emissions, but clearly the biggest problem with this vehicle is NO_x emissions.
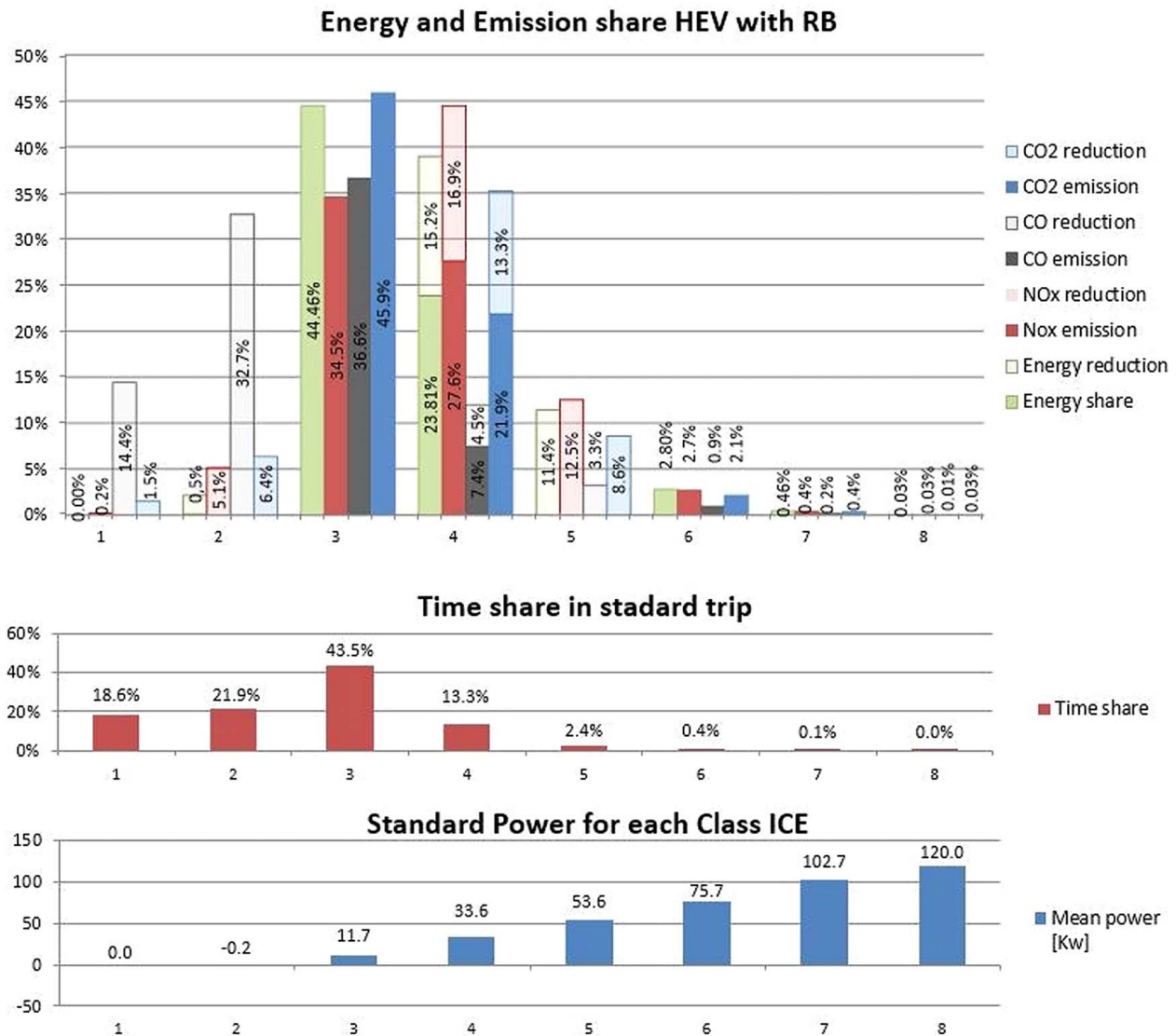

Fig. 11 Emissions and mechanical energy divided into power classes of standard and hybrid drive with regenerative braking
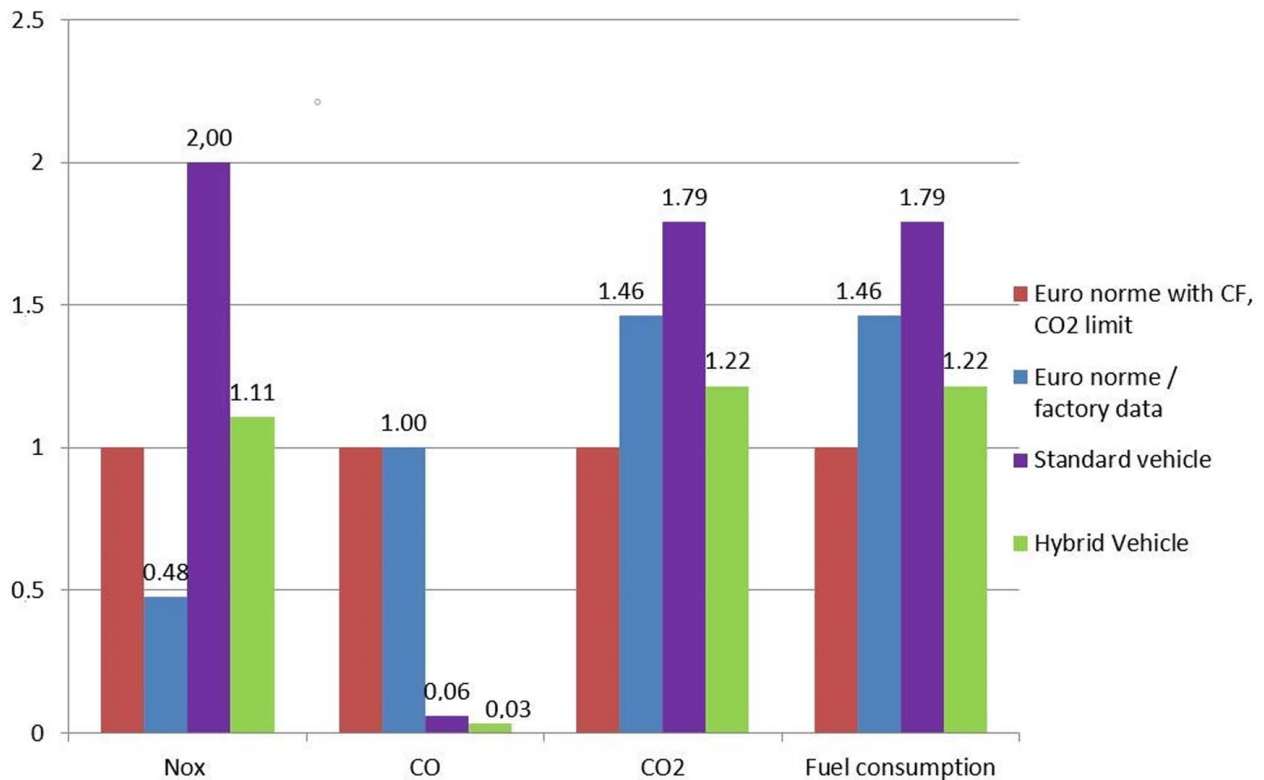
Fig. 12 Comparison of conventional and hybrid powertrain emissions

For these reasons, no energetic changes were made in the power class 3.

The output of internal combustion engines of power classes 4 and 5 is reduced to power class 3 with an average mechanical power of 11.7 kW. The regenerated energy amount of 5.48 kWh is sufficient to completely replace the mechanical energy of power class 2, i.e., without the use of a diesel engine, and power class 4, if the diesel engine is operated in the parameters of power class 3 with an average power of 11.7 kW and 50% of power class 5. The engine should operate only half the time with the parameters of power class 3 with an average power of 11.7 kW and the rest unchanged with an average power of 53.55 kW. In this way, around 0.09 kWh should be consumed to replace class 2, 5.25 kWh for class 4, and 0.9 kWh for class 5.

The differences of the hybrid system compared to the conventional system are shown by the gaps in the bar chart in Fig. 11. The final effect of the described hybrid drive strategy is shown in Fig. 12. The NO_x emissions are reduced to almost 50% of the initial values, and they are now 10% above the prescribed limit, which is simply solved by an engine management strategy. CO_2 emissions and fuel consumption have been reduced to 113 g/km or 68% of the initial value, and they are now 20% above the penalty limit, which is acceptable for an upper mid-range vehicle. The remaining CO emissions have been reduced to 31% of the initial value, which is negligible compared to the legal limit. The described hybrid drive strategy has been simplified, further improvements are possible by optimization and introduction of shifting operating point of the combustion engine. Such or similar strategies could be applied to smaller vehicles in the future, as their engines generally use low-cost emission control systems that only partially solve the NO_x problem at the expense of fuel economy, i.e., both in hybrid and diesel management strategies. The propulsion engines of larger vehicles will be equipped with more expensive exhaust after-treatment systems that incorporate SCR technology and that fully solve the NO_x problem. Hybrid powertrain management strategy for larger vehicles, i.e., optimization, will be reduced to minimize CO_2 emissions and consumption.

4 Conclusion

The herein reported study elaborated and discussed the problem of diesel engine emissions under realistic driving (operating) conditions. An extensive experiment was conducted on several vehicles during the realistic on-road driving cycles. The analysis performed on vehicles with the correct emission system shows significant discrepancies between the measurements obtained under real driving conditions and the homologated values. For vehicles with newer emission standards, the deviation is even higher. These deviations are mainly due to the outdated NEDC procedure for homologation of all tested vehicles. The situation is significantly deteriorated by the failure of the emission control components. The non-original components are used for replacement ones or even removed from the system. A significant increase in NO_x relative to the prescribed euro limit multiplied by CF was recorded, 21% for Euro 5 vehicles, 82% for Euro 4 vehicles, and 38% for Euro 3, mainly due to a defective EGR system or less significant, the absence of the DPF. The largest relative deviation of defective vehicles with respect to NO_x emissions is recorded for the vehicles with the euro 5 standard of 3.28 times, for euro 4 of 1.86 times, and for euro 3 of 9% below, compared to the related standard and CF 2.1. An increase in CO by three times for Euro 3, more than five times for Euro 4, and nearly nine times for Euro 5 were recorded due to a missing of the oxidation catalyst. The content of sulfur oxides is negligible due to the use of quality fuel with very low sulfur content. Fuel consumption and CO_2 emissions are several percents lower, i.e., up to 3% for the vehicle without EGR, catalytic converter, and DPF. This occurs due to more complete combustion without exhaust gas recirculation and lower backpressure. Fuel consumption can be reduced by adjusting the injection phase, but then the NO_x level increases significantly.

Standard technical inspection cannot detect a defective emission control system or significant modification of the engine management software. The new procedure is proposed to detect a missing oxidation catalyst. For this purpose, the standard emission measuring devices used for gasoline engines are proposed for measuring CO and HC. Another novelty is the detection of defective

EGR by measuring excess oxygen. Previous could also be detected with the lambda ratio, which is between 40 and 90% higher in a defective engine at idling.

In addition, the impact of the hybrid powertrain on exhaust emissions and consumption was also analyzed. NO_x emissions are reduced by almost 45% and are only 10% above the permissible limit, which is easily remedied by modifying the engine management parameters. CO emissions have been reduced to 31% compared to conventional propulsion, and CO_2 emissions are 113 g/km, which is about 20% above the penalty limit that has been applied since 2020. The result of CO_2 emissions is quite acceptable today as it is an upper mid-range vehicle, and the penalty is calculated at the level of the manufacturer's fleet, which includes on average all classes of vehicles. The measured data clearly showed that additional monitoring of the correctness of all antipollution components is required to regulate emissions throughout the whole life cycle of the vehicles if they want to achieve air quality standards. Measurement data from the long-term operation are not yet available for the latest vehicles generation homologated under real driving conditions, due to the short period of use. However, from the applied technologies, it can be concluded that the control of emission reduction components in vehicles with the latest technologies will have a much greater impact than before.

Future research should include the investigation of the latest Euro 6d standard vehicles with defective "antipollution" components during out-of-warranty exploitation. Secondly, a method for evaluation exhaust emission of hybrid powertrains and management strategy based on distributions by power classes would be developed. Increasing the efficiency of modern diesel engines within hybrid powertrains, in particular the exhaust after-treatment systems, in conjunction with a robust control system, will enable permanent compliance with strict environmental standards. This will provide a cleaner and near-zero-emission powertrain in terms of harmful gases and reduce CO_2 emissions to the lowest possible level.

Acknowledgment

Conflict of Interest

There are no conflicts of interest.

Data Availability Statement

The datasets generated and supporting the findings of this article are obtainable from the corresponding author upon reasonable request.

Nomenclature

j = power class on drive wheels from 1 to 9
k = time-step
a_{ref} = reference acceleration for P_{drive} (0.45 m/s^2)
$f_0, f_1,$ and f_2 = drag coefficients of the vehicles
m_{gas} = average emission value of an exhaust gas component (g/s)
$m_{gas,i}$ = instantaneous mass of the exhaust component "gas" at time-step i (g/s)
$m_{gas,j}$ = average emission value of an exhaust gas component in the wheel power class j (g/s)
$m_{gas,3s,k}$ = 3-s moving average mass flow of the exhaust gas component "gas" in time-step k given in 1 Hz resolution (g/s)
$t_{c,j}$ = time share of the wheel power class j (%)

$M_{gas,d}$ = distance-specific emissions for the exhaust gas component "gas" (g/km)
$P_{c,norm,j}$ = wheel power class limits for class j as normalized power value (–)
$P_{c,j}$ = wheel power class limits for class number j (kW)
P_{drive} = power demand at the wheel hub for a vehicle at reference speed and acceleration (kW)
$P_{w,3s,k}$ = 3-s moving average power demand at the vehicle's wheel to overcome driving resistances in time-step k in 1 Hz resolution (kW)
$P_{w,i}$ = actual power demand (kW)
TM = test mass of the vehicle (kg)
$v_{3s,k}$ = 3-s moving average of the vehicle velocity in time-step k (km/h)
v_i = actual vehicle speed in time-step i (km/h)
v_{ref} = reference velocity for P_{drive} (70 km/h)
v_j = average speed in power class (km/h)
ξ = regenerative energy conversion factor wheel-to-wheel

References

[1] Nižetić, S., Penga, Ž, and Arıcı, M., 2017, "Contribution to the Research of an Alternative Energy Concept for Carbon Free Electricity Production: Concept of Solar Power Plant With Short Diffuser," Energy Convers. Manage., **148**, pp. 533–553.

[2] Nižetić, S., Djilali, N., Papadopoulos, A., and Rodrigues, J. J. P. C., 2019, "Smart Technologies for Promotion of Energy Efficiency, Utilization of Sustainable Resources and Waste Management," J. Cleaner Prod., **231**, pp. 565–591.

[3] Hooftman, N., Messagie, M., Mierloi, V. J., and Coosemans, T., 2018, "A Review of the European Passenger car Regulations—Real Driving Emissions vs Local air Quality," Renewable Sustainable Energy Rev., **86**, pp. 1–21.

[4] Matulić, N., Radica, G., Barbir, F., and Nižetić, S., 2019, "Commercial Vehicle Auxiliary Loads Powered by PEM Fuel Cell," Int. J. Hydrogen Energy, **44**(20), pp. 10082–10090.

[5] Kozina, A., Radica, G., and Nižetić, S., 2020, "Analysis of Methods Towards Reduction of Harmful Pollutants From Diesel Engines," J. Cleaner Prod., **262**, p. 121105.

[6] O'Driscol, R., Stettler, M., Molden, N., Oxley, T., and Apsimon, H. M., 2018, "Real World CO_2 and NO_x Emissions From 149 Euro 5 and 6 Diesel, Gasoline and Hybrid Passenger Cars," Sci. Total Environ., **621**, pp. 282–290.

[7] Brand, C., 2016, "Beyond 'Dieselgate': Implications of Unaccounted and Future air Pollutant Emissions and Energy use for Cars in the United Kingdom," Energy Policy, **97**, pp. 1–12.

[8] Degraeuwe, B., and Weiss, M., 2017, "Does the New European Driving Cycle (NEDC) Really Fail to Capture the NO_X Emissions of Diesel Cars in Europe," Environ. Pollut., **222**, pp. 234–241.

[9] Burkhardt, T., 2019, "ADAC Testing Finds new Diesel Cars Cleaner Than Required; Euro 6c and 6d-Temp Vehicles Well Below the Permissible NO_x Limits," Green Car Congress 2019, Energy, Technologies, Issues and Policies for Sustainable Mobility. https://www.greencarcongress.com/2019/02/201902-22-adac.html

[10] Sanchez, P. F., Bandivadekar, A., and German, J., 2012, "Estimated Cost of Emission Reduction Technologies for Light-Duty Vehicles," The International Council on Clean Transportation 2012. www.theicct.org

[11] Zhuang, W., Li, S., Zhang, X., Kum, D., Song, Z., Yin, G., and Ju, F., 2020, "A Survey of Powertrain Configuration Studies on Hybrid Electric Vehicles," Appl. Energy, **262**, p. 114553.

[12] Agarwal, A. K., Park, S., Dhar, A., Lee, C. S., Park, S., Gupta, T., and Gupta, N. K., 2018, "Review of Experimental and Computational Studies on Spray, Combustion, Performance, and Emission Characteristics of Biodiesel Fueled Engines," ASME J. Energy Resour. Technol., **140**(12), p. 120801.

[13] Singh, A. P., Sharma, N., Satsangi, D. P., and Agarwal, A. K., 2020, "Effect of Fuel Injection Pressure and Premixed Ratio on Mineral Diesel-Methanol Fueled Reactivity Controlled Compression Ignition Mode Combustion Engine," ASME J. Energy Resour. Technol., **142**(12), p. 122301.

[14] Benajes, J., García, A., Monsalve-Serrano, J., and Boronat, V., 2017, ""Achieving Clean and Efficient Engine Operation up to Full Load by Combining Optimized RCCI and Dual-Fuel Diesel-Gasoline Combustion Strategies," Energy Convers. Manage., **136**, pp. 142–151.

[15] Gürbüz, H., and Demirtürk, S., 2020, "Investigation of Dual-Fuel Combustion by Different Port Injection Fuels (Neat Ethanol and E85) in a DE95 Diesel/Ethanol Blend Fueled Compression Ignition," ASME J. Energy Resour. Technol., **142**(12), p. 122306.

[16] Chen, Y., and Borken-Kleefeld, J., 2014, "Real-driving Emissions From Cars and Light Commercial Vehicles e Results From 13 Years Remote Sensing at Zurich/CH," Atmos. Environ., **88**, pp. 157–164.

[17] Kerbachi, R., Chikhi, S., and Boughedaoui, M., 2017, "Development of Real Exhaust Emission From Passenger Cars I Algeria by Using on-Board Measurement," Energy Procedia, **136**, pp. 388–393.

[18] Nesbit, M., Fergusson, M., Colsa, A., Ohlendorf, J., Hayes, C., Paquel, K., and Schweitzer, J.-P., 2016, "Comparative Study on the Differences Between the

EU and US Legislation on Emissions in the Automotive Sector," Policy Department A: Economic and Scientific Policy, https://www.europarl.europa.eu/committees/en/supporting-analyses

[19] Cheng, W., Li, X., and Yi, X., 2017, "Influence of Exhaust Gas Recirculation on Low-Load Diesel Engine Performance," Wuhan Univ. J. Nat. Sci., **22**(5), pp. 443–448.

[20] Simoson, C., and Wagner, J., Mar 2008, "Effects of Cooled EGR on a Small Displacement Diesel Engine: A Reduced-Order Dynamic Model and Experimental Study," ASME J. Energy Resour. Technol., **130**(1), p. 011102.

[21] Ghodke, P. R., and Suryavanshi, J. G., 2012, "Review of Advanced EGR and Breathing Systems for High Performance and Low Emission HSDI Diesel Engine," Int. J. Mod. Eng. Res., **2**(5), pp. 3138–3142.

[22] Park, Y., and Bae, C., 2014, "Experimental Study on the Effects of High/low Pressure EGR Proportion in a Passenger car Diesel Engine," Appl. Energy, **133**, pp. 308–316.

[23] Huang, Y., Organ, B., Zhou, J. L., Surwaski, N. C., Hong, G., Chan, E. F. C., and Yam, Y. S., 2018, ""Emission Measurement of Diesel Vehicles in Hong Kong Through on-Road Remote Sensing: Performance Review and Identification of High-Emitters," Environ. Pollut., **237**, pp. 133–142.

[24] Kozina, A., Radica, G., and Nižetić, S., 2020, "Emission of Diesel Powered Vehicle Under Real Operating Conditions-Impact of Emissions Control System Failure," 2020 5th International Conference on Smart and Sustainable Technologies (SpliTech).

[25] Varella, R., Duarte, G., Baptista, P., Sousa, L., et al., 2017, "Comparison of Data Analysis Methods for European Real Driving Emissions Regulation," SAE Technical Paper 2017-01-0997.

[26] Preda, I., Covaciu, D., and Ciolan, G., 2010, "Coast Down Test-Theoretical and Experimental Approach," Transilvania Universiti of Brasov.

[27] Commission Regulation (EU) 2016/427. Amending Regulation (EC) No 692/2008 as Regards Emissions From Light Passenger and Commercial Vehicles (Euro 6). Official Journal of the European Union.

[28] Mikulic, I., Zhan, R., and Eakle, S., 2010, "Dependence of Fuel Consumption on Engine Backpressure Generated by a DPF," SAE International.

[29] Stamatellou, A.-M., and Stamatelos, A., 2017, "Overview of Diesel Particulate Filter Systems Sizing Approaches," Appl. Therm. Eng., **121**, pp. 537–546.

[30] Mittal, M., Donahue, R., and Winnie, P., 2015, "Evaluating the Influence of Exhaust Back Pressure on Performance and Exhaust Emissions Characteristics of a Multicylinder, Turbocharged, and Aftercooled Diesel Engine," ASME J. Energy Resour. Technol., **137**(3), p. 032207.

[31] Pielecha, I., Cieslik, W., and Szalek, A., 2019, "Energy Recovery Potential Through Regenerative Braking for a Hybrid Electric Vehicle in a Urban Conditions," IOP Conf. Ser. Earth Environ. Sci., **214**, p. 012013.

[32] Sovran, G., 2011, "The Impact of Regenerative Braking on the Powertrain-Delivered Energy Required for Vehicle Propulsion," SAE International 2011-01-0891.

[33] Yusaf, T. F., 2009, "Diesel Engine Optimization for Electric Hybrid Vehicles," ASME J. Energy Resour. Technol., **131**(1), p. 012203.

PRILOG D

Naslov rada: A New Vehicle-Specific Power Model for the Estimation of Hybrid Vehicle Emissions

Autori: Ante Kozina, Tino Vidović, Gojmir Radica, Ante Vučetić

Izvornik: *Energies*

Broj izdanja, stranice, godina: vol. 16, no. 24, p. 8094, 2023.

Vrsta rada: izvorni znanstveni

Izvorni jezik: engleski

Ključne riječi: hybrid electric vehicles; vehicles models; VSP analyses

Sažetak: Hybrid electric vehicles are certainly one of the key solutions for improving fuel efficiency and reducing emissions, especially in terms of special vehicles and with the use of CO_2-neutral fuels. Determining the energy management strategy and finding the optimal solution with regard to the aforementioned goals remains one of the main challenges in the design of HEVs. This paper presents a new vehicle modeling method, with an emphasis on HEVs, which is based on the frequency analysis of emissions and consumption according to the current specific traction power of the vehicle. An evaluation of the newly introduced model in the RDE, NEDC and WLTP cycle was performed, and the results were compared with the standard verified vehicle model that was created in AVL's CruiseM R2021.2 software package. Positive traction energies have positive deviations of between 0.35% and 2.85%. The largest deviation in CO_2 emissions was recorded for the HEV model in the RDE cycle and in the non-hybrid model in the WLTP cycle and were 3.79% and 4.4%, respectively. All other combinations of cycle and vehicles had deviations of up to about 1%. As expected, the largest relative deviations were recorded for NO_X emissions and ranged from 0.13% to 9.62% for HEVs in the WLTP cycle.

A New Vehicle-Specific Power Model for the Estimation of Hybrid Vehicle Emissions

Ante Kozina [1], Tino Vidović [1], Gojmir Radica [1,*] and Ante Vučetić [2]

1 Faculty of Electrical Engineering, Mechanical Engineering and Naval Architecture, University of Split, R. Boškovića 32, 21000 Split, Croatia; ante.kozina.00@fesb.hr (A.K.); tino.vidovic.00@fesb.hr (T.V.)
2 Faculty of Mechanical Engineering and Naval Architecture, University of Zagreb, Ivana Lučića 5, 10000 Zagreb, Croatia; ante.vucetic@fsb.hr
* Correspondence: goradica@fesb.hr

Abstract: Hybrid electric vehicles are certainly one of the key solutions for improving fuel efficiency and reducing emissions, especially in terms of special vehicles and with the use of CO_2-neutral fuels. Determining the energy management strategy and finding the optimal solution with regard to the aforementioned goals remains one of the main challenges in the design of HEVs. This paper presents a new vehicle modeling method, with an emphasis on HEVs, which is based on the frequency analysis of emissions and consumption according to the current specific traction power of the vehicle. An evaluation of the newly introduced model in the RDE, NEDC and WLTP cycle was performed, and the results were compared with the standard verified vehicle model that was created in AVL's CruiseM R2021.2 software package. Positive traction energies have positive deviations of between 0.35% and 2.85%. The largest deviation in CO_2 emissions was recorded for the HEV model in the RDE cycle and in the non-hybrid model in the WLTP cycle and were 3.79% and 4.4%, respectively. All other combinations of cycle and vehicles had deviations of up to about 1%. As expected, the largest relative deviations were recorded for NOx emissions and ranged from 0.13% to 9.62% for HEVs in the WLTP cycle.

Keywords: hybrid electric vehicles; vehicles models; VSP analyses

1. Introduction

The constant increase in transport needs and the desire for sustainability is forcing vehicle manufacturers towards significant reductions in harmful exhaust emissions and emissions of greenhouse gases, especially carbon dioxide. Several countries, especially EU members and some US states, want to restrict the sale of new passenger vehicles fueled by fossil fuels [1,2]; however, this ban policy has proven difficult to implement in less developed parts of the world with inadequate infrastructure [3]. The EU plans to reduce CO_2 emissions to 95 g/km for new passenger vehicles by 2025 [4], an additional reduction of 17% is planned between 2025 and 2030, and a reduction of 37.5% from 2030 onwards [5]. In the last 15 years, high-speed internal combustion engines have achieved very high efficiency, diesel engines achieve peak mechanical efficiency of over 40% [6], but it is still questionable whether they will be able to satisfy newly proposed Euro 7 standard [7,8] as stand-alone powertrains [9]. The main reason for this is the inefficient energy management that is due to the absence of regenerative braking and the large drop in efficiency at low loads for which the engine operates in a low efficiency region. Hybrid electric vehicles (HEVs) combine the advantages of EVs and standard vehicles, they have a high degree of flexibility as well as the ability to meet a wider range of driving requirements [10]. The most significant advantage over standard vehicles powered solely by an ICE is the ability to save energy from regenerative braking and store excess energy by shifting the engine operating region towards that of a higher efficiency, as well as the use of smaller, lighter, and simpler single-range ICEs. Additionally, the ever-present possibility of choosing different operating

parameters of the ICE enables better emission control management and almost completely solves the problems associated with their use [11]. The most significant advantage of HEVs compared with fully electric vehicles (EVs) is their superior range over a single charge and their fast refueling, which is achieved by using chemical energy instead of electrical [12]. Hybrid electric vehicles together form a key solution for increasing efficiency and lowering emissions and a viable strategy for developing countries> This is particularly so with the use of environmentally friendly, synthetic CO_2-neutral fuels at an affordable price [13] or with the use of alternative fuels, such as LPG, which have significantly lower emissions and a lower CO_2 footprint [14]. Such power trains will certainly find their application in heavy trucks for long distances, special purpose vehicles or off-road and military vehicles [15,16]. The share of hybrid vehicles, with all levels of hybridization, from plug-in and full hybrid electric vehicles to mild hybrid vehicles, is predicted to be over 36% by 2030 [17]. The above indicated advantages are made possible due to the high complexity of the HEV system, which is also the biggest challenge both in terms of the number of installed systems and in terms of finding the optimal control method [18–20]. The use of multiple energy sources and the high complexity of the HEV drive system require a more complex high-level control system. This, in turn, requires complex modeling methods with highly demanding models in terms of the user and in computation [21–23]. Various approaches to the modeling of hybrid road vehicles have been developed and, according to the literature, we are able to distinguish kinematic (backward), quasi-static (forward) and dynamic approaches [24,25]. The optimal solution depends on the specifics of the application, but in most cases the energy management strategy (EMS) is a compromise between minimizing energy consumption and exhaust gas emissions [26], increasing the durability of components such as batteries, meeting power requirements, and ensuring vehicle performance and comfort [27]. Each of these requirements depend on a large number of parameters and it is very difficult and impractical to cover them all in one model. Because of these reasons, the authors in the relevant literature mainly observe, in detail, the influence of certain specific parameters on one of the aforementioned requirements. In [28], an EMS plug-in HEV bus was proposed based on an equivalent consumption minimization strategy by using real-time traffic information described by the average speed, average acceleration, and standard deviation of speed for different road sections. In [29], a method based on gear shift control was proposed in order to improve further research on the relationship between different road sections and vehicle driving conditions and gears. In [28,29] steady-state map-based ICE models were used, which are an efficient solution to the estimation of fuel consumption. In contrast with consumption models that do not depend heavily on transient behaviors, emission models are much more sensitive to them. Due to its complexity, the usual way of modeling a complete HEV does not include complex and detailed ICE emission models, but relies on lower-level models that include steady-state emission maps that introduce a certain emission estimation error [30]. Modal vehicle specific power (VSP) analysis is also used in fuel consumption and emissions estimations. Unlike most consumption models that depend on steady-state maps, in [31] a fuel consumption model for passenger cars was developed that includes an analysis of the influence of transient loads. Such an analysis gives an essential advantage when estimating emissions. In [32], a VSP model of a full HEV was built with 14 modes by measuring emissions and consumption using a PEMS device, the model was then validated in an NEDC cycle by which the vehicle is type approved. This used a simplified universal definition of vehicle specific power according to [33], one which simplifies the model but also reduces the accuracy. The deviation of the model from the certified data according to the NEDC protocol was for fuel consumption −3.2%, for CO emission +18.1% and for NOx emission 26.2%.

Modal VSP analysis is used to form incomplete models of HEVs, mainly for the assessment of the total vehicle fuel consumption and emissions of the ICE on its own and of HEVs in different driving conditions. This is because they do not apply the energy flows necessary for the creation of a complete model that enables the application of an

appropriate management strategy, i.e., the assessment of the maximum hybridization efficiency. Additionally, the definition of modal emissions as flow per unit of time in relation to modal emissions per unit of energy introduces additional error into the model. The main goal of this paper was to present a new model of a hybrid vehicle based on modal analysis of vehicle consumption, emissions and energy flows. Because it takes into account transitory events, this approach should allow for a faster and simpler arrival at the pre-set HEV optimization target, especially for the emission objective. The model can also be used as a guideline for a standard time-based model that leads to an optimal solution, avoiding local minima. The model was based on real vehicle emissions, fuel and energy consumption data which were recorded in real driving conditions according to the Real Driving Emissions (RDE) rules, which are today a mandatory segment of the type approval process. Validation and result comparison was undertaken with regard to standard time-based CruiseM model results.

2. Materials and Methods

First, a non-hybrid vehicle model was created and validated in AVL's CruiseM R2021.2 software package. CruiseM is a versatile system simulation tool supporting model-based development across various domains, such as engine, flow, aftertreatment, driveline, electrics, and hydraulics. It enables efficient multi-physics system simulation through a flexible, multi-level modeling approach and has interfaces with third-party tools via the functional mock-up interface (FMI) standard [34]. The software addresses complex areas in vehicle development, including electrical networks, thermoregulation systems, mechanical and thermodynamic systems, and control tasks. For battery electric vehicles, it aids in answering critical questions about battery packs, thermal management, electric motors, transmission coordination, and operating strategies. Benefits include easy-to-parameterize models for concept studies, and the ability to study interrelationships between domains, to control calibration in a virtual environment, and to serve as a starting point for detailed 3D simulations in order to evaluate component requirements. The purpose of the non-hybrid model created in CruiseM was to check the accuracy of the newly introduced VSP frequency model in different tested conditions and cycles. A new VSP model was developed based on the specific power of the vehicle, and frequency analysis. The CruiseM model was based on maps of consumption and emissions which were obtained with chassis dynamometer in laboratory conditions. The vehicle models were validated with obtained parameters under RDE driving cycle. The next step was the hybridization of both models into a parallel hybrid architecture under equal conditions. The CruiseM model was used as a control model. At the end, the obtained results of the newly developed VSP frequency model and the time domain CruiseM model were compared. The comparison was made on a non-hybrid and hybrid vehicle in RDE, NEDC and WLTC cycles.

2.1. Measurement and Equipment

The portable emissions measurement system (PEMS) AVL M.O.V.E. was installed on a test vehicle for the purpose of measuring emissions of carbon dioxide and other pollutants in real driving conditions. This system continuously monitors and records vehicle emissions data. The PEMS device is composed of several basic parts that are interconnected and controlled by a central computer. More detailed information about the AVL M.O.V.E. measuring instrument is shown in Table 1.

To diminish impact on the driving dynamics, the majority of equipment was installed in the trunk of the vehicle: gas analyzers, solid particle counter, and central computer with battery. Exhaust gas mass flow meter, GPS receiver and meteorological station for monitoring atmospheric conditions were installed outside. A photo of the vehicle with all the measuring equipment is shown in Figure 1. Measurements of current power, consumption and emissions were recorded along an 87 km long route that meets the RDE measurement criteria, and all measurements were performed according to the RDE test procedure. The calibration of the measuring instruments was performed before the

start of the measurement and after the measurement was completed. Continuous power measurement was carried out via OBD diagnostics, whose power values were previously calibrated on a chassis dynamometer at several operating points throughout the entire engine operating range. The emission maps and consumption maps that were used in the creation of the time domain CruiseM model were obtained by measuring emissions and consumption on the chassis test bed at different engine loads and speeds. In all laboratory measurements, a MAHA LPS 3000 chassis dynamometer was used, equipment was sourced from MAHA Maschinenbau Haldenwang GmbH & Co. KG, Haldenwang, Germany. The vehicle was type approved according to the EURO6b standard [35], based on the laboratory NEDC test cycle and is powered by a 1.6 L diesel engine with a maximum power of 77 kW with EGR, DOC and DPF antipollution systems and a 5 speed manual gearbox. Coast-down analysis was used to determine the resistances of the vehicle. This was obtained by recording the speed from the OBD system with a resolution of 1 s. The measured speed from the OBD was previously calibrated with the GPS system.

Table 1. Technical features of PEMS devices.

Analyzer	NO/NO_2 and $CO/CO_2/N_2O$	THC/CH_4	Particle Counter
Measuring method	Non-Dispersive Ultra Violet-NDUV Non-Dispersive Infra Red-NDIR	Flame Ionization Detector-FID	Advanced diffusion charger
Measuring range	NO: 0–5000 ppm		
	NO_2: 0–2500 ppm	THC: 0–30,000 ppmC1	
	CO: 0–5% vol.		$\sim$1500–$\sim$2.5 $\times$ 10^7 #/cm^3
	CO_2: 0–20% vol.	CH_4: 0–10,000 ppmC1	
	N_2O: 0–2000 ppm		
Zero Drift/8 h	NO/NO_2: 2 ppm		
	CO: 20 ppm	$\pm$5 ppm C1/8 h	
	CO_2: 0.1% vol.		
	N_2O: 20 ppm		
Accuracy	0.3% FS		

Figure 1. Test vehicle with built-in measuring equipment.

The vehicle model was created in the CruiseM software package with a quasi-static approach, which starts from the driver's request to follow a predetermined speed pattern or driving cycle, with a schematic representation shown in Figure 2. The request is transmitted to the drive system via the appropriate regulator and accelerator pedal which has its own characteristics and transient response. The torque is transmitted to the transmission system,

which has its own gear ratios and losses all the way to the wheels and which needs to achieve the necessary torque or driving force to meet the required velocity pattern. This approach gives particularly good results in CO_2 emissions, consumption estimation as well as NOx emissions estimation [24].
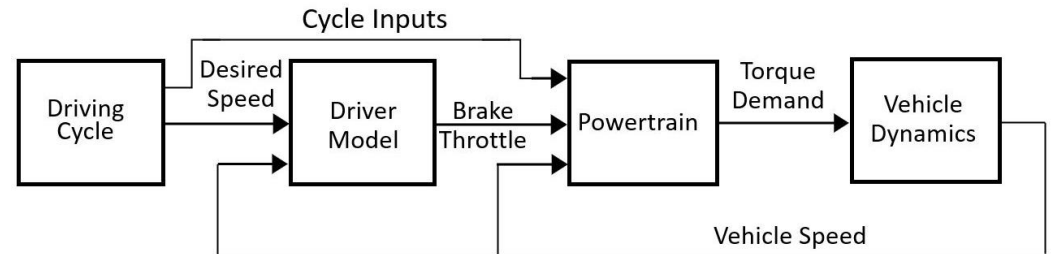

Figure 2. Schematic representation of the quasi-static or forward model of the vehicle.

The next step was the modelling of a full hybrid vehicle with a parallel configuration. An identical model was also used in the simulation of a non-hybrid vehicle with the exclusion of the components marked blue in Figure 3. As measurements were taken with a moderate driving style, the transverse and vertical dynamics have negligible influence on fuel consumption and emissions, so the vehicle dynamics model was reduced to solely reflect longitudinal dynamics. The vehicle resistance forces were defined as a function of the vehicle speed, by a polynomial of second degree (1) obtained from the coast down analysis [36]. The vehicle drag force equation is defined as:

$$f_0 + f_1 \times v + f_2 \times v^2 = TM\frac{dv}{dt} \tag{1}$$

where parameter f_0 is the free term, f_1 is the linear component and f_2 is the quadratic component.

The internal combustion engine was modeled as a black box based on the corresponding consumption or CO_2 maps and NOx maps, which give the correlation of the corresponding emissions with the engine current operating point. Engine maps were also obtained by testing on chassis test bed sweeping the entire operating range. The engine is controlled by desired load from a controller. Engine limits were determined by the maximum torque as a function of rotation speed. The motoring torque losses were set up with an interpolation curve depending on the rotation speed. A classic gearbox with five forward gears was modeled, with the same transmission ratios as the physical gearbox. The efficiency and the moments of inertia were held constant. The vehicle powertrain contains two clutches, the first (separator) serves to separate the ICE from the rest of the powertrain and the second is a standard clutch for coupling power devices with the transmission. The separator enables one to connect/disconnect the ICE to/from the whole system according to the applied HEV strategy (e.g., e-drive, e-brake regeneration, etc.). In addition, a transmission controller is required for gear up-/downshifting as well as actuating both clutches. Both clutches are driven by thrust force and modeled with the following parameters: maximum torque, moment of inertia and "clutch release" dependence characteristic on thrust force.
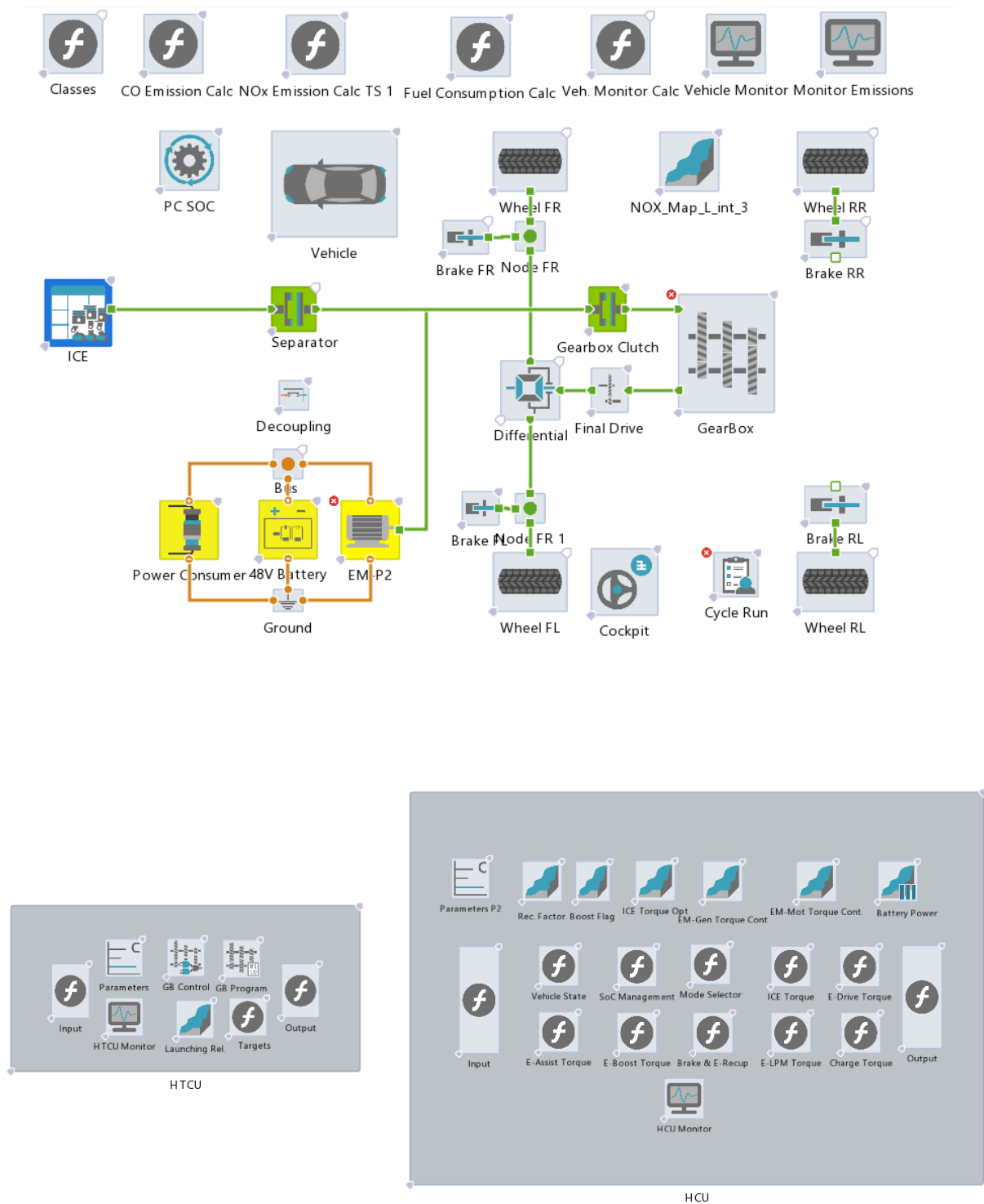
Figure 3. Schematic representation of the CruiseM vehicle model.

A 48 V electric drive system was used, which consists of a battery, a power consumer and an electric machine (EM) that is mechanically connected between two clutches. The EM is modeled as a basic quasi-static model that instantly responds to the torque demand. The characteristics of EM are defined in both working quadrants separately. The maximum torque limit is defined in generator and motor mode depending on the rotation speed as well as the efficiency characteristics with an additional parameter of the operating voltage. The drive control calculates the e-motor load signal in both traction and recuperation conditions, by modifying the cockpit output signals. If the braking effect of the e-motor torque is below

the driver's request in terms of equivalent brake pressure, then the mechanical brakes are supplied with pressure. The HEV controller contains a basic state machine which smoothly applies different hybrid strategies according to the current driving situation. A baseline management strategy was chosen according to the rules and which does not have the ability to adapt to different driving conditions [37]. Consequently, change of control parameters during testing in different cycles was undertaken manually. For an easier comparison of fuel and energy consumption between different models, the charge sustain mode was used, which requires the battery to be equally charged at the beginning and at the end of each testing cycle.

2.2. VSP Model

Vehicle specific power (*VSP*) is defined as a ratio of the instantaneous power to the vehicle's mass and is used to overcome the vehicle's resistances, including rolling and aerodynamic resistances, and kinetic and potential energies (2) [33]:

$$VSP = \frac{\frac{d}{dt}(KE+PE)+F_{roll}\cdot v+F_{aero}\cdot v}{m} = \frac{\frac{d}{dt}(KE+PE)+F_{res}\cdot v}{m}$$
$$= \frac{\frac{d}{dt}\left(\frac{1}{2}m\cdot v^2+mgh\right)+\left(f_0+f_1\cdot v+f_2\cdot v^2\right)\cdot v}{m} \tag{2}$$

All vehicle resistances, including rolling resistances, are also defined by longitudinal dynamics as in the classic Cruise M model in which moments of inertia are approximated with a 3% increase in vehicle mass [38]. The total traction energy is calculated according to:

$$E_{tr} = \int_0^T mVSPdt \tag{3}$$

The mathematical description of the vehicle's specific power (2) is the basis for the model of the current traction power or energy consumption. This model was created using a kinematic or backward approach that starts from the end components of the vehicle, i.e., the wheels, which require a certain torque to follow the cycle. The schematic representation of the backward model is shown in Figure 4, the flow of information or requests is opposite to the flow of energy. The movement of the vehicle absolutely coincides with the cycle being followed, so an additional condition is added which takes into account whether the vehicle can meet the power request at every point of the driving cycle.
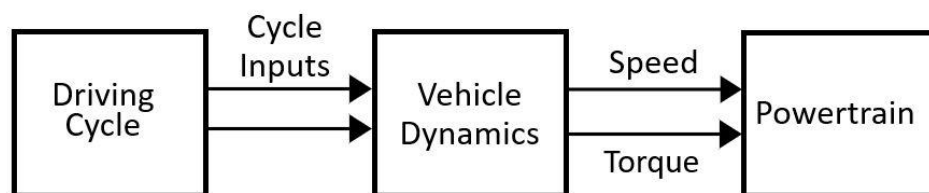

Figure 4. Schematic representation of the kinematic or backward model of the vehicle.

The VSP model is a discrete model formed by frequency analysis of measured emissions and consumption within certain power ranges or classes. The starting assumption is that the amount of each emission per unit of traction energy is always equal within the observed power class, regardless of the driving cycle. More accurate results are obtained by using a larger number of small ranges classes, but a large number of classes increases the complexity of data processing. The power classes are determined according to the power binning method within EU regulation 2016/427 [39], which gives normalized values of their power ranges. Some changes were introduced in classes 2 and 3. The change in the 2nd class refers to the division into its positive and negative parts separately, and class 3 is divided into two equal parts in order to increase the accuracy of the model. The denormalized values of power class ranges for the tested vehicle are shown in Table 2.

Table 2. Power classes for the modelled vehicle.

Power Class No.	$P_{c,j}$ (kW) from	$P_{c,j}$ (kW) to
1	$-\infty$	-2.368
2	-2.368	0.000
3	0.000	2.368
4	2.368	11.840
5	11.840	23.680
6	23.680	44.992
7	44.992	66.304
8	66.304	∞

The bin classification is undertaken according to the limits specified in Table 2, and according to the conditions of maximum and minimum traction power according to (4):

$$P_{c,j\ lower\ bound} < P_{wheel} \leq P_{c,j\ upper\ bound} \tag{4}$$

$$m_{x,j} = \sum_{all\ k\ in\ class\ j} m_{x,k} \tag{5}$$

The traction energy of the *j* class is calculated according to (6):

$$W_{tr,j} = m_{vehicle} \sum_{all\ k\ in\ class\ j} VSP_{tr,k} t_k \tag{6}$$

The value of individual emissions per unit of traction energy of the *j* class is equal to the ratio of the total amount of emissions of the grade and its total traction energy (7):

$$\dot{m}_{x,j} = \frac{m_{x,j}}{W_{tr,j}} = \frac{\sum\limits_{all\ k\ in\ class\ j} m_{x,k}}{\sum\limits_{all\ k\ in\ class\ j} P_{tr,k} t_k} = \frac{\sum\limits_{all\ k\ in\ class\ j} m_{x,k}}{m_{vehicle} \sum\limits_{all\ k\ in\ class\ j} VSP_{tr,k} t_k} \tag{7}$$

The distribution of emissions and energy by power classes during the testing in real driving conditions are shown in diagram in Figure 5. The energy shares of the classes are expressed in percentages relative to the total positive traction energy.
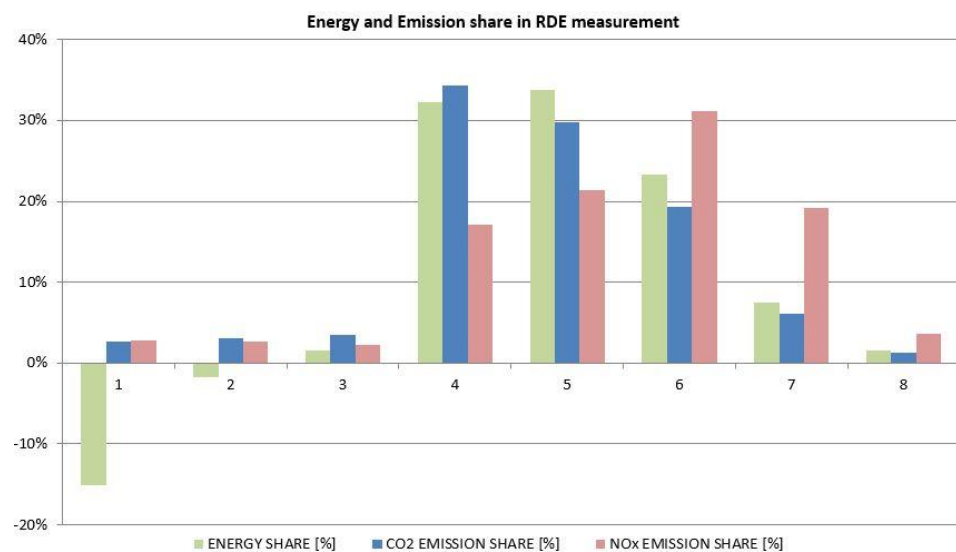

Figure 5. Class distribution of traction energy, CO_2 emissions and NOx emissions during the RDE route.

The total amount of emissions and consumption is obtained by summing the emissions of all individual classes, i.e., the product of specific emissions and the traction energy coming from the internal combustion engine, according to (8):

$$M_x = \sum_j m_{x,j} = \sum_j \dot{m}_{x,j} W_{tr,j} \tag{8}$$

When modelling a non-hybrid vehicle, all power classes were calculated in the assessment of complete cycle emissions. The main point of hybrid vehicles, including this hybrid vehicle model, is to use the most favorable operation regions for each available power source, according to a defined objective function that usually evaluates emissions and consumption. Traction energy of the j-class produced by an internal combustion engine is given in (9):

$$W_{tr,j} = w_{tr,j} + w_{mwa,j} - \gamma_j w'_{stored} \tag{9}$$

where $w_{tr,j}$ represents the total traction energy of j class that the engine would generate without hybrid drivetrain components, and $w_{mwa,j}$ represents the additional mechanical energy due to the shift of the operating region of the engine to the more favorable class. Stored energy w'_{stored} (10) consists of the regenerative braking energy W_{br} and the stored energy of the engine produced by moving operating region $W_{s,mwa}$

$$w'_{stored} = \eta_g \eta_{st} \eta_m \left(\alpha \eta_{gb}^2 \eta_f^2 W_{br} + \eta_{gb} \eta_f W_{s,mwa} \right) \tag{10}$$

Inserting Equation (10) into Equation (9) gives Equation (11):

$$W_{tr,j} = w_{tr,j} + w_{mwp,j} - \gamma_j \eta_g \eta_{st} \eta_m \left(\alpha \eta_{gb}^2 \eta_f^2 W_{br} + \eta_{gb} \eta_f W_{s,mwa} \right) \tag{11}$$

The energy flows are based on the flow diagram from [40], with slightly modified labels and definitions of all energy sources and sinks with regard to the drive shaft. The objective function is the minimum product of certain emissions and associated weighting factors (12):

$$J = A M_{CO2} + B M_{NOx} + C M_{PN} + D M_{CO} \tag{12}$$

Due to the limitations of the classic CruiseM model, only CO_2, fuel consumption and NOx emissions were retained, and the objective function (13) preferred only the minimization of consumption and CO_2 emissions:

$$J = A M_{CO2} = \sum_j \dot{m}_{CO2,j} W_{tr,j} \tag{13}$$

Inserting Equation (11) into Equation (13) gives Equation (14):

$$J = A \sum_j \dot{m}_{CO2,j} \left[w_{tr,j} + W_{mwp,j} - \gamma_j \eta_g \eta_{st} \eta_m \left(\alpha \eta_{gb}^2 \eta_f^2 W_{br} - \eta_{gb} \eta_f W_{s,mwa} \right) \right] \tag{14}$$

The total stored engine moving operating region energy is obtained by multiplying power differences between the engine's average j-class power, $P_{e,j}$, and the required traction power, j-th class, with the engine's operating time, $T_{j,mwa}$ (15):

$$W_{s,mwa} = \sum_j T_{j,mwa} \left(P_{e,j} - P_j \right) \tag{15}$$

The total recuperated energy from braking is obtained by the sum of the braking energies of all individual classes (16):

$$W_{br} = \sum_j W_{br,j} \tag{16}$$

3. Results and Discussion

3.1. Vehicle Models

Based on emission measurements and other relevant parameters, a CruiseM model, as well as a new frequency model of a non-hybrid vehicle was created. The vehicle energy balance and the main conversion pathways of chemical energy derived from the fuel are shown in the diagram in Figure 6 below:
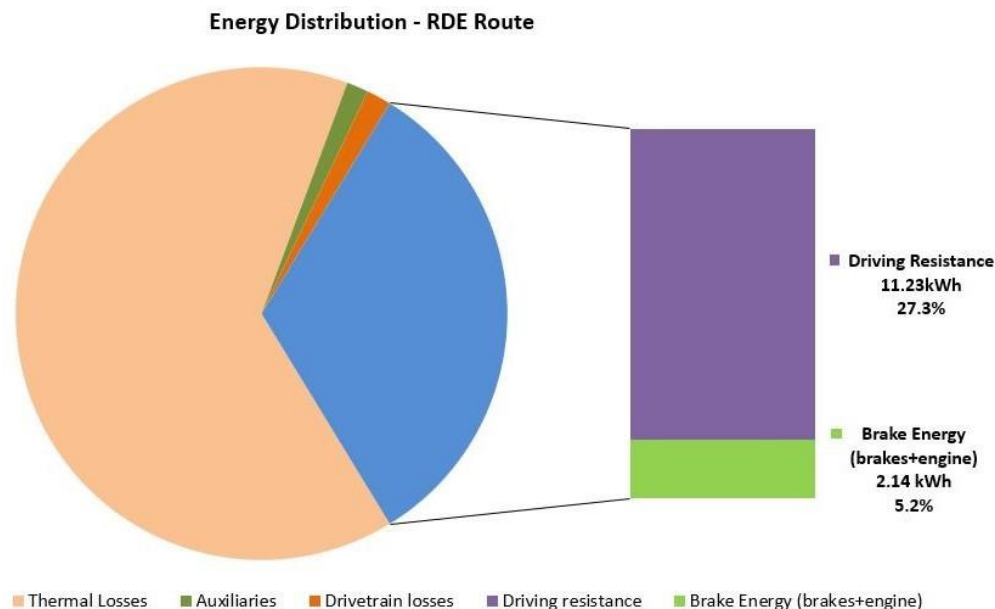

Figure 6. Vehicle energy balance.

The overall efficiency of the internal combustion engine in the test conditions of the vehicle was quite high, over 32%, but it should be emphasized that the efficiency in city driving conditions is far lower and in certain conditions falls below 10%, while the maximum engine efficiency is around 42%. This difference shows the utility of the hybrid drive, which has the ability to move the load point towards the higher efficiency. Of the total traction energy, 84% was spent on overcoming the vehicle's resistances and that part of the energy is irreversible, while the rest was spent on vehicle braking which can be returned to the system through regenerative braking. The testing was carried out on roads without a significant change in altitude and in conditions of moderate traffic, which resulted in more uniform driving with only 16% reversible energy. The distribution of emissions and traction energy according to power classes is shown in a bar graph in Figure 5, where all energy values are shown relative to the total positive traction energy of the RDE cycle, while emissions are shown as a percentage of the total emissions generated during the cycle. The relevant parameters for the comparison of the VSP non-hybrid model and CruiseM non-hybrid vehicle model are presented in Table 3.

Table 3. The relevant parameters for the comparison of the VSP and CruiseM models.

| Classic Vehicle	RDE Cycle			RDE (1/km)			Deviation			
	Measured	CruiseM	VSP	Measured	CruiseM	VSP	CruiseM	CruiseM (%)	VSP	VSP (%)
Distance (km)	86.21	86.63	86.21	1.000	1.005	1.000	0.005	0.48%	0.000	0.00%
Positive traction energy (kWh)	13.37	13.33	13.46	0.155	0.154	0.156	−0.035	0.22%	0.092	0.69%
Negative traction energy (kWh)	−2.14	−2.22	−2.27	−0.0248	−0.0256	−0.0263	−0.080	3.26%	−0.130	6.08%
CO_2 emission (g)	10,540	10,556	10,540	122.2	121.9	122.2	16.259	−0.33%	0.000	0.00%
NOx emission (mg)	39,806	40,051	39,806	461.7	462.3	461.7	245.136	0.13%	0.000	0.00%
Consumption (kg)	3.366	3.371	3.366	0.039	0.039	0.039	0.005	−0.33%	0.000	0.00%

The distance and emissions of the VSP non-hybrid model match the measured data perfectly because the model was calculated using those parameters. Positive and negative traction energy deviate from the measured values because they are calculated via Equation (2) based on current specific power. The distance deviation of the CruiseM model is a consequence of the forward approach, which controls velocity using a PI regulator. In this approach the driving cycle is not perfectly followed because it considers system response time. Deviations of positive traction energy, distance, consumption and CO_2 emissions are within 1% of actual values. Only the relative negative traction energy significantly deviates between the two models, while the absolute deviation is small due to the small value of negative traction energy. The reason for this deviation is the same as for the distance deviation.

3.2. Testing of Hybrid and VSP Vehicle Models in RDE, NEDC and WLTC Driving Cycles

Both hybrid models were tested and compared using standard cycles: the RDE cycle, which is identical to the already performed measurement; the NEDC cycle, which is outdated by today's standards; and the WLTC cycle, which has gradually replaced NEDC. The CruiseM model is optimized based on a set of simple rules described with global objective function. The VSP model works in the frequency domain, so it does not have the possibility of real-time optimization, but the same rules can be used to compare these two models. In this case, the primary goal is to compare the two models so that the VSP frequency model follows the conditions of the CruiseM model. The objective function is a minimization of CO_2 emissions or consumption, so the optimization prefers medium and higher power classes in which the internal combustion engine works more efficiently. On the other hand, the highest classes generate high NOx emissions, which in this case are not penalized because they are not covered by the objective function (14). The distribution of traction energy, emissions, and consumption for the hybrid vehicle under the RDE cycle is graphically depicted in Figure 7A using a bar chart.

All emissions and energy shares are expressed relative to the emissions of a non-hybrid vehicle and to the positive traction energy of each cycle. Classes 1 and 2 have a negative traction power where any engine operation is generally unnecessary, but regenerative braking is possible. The internal combustion engine remains switched on in class 2 only 1.92% of the time, as shown in Figure 7B, and consumes 0.2% of the total traction energy, as shown in Figure 7A. This small amount of energy consumption is not the most optimal solution from an energy point of view, but is a consequence of replicating the energy management strategy of the CruiseM model.

Class 3 represents the lowest values of positive traction power with a mean power of 1.1 kW, as shown in Figure 7C. This engine's operating region is very inefficient, so the goal is to completely eliminate the engine's work and replace that energy with stored regenerative braking energy. Similar to the CruiseM model The engine remained in operation for only 1.28% of the operation time compared with the 11.3% of the total operation time of the non-hybrid vehicle, as shown in Figure 7B and generated 0.2% of the total traction energy, as shown in Figure 7A. In class 3, the vehicle emits 0.4% instead of the initial 3.5% of CO_2 emissions and 0.3% of NOx emissions instead of the initial 2.3%.
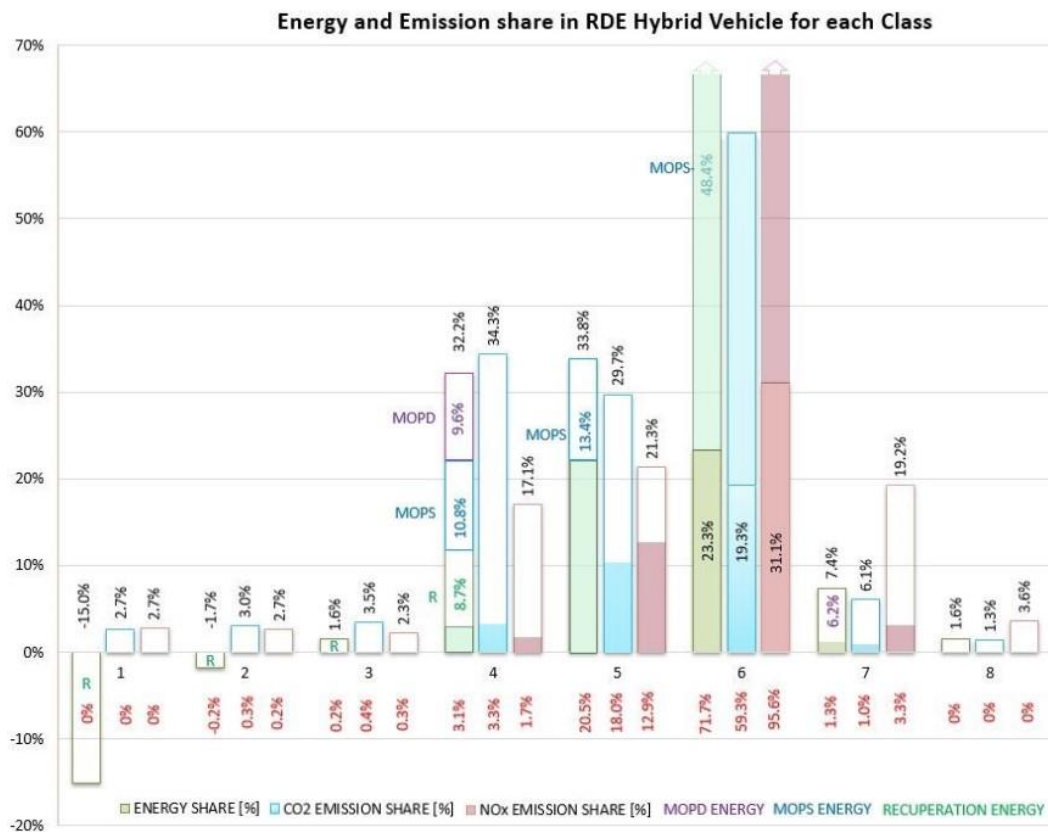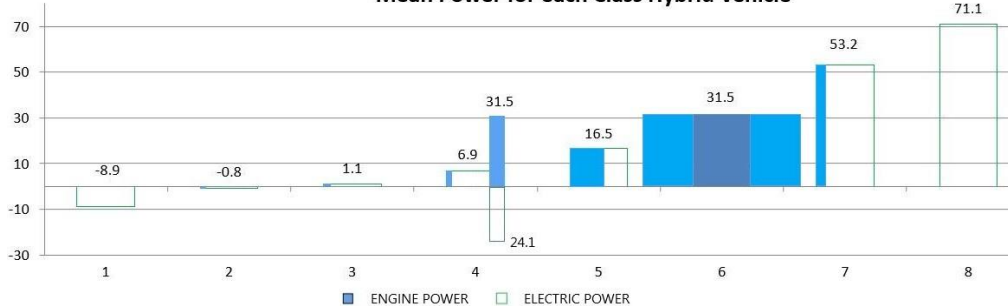
Figure 7. (**A**) Energy distribution and emissions of the VSP hybrid model in the RDE cycle. (**B**) Time shares of power classes. (**C**) Mean power for each class hybrid vehicle.

Class 4 has a slightly higher average power of 6.9 kW but is still deep in the inefficient region in terms of consumption and CO_2 emissions. With a hybrid drive, it would also be desirable to completely eliminate the operation of the engine in this region, but the

engine remains on for 3.6% of the total driving time, as in Figure 7B, generating 3.1% of the total traction energy. Class 4 contains 32.2% of the total traction energy, where 8.7% of the energy was gained from regenerative braking. The remaining 20.4% was obtained by moving the operating region of the engine to the more efficient class 6. Of the 20.4% of the mentioned energy, 9.6% was obtained directly from the internal combustion engine operating in a higher class and this is marked in Figure 7A as moving operating point direct (MOPD), while 10.8% is obtained from stored energy from the battery, which is generated as the excess engine energy gained from the moving engine operating point, marked on the graph as moving operating point stored (MOPS). Considering the time shares of individual classes, as in Figure 7C, the engine works only 3.6% of the time with the power of the original class, it works 10.9% of the time with the average power of the preferred 6th class, and in the remaining time the vehicle is powered by energy from the battery, 9.9% from regenerative braking and 12.3% from MOPS. In class 4, the vehicle emits 3.3% instead of the initial 34.3% of CO_2 emissions and 1.7% of NOx emissions instead of the initial 17.1%.

In class 5, 20.5% of the energy comes from the internal combustion engine, while the remaining 13.4% is used from the battery and gained through MOPS. The engine generates 18% of CO_2 emissions instead of the initial 29.7% and 12.9% of NOx emissions instead of the initial 21.3%. Class 6 is the preferred choice given its engine efficiency, so the share of internal combustion engine energy increases in favor of other classes from 23.3% to 71.7% of the total initial traction energy. At the same time, the CO_2 emissions of class 6 increase from 19.3% to 29.3% of initial total CO_2 emissions, while NOx emissions increase from 31.1% to 95.6%.

Class 7 also belongs to the less efficient region, compared with class 6, and engine energy covers only 1.3% of the initial required 7.4%. This 1.3% of the traction energy also results from the CruiseM model energy management strategy. The total CO_2 emissions of the hybrid vehicle were reduced from 6.1% to 1%, while NOx emissions were reduced from 19.2% to 3.3%. The bar diagram in Figure 8 shows the respective comparative results of the vehicle travelled distance for the VSP and CruiseM models of hybrid and non-hybrid vehicles in RDE, NEDC and WLTP cycles. In contrast with Table 3, where the deviations are expressed in relation to the measured values of the RDE cycle, the following bar diagrams show the deviations between the VSP and CruiseM models.
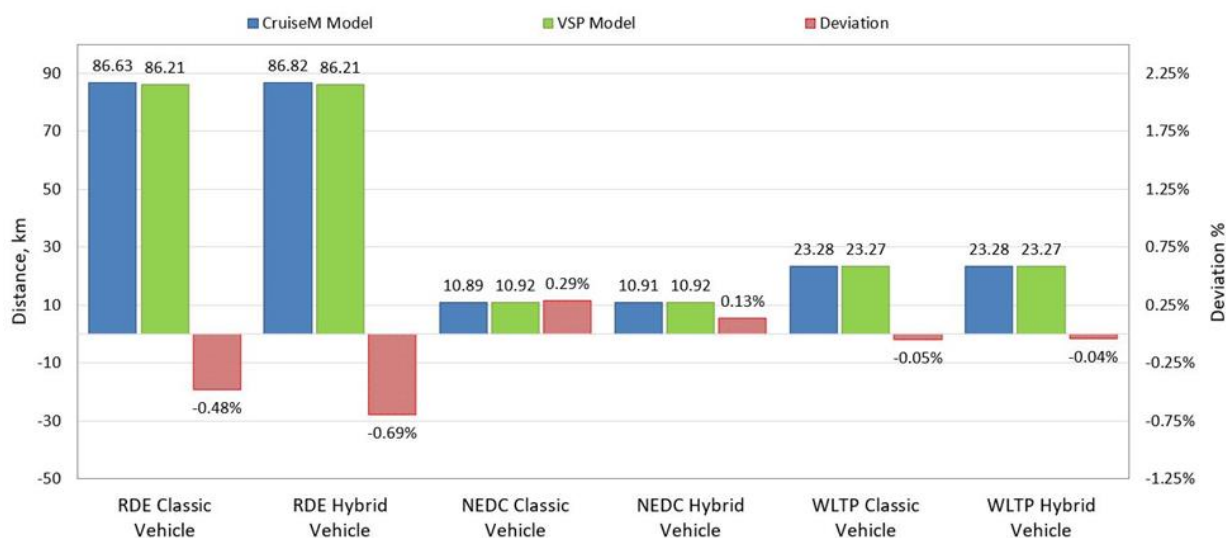

Figure 8. Comparison of distances covered for different models and cycles.

As mentioned above, the cause of the deviation between the two models lies in the different modeling approaches. The VSP was created as a backward model that perfectly follows the given speed profile, while the deviation of the travelled distance of the CruiseM model is a consequence of the forward approach, which in this case includes the PI regulator.

Despite the different approaches, the maximum deviation of the travelled distance is less than 0.7%, which is a more than acceptable result. In the RDE cycle, the travelled distance of both models deviates the most, −0.69% for the hybrid model, and −0.48% for the non-hybrid model. Better results were achieved with laboratory cycles compared with the RDE cycle. One of the important reasons is certainly the influence of altitude, which laboratory cycles cannot replicate. In the NEDC cycle, the travelled distance of classic vehicles differs by 0.29% for a non-hybrid vehicle and 0.13% for a hybrid vehicle. The smallest deviations, of 0.05% for the non-hybrid vehicle and 0.04% for the hybrid vehicle, were recorded in the WLTP cycle. Although the deviations in the travelled distance are small, they were taken into account as a corrective factor when comparing other parameters. The bar graphs in Figures 9 and 10 show the comparative results of the positive and negative traction energies required for the vehicle to overcome the test driving cycles for different cycles. The differences that arise in the traction energies are also a consequence of the forward model, i.e., the settings of the PI regulator. The largest deviation of positive traction energy was recorded between RDE models of hybrid vehicles at 2.85%. Relative deviations of negative traction energies are significantly higher due to small absolute amounts, but the absolute amounts are small and acceptable considering the impact on emissions and consumption. The largest relative deviation of negative traction energies is shown by the non-hybrid vehicle model in the WLTP cycle of over 8%, but on an absolute scale only 0.07 kWh.
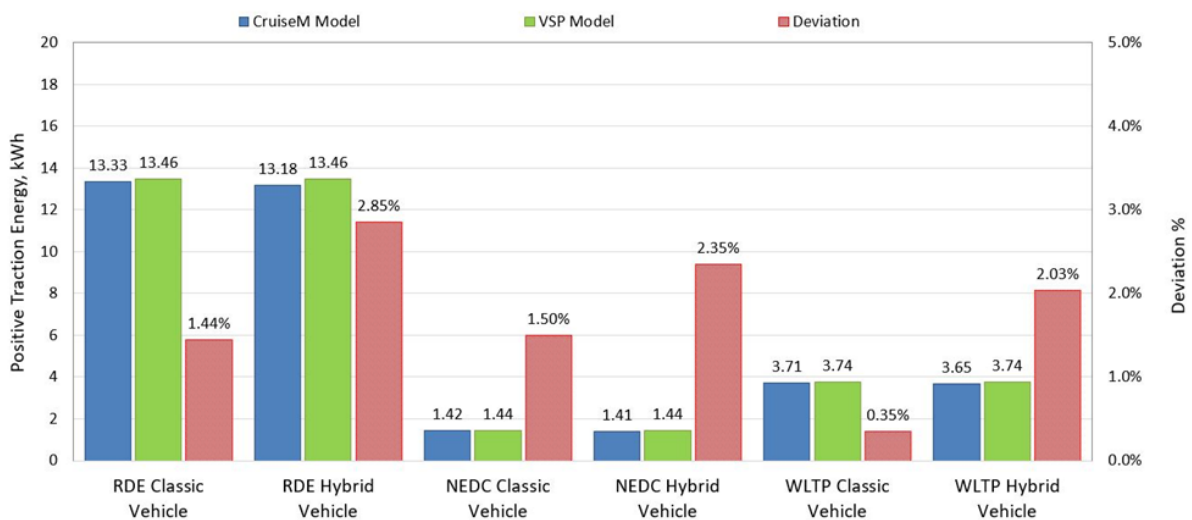

Figure 9. Comparison of positive traction energies for different models and cycles.
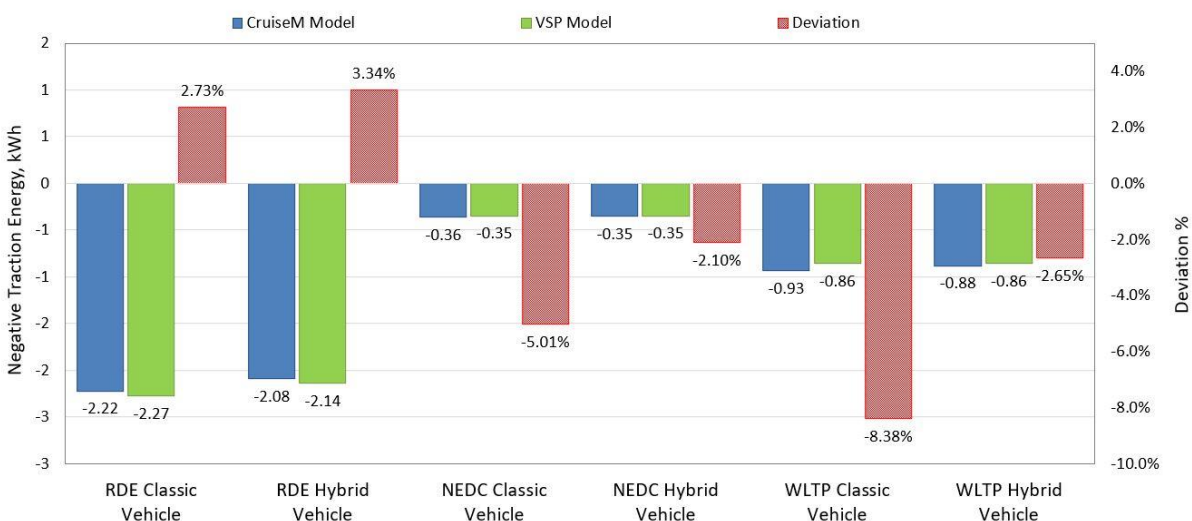

Figure 10. Comparison of negative traction energies for different models and cycles.

The comparison of CO_2 emissions and fuel consumption is shown in the bar diagrams in Figures 11 and 12. CO_2 emissions are expressed in absolute values i.e., in grams that are corrected according to the travelled distance, while consumption is traditionally expressed in liters per 100 km. The most significant deviations were recorded for the hybrid vehicle model in RDE conditions at 3.79% and for the non-hybrid vehicle model in the WLTP cycle at 4.4%. If we compare the results according to cycles, the NEDC cycle in both modelled vehicles, hybrid and classic, gives deviations slightly higher than 1%. The CruiseM model was used as a reference, but it is possible that this model also causes some deviations because it does not include transients.
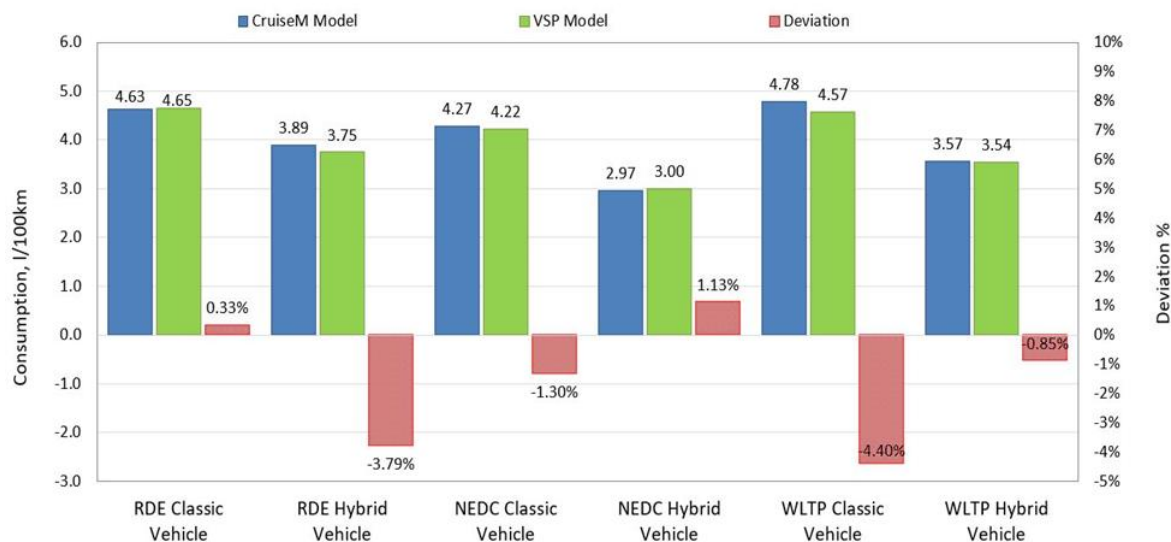

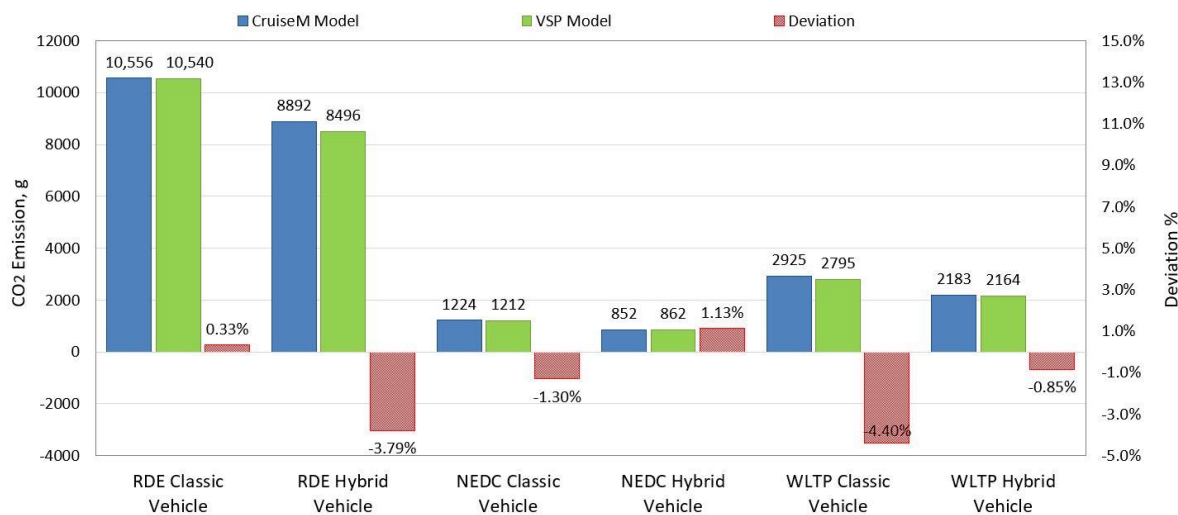**Figure 11.** Comparison of consumption per 100 km for different models and cycles.

Figure 12. Comparison of CO_2 emissions for different models and cycles.

The reason for the good overlap between the results of the NEDC cycle lies in the cycle itself, with constant accelerations where the classic CruiseM model, which is based on consumption and emission maps, approximates the real situation relatively well due to a reduced influence of transient phenomena.

Because the vehicle is type approved according to the Euro 6b standard, which includes testing in laboratory conditions according to the NEDC cycle, it is possible to compare the results with the type approved values. The declared value of CO_2 emissions in the NEDC cycle for the tested vehicle is 102 g/km, while the value of CO_2 emissions of the modelled

vehicle is slightly less than 111 g/km. A deviation of 8.8% was expected, considering that the type approval procedure at that time was performed on a "golden vehicle" which gave significantly better results than the tested one. All of the results derived from the hybrid models were achieved by following the strategy of the CruiseM model based on set of rules. However, the best result was achieved by optimizing the VSP hybrid model without taking into account the CruiseM strategy, which, in terms of CO_2 emissions, gives about 4% better results than those shown in Figure 12, and would put this vehicle inside the legal limit of 95 g of CO_2 emissions in real conditions.

The absolute amounts and corrected deviations of NOx emissions of both models applied to different cycles are shown by the bar graph in Figure 13. The deviations of NOx emissions are, on average, slightly higher than CO_2 emissions and fuel consumption, primarily due to the larger possible deviations of the classic map-based CruiseM model that does not include transients. Transient phenomena in the assessment of NOx emissions have a greater impact due to the way that NOx emissions are regulated through exhaust gas recirculation [11].
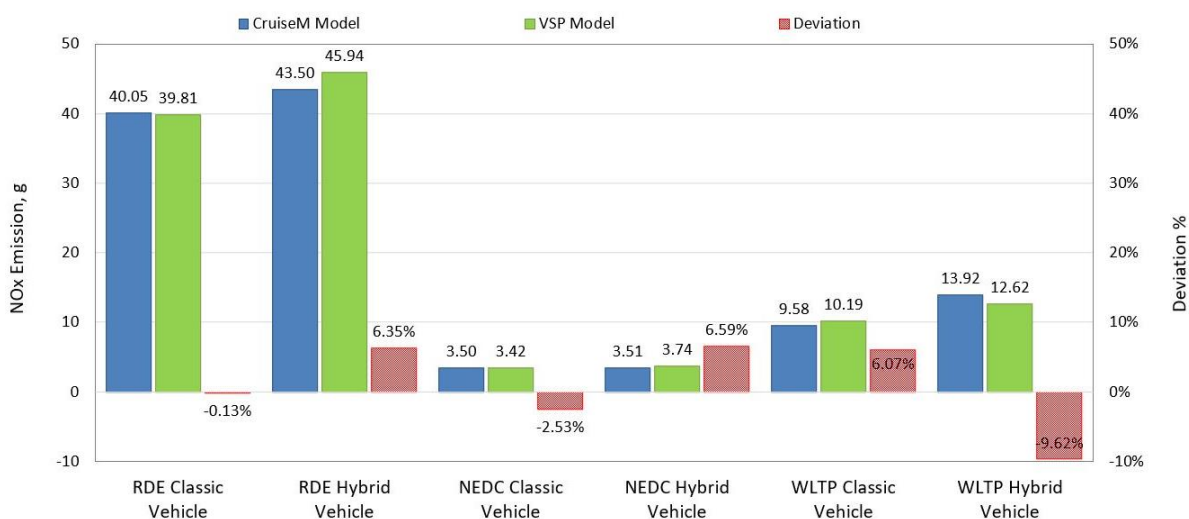

Figure 13. Comparison of NOx emissions for different models and cycles.

The largest deviations of NOx emissions, of 9.62%, are shown with the hybrid vehicle models in the WLTP cycle, while the same models in the NEDC and RDE cycles show deviations slightly higher than 6%. The non-hybrid vehicle models in the RDE, NEDC and WLTP conditions differ by 0.13%, 2.53% and 6.07%, respectively. Larger deviations in the WLTP cycle, especially in NOx emissions, are expected due to extremely dynamic driving.

4. Conclusions

This paper presents a VSP model based on frequency analysis, which represents a new way of modeling primarily hybrid, but also classic non-hybrid vehicles. A comparison of two independent models, VSP and one made in CruiseM, was performed in order to prove the usefulness of the much simpler VSP model with the possibility of obtaining results with similar accuracy. Positive and negative traction energies data, which are necessary to follow the desired cycle, as well as CO_2 emissions data, fuel consumption and NOx emissions, were analyzed and compared. First, the VSP model was tested on a hybrid vehicle under RDE conditions following the same rule-based strategy as the CruiseM model. Furthermore, the energy balance calculation is presented in detail, as well as the calculation of the corresponding CO_2 and NOx emissions for each individual class. All hybrid modes time shares, as well as the shares of individual traction energy components and average ICE power, are graphically presented and classified into the necessary traction power classes. Absolute comparative data are presented graphically with all deviations expressed relatively with a correction according to the travelled distances. The deviations of

the travelled distances are very low, with the highest value of 0.69% for the hybrid vehicle and the RDE cycle. The causes of the deviations lie in the different modeling approaches, a backward approach for the VSP model and a forward approach for the CruiseM model, where the PI controller causes slight deviations. All positive traction energies have positive deviations in the VSP model of between 0.35% for the WLTP model of the non-hybrid vehicle to a maximum of 2.85% for the RDE hybrid model. The deviations of the negative traction energy are relatively higher, up to 8.38%, which is expected because of their small absolute values compared with the total positive traction energy, so they have negligible impact to the overall results. The most important elements of the comparison of the two models are CO_2 emissions and fuel consumption, where the biggest deviation of the results was recorded for the hybrid model of the vehicle in RDE cycle conditions of 3.79% and for the non-hybrid vehicle model in WLTP conditions of 4.4%. All other combinations of cycles and models give deviations of about 1%, which is an excellent result that directly proves the reliability of the model. The best result obtained by optimizing the VSP model of the hybrid vehicle in RDE conditions, independently of the CruiseM model, is about 4% better relative to the result obtained following the CruiseM strategy. This outcome means that this vehicle would reach the legally prescribed, penalty-free limit of 95 g/km under real-world conditions. Regarding the results of the comparison of NOx emissions, the deviations are somewhat larger compared with CO_2 emissions and consumption. The largest deviations of NOx emissions, of 9.62%, are shown by the hybrid vehicle models in the WLTP cycle, while the same models in the NEDC and RDE cycles show deviations slightly higher than 6%. The models of non-hybrid vehicles in the RDE, NEDC and WLTP conditions differ by 0.13%, 2.53% and 6.07%, respectively. Larger deviations of these emissions are expected due to the reduced performance of the CruiseM model when predicting the NOx emissions that are controlled by the EGR system, which in turn is very sensitive to transient phenomena that are not described by this model. This research has shown very good results for the simpler VSP model when predicting fuel consumption and CO_2 and NOx emissions without using complex time domain models which require great skills and complex algorithms to realize real objective functions. Another problem of the time domain model is that it sometimes gets stuck in local minima without finding an optimal global solution, so there is also the possibility to use the VSP model as a control mechanism for the time domain model. Such a model enables a much simpler definition of the objective function, and thus also enables the simplification of the optimization of complex energy management systems such as hybrid propulsion systems. Future research should be directed towards determining the influence of various parameters of the VSP model on its accuracy, especially the selection of the number of classes and their ranges. The possibility of expanding the model in a multidimensional domain should also be investigated, i.e., that it should be expanded with additional influential parameters.

Abbreviations

DOC	Diesel oxidation catalyst
DPF	Diesel particulate filter
EGR	Exhaust gas recirculation
EM	Electric machine
EMS	Energy management strategy
EV	Electric vehicle
GPS	Global position system
HEV	Hybrid electric vehicle
ICE	Internal combustion engine
KE	Kinetic energy
LPG	Liquid petroleum gas
NEDC	New European driving cycle
OBD	On-board diagnostics
PE	Potential energy
PEMS	Portable emission measurement system
RDE	Real driving emission
TM	Technical mass
VSP	Vehicle specific power
WLTP	Worldwide harmonized light vehicle test procedure
f_0, f_1, f_2	Coast down analyses free factor, linear factor, quadratic factor
E_{tr}	Traction energy
F_{aero}	Aerodynamics resistance force
F_{roll}	Rolling resistance force
F_{res}	Resistance force
h	Height
m	Mass
M_x	Total mass of x emission
$m_{x,j}$	Mass of x emission in j power class
$m_{x,k}$	Mass of x emission in k interval
$P_{c,j}$	Power j-class
$P_{e,j}$	Engine power j-class
P_{wheel}	Wheel power
$T_{j,mwa}$	j class engine ICE operating time
v	Velocity
W_{br}	Braking energy
$w_{mwa,j}$	Mechanical energy due to the shift of the ICE operating region
$W_{s,mwa}$	Total stored energy due to the shift of the ICE operating region
$W_{tr,j}$	Traction energy from ICE in class j
$w_{tr,j}$	Drive shaft traction energy in class j
α	Regenerative braking factor
γ_j	Stored energy share in class j
$\eta_g, \eta_{st}, \eta_m$	Generator, storage, motor efficiency
η_{gb}, η_f	Gearbox, final drive efficiency

References

1. News European Parliament. EU Ban on the Sale of New Petrol and Diesel Cars from 2035 Explained. Available online: https://www.europarl.europa.eu/news/en/headlines/economy/20221019STO44572/eu-ban-on-sale-of-new-petrol-and-diesel-cars-from-2035-explained (accessed on 26 August 2023).
2. Regulation (EU) 2023/851 of the European Parliament and of the Council of 19 April 2023. Available online: https://eur-lex.europa.eu/eli/reg/2023/851 (accessed on 5 December 2023).
3. Mali, B.; Shrestha, A.; Chapagain, A.; Bishwokarma, R.; Kumar, P.; Gonzalez-Longatt, F. Challenges in the penetration of electric vehicles in developing countries with a focus on Nepal. *Renew. Energy Focus* **2022**, *40*, 1–12. [CrossRef]
4. Ktistakis, M.A.; Pavlovic, J.; Fontaras, G. *Sampling Approaches for Road Vehicle Fuel Consumption Monitoring*; EUR 30420 EN; Publications Office of the European Union: Luxembourg, 2021; ISBN 978-92-76-23986-4. [CrossRef]
5. Regulation (EU) 2019/631 of the European Parliament and of the Council of 17 April 2019 Setting CO2 Emission Performance Standards for New Passenger Cars and for New Light Commercial Vehicles, and Repealing Regulations (EC) No 443/2009 and (EU) No 510/2011. 2019. Available online: http://data.europa.eu/eli/reg/2019/631/oj (accessed on 5 December 2023).

6.   Takaishi, T.; Numata, A.; Nakano, R.; Sakaguchi, K. Approach to High Efficiency Diesel and Gas Engines. *Mitsubishi Heavy Ind. Rev.* **2008**, *45*, 21–24.

7.   Regulation of the European Parliament and of the Council on Type-Approval of Motor Vehicles and Engines and of Systems, Components and Separate Technical Units Intended for such Vehicles, with Respect to Their Emissions and Battery Durability (Euro 7) and Repealing Regulations (EC) No 715/2007 and (EC) No 595/2009. Available online: https://ec.europa.eu/transparency/documents-register/api/files/COM(2022)586_0/090166e5f39c64d8?rendition=false (accessed on 5 December 2023).

8.   Annexes (1–6) to the Proposal for a Regulation of the European Parliament and the Council on Type-Approval of Motor Vehicles and Engines and of Systems, Components and Separate Technical Units Intended for Such Vehicles, with Respect to Their Emissions and Battery Durability (Euro 7) and Repealing Regulations (EC) No 715/2007 and (EC) No 595/2009. Available online: https://ec.europa.eu/transparency/documents-register/api/files/COM(2022)586_1/090166e5f39c64bb?rendition=false (accessed on 5 December 2023).

9.   Maurer, R.; Kossioris, T.; Sterlepper, S.; Günther, M.; Pischinger, S. Achieving Zero-Impact Emissions with a Gasoline Passenger Car. *Atmosphere* **2023**, *14*, 313. [CrossRef]

10.   Morgan, J.P. Driving into 2025: The Future of Electric Vehicles. Available online: https://www.jpmorgan.com/insights/global-research/autos/electric-vehicles (accessed on 25 May 2022).

11.   Kozina, A.; Radica, G.; Nižetić, S. Analysis of methods towards reduction of harmful pollutants from diesel engines. *J. Clean. Prod.* **2020**, *262*, 121105. [CrossRef]

12.   Reshma, S.; Samuel, E.R.; Unnikrishnan, A. A Review of various internal combustion engine and electric propulsion in hybrid electric vehicles. In Proceedings of the 2019 2nd International Conference on Intelligent Computing, Instrumentation and Control Technologies (ICICICT), Kannur, India, 5–6 July 2019; IEEE: Piscataway, NJ, USA, 2019; Volume 1, pp. 316–321.

13.   Ravi, S.S.; Mazumder, J.; Sun, J.; Brace, C.; Turner, J.W. Techno-Economic assessment of synthetic E-Fuels derived from atmospheric CO_2 and green hydrogen. *Energy Convers. Manag.* **2023**, *291*, 117271. [CrossRef]

14.   Vučetić, A.; Sraga, V.; Bućan, B.; Ormuž, K.; Šagi, G.; Ilinčić, P.; Lulić, Z. Real Driving Emission from Vehicle Fuelled by Petrol and Liquefied Petroleum Gas (LPG). *Cogn. Sustain.* **2022**, *1*, 1–8. [CrossRef]

15.   Medževeprytė, U.K.; Makaras, R.; Lukoševičius, V.; Kilikevičius, S. Application and Efficiency of a Series-Hybrid Drive for Agricultural Use Based on a Modified Version of the World Harmonized Transient Cycle. *Energies* **2023**, *16*, 5379. [CrossRef]

16.   Schulze, S.; Feyerl, G.; Pischinger, S. Advanced ECMS for hybrid electric heavy-duty trucks with predictive battery discharge and adaptive operating strategy under real driving conditions. *Energies* **2023**, *16*, 5171. [CrossRef]

17.   Kampker, A.; Offermanns, C.; Heimes, H.; Bi, P. Meta-analysis on the Market Development of Electrified Vehicles. *ATZ Worldw.* **2021**, *123*, 58–63. [CrossRef]

18.   Sabri, M.; Danapalasingam, K.A.; Rahmat, M.F. A review on hybrid electric vehicles architecture and energy management strategies. *Renew. Sustain. Energy Rev.* **2016**, *53*, 1433–1442. [CrossRef]

19.   Bayindir, K.Ç.; Gözüküçük, M.A.; Teke, A. A comprehensive overview of hybrid electric vehicle: Powertrain configurations, powertrain control techniques and electronic control units. *Energy Convers. Manag.* **2011**, *52*, 1305–1313. [CrossRef]

20.   Zhang, P.; Yan, F.; Du, C. A comprehensive analysis of energy management strategies for hybrid electric vehicles based on bibliometrics. *Renew. Sustain. Energy Rev.* **2015**, *48*, 88–104. [CrossRef]

21.   Salmasi, F.R. Control strategies for hybrid electric vehicles: Evolution, classification, comparison, and future trends. *IEEE Trans. Veh. Technol.* **2007**, *56*, 2393–2404. [CrossRef]

22.   Ali, A.M.; Söffker, D. Towards optimal power management of hybrid electric vehicles in real-time: A review on methods, challenges, and state-of-the-art solutions. *Energies* **2018**, *11*, 476. [CrossRef]

23.   Liu, W. *Introduction to Hybrid Vehicle System Modeling and Control*; John Wiley & Sons: Hoboken, NJ, USA, 2013.

24.   Enang, W.; Bannister, C. Modelling and control of hybrid electric vehicles (A comprehensive review). *Renew. Sustain. Energy Rev.* **2017**, *74*, 1210–1239. [CrossRef]

25.   Chan, C.C.; Bouscayrol, A.; Chen, K. Electric, hybrid, and fuel-cell vehicles: Architectures and modeling. *IEEE Trans. Veh. Technol.* **2009**, *59*, 589–598. [CrossRef]

26.   Onori, S.; Serrao, L.; Rizzoni, G. *Hybrid Electric Vehicles: Energy Management Strategies*; Springer: Berlin/Heidelberg, Germany, 2016.

27.   Tran, D.-D.; Vafaeipour, M.; El Baghdadi, M.; Barrero, R.; Van Mierlo, J.; Hegazy, O. Thorough state-of-the-art analysis of electric and hybrid vehicle powertrains: Topologies and integrated energy management strategies. *Renew. Sustain. Energy Rev.* **2020**, *119*, 109596. [CrossRef]

28.   Sun, X.; Cao, Y.; Jin, Z.; Tian, X.; Xue, M. An adaptive ECMS based on traffic information for plug-in hybrid electric buses. *IEEE Trans. Ind. Electron.* **2022**, *70*, 9248–9259. [CrossRef]

29.   Sun, X.; Jin, Z.; Xue, M.; Tian, X. Adaptive ECMS with Gear Shift Control by Grey Wolf Optimization Algorithm and Neural Network for Plug-in Hybrid Electric Buses. *IEEE Trans. Ind. Electron.* **2023**, *71*, 667–677. [CrossRef]

30.   Ciesla, C.; Keribar, R.; Morel, T. *Engine/Powertrain/Vehicle Modeling Tool Applicable to All Stages of the Design Process*; SAE Technical Paper; SAE International: Warrendale, PA, USA, 2000; ISSN 0148-7191.

31.   Zhou, M.; Jin, H. Development of a transient fuel consumption model. *Transp. Res. Part D Transp. Environ.* **2017**, *51*, 82–93. [CrossRef]

32.   Duarte, G.; Varella, R.A.; Gonçalves, G.; Farias, T. Effect of battery state of charge on fuel use and pollutant emissions of a full hybrid electric light duty vehicle. *J. Power Source* **2014**, *246*, 377–386. [CrossRef]

33. Jimenez-Palacios, J.L. *Understanding and Quantifying Motor Vehicle Emissions with Vehicle Specific Power and TILDAS Remote Sensing*; Massachusetts Institute of Technology: Cambridge, MA, USA, 1998.

34. Functional Mock-Up Interface Specification. Available online: https://fmi-standard.org (accessed on 5 December 2023).

35. Commission Regulation (EU) No 459/2012 of 29 May 2012 amending Regulation (EC) No 15/2007 of the European Parliament and of the Council and Commission Regulation (EC) No 692/2008 as Regards Emissions from Light Passenger and Commercial Vehicles (Euro 6) Text with EEA Relevance. Available online: https://eur-lex.europa.eu/eli/reg/2012/459/oj (accessed on 5 December 2023).

36. Preda, I.; Covaciu, D.; Ciolan, G. *Coast Down Test–Theoretical and Experimental Approach*; Transilvania University Press: Braşov, Romania, 2010.

37. Zhang, F.; Wang, L.; Coskun, S.; Pang, H.; Cui, Y.; Xi, J. Energy management strategies for hybrid electric vehicles: Review, classification, comparison, and outlook. *Energies* **2020**, *13*, 3352. [CrossRef]

38. Lee, J.; Nelson, D.J. Rotating inertia impact on propulsion and regenerative braking for electric motor driven vehicles. In Proceedings of the 2005 IEEE Vehicle Power and Propulsion Conference, Chicago, IL, USA, 7 September 2005; IEEE: Piscataway, NJ, USA, 2005; p. 7.

39. Commission Regulation (EU) 2016/427; Amending Regulation (EC) No 692/2008 as Regards Emissions from Light Passenger and Commercial Vehicles (Euro 6). 2016. Available online: https://eur-lex.europa.eu/legal-content/EN/TXT/?uri=CELEX:32016R0427 (accessed on 5 December 2023).

40. Kozina, A.; Radica, G.; Nižetić, S. Hybrid Vehicles Emissions Assessment. In Proceedings of the 2021 6th International Conference on Smart and Sustainable Technologies (SpliTech), Bol and Split, Croatia, 8–11 September 2021; IEEE: Piscataway, NJ, USA, 2021; pp. 1–5.

ŽIVOTOPIS

Ante Kozina rođen je 2. travnja 1980. u Sinju. Pohađa osnovnu školu Trilj, nastavlja školovanje u Elektrotehničkoj školi u Splitu, a 1998. upisuje dodiplomski studij elektrotehnike, smjer elektronika na Veleučilištu u Splitu. U prosincu 2001. stječe naziv inženjera elektrotehnike. Sveučilišni studij strojarstva na Fakultetu elektrotehnike strojarstva i brodogradnje upisuje 2004. U siječnju 2009. stječe titulu diplomiranog inženjera strojarstva. Za uspjeh tijekom studija dobiva nagrade za najbolje studente završnih godina FESB-a za 2007. i 2008. te pohvalnicu za izvrstan uspjeh. Nakon završetka studija nepune tri godine radi kao voditelj gradilišta strojarske grupe poslova na nekoliko velikih građevinskih projekata. U tvrtki Tromont zapošljava se 2012. kao projektant strojarskih konstrukcija, gdje ubrzo postaje voditelj odjela projektiranja, konstrukcije i tehnologije. Poslijediplomski studij strojarstva na FESB-u upisuje 2014. godine pod mentorstvom prof. dr. sc. Gojmira Radice. Objavljuje ukupno deset znanstvenih radova iz područja procjene emisija ispušnih plinova, sudjeluje na međunarodnim konferencijama. U tvrtki Espera zapošljava se 2017. gdje radi kao voditelj strojarske grupe poslova, voditelj projekta i konstruktor. Od 2020. je zaposlen u vlastitoj tvrtki Mechtron, gdje radi na razvoju sustava vojne opreme u suradnji s više europskih i svjetskih tvrtki.

BIOGRAPHY

Ante Kozina, born on April 2, 1980, in Sinj, attended elementary school in Trilj and pursued his studies at the School of Electrical Engineering in Split. In 1998, he enrolled in an undergraduate course in electrical engineering, specializing in electronics, at the University of Split, where he obtained the title of electrical engineer in December 2001. Continuing his academic journey, Ante Kozina enrolled in the university study of mechanical engineering at the Faculty of Electrical Engineering, Mechanical Engineering, and Naval architecture in 2004. In January 2009, he achieved the title of Mag. Ing. of Mechanical Engineering. His academic excellence was recognized through awards for being the best student in the years 2007 and 2008, along with a certificate of commendation for outstanding success. After completing his studies, Ante Kozina gained experience as a construction site manager on several large engineering projects for three years. In 2012, he joined the company Tromont as a design engineer, quickly progressing to become the head of the department for design, construction, and technology. Subsequently, in 2014, he pursued postgraduate studies in mechanical engineering at FESB under the mentorship of Prof. Ph.D. Gojmir Radica. During this time, he authored ten scientific papers focusing on exhaust gas emissions assessment and actively participated in international conferences. Simultaneously, Ante Kozina worked as a consulting engineer in structural engineering, production technology, and maintenance of industrial electronics. In 2017, he transitioned to Espera, where he was head of the mechanical work group, project manager, and constructor. In 2020, he founded Mechtron, a company dedicated to developing military equipment systems in collaboration with various European and international companies.